

Modelling Landslide Dynamics in Forested Landscapes

Promotor: Prof. dr. ir. A. Veldkamp
Hoogleraar in de bodeminventarisatie en landevaluatie
Laboratorium voor Bodemkunde en Geologie
Wageningen Universiteit

Co-promotor: Dr. J.M. Schoorl
Universitair Docent
Laboratorium voor Bodemkunde en Geologie
Wageningen Universiteit

Samenstelling promotiecommissie (members of the promotion - examination committee):

| | |
|-------------------------------|--|
| Prof. dr. M.J. Crozier | University of Wellington, New Zealand |
| Prof. dr. G. Govers | Katholieke Universiteit Leuven, België |
| Prof. dr. T.W.J. Van Asch | Universiteit Utrecht, Nederland |
| Prof. dr. ir. L. Stroosnijder | Wageningen Universiteit, Nederland |

Dit onderzoek is uitgevoerd binnen de onderzoekschool C.T. de Wit Graduate School for Production Ecology and Resource Conservation (PE&RC).

Modelling Landslide Dynamics in Forested Landscapes

Addressing landscape evolution, landslide soil redistribution and vegetation patterns in the Waitakere Ranges, west Auckland, New Zealand

Lieven Claessens

PROEFSCHRIFT

ter verkrijging van de graad van doctor
op gezag van de rector magnificus
van Wageningen Universiteit
Prof. dr. ir. L. Speelman
in het openbaar te verdedigen
op vrijdag 22 april 2005
des namiddags te vier uur in de Aula

CIP-DATA Koninklijke Bibliotheek, Den Haag

Claessens, L., 2005

Modelling Landslide Dynamics in Forested Landscapes. Addressing landscape evolution, landslide soil redistribution and vegetation patterns in the Waitakere Ranges, west Auckland, New Zealand.

PhD Thesis Wageningen University, The Netherlands. - With ref. - With summaries in Dutch and English.

ISBN 90-8504-145-7



Toitū he whenua, whatungarongaro he tangata
(Land is permanent, man disappears)

Traditional Maori proverb

Is this the real life
Is this just fantasy
Caught in a landslide
No escape from reality

© *Queen - Bohemian Rhapsody (1975)*

This research was supported by the Netherlands Organisation for Scientific Research (NWO) under project number 810.62.013.



Netherlands Organisation for Scientific Research

Cover illustration ‘desaggregating the landscape’: 3D representation of the upper part of the Waitakere River Catchment (above the Waitakere Dam). On top is an orthophoto of the area ‘draped’ over a Digital Elevation Model. The three underlying data layers represent (from top down) landslide hazard, elevation and geology.

Acknowledgements

Looking back at the past four years of work that resulted in this thesis, I really feel privileged for all the chances I've got, the inspiring and highly varied working environment and the many colleagues and friends I got to know along the way! I owe a lot of thanks to a lot of people and I apologise to those I might forget.

In the first place, I want to thank my promotor Tom Veldkamp: Tom, I really enjoyed the amount of freedom you gave me to gradually come up with the different subjects of research resulting in this little but highly diverse book. The fact that field work areas were a little bit 'free flowing' in the beginning, made it necessary to be creative with the original research questions, a process we always managed to accomplish in mutual agreement. This eventually gave me the chance to have a taste of a very broad spectrum of subjects in the fields of geology, geomorphology, soil science and ecology. You also gave me the chance to gain a lot of field experience, building up a database of 'reference landscapes' in different and truly interesting parts of the world. Believe me, looking at a landscape will never be the same again, you managed! What made it even more rewarding was the fact that you very often joined me in the field, sharing your own incredible amount of field experience with me (a total of 14 weeks, I counted it!). In addition, my background in geology and landscape processes (and mini-packs and scissors...) was highly enriched when you gave me the opportunity to join the Ishiara fieldwork project in Kenya in 2001. Quite an eye-opener to see the same rocks and landscapes appearing in this quite distant location of New Zealand in 2003! You were right: geologically speaking, it's a small world...I would be delighted if we can still work together in the future, hopefully also in the field!

I also want to thank my co-promotor Jeroen Schoorl. You introduced me to the mighty LAPSUS-world, and helped me making the first steps in programming the landslide component of the model which forms the core of this work. I really appreciated the informal way of exchanging ideas and working together; you were also always very efficient in making helpful comments on premature manuscripts. I very much enjoyed the practical periods in Álora, especially the enthusiasm and hospitality with which you introduced me (and other people) to your true second home. I really hope we can keep developing the LAPSUS framework together and I wish you lots of success in your new Dutch/Spanish home!

This work was carried out within the main research programme 'Podzolisation under Kauri (*Agathis australis*): for better or worse?' In this context I want to thank Nico van Breemen for starting and leading this programme in an enthusiastic way, despite the political difficulties regarding study areas we experienced at the start. I also thank Johan Bouma for acting as my first interim promotor in the beginning of the project. I owe a lot of thanks to my 'kauri-

colleagues' Anne Jongkind and Eric Verkaik. It was not always easy to tune the timing of our different subjects but we did have some nice fieldwork time together in New Zealand. Sharing the house (or rather camping) in Titirangi and 'Hindersun' was really cosy and I still wish you both good luck in finishing your kauri research.

A lot of work in the Waitakere Ranges was done in co-operation with MSc students who joined me in New Zealand to carry out fieldwork for their theses: Bas, Wouter, Emile, Hans, Ben, Marijn, thanks a lot guys, 'herders', for the good work and discussions in the field, for keeping me company during the incredible distances we covered, the exchange of weird music styles, 'fush 'n chups', flat whites and Steinies and the awful KFC moments with mashed potatoes and gravy...

The Laboratory of Soil Science and Geology provided an exceptionally nice and friendly working environment and I really enjoyed getting to know a lot of excellent colleagues over the years. I thank Henny and Thea for the valuable administrative and logistic support during the whole process of working in projects and travelling a lot. I especially enjoyed (and still enjoy) the company of the 'lunch bunch'; work and non-work related issues all passed the scene and this always served as a welcome mid-day break. Absolutely no work related issues at Tuesday's pub quiz nights though: thanks to the BenG quiz team for these rewarding social events, we rule (provided with some Leffe blond...)!

Several people in Wageningen and New Zealand were closely involved in working on some papers included in this thesis. I want to thank Peter Verburg and Gerard Heuvelink (Wageningen), Bruce Hayward (Geomarine Research, Auckland) and David Lowe (Waikato University, Hamilton) for their highly appreciated contributions to several chapters of this thesis. Hopefully we find a way to cooperate on some more interesting subjects in the future.

Thanks to Toine Jongmans for the nice company in the field in New Zealand in 2002 and the occasional intro to antique Dutch vases and the historical links between the Netherlands and Belgium. I also very much appreciated the company of Rob van den Berg van Saporoea on various moments and locations in Álora, France and Germany, occasionally accompanied by a good rioja wine and some gambas al pil pil !

Starting as a complete novice in landslide research I appreciated very much the help and advice I got from various colleagues at the universities of Utrecht and Amsterdam: Theo Van Asch, Thom Bogaard, Rens van Beek and Erik Cammeraat, thanks for helping me on the way. Quite some people provided support and advice for carrying out the fieldwork in New Zealand. I want to thank Bruce Burns and Warwick Silvester: your help and advice during the first weeks down under were really appreciated. Rhys Gardner showed us our first kauri tree (less impressive than we thought, it was a seedling...) and has always been very helpful and hospitable during the fieldwork periods in the Waitakere Ranges. Our first and politically rather difficult stay in New Zealand was located in the far north of the North Island; I really enjoyed our stay at the Tree House in Kohukohu in the nice company of the Evans family and Tony Watkins. Tipo, Abraham and Kamira of the Matihetihe Community Development Centre in Mitimiti guided us on a few very (in every sense) breathtaking tramps in the Warawara Forest, cheers mates! When we finally ended up in the Waitakere Ranges, we got the support from Brenda Greene, Scott da Silva and other rangers from the Auckland Regional Council and the Arataki Visitor Centre, Te Kawerau a Maki, the Department of Conservation and Watercare Services Ltd. (Cameron King), this support was very welcome, thanks for that! Our work was also valued by John Edgar from the Waitakere Ranges

Protection Society and John Staniland from the Royal Forest and Bird Protection Society kindly gave us permission to work in the Matuku Reserve in Bethells Swamp, Te Henga.

During the last months I was able to broaden again my 'database' on soils and landscapes, by working in the TOA project in Machakos, Kenya. I want to thank Jetse Stoorvogel for giving me this opportunity and agent Alejandra Mora Vallejo for being part of the excellent fieldwork team that accomplished this 'mission'.

I also spend a lot of time in my car over the last years travelling between Belgium, the Netherlands and France... Besides Lies and my family, there were several other reasons for that: one important one was the fact that I've been lucky to play in some very nice bands with very good musicians/friends. Thanks to all the rockers of Stampede, Dynamic Trio and the Melsele All Star Band for some very special moments on and off stage at some hilarious events and locations all over Belgium! I also wouldn't have driven so many kilometres if it wasn't for this amazing group of friends I'm glad to keep on seeing from both the period in Leuven and from before (Melsele and Antwerp). Thanks everybody for just staying who you are and doing that effort to keep meeting each other from time to time, even though we're living in places all over the world and kids are gradually taking over.... !

Tot slot wil ik hier in het bijzonder mijn ouders en familie bedanken, zonder wie dit boekje hier niet had gelegen. Jullie hebben mij de laatste jaren waarschijnlijk wel wat minder gezien dan voorheen, maar ik kan mij niet van de indruk ontdoen dat die momenten dat we er dan toch in slagen samen te komen, nog steeds deugd doen en misschien zelfs in waarde toenemen! Mijn vader bedank ik nog eens extra voor de logistieke steun, zonder welke ik 'én/én' waarschijnlijk wat meer in 'of/of' had moeten veranderen...

Ik heb gedurende de laatste maanden afscheid moeten nemen van mijne beide grootvaders, ondanks het verdriet kijk ik vol dankbaarheid terug op hun leven en wil dan ook graag mijn proefschrift aan mijn grootouders opdragen.

En 'last but not least' wil ik Liesje bedanken voor de steun, de humor, de aangename avonden in Gent en vooral voor het blijven wachten al die jaren... Het was en is zeker niet vanzelfsprekend om diergeneeskunde studeren in Gent, promotieonderzoek in Wageningen en Nieuw- Zeeland en 'césariennes' in Aigurande te combineren. Toch vind ik dat we dat tot hier toe al behoorlijk goed hebben gedaan, hopelijk vloeien beide wegen binnenkort dan toch eindelijk in elkaar...

Bedankt, thanks, kia ora!

Table of Contents

| | |
|--|-----------|
| CHAPTER 1: GENERAL INTRODUCTION..... | 13 |
| 1.1 RESEARCH FRAMEWORK | 13 |
| 1.2 STUDY AREA..... | 14 |
| 1.2.1 Geological history..... | 15 |
| 1.2.2 Climate..... | 19 |
| 1.2.3 Socio-economic history and land use..... | 20 |
| 1.3 MAIN OBJECTIVES AND RESEARCH QUESTIONS..... | 20 |
| 1.4 THESIS OUTLINE | 21 |
| CHAPTER 2: TECTONIC SETTING AND TERRACES | 25 |
| 2.1 INTRODUCTION | 26 |
| 2.1.1 Terrace research in New Zealand..... | 26 |
| 2.1.2 Terraces in the Auckland-Northland region | 28 |
| 2.2 STUDY AREA..... | 28 |
| 2.2.1 Te Henga – Muriwai Coastal Section | 28 |
| 2.2.2 Kumeu River | 30 |
| 2.3 METHODS | 31 |
| 2.3.1 Terrace level mapping, stratigraphic descriptions and altitude measurements..... | 31 |
| 2.3.2 Tephrochronology..... | 31 |
| 2.3.3 Paleoclimatic records..... | 32 |
| 2.4 RESULTS..... | 33 |
| 2.4.1 Terrace level mapping | 33 |
| 2.4.2 Tephrochronology..... | 34 |
| 2.4.3 Correlation with paleoclimatic records and calculation of uplift rates | 36 |
| 2.5 DISCUSSION | 38 |
| 2.6 CONCLUSION | 41 |
| CHAPTER 3: LANDSCAPE PROCESS MODELLING..... | 43 |
| 3.1 INTRODUCTION | 43 |
| 3.2 MATERIALS AND METHODS | 45 |
| 3.2.1 Study area | 45 |
| 3.2.2 Modelling framework..... | 47 |
| 3.2.3 Landslide hazard modelling..... | 47 |
| 3.2.4 Trajectories of failed slope material | 49 |
| 3.2.5 Input data..... | 52 |
| 3.3 RESULTS AND DISCUSSION | 53 |
| 3.3.1 Application for Waitakere Ranges catchment..... | 53 |
| 3.3.2 Model validity..... | 54 |
| 3.4 CONCLUSIONS | 57 |

| | |
|--|------------|
| CHAPTER 4: DEM RESOLUTION EFFECTS..... | 59 |
| 4.1 INTRODUCTION | 60 |
| 4.2 INFLUENCE OF DEM RESOLUTION ON DIGITAL TERRAIN ANALYSIS | 61 |
| 4.2.1 DEM resolution and topographic index..... | 61 |
| 4.2.2 DEM resolution and influence on topographical attributes and modelling results | 62 |
| 4.2.3 DEM resolution and landslide modelling | 63 |
| 4.3 MATERIALS AND METHODS | 63 |
| 4.3.1 Study area | 63 |
| 4.3.2 LAPSUS-LS..... | 64 |
| 4.3.3 Terrain analysis: DEM, slope and specific catchment area | 65 |
| 4.4 RESULTS AND DISCUSSION | 66 |
| 4.4.1 Influence of grid size on slope, specific catchment area and critical rainfall..... | 66 |
| 4.4.2 Influence of grid size on landslide soil redistribution quantities and spatial patterns..... | 69 |
| 4.5 CONCLUSIONS | 73 |
| CHAPTER 5: LANDSLIDE MAGNITUDE AND FREQUENCY | 75 |
| 5.1 INTRODUCTION | 75 |
| 5.2 MATERIALS AND METHODS | 78 |
| 5.2.1 Study area | 78 |
| 5.2.2 LAPSUS-LS, delivery ratio and sediment yield..... | 79 |
| 5.2.3 Sediment record | 81 |
| 5.3 RESULTS AND DISCUSSION | 82 |
| 5.3.1 LAPSUS-LS and sediment yield | 82 |
| 5.3.2 Sediment record interpretation | 84 |
| 5.4 CONCLUSIONS | 91 |
| CHAPTER 6: VEGETATION PATTERNS AND LANDSCAPE STABILITY | 95 |
| 6.1 INTRODUCTION | 96 |
| 6.1.1 Kauri and its distribution..... | 96 |
| 6.1.2 Vegetation patterns | 98 |
| 6.1.3 Digital terrain analysis for ecological applications | 98 |
| 6.2 MATERIALS AND METHODS | 100 |
| 6.2.1 Study area | 100 |
| 6.2.2 DEM analysis and LAPSUS-LS | 100 |
| 6.2.3 Presence-absence analysis..... | 101 |
| 6.3 RESULTS..... | 104 |
| 6.3.1 DEM analysis and LAPSUS-LS | 104 |
| 6.3.2 Logistic regression..... | 104 |
| 6.4 DISCUSSION AND CONCLUSIONS | 106 |
| CHAPTER 7: SYNTHESIS..... | 111 |
| 7.1 TECTONIC UPLIFT, PALEOCLIMATE AND GEOMORPHIC ACTIVITY..... | 111 |
| 7.2 DYNAMIC LANDSCAPE PROCESS MODELLING: LAPSUS-LS..... | 112 |
| 7.2.1 Validity of the LAPSUS-LS model..... | 112 |
| 7.2.2 DEM resolution | 113 |
| 7.2.3 Magnitude-frequency..... | 113 |
| 7.3 KAURI AS A SOIL-LANDSCAPE ENGINEER ?..... | 114 |
| 7.4 IDEAS FOR FUTURE RESEARCH..... | 115 |
| 7.4.1 Tectonic history, uplift rates and terraces in the Auckland-Northland area | 115 |
| 7.4.2 Improvements LAPSUS-LS | 116 |
| 7.4.3 Integration of geomorphic process models and landuse change models | 117 |
| REFERENCES..... | 119 |
| SUMMARY | 135 |
| SAMENVATTING..... | 139 |
| CURRICULUM VITAE | 143 |

Chapter 1

General Introduction

1.1 Research framework

The research resulting in this thesis has been carried out within the programme entitled ‘Podzolisation under kauri (*Agathis australis*): for better or worse ?’, supported by the Netherlands Organisation for Scientific Research (NWO Project 810.62.013). The general goal of the research programme was providing new insights in the linkages between biota and their abiotic environment. Kauri, an endemic conifer from New Zealand, was put forward as an extreme example of a tree which strongly decreases soil fertility and rootability. By worsening local soil conditions to a level it endures better than its competitors, kauri enhances the advantage of its great longevity (500-2000 years) relative to other species, in this way increasing its own fitness. Regeneration of other trees however, including young kauri, becomes restricted on these soils. It was therefore hypothesised that soil rejuvenation (exposure of ‘new’ soil substrates), possibly associated with fire, windthrow or mass movement, is a prerequisite for regeneration of the forest ecosystem (including persistence of kauri itself), necessary to undo kauri’s destructive effects on soil conditions.

Because of the interdisciplinary content of the overall research framework, objectives and research questions were split up in three parts, each covering the scope of one individual doctorate study:

1. Plant characteristics and stand dynamics
2. Soil processes under kauri
3. Soil distribution and landscape dynamics (this study)

This thesis covers the geological, geomorphological and landscape ecology related issues of the main research programme, aiming to link results with the other two subjects which are dealing with ecological and soil chemical processes. In the next paragraphs, the study area, the main objectives and research questions as well as the outline of this thesis are described in more detail.

1.2 Study area

Fieldwork has been carried out in the Waitakere Ranges Regional Park, west of Auckland City on the North Island of New Zealand (Fig. 1.1). Several river catchments within the Waitakere Ranges were studied in the different chapters of this thesis; these study areas are located and described in detail therein. In the following sections, the geological history of New Zealand and the Waitakere Ranges is summarised and the climate and some socio-economic factors of the region are briefly discussed.

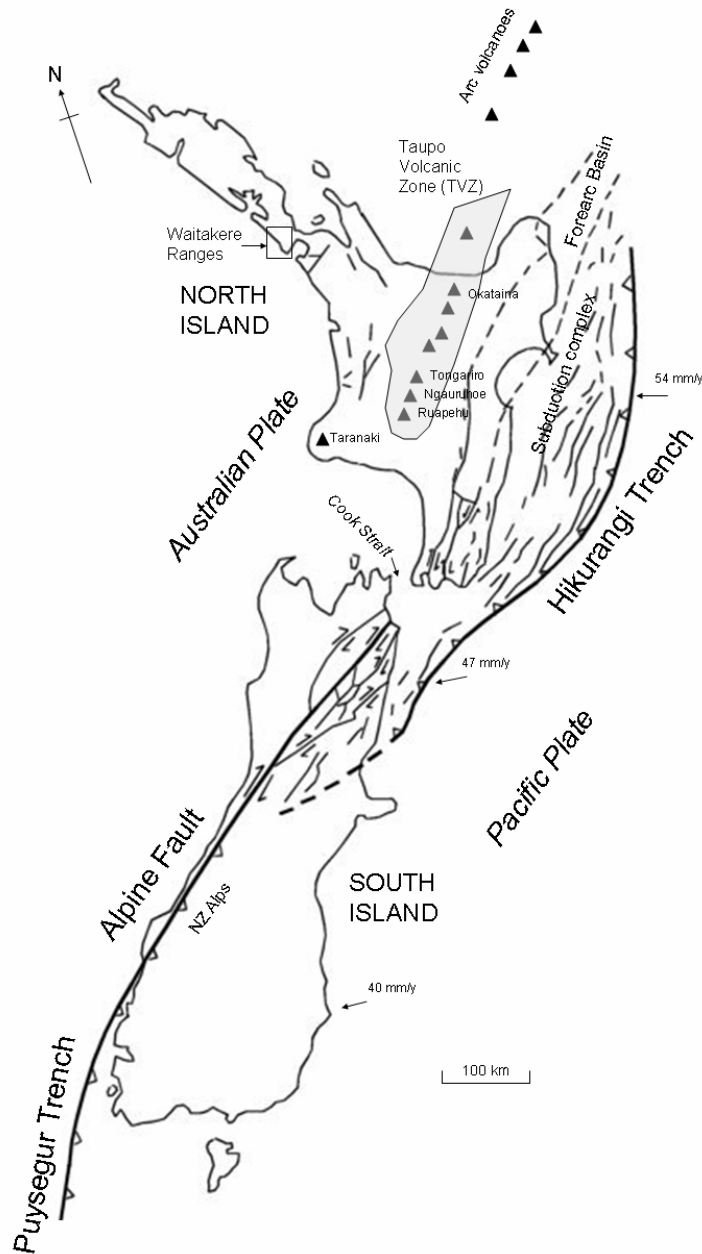


Fig.1.1 General tectonic setting of New Zealand (modified after Kamp, 1992a, Fig. 1.3 and Shane, 2000, Fig. 1).

1.2.1 Geological history

General tectonic setting of New Zealand

The New Zealand landmass is part of a large, thin piece of continental crust of which the major part is covered by sea and situated on the convergent plate boundary between the Pacific and Australian plates (Fig. 1.1).

About 25 Ma BP this active plate boundary developed a new position right through the New Zealand subcontinent (Cooper et al., 1987). A convergent plate margin evokes tectonism which is a fundamental control of the New Zealand landforms and their development (Kamp, 1992a). The boundary between the two plates is marked by the Hikurangi Trough off the East Coast of the North Island and continues along the Alpine Fault on the South Island (Fig. 1.1). In the north, convergence of the two plates is approximately at right angle, which leads to subduction of one plate beneath the other. At the Hikurangi Trough, the dense oceanic crust of the Pacific Plate subducts with a rate of 54 mm yr^{-1} beneath the lighter continental crust of the Australian Plate (Kamp, 1992a). In the subduction zone, slabs of crust descend into the mantle, melt, move to the surface as magma and give rise to active andesitic volcanism, nowadays apparent as four stratovolcanoes on the North Island (Taranaki, Tongariro, Ngauruhoe and Ruapehu, Fig. 1.1). The angle of subduction is small under the North Island so the distance between the subducting crust and the continental plate is relatively small as well. The subducting crust pulls the continental crust downward which leads to the formation of a basin behind the volcanic arc. Partial melting of the acidic continental crust and magma differentiation give rise to the rhyolitic volcanism of the Taupo Volcanic Zone (TVZ). The subduction of the Pacific Plate at more or less right angle at the Hikurangi Trough is transformed into an oblique slip movement of the two plates along the Alpine Fault on the South Island with the Cook Strait as the transitional area. The angle of convergence becomes smaller and smaller when going south and more and more slippage occurs until the angle becomes zero and the plates are sliding past each other causing major uplift and the formation of the New Zealand Alps (Campbell, 1998; Fig. 1.1). Because of the oblique slip movement, the South Island is growing in NE-SW direction. Southwest of the South Island the movement of the two plates changes again. Here the dense oceanic crust of the Australian Plate descends at the Puysegur Trench and subducts beneath the Pacific plate (Kamp, 1992a).

Geological history of New Zealand, the Auckland area and the Waitakere Ranges

Late Precambrium – Jurassic (600 – 140 Ma BP)

The major ‘building blocks’ of New Zealand are a series of fault-bounded tectonostratigraphic terranes accreted at an active margin of the Gondwana supercontinent in Late Paleozoic to Early Cretaceous time and amalgamated in the late Mesozoic (Bradshaw, 1989; Edbrooke, 2001). The basement terranes can be subdivided in two groups. The oldest is the Tuhua Orogen, which comprises two terranes of late Precambrian to Devonian age (600–350 Ma BP). Rocks of the Tuhua Orogen only crop out on parts of the west coast of the South Island. The second group is the Rangitata Orogen, formed in the Carboniferous, Permian, Triassic and Jurassic (350–140 Ma BP), which makes up the bulk of onshore New Zealand. The boundary between the Tuhua and Rangitata orogens, known as the Median Tectonic Line,

marks the mid-Paleozoic edge of the continental lithosphere of eastern Gondwanaland (Kamp, 1992a).

The basement terrane of the Auckland area including the Waitakere Ranges is mainly composed of two distinctive accumulations of sediments eroded from the Gondwana supercontinent from the Late Triassic until the Late Jurassic (200-140 Ma BP). Sediments of the Murihuku Supergroup were deposited in coastal and near-shore environments; sediments of the Waipapa Group were deposited farther offshore in deeper water (Kermode, 1992). The Waipapa terrane was formed as an accretionary prism, the Murihuku terrane in a forearc basin setting (Kamp, 1992a). The sediments continued to compact and harden for the next 60 million years, until tectonic movements began to bring the sediments together and raised them above sea-level around the Late Jurassic. During these processes, the coarser grained shallow water 'greywacke' of the Murihuku Supergroup was gently folded, the finer grained deepwater 'greywacke' of the Waipapa Group was intensely folded, faulted and overthrust. The contact zone of these two terranes is now known as the Junction Magnetic Anomaly (Kermode, 1992). Murihuku terrane outcrops in the southwest and Waipapa terrane in the east of the Auckland area (Edbrooke, 2001). From magnetic anomaly patterns, an intervening narrow belt of Dun Mountain-Maitai terrane is inferred to be present at depth beneath Auckland (Hunt, 1978).

Cretaceous – Late Oligocene (140 Ma – 23 Ma BP)

During the Cretaceous New Zealand separated from the Australian continent through the process of seafloor spreading and moved eastwards. Substantial crustal thickening occurred in the final stage of the assembling of the Murihuku and Waipapa terranes in the Early Cretaceous (144-105 Ma BP; Kamp, 1992a). At the end of this period subduction terminated and extension of the crust started in the Mid Cretaceous (105 Ma BP). This crustal extension was the onset of the continental rifting that separated New Zealand from Australia and Antarctica. The land that earlier had been raised above the sea was slowly eroded to form a group of large islands surmounting a much larger submerged plateau. During the Late Eocene (40-37 Ma BP) swamps and estuaries developed and peat started to accumulate. A marine transgression started in the Early Oligocene (35 Ma BP), the swamps were inundated and the peat was transformed into coal (known as Waikato Coal Measures, Kermode, 1992). The marine transgression also caused the accumulation of a thick sequence of calcareous marine sedimentary deposits during the Late Oligocene and Early Miocene (37-20 Ma BP) covering the Waikato Coal Measures, together forming the Te Kuiti Group (Isaac et al., 1994).

Miocene - Pliocene (23 Ma – 2 Ma BP)

By the Early Miocene New Zealand had reached its present day position with respect to other nearby lands (Hayward, 1979). The convergent plate boundary between the Australian and Pacific plates passed through eastern New Zealand. The Hikurangi trench marked this boundary and was situated somewhere east of northern New Zealand. Subduction at the trench caused the formation of two parallel, southeast trending volcanic arcs (Ballance, 1976a). The first, older, mainly submarine arc (Northland-Coromandel chain) commenced activity in the Late Oligocene (c. 25 Ma BP) and lay west off the present day west coast of Northland. A second, probably more terrestrial volcanic arc (Waitakere chain) developed west

of the first one (Ballance and Williams, 1992). Between the arcs an elongate marine basin formed, the Waitemata basin. The basin gradually deepened during the Early Miocene (22–19 Ma BP) and was filled with 2 km of flysch sediments (alternating sandstone and mudstone), forming the Waitemata Group (Ballance et al., 1977). The sediments were derived from neighbouring lands, mainly northwest of the basin which accumulated as extensive fans around submarine canyons. Turbidity currents from the northwest deposited sediment in the outer fan regions. Cornwallis Formation (Hayward, 1976), consisting of thick graded turbidite sandstone interbedded with laminated siltstone, is inferred to have come from a northwestern source area (Hayward and Smale, 1992) and outcrops along the east side of the study area.

During the Early Miocene and the beginning of the Mid Miocene (18–16 Ma BP) volcanism of the Waitakere volcanic chain increased and the margin of the volcanic centre began to migrate eastwards. In the Auckland area, volcanic rocks of the Waitakere Group originate from two large stratovolcano complexes (Manukau and Kaipara) and several smaller volcanoes 1–10 km across (Edbrooke, 2001). The mainly offshore Manukau centre was a predominantly submarine stratovolcano that was periodically emergent, and only in its final phases produced significant terrestrial flows and pyroclastics, at least on its eastern flanks which now form the Waitakere Ranges (andesite and basaltic andesites of the Manukau Subgroup of the Waitakere Group, Hayward, 1976, 1993). A combination of K-Ar dates and detailed biostratigraphy indicates that the Manukau volcano was active during most of the Early Miocene (23–16 Ma BP; Isaac et al., 1994). The Manukau Subgroup includes a submarine eruptive facies comprising lava flows, pillow lavas and hyaloclastite breccia (Waiatarua Formation), and coarse volcanoclastic breccia and conglomerate, locally interbedded with volcanoclastic sandstone and (rarely) siltstone (Piha Formation). The Piha Formation volcanoclastics are interpreted as debris flow lag deposits that accumulated on the bathyal slopes of the Manukau volcano (Isaac et al., 1994). They grade into a more distal, fine-grained facies of planar-bedded, volcanoclastic grit, sandstone and siltstone (Nihotupu Formation), which overlies and interfingers with sandstone and mudstone of the Waitemata Group to the east (Edbrooke, 2001). Submarine channels in the Piha and Nihotupu Formations are up to 1.5 km across and filled with cross-bedded or structureless mass flow deposits of volcanic conglomerate, sandstone and minor siltstone (Tirikohua Formation). During the last phases of eruption (16 Ma BP), the volcanic cone was breached on its eastern flanks by several conduits of magma which probably reached the surface along pre-existing faults and formed two NNW trending alignments of small parasitic cones. Predominantly terrestrial andesite flows and minor pyroclastic sediments from these cones (Lone Kauri Formation) covered most of the submarine volcanic facies and still cap large parts of the present Waitakere Ranges (Hayward, 1983).

Volcanism in the Waitakere ranges ceased during the Mid Miocene (15 Ma BP), the floor of the Waitemata Basin was slowly uplifted and the Auckland area became emergent. An 8 million year period of relatively low geological and tectonic activity followed and the large volcanoes and the new lands to the west were eroded to almost a plain (Kermode, 1992). Tectonic activity resumed during the Late Miocene and Pliocene (7–2 Ma BP) causing block faulting and uplift in the Auckland Area. The Waitakere Ranges sank in relation to the Auckland block and the Waitemata Basin sediments were compacted and covered with mainly estuarine sediments (Kermode, 1992). Since the period of block faulting, large proportions of the softer rocks mainly in the north and the east of the Waitakere Ranges (Waitemata Group and Nihotupu Formation) have been eroded. The harder rocks (Lone

Kauri and Piha Formations) were more resistant and are still upstanding, though deeply dissected (Hayward, 1983). A simplified geological map of the present Waitakere Ranges, mainly composed of Miocene volcanic rocks, is presented in Fig. 1.2.

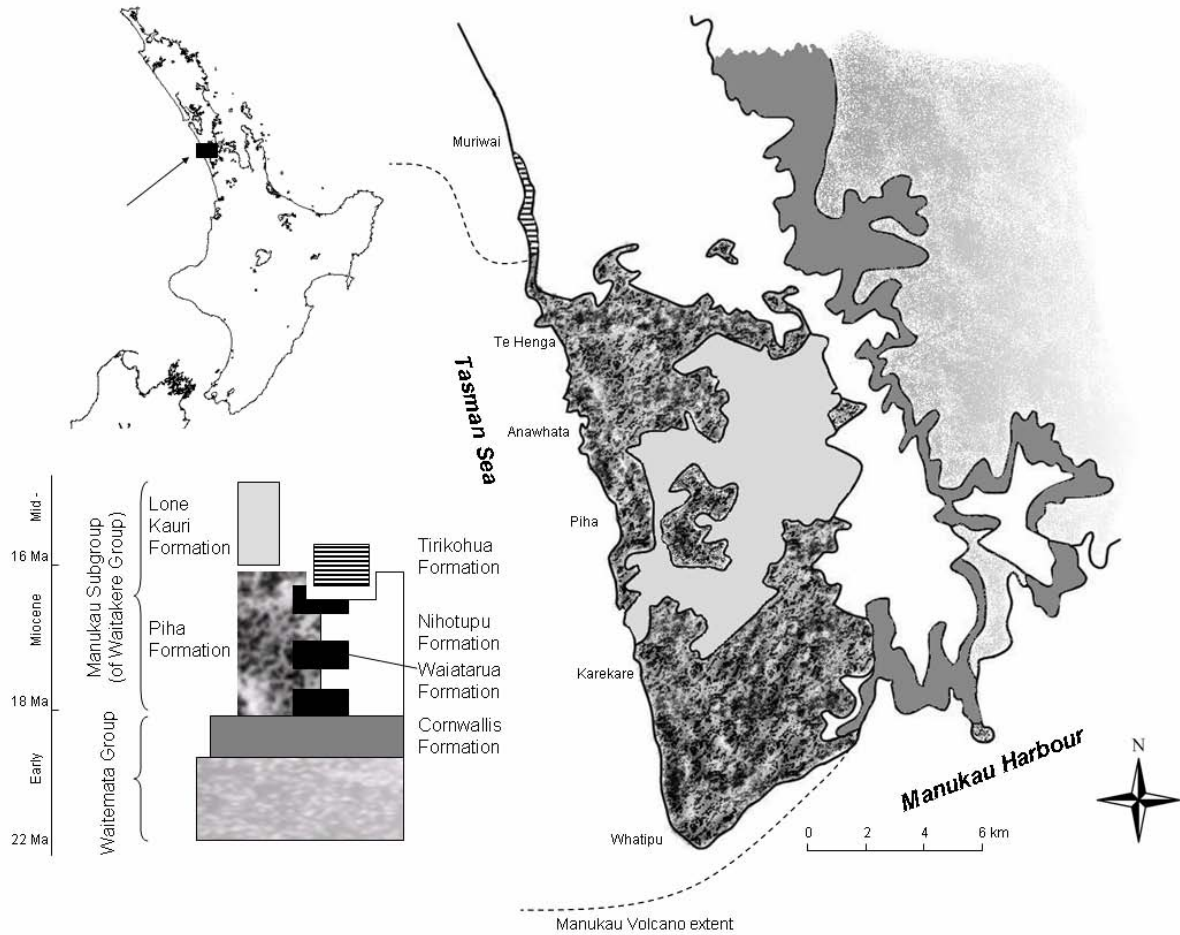


Fig. 1.2 Location and generalised geological map of the Waitakere Ranges (modified after Hayward, 1979, Fig. 11 and Edbrooke, 2001).

Pleistocene - Holocene (2 Ma - Present)

During the Late Pliocene and Early Pleistocene, large coastal sand barriers developed along the west coast of the Auckland area (Edbrooke, 2001). These dune sands and interdune facies are part of the Awhitu Group (Isaac et al., 1994) and outcrop in the northern part of the Waitakere Ranges (Te Henga to Muriwai) and south on the Awhitu Peninsula. Much of the sand is probably derived from silicic volcanics and volcanoclastics and now mainly apparent as moderately to poorly consolidated, large-scale cross-bedded sandstone. Mafic-rich sands, conglomerates and rhyolitic ignimbrites and tephras are present locally. Dips on cross-bedded foresets are consistent with deposition from westerly winds, and intercalated paleosols indicate that sand deposition alternated with periods of dune stabilisation and development of vegetation (Edbrooke, 2001). If induced by climate change, then dune building would probably occur in times of low sea-level glacial periods (Isaac et al., 1994). During the

Pleistocene ice ages left their marks on the landscape of the Waitakere Ranges. Several coastal terraces were formed and the drop in base level caused the rivers to incise. At the same time, series of terrace surfaces were cut in the headwaters of the Kumeu River in the northeast of the study area (Hayward, 1983, see Chapter 2). At the beginning of the Pleistocene the Hauraki Rift was formed and rhyolitic volcanic activity began in the Taupo Region (Spörli, 1989). Throughout the Pleistocene and Holocene there have been many violent rhyolitic eruptions from a number of volcanic centres in the Central North Island (Okataina, Taupo and Tongariro Volcanic Centres; Kermode, 1992). During these eruptions parts or the whole of the study area got covered with airfall ash and this can still be recognised in the landscape as distinct white layers.

Early Pleistocene to Holocene, moderately consolidated to unconsolidated coastal sand deposits of shallow marine, beach and dune origins (Karioitahi Group, Isaac et al., 1994) disconformably overlie Awhitu Group sands and unconformably overlie Miocene volcanic rocks. Dune morphology is typically moderately to well preserved and several geomorphic forms and lithologies can be differentiated (see Isaac et al., 1994). West coast Karioitahi Group sands include significant titanomagnetite and derivation from the Pleistocene hornblende andesites of Mount Taranaki is inferred (e.g. Carter, 1980). Quartz and feldspar components originate from sand derived from the Taupo Volcanic Zone, transported to the west coast by the Waikato River during the last 20 000 years (Nelson et al., 1988). In the study area both stable and moving dune sands as well as modern beach sands are present along the coast. Fixed sand covers an extensive area behind Muriwai beach where in places it has been blown inland for 3.5 km and heights up to 140 m. It forms a coastal belt behind Anawhata, Piha and Karekare where dunes have blown a shorter distance inland (Hayward, 1983). Active dune fields are also present although sometimes recently stabilised by planting of exotic forests (Edbrooke, 2001). At Te Henga, active dune fields have blocked inland river valleys and impounded lakes Wainamu, Kawaupaka and the Te Henga wetland (see Chapter 5). Stratigraphic relationships indicate the moving dune fields have probably accumulated in the last 800-1000 years (Isaac et al., 1994). In the south, at Whatipu, a vast low lying sandy flat (c. 8 km²) has built up over the last decades (Williams, 1977).

At present, the Waitakere Ranges show a rugged, deeply dissected topography and are covered with dense rainforest or regenerating native vegetation. The landscape is mantled by very deep soils (up to 20 m) which are classified as haplic Acrisols according to the WRB classification (Deckers et al., 2002). The clay composition of the soils is dominated by kaolinite but varying fractions of smectite, halloysite and vermiculite clays are also present. Although landslides are usually less common under native forest than under e.g. pasture because of protection by vegetation cover and reinforcement by tree root systems (Phillips and Watson, 1994), they still form the dominant erosion process in the study area. Slope failure occurs frequently involving 1 to 40 m³ of soil material (Hayward, 1983). The bold rocky coastline experiences rapid marine erosion caused by prolonged periods of high energy wave conditions produced by prevailing westerly winds (Denyer et al., 1993). Active marine erosion processes are illustrated by the presence of steep cliffs, intertidal platforms, islands, stacks, caves and blowholes along the present coastline.

1.2.2 Climate

The climate of the the Auckland Region in general is mild because of its maritime location, lacking extremes of temperature, rainfall, and wind. In the Waitakere Ranges however, there

are some significant microclimatic effects, occurring as a response to the relative high exposure to prevailing westerly winds and marine processes along the high energy Tasman coast (Denyer et al., 1993). Due to orographic processes, the Waitakere Ranges experience the highest recorded annual rainfall in the Auckland Region, together with an increase in the number of rainy days and a lower mean annual temperature. The mean annual rainfall ranges from about 1400 mm near the Tasman coast up to 2030 mm at the higher altitudes (altitude ranges from sea-level to 474 m; Auckland Regional Council, 2002). The mean daily air temperature (at Nihotupu Dam) varies between 9° and 18° and the mean annual temperature is 14° C (National Institute of Water and Atmospheric Research Ltd., Wellington, New Zealand).

1.2.3 Socio-economic history and land use

The Waitakere Ranges have a history of human modification and use extending back one thousand years (Denyer et al., 1993). The coastal fringes were extensively modified in the pre european era (before the 1830s). The interior part however, was left virtually untouched during this period. The vegetation of the Ranges was dense rainforest (podocarp-broadleaf) with kauri (*Agathis australis*) forest on the eastern slopes and ridges (Millener, 1965). After more than a century of intensive modification by extractive industries, there are few areas of pre european forest left, and the forest is now composed of extensive areas of regenerating and succesional vegetation. Timber milling drastically altered the original characteristics of the vegetation and wildlife habitats, by selective species removal or clearfelling. Other industries included flaxmilling, gumdigging, mineral extraction and quarrying (Murdoch, 1991; Diamond and Hayward, 1980). Farming also resulted in extensive areas being cleared of their original vegetation (Denyer et al., 1993). The development of a water supply headworks system for metropolitan Auckland from 1907 onwards ultimately lead to the opportunity to preserve a large part of the selectively logged but regenerating indigenous forest. Initially large areas of forest were cleared for the reservoir lakes and dam sites. Three concrete dams had been completed by 1929; the last two dams (earth) were completed in 1948 and 1971 (Auckland Regional Council, 2002). To ensure the purity of the water supply, the catchments were retired from development and allowed to recover naturally. The closing of the catchments allowed the regeneration of 2610 ha of forest and provided the only example of a large area of indigenous forest in the Auckland Region with some form of protection (Murdoch, 1991). Most of the Waitakere Ranges is now administered by the Auckland Regional Council and used for recreation and conservation. The area is not densely populated, although beach settlements of Te Henga, Piha and Karekare are all busy summer locations (Auckland Regional Council, 2002).

1.3 Main objectives and research questions

The general objective of this thesis is to investigate soil-landscape-vegetation dynamics in the Waitakere Ranges. The main core consists of the development of a dynamic landscape process model to simulate soil redistribution by shallow landsliding. Resulting spatial patterns of soil redistribution, changes in landslide susceptibility over time and the relation of spatially explicit landscape attributes with vegetation patterns are further explored. This general objective can be divided into the following, more specific themes, each formulated by a number of research questions:

1. Geological and tectonic context of the study area.
 - What is the geological and geomorphological background leading to the different parent materials, soil types, landforms and geomorphic processes in the study area ?
 - How do present landforms relate to geological and tectonic processes in the past and how is this linked to global sea-level and climate change ?
 - What are the historic and present uplift rates of the area and how do they relate to landscape processes ?
 - How are marine and terrestrial (fluvial) landforms correlated ?
2. Development of a simple, dynamic landscape process model, incorporating the main landscape evolution processes in the study area.
 - What is the dominant process of long term hillslope denudation and soil redistribution in the study area ?
 - Which parameters determine this process and should be incorporated in the model structure ?
 - What are the long term effects of landscape evolution and can spatial patterns of geomorphic attributes be visualised by dynamic landscape process modelling ?
3. Effect of resolution of a digital elevation model (DEM) upon modelling results.
 - Does the grid size of a DEM representing the landscape has influence on modelled soil redistribution quantities and resulting spatial patterns ?
 - What is the most appropriate DEM resolution for landscape process modelling in general ?
4. Magnitude and frequency of soil erosion and sedimentation in the study area.
 - How can long term high-magnitude/low-frequency soil erosion events be assessed without quantitative data covering this timeframe ?
 - Is the landscape process model capable of back-calculating soil redistribution and basin sediment yield scenarios from historic sediment records ?
5. Terrain analysis, geomorphic process modelling and spatial vegetation patterns.
 - How does the ecological cycle of kauri trees result in a typical mosaic pattern of dense stands of mature trees on specific landscape positions ?
 - Can topographical terrain analysis and landscape process modelling contribute to the interpretation of kauri tree stand dynamics ?
 - Are there any feedback mechanisms concerning landscape stability between geomorphic processes and the ecology of kauri trees ?

1.4 Thesis outline

Following this introductory chapter, the thesis is composed of 5 chapters dealing with different aspects covering the main objective and research questions mentioned in the previous paragraph. These chapters (2-6) are based on and structured as scientific papers published in or submitted to peer reviewed journals (introduction, materials and methods, results, discussion, conclusions). Finally, a synthesis is given in Chapter 7. A schematic overview of the framework covering the different chapters is shown in Fig. 1.3.

- Chapter 2 deals with the general geological and tectonic setting of the study area. Quaternary coastal and fluvial terrace morphology and chronology in and near the Waitakere

Ranges are explored to reconstruct the tectonic history of the south-west coast of the Northland region in New Zealand. This chapter is situated on the geological timescale (1.8 Ma BP till present) and places the subsequent chapters dealing with the landscape process model and its applications, acting on a timescale of years to decades, in a broader spatio-temporal perspective.

- Chapter 3 deals with the development and application of the LAPSUS-LS model. The model is constructed as a component of the overall LAPSUS modelling framework (LandscApe ProcesS modelling at mUlti dimensions and scaleS, Schoorl et al., 2000; -LS: LandSlide refers to the process specific model component). LAPSUS originally addresses on-site and off-site effects of current and possible water and soil redistribution by water run-off and tillage erosion. Landscape evolution within a timeframe of decades is simulated in a dynamic way by adapting digital elevation data between yearly timesteps according to calculated soil erosion and sedimentation. Because shallow landsliding is the main soil redistribution process in the study area, there was a need to develop an additional spatially explicit model component dealing with erosion and sedimentation processes caused by landsliding and the associated long term effects on landscape dynamics. LAPSUS-LS delineates the location of shallow landslide initiation sites and simulates the effects on spatial patterns of soil redistribution and resulting landslide hazard in a large watershed within the study area.
- Chapter 4 zooms in on a more theoretical aspect of the LAPSUS-LS model and evaluates digital elevation model (DEM) resolution effects on model results. The focus is on influences of grid size on landslide soil redistribution quantities and resulting spatial patterns and feedback mechanisms.
- Chapter 5 and 6 describe two distinct applications of the LAPSUS-LS model: in Chapter 5, a sediment record from a wetland at the outlet of the largest river catchment in the Waitakere Ranges is used to assess the common issue of dealing with magnitude and frequency of landsliding. The stratigraphy and chronology of sedimentation pulses present in sediment cores taken along a transect covering the wetland are used to represent landslide sediment yield from the catchment upstream. Upland landslide erosion- and sedimentation quantities and sediment delivery ratios are simulated in a spatially explicit way by running different model scenarios with LAPSUS-LS, expanded with algorithms to model sediment yield.
- Finally, Chapter 6 is a more ecologically focused application of the model and links digital terrain analysis and landslide modelling with the spatial distribution of mature kauri trees. Relative landslide hazards, calculated with the LAPSUS-LS model, and logistic regression techniques are used to gain insight in the occurrence of mature kauri trees, their ecological cycle and their effect on landscape stability.

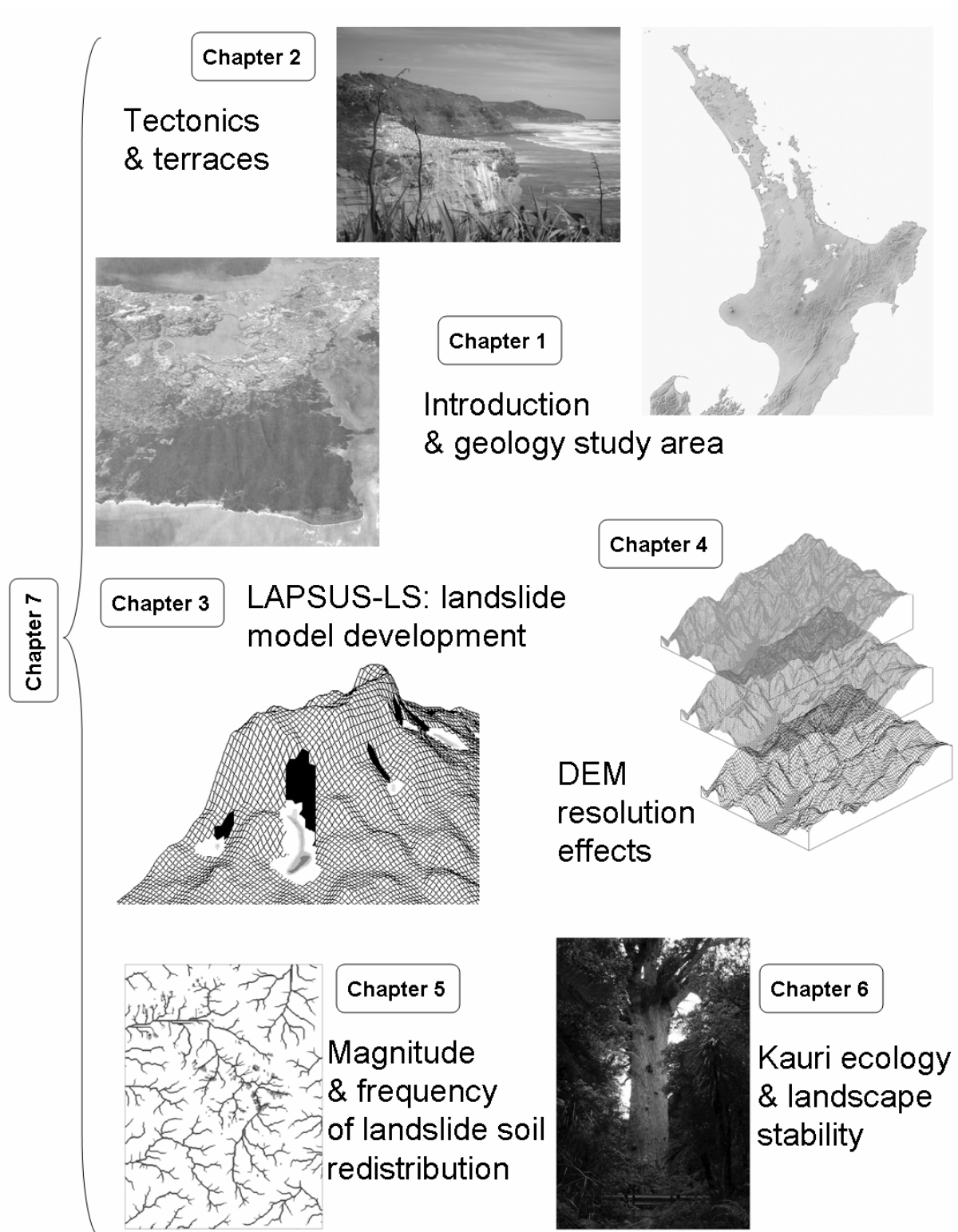


Fig. 1.3 Overview of the content of the different chapters forming this thesis.



Chapter 2

Tectonic Setting and Terraces

In this chapter, marine and fluvial terrace sequences from the northern region of the Waitakere Ranges study area are correlated. Field surveys and the analysis of aerial photography yielded an inventory of 13 fluvial and 12 marine terrace levels. Due to poor exposure of distinct field evidence in the form of e.g. wave-cut platforms or river sediments, planar landscape morphology was the main criterion for terrace remnant identification. Based on the record of terrace height spacings, sparse tephra age control and correlation with global paleoclimatic records, an attempt is made to reconstruct the regional Quaternary uplift rates. Because no hard chronostratigraphic marker is present within the fluvial terrace sequence, fluvial terrace levels are linked to the marine sequence by using the mean uplift rates calculated from the marine terraces (0.35 mm yr^{-1} from 0-0.1 Ma and 0.26 mm yr^{-1} from 0.1-0.3 Ma). Both sets of terraces are then correlated with oxygen isotope fluctuations and the astronomically tuned timescale from ODP Site 677 and the Vostok ice core paleoclimatic records. Oldest marine and fluvial terrace levels are estimated 1.21 Ma and 0.242 Ma respectively. Although there seems to be some form of controversy about the uplift history and especially the preservation of marine terraces in the study area, a general regional uplift, superimposed on glacio-eustatic sea-level changes, is substantiated as the only possible mechanism leading to the maintenance of a considerable relief and active denudation processes inland. Regarding the fluvial terrace sequence, the proposed general model is an actively incising river, carving out strath terraces. The incision phases are reactivated by sea-level lowering and interrupted by net aggradation events due to changing fire regimes during the somewhat drier glacials/stadials or volcanic ash falls, all leading to a temporary increased sediment supply. Since fluvial terrace research is now mainly conducted in geological settings where formation and preservation of terrace surfaces and sediments are most likely, this

Based on: Claessens L. and Veldkamp, A., 2005a. A Quaternary uplift record for the northern Waitakere Ranges, Te Henga-Muriwai, New Zealand, based on marine-terrestrial correlations of coastal and fluvial terraces. *Quaternary Science Reviews*. Submitted.

© 2005 Elsevier Science B.V.

chapter can possibly motivate future researchers to study fluvial terraces in less obvious rapid uplift settings as well.

2.1 Introduction

Both fluvial and marine terraces signify a long term uplifting setting. Fluvial terraces are known to register both glacial and interglacial conditions while coastal terraces have only the ability to register interglacial sea-level high stands. Fluvial terraces are often studied to record a river's response to climatic, tectonic and eustatic processes causing a base level change. Two separate ingredients are required for the formation of aggradational terraces: (i) surface uplift to provide the impetus for fluvial incision and (ii) climatic fluctuation which drives the fluvial activity leading to terrace formation (Bridgland et al., 2004). Sea-level change, itself related to climate change, is only of direct influence to river terrace formation in areas close to the coast and where the continental shelf is narrow (Schumm, 1993; Veldkamp and Tebbens, 2001). The height of terraces above the modern river profile is commonly used to calculate incision rates that are used as a proxy for uplift rates either assuming a time-invariant river profile (Molnar et al., 1994) or using a reconstructed river profile (Lavé and Avouac, 2000). If terraces are present in a tilted, faulted, or folded setting, they can also be used to deduce history and rates of local tectonic deformation (Rockwell et al., 1984; Lavé and Avouac, 2000). When age and (relative) heights of terrace levels above the floodplain are known, minimum regional uplift rates can be calculated.

Marine terrace sequences have been combined worldwide with deep-sea oxygen isotope records to reveal Quaternary sea-level changes and rates of uplift. Interglacial and interstadial sea-levels have been estimated from dated terraces. Examples include Barbados (Bender et al., 1979), Timor (Chappell and Veeh, 1978), New Zealand (Pillans, 1983) and Sumba (Pirazzoli et al., 1991), but the most detailed record is based on an extensive flight of coral terraces at Huon Peninsula, Papua New Guinea, widely regarded as a global reference (Chappell, 1974 and 1983; Chappell et al., 1996). Upper Quaternary coral reef terraces rise to about 1000 m above sea-level and record the history of glacio-eustatic sea-level oscillations superimposed on a history of fast tectonic uplift during the last 300 ka. Another example is the preservation of barrier shorelines located in the Coorong Coastal Plane (southern Australia) which preserves the most complete Middle Pleistocene to Holocene sea-level highstand record in Australia, and globally represents one of the longest Pleistocene highstand records (Murray-Wallace, 2002). However, because marine terrace sequences are restricted to only recording the highest interglacial sea-levels, they rarely have comparable numbers of elements as fluvial terrace staircases. Still, evidence from marine terraces can complement that from river terraces (Pillans, 1994; Bridgland et al., 2004).

2.1.1 Terrace research in New Zealand

Suites of fluvial terraces stepping down towards the modern floodplain characterise many rivers in New Zealand and for the last decades they have been studied intensively due to their link with climatic change (Formento-Trigilio et al., 2002). River systems with their terrace sequences have been analysed both on the North Island (e.g. Vella et al., 1988; Neall, 1992; Heerdegen and Sheperd, 1992; Formento-Trigilio et al., 2002) and the South Island (Eden, 1989; Bull, 1991; Table 2.1; Fig. 2.1). Since the North Island has a history of large volcanic eruptions spanning the entire Quaternary, widespread tephra layers preserved in river terraces

have often been used as stratigraphic markers (Campbell, 1973; Eden, 1989; Marden and Neall, 1990; Pillans et al., 1993; Vucetich et al., 1996; Berryman et al., 2000).

| River (North/South Island) | # River terraces/sets | Age highest terrace | Reference |
|-------------------------------|--------------------------|------------------------|---|
| Huangaia (NI) | 4 – 7 | 460 ka | Formento-Trigilio et al. (2002) |
| Waipaoa (NI) | 4 | 90-140 ka | Berryman et al. (2000); Eden et al. (2001) |
| Manawatu (NI) | 4 | > 45 ka | Fair (1968) |
| | 5 | | Kamp (1992b) |
| | 3 | 18 ka | Marden and Neall (1990) |
| Wanganui (NI) | - | 20 ka | Campbell (1973) |
| Rangitikei (NI) | 3 | 18 ka | Pillans et al. (1993) |
| | 11 | >245 ka | Milne (1973) |
| | | 360-370 ka | Pillans (1994) |
| Wairarapa (NI) | 4 | 85 ka | Vucetich et al. (1996) |
| | 9 | >300 ka | Vella et al. (1988) |
| Waiohine (NI) | 6 | 20 ka | Lensen and Vella (1971) |
| Kaipara (NI) | 3 | Late Pleistocene ? | Hayward (1983) |
| Charwell (SI) | 11 | 53 ka | Bull (1991) |
| Awatere (SI) | 6 | 270 ka | Eden (1989) |

Table 2.1 Examples of former research on river terraces in New Zealand.

The study of coastal terraces in New Zealand dates back more than 150 years ago (review in Gage, 1953). Following the development of plate tectonic theory over the last decades, the introduction of new dating techniques and the publication of the above mentioned sea-level curve for Papua New Guinea (Chappell, 1974), many studies have been undertaken on marine terrace sequences all over New Zealand. Many coastal terrace sequences in New Zealand include tephra layers, produced by numerous volcanic eruptions from the Central North Island. In this context, fission track dating has become a popular technique for dating coastal terraces or marine strata in general (Milne, 1973; Chappell, 1975; Pillans, 1990; Shane et al., 1996a; Lowe et al., 2001; Alloway et al., 2004). Marine terraces in New Zealand have been studied mainly in locations with softer lithologies and moderate to high uplift rates, such as the Wanganui basin and east coasts of the North Island and northern South Island (Williams, 1982; Berryman, 1993; Hesp et al., 1999). The flight of coastal terraces in the South Taranaki-Wanganui region (North Island) is one of the best studies on upper Quaternary coastal terrace chronology in New Zealand where tephra markers are used for terrace age estimation (Pillans, 1983). Correlations with river terraces and marine shelf sediments were made and yield one of the most complete Quaternary stratigraphic records in the world (Pillans, 1994). A summary of methods and results of studies of Pleistocene marine terraces in New Zealand undertaken prior to 1990 is given in Pillans (1990). More recent research, also covering the new focus on Holocene marine terraces and coastal deposits as evidence for shorter term tectonic deformation is summarised in Hesp et al. (1999).

2.1.2 Terraces in the Auckland-Northland region

Before going into detail about the study area, a short overview of previous related research and the issues which complicate the interpretation of marine terraces in the Auckland-Northland region is given: Over the last decades, several researchers described coastal terraces and deduced uplift rates along the east and west coasts of the Auckland and Northland region (Table 2.2). Still, there seems to be an ongoing debate on whether marine wave-cut platforms or comparable marine erosion levels are preserved and apparent coastal terrace morphology can be interpreted as such (B. Alloway, pers. comm.). Current fieldwork has revealed the inadequacy of some earlier definitions and revision has commenced (Kermode, 1992; McMahan, 1994). There are indeed some complications regarding marine terrace interpretation and the calculation of uplift rates:

1. For New Zealand in general, the formation of terraces is initially erosional (in contrast with e.g. the constructional coral terraces in New Guinea) and their survival after uplift is controlled by subaerial erosional and depositional processes, and in part by subsequent marine cliffing (Pillans, 1990). Therefore, there will be extensive preservation of marine terraces in 'favourable' areas, whereas in other places only small isolated remnants remain.
2. If marine terrace surfaces are preserved, they are often overlain by or interfingering with terrestrial, marine or estuarine coverbeds. Almost no direct evidence in the form of wave-cut surfaces (uplifted 'abrasion plateaus', bored surfaces, dateable shell material etc.) are outcropping or have been intersected by drilling.
3. There is no real evidence for (convergent) tectonic activity (with associated volcanism and displacement of older sediments) after the end of the Early Miocene for the region in general, indicating a relative tectonic quiescence since then (e.g. Isaac et al., 1994).
4. Finally, when computing rates of uplift from terrace heights, the long term average rates can be the result of highly episodic events (e.g. earthquakes) in which sudden displacements of metres are separated by decades or centuries of 'stability'.

2.2 Study area

2.2.1 Te Henga – Muriwai Coastal Section

The coastal section for this study is situated along the Te Henga-Goldie Bush Walkway, administered by the Department of Conservation, between Te Henga (Bethells Beach) and Muriwai on the northern foothills of the Waitakere Ranges (Fig. 2.1). The geological and tectonic history of the Waitakere Ranges and the resulting parent materials were described in more detail in Chapter 1 (Fig. 1.2).

After an 8 Ma period of relative geological quiet from the Mid Miocene (15 Ma BP, Kermode, 1992), tectonic activity resumed during the Late Miocene and Pliocene (7-2 Ma BP) causing block faulting and uplift in the Auckland area (Hayward, 1983). Extensional tectonics in the Late Neogene (Pliocene-Quaternary) led to the development of a basin and range topography, probably involving reactivation of deepseated Cretaceous palaeofaults (Kamp, 1988). A vestige of this basin and range topography prior to Quaternary sediment deposition is seen in the north-trending residual fault scarp east of the line Muriwai to Parakai (Fig. 2.1). This fault marks an important boundary between footwall Waitakere Volcanics and younger sediments on the hanging wall, i.e. the South Kaipara Barrier (McMahan, 1994). The

fault is indicated on the older geological map of Auckland (Schofield, 1967) but does not re-appear on the more recent one (Edbrooke, 2001).

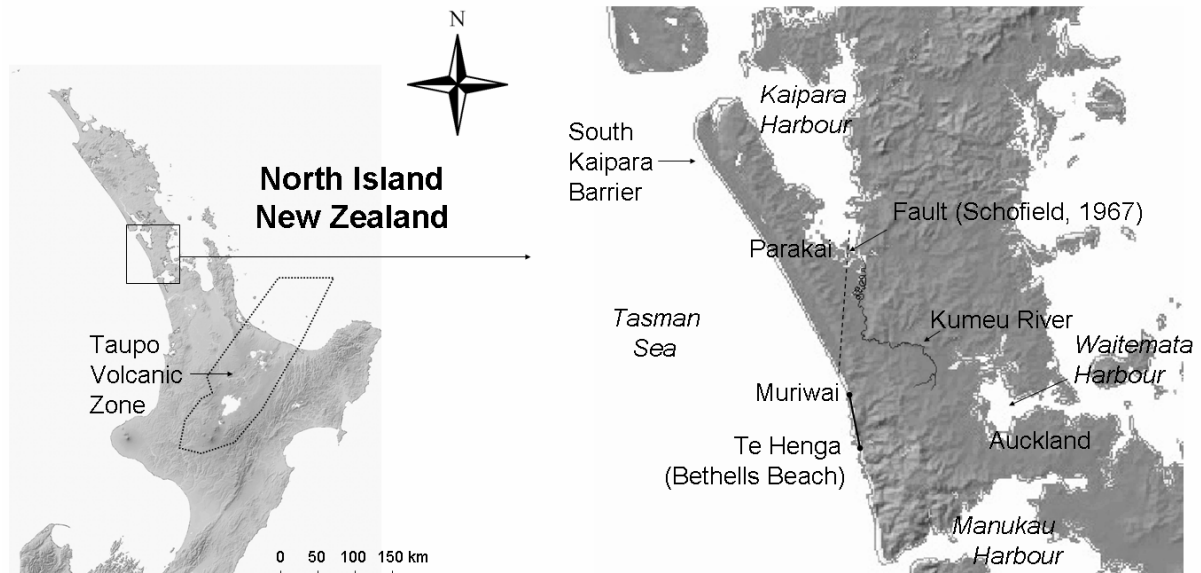


Fig. 2.1 Location of the study area and other localities referred to in the text.

| Area | Coastal terraces [#]/presence | Highest terrace [m] | Uplift rate [mm yr ⁻¹] | Reference |
|-----------------------|----------------------------------|------------------------|---------------------------------------|----------------------|
| Awhitu | 7 | 165-180 | - | Barter (1976) |
| Auckland | 8 | 150-180 | - | Ballance (1968); |
| | 6 | - | 0.30 | Chappell (1975) |
| South Kaipara | 6 | 167 | - | Brothers (1954) |
| North Kaipara | 6 | 105 | - | Richardson (1985) |
| Aupouri-Karikari | 8 | 167-183 | 0.35 | Goldie (1975); |
| | | | 0.35 | Ricketts (1975); |
| | | | 0.21 | Hicks (1975) |
| Waitakere-Auckland | 8 | 167-183 | - | Searle (1944); |
| | 'presence' | - | - | Hayward (1983) |
| Waitemata-Helensville | 8 | 167 | - | Clark (1948) |
| North Cape | 5-6 | 116-182 | 0.30 | Leitch (1966) |
| Ahipara-Doubtless Bay | 'presence' | - | - | Isaac (1996) |
| Hauraki Gulf and | 'presence' | - | - | Isaac et al. (1994); |
| Firth of Thames | 'presence' | - | - | Edbrooke (2001) |

Table 2.2 Examples of previous research on marine terraces and inferred uplift rates in the Auckland-Northland region.

During the Late Pliocene and Early Pleistocene, large coastal sand barriers (Awhitu Group, Isaac et al., 1994) developed along the west coast of the Auckland area (Edbrooke, 2001). On the Te Henga track, the contact between Miocene volcanic rocks and overlying Plio-

Pleistocene sands is hardly exposed. However, coastal cliff sections show up to 30 m thick deposits of Awhitu Group sands unconformably overlying an irregular surface of Waitakere Group volcanics (Hayward, 1983). One drill-hole at Parakai (Fig. 2.1) intersected Waitemata Group turbidites at 30 m below surface (Calavache, 1984). Much of the sand is probably derived from silicic volcanics and now mainly apparent as moderately to poorly consolidated, large-scale cross-bedded sandstone.

At the beginning of the Pleistocene, rhyolitic volcanic activity began in the Central North Island. Throughout the Quaternary there have been a number of violent rhyolitic eruptions from the Taupo Volcanic Zone (Fig. 2.1) resulting in several distal tephra deposits which have been preserved and identified in coastal sequences and lake deposits in the Auckland area (e.g. Newnham et al., 1999; Sandiford et al., 2003; Alloway et al., 2004).

Regarding coastal terraces in the study area, the early works of Searle (1944) and Brothers (1954) were done at nearby locations (north shores of Manukau Harbour and South Kaipara Barrier respectively; Fig. 2.1). The contention was that Pleistocene sea-level regression took place from 167 m higher than present sea-level and that four periods of glacial eustasy were reflected in the terrace surfaces. Tectonic stability of North Auckland since the Kaikoura Orogeny (26 Ma BP) was assumed, a notion contradicted by several indications of differential Pleistocene earth movement (Ballance, 1968). In the Waitakere geological map report (Hayward, 1983), glacial eustasy related coastal terraces are mentioned but they were not mapped as such. Unpublished work by McMahan (1994) was conducted on the South Kaipara Barrier, just north of Muriwai (Fig. 2.1). The section is interpreted as a composite barrier depositional system: coastal terrace formation is not substantiated and the terrace surfaces are considered to be of large scale aeolian bounding surface origin (also called 'Stokes surfaces'). It is important to notice that the South Kaipara Barrier should be treated as a different local 'tectonic block' (north-west of the faultline Muriwai-Parakai, see Fig. 2.1) where Awhitu sands are underlain by soft Waitemata Group turbidites in which cutting and preservation of coastal terraces or erosion levels is not likely. In the Te Henga-Muriwai section however, south-east of the fault, more resistant Waitakere Group volcanics are underlying the Awhitu sand deposits.

2.2.2 Kumeu River

The Kumeu River originates in the northern part of the Waitakere Ranges, where volcanic parent materials from the Nihotupu and Piha Formations (see Chapter 1) scarcely contribute to the river sediments (Fig. 2.1). Most of the c. 30 km² catchment area is comprised of sand-, mud- and siltstones of the Waitemata Group (see Chapter 1). In the Early Miocene a marine basin (Waitemata Basin) lay east of the Manukau volcanic chain and was mainly filled with turbidite deposits (Kermode, 1992; Edbrooke, 2001). The sediments were derived from neighbouring lands, mainly northwest of the basin which accumulated as extensive fans around submarine canyons. Turbidity currents from the northwest deposited sediment in the outer fan regions. The Kumeu River mainly intersects the alternating, graded sandstones and laminated mudstones of the East Coast Bay Formation (Ballance, 1976b) and the thick turbidite sandstones interbedded with laminated siltstones of the Cornwallis Formation (Hayward, 1983). In the town of Kumeu, the river bends to the west to join two other streams and form the Kaipara River, which drains north into the Kaipara Harbour (Fig. 2.1).

Unpublished early work of Clark (1948) deals with the evolution of the drainage between the Kaipara and Waitemata Harbours (Fig. 2.1). He describes eight 'erosion-level' terraces

attributed to changes in uplift and subsidence. Two instances where this terrace surfaces have an appreciable slope and may have been warped are seen as indications for Pleistocene differential earth movement in the area by Ballance (1968). Based on borehole data and mainly geomorphic criteria (two north-south faultlines, assymetry of stream valleys and direction of current tributaries), Clark also suggests the Kumeu River used to be a tributary of an ancestral Waitemata River draining to the east (now reduced to Rangitopuni Stream) and was later captured by the Kaipara River draining to the north.

Three groups of Kumeu River terraces are mentioned and mapped on the 1:50 000 Waitakere geological map (Hayward, 1983). They are described as poorly exposed, highly weathered, mostly silt and clay and often impossible to distinguish from weathered exposures of lower Miocene parent rocks. The deposits underlie a number of surfaces which roughly parallel modern stream profiles. They have been divided in groups of terraces lying 35 m, 15-25 m and 2-8 m above local stream level, and inferred to relate to marine base levels at these altitudes (Hayward, 1983). In the more recent 1:250 000 geological map of the Auckland area (Edbrooke, 2001), the terraces are mapped as a lumped alluvium/colluvium unit.

2.3 Methods

2.3.1 Terrace level mapping, stratigraphic descriptions and altitude measurements

Based on aerial photography, digital elevation models, earlier mapping (Hayward, 1983; Edbrooke, 2001) and intensive field surveys, fluvial- and marine terraces were localised and mapped in the Kumeu River valley and along the Te Henga-Muriwai coastal section respectively. Due to poor exposure of obvious fluvial terrace deposits and wave-cut marine terrace surfaces (see further in discussion), subplanar morphology and front scarps forming stair-like landforms were the most important and first field criteria to recognise and map terrace remnants. Positioning and barometric altitude measurements were performed with a calibrated GPS device. For fluvial terraces, the altitude of the top of a (mostly weathered) fluvial terrace remnant was taken as reference.

Although a wave-cut platform is often the most readily identifiable paleosea-level, the height of the maximal strandline (intersection of platform and the base of a fossil sea cliff) is the the most useful field datum and recommended for reporting the age of a marine terrace (Pillans, 1990). The surface expression of a strandline is typically the base of a terrace riser (the ascending slope bordering the subplanar terrace landform). Strandlines were located and mapped in the field including reference altitudes for each marine terrace level. Relative terrace height rather than absolute height has long been regarded vital in interpreting terrace ages and reconstructing uplift scenarios (e.g. Chappell, 1975).

For later correlation of terrace remnants and because tephra layers were present in exposures within both marine- and fluvial terraces, detailed stratigraphic descriptions of 38 marine terrace-and 19 fluvial terrace sections were made (ten Broeke, 2002; Vloemans, 2004).

2.3.2 Tephrochronology

The assignment of terrace ages based solely on height spacings is found to be unreliable in the absence of other dating methods (Pillans, 1990). Tephra (volcanic ash) layers when correlated and dated help provide a chronology for sedimentary records, river terraces, coastal terraces or marine strata in general (Milne, 1973; Chappell, 1975; Vella et al., 1988; Eden, 1989;

Marden and Neall, 1990; Pillans, 1990 and 1994; Newnham and Lowe, 1991; Eden and Froggatt, 1996; Shane et al., 1996a; Naish et al., 1996; Lowe et al., 1999 and 2001; Shane and Hoverd, 2002; Sandiford et al., 2002; Newnham et al., 2004; Alloway et al., 2004). In New Zealand, the recently-active rhyolitic Taupo and Okataina caldera volcanoes, within the central Taupo Volcanic Zone (TVZ), are the two most frequently active rhyolite centres on Earth and their tephra deposits have been the focus of study for much of the 20th century (Wilson, 1993; Black et al., 1996; Shane, 2000). Positive correlations of tephra commonly require multiple criteria (Froggatt and Lowe, 1990). In proximal settings (<50 km from vent), tephra beds can usually be identified from their stratigraphic position, lithology, and ferromagnesian mineral assemblages. In more distal settings, however, these features become less diagnostic and geochemical fingerprinting must be employed. Major element compositions of glass shards of rhyolitic tephra deposits are often analysed by electron microprobe. The efficacy of this technique to fingerprint tephra deposits was established by Froggatt (1983) and has been widely used (e.g., Lowe, 1988; Shane, 2000). A number of shards per sample are analysed and populations of identical composition are expressed as a mean and standard deviation. Glass compositions can then be compared with those from known (and dated) tephra deposits elsewhere. Still, some tephras may have indistinguishable glass chemistries and the possibility remains that equivalent-aged tephra correlatives might represent different eruptive events from the same volcanic centre (Alloway et al., 2004).

2.3.3 Paleoclimatic records

During a glacial, skeletons of Benthic Foraminifera microfossils take up more ¹⁸O isotopes since lighter ¹⁶O isotopes are preferentially locked away in ice sheets and because of changes in response to water temperature and salinity. Glacial-interglacial oxygen isotope oscillations have been established from oxygen stable isotope measurements on foraminiferal shells from deep sea sediment cores all over the world and they can be used to calibrate global climate and sea-level changes throughout the Quaternary. The amplitudes of correlative waves in different cores diverge to a significant degree due to limited sampling density, burrowing, selective dissolution, delay in ocean mixing. The shape of the curve, rather than absolute changes of the ¹⁸O/¹⁶O ratios, are used for stratigraphic correlation (Kukla and Cilek, 1996). ODP (Ocean Drilling Program) and DSDP (Deep Sea Drilling Program) cores have shown that there have been about 50 glacial periods and, therefore, 50 cycles of sea-level change during the last 2.6 Ma. These cycles, or oscillations, are numbered from the top (stage 1 as last interglacial) downwards and are known as "Marine Isotope Stages" (MIS). An even number correlates to a glacial and an uneven number to an interglacial. A total of 104 marine isotope stages have been identified. Isotopic data suggest that glacial cycles are "sawtoothed", consisting of a long period of ice build-up and falling sea-level during the glaciation phase, and a much shorter period of rising sea-level during deglaciation (Trenhaile, 2001). For correlations in this study the isotopic record and astronomically tuned timescale of Site ODP 677 (Shackleton et al., 1990) are used because they are recommended for global correlations (Pillans, 1994; Bridgland et al. 2004).

Other high resolution records for paleoclimatology are the polar ice caps. Ice cores were taken from these polar ice sheets on high elevations, called the dry snow zone where snow melt and sublimation are lowest. Here the accumulation of snow has been continuous and can provide a paleoclimatic record of up to several hundred thousand years (Bradley, 1999). From the ice cores precipitation, air temperature, atmospheric composition (CO₂), explosive volcanic

eruptions and variations in solar activity can be determined (Bradley, 1999). The records of past air temperatures are obtained from stable isotope variations in the ice cores (^2H and ^{18}O). The ratios between the heavier and lighter isotopes can be used to determine temperature variations in a similar manner as with the deep sea records. The two longest and most prominent ice core records obtained are the Vostok ice core in Antarctica and the GISP2/GRIP ice cores in Greenland. For detailed correlations for the last 0.4 Ma, temperature variations and the glaciological timescale of the Vostok ice core were used (Petit et al., 1999).

2.4 Results

2.4.1 Terrace level mapping

Along the Te Henga-Muriwai coastal section, a total of 12 groups (levels) of coastal terrace remnants were found (Fig. 2.2). The highest point where a volcanic rock surface underlying an Awhitu sand covered bed was exposed was present at 108 m. No wave-cut platforms are outcropping but, besides subplanar morphology of the Awhitu sand deposits, field indications for marine terrace formation and uplift are:

1. Presence of traces of jarosite, produced by oxidation of pyrite FeS_2 in a non calcareous sediment, within Awhitu sand exposures up to 170 m. The formation of pyrite can only take place during sedimentation in a marine or intertidal environment. Conditions are: (i) Fe and S from seawater or brackish water (ii) anaerobic conditions and Fe and S-reducing microbes to allow reduction of sulfate and Fe-oxides (this is met in fresh coastal sediments) (iii) organic matter as energy source for microbes: comes from mangroves, reeds or sedges (iv) tidal flushing: to remove the alkalinity formed in the process of pyrite formation (v) slow sedimentation: to form sufficient pyrite for potentially acid sediment (FAO, 2001).
2. The Pleistocene marine Awhitu sand covered beds, which are interpreted to be deposited by wave action (McMahon, 1994), as admixture of marine and freshwater sediment with aeolian dune sand (Hayward, 1983) or as accumulated in a range of fluvial, estuarine and marine environments (Isaac, 1996), occur high in the landscape (up to 200 m). If the deposition environment is indeed (partly) shallow marine/coastal (indicated by presence of jarosite, see previous point), there should have been at least 200 meters of uplift since deposition (Late Pliocene to Early Pleistocene, Isaac, 1996). Edbrooke (2001) however, found dips on foreset crossbeds more consistent with the sands being dune remnants from aeolian deposition from southwesterly winds.
3. Shallow landsliding is a highly active, historical but also ongoing geomorphic process in the Waitakere Ranges study area (Hayward, 1983; Chapters 3, 5 and 6). On the long term, continued hillslope denudation by landsliding can only be accomplished if the potential energy for transport of material is provided by base level lowering. This is in turn provoked by local tectonic uplift or global sea-level fluctuations, or a combination of both, forcing graded rivers to incise, undermine hillslopes and in this way triggering upslope (headward) soil erosion processes.

In the Kumeu River valley at least 13 sets of fluvial terraces (excluding the current floodplain) were recognised (Fig. 2.3). Fluvial sediments, though highly weathered and hard to distinguish from the in situ parent materials, were found up till level 11. The two upper terrace levels (R12 and R13) are only based on planar morphology in the field. By plotting

fluvial terrace levels along the baseline of the Kumeu River (Fig. 2.3), no obvious pattern of downstream convergence or divergence of terraces becomes apparent. Downstream convergence (i.e. decreasing altitude differences between terrace levels) would generally indicate tilting. Downstream divergence on the other hand is common in areas with little or no uplift. The apparent parallel arrangement of the terrace levels indicates formation controlled by tectonic uplift (Bull, 1991). Note that in Fig. 2.3, parallel arrangement is presumed to project the baseline on the different terrace levels by plotting the curve through the mean terrace altitudes. Because of less likely preservation of older terrace levels, an increase in vertical spacing between terrace levels with increasing age can also be observed.

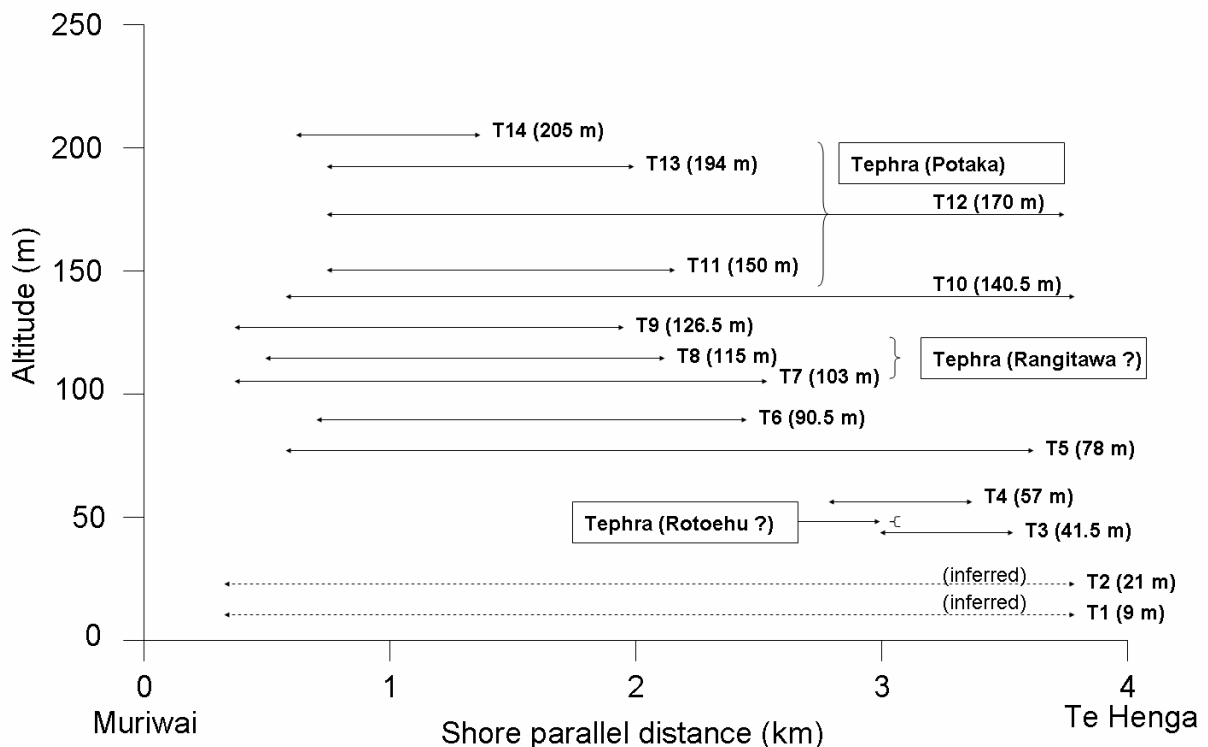


Fig. 2.2 Shore-parallel pattern of marine terrace levels between Te Henga and Muriwai with position of tephra deposits.

2.4.2 Tephrochronology

Three rhyolitic tephra deposits were exposed at different levels in the Te Henga-Muriwai marine section (Fig. 2.2) and were sampled for geochemical analysis to be correlated with known tephtras and serve as stratigraphic markers. Unfortunately, only one sample (3 m thick Te Henga 1 tephra, altitude 143-200 m) out of twelve contained sufficient glass shards for electron microprobe analysis. After comparison, this tephra is correlated with Potaka tephra, although values for Na_2O are significantly different (Table 2.3). The Early Pleistocene Potaka tephra (dated c. 1 Ma, Shane et al., 1996b) is one of the most far traveled ignimbrites known and it covers much of the North Island (Wilson et al., 1995). It has been deposited as a pyroclastic density current (primary emplacement), identified at a number of Auckland localities (Alloway and Newnham, 1995) and informally named Waiuku tephra (Alloway et al., 2004).

The two other tephra deposits could not be geochemically characterised and were inferred to correlate with two other widespread macroscopic tephra (distal ignimbrites) associated with large Quaternary eruptions from the TVZ. A 1-2 m thick tephra deposit (103-123 m altitude) is correlated with Rangitawa (formerly Mt Curl) tephra (c. 0.345 Ma, Froggatt et al., 1986; Shane, 2000). The youngest, c. 20 cm thick tephra deposit (44 m altitude) is correlated with Rotoehu tephra (c. 44 ka, Shane and Sandiford, 2003; c. 55 ka, Newnham et al., 2004). Both tephra have been previously identified in the Auckland-Northland area and in deep sea cores around New Zealand (e.g. Froggatt et al., 1996; Pillans et al., 1996; Shane, 2000; Newnham et al., 2004).

In the Kumeu River terrace sequence, one macroscopic tephra deposit was found in fluvial terrace level 2. This sample in turn did not contain enough glass shards for analysis but considering the probable range of terrace age it could be tentatively correlated with Kawakawa tephra (c. 24 ka, Pillans, 1994; 26.4 ka Shane and Hoverd, 2002). Kawakawa Tephra erupted from the Taupo Volcanic Centre during the Last Glacial Maximum (Pillans et al., 1993) and is widely preserved in New Zealand, also in the Auckland area (Carter et al., 1995; Shane, 2000; Shane and Hoverd, 2002). However, because the tephra is probably present in reworked form (as a channel fill), it can hardly be used to assign an age to the terrace level (only a minimum age) nor for straightforward correlation with the Last Glacial Maximum.

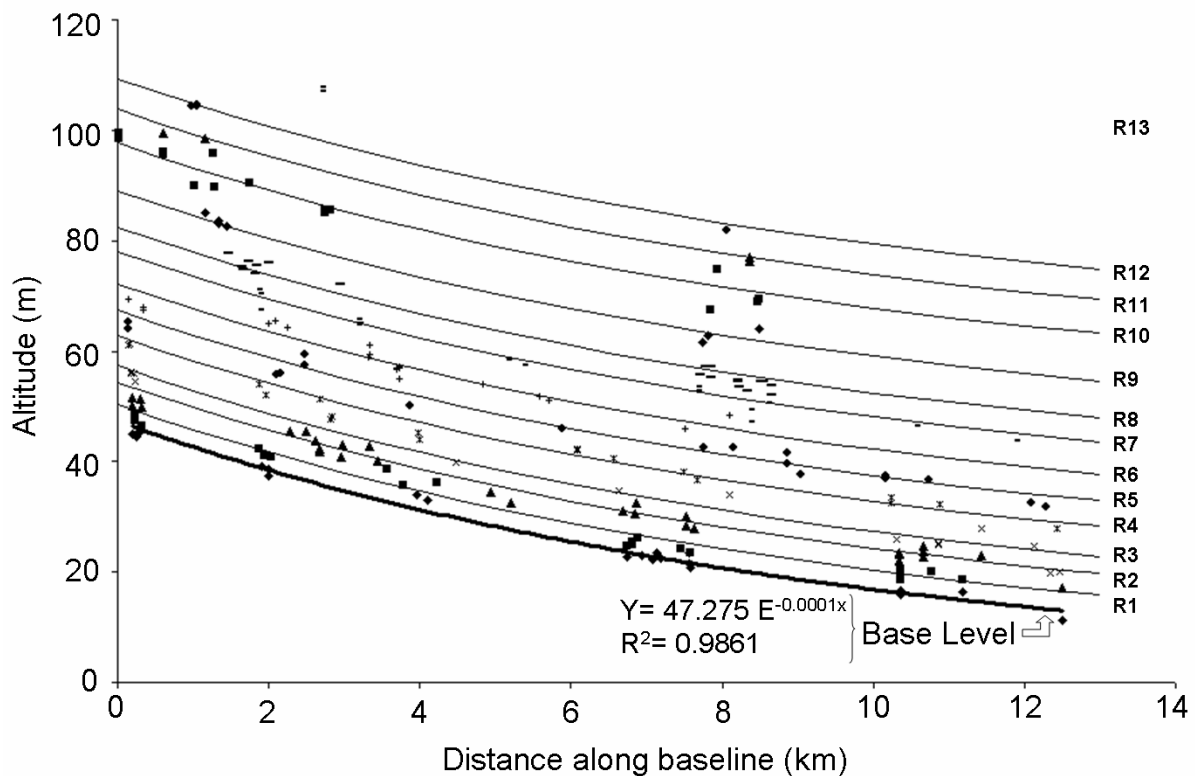


Fig. 2.3 Overview of fluvial terrace levels plotted along the longitudinal profile of the Kumeu River. Start of river baseline is at Hunter Road (New Zealand topographic map 260-Q11 & Pt. R11 484840).

| | Te Henga 1 | Waiuku 1 Alloway et al., 2004 Auckland | Waiuku 2 Auckland | Potaka 1 Shane et al., 1996a Cape Kidnappers | Potaka 2 Shane et al., 1996b |
|--------------------------------|--------------|--|----------------------|--|---------------------------------|
| SiO ₂ | 78.82 (0.54) | 78.12 (0.29) | 77.72 (0.13) | 77.34 (0.52) | 78.33 (0.25) |
| Al ₂ O ₃ | 12.83 (0.13) | 12.41 (0.13) | 12.36 (0.13) | 12.36 (0.27) | 12.38 (0.17) |
| TiO ₂ | 0.12 (0.07) | 0.14 (0.07) | 0.10 (0.03) | 0.12 (0.02) | 0.09 (0.03) |
| FeO* | 1.16 (0.09) | 1.14 (0.13) | 1.14 (0.11) | 1.17 (0.08) | 0.90 (0.13) |
| MgO | 0.10 (0.03) | 0.10 (0.03) | 0.07 (0.02) | 0.13 (0.01) | 0.10 (0.02) |
| CaO | 0.92 (0.10) | 0.88 (0.14) | 0.89 (0.10) | 1.00 (0.01) | 0.82 (0.12) |
| Na ₂ O | 2.21 (0.47) | 3.26 (0.20) | 3.82 (0.13) | 3.82 (0.12) | 3.73 (0.14) |
| K ₂ O | 3.58 (0.32) | 3.71 (0.36) | 3.68 (0.22) | 3.85 (0.16) | 3.65 (0.28) |
| Cl | 0.23 (0.04) | 0.19 (0.02) | 0.19 (0.02) | 0.22 (0.02) | - |
| H ₂ O [†] | 7.49 (1.41) | 5.02 (0.66) | 7.33 (0.60) | 7.02 (1.08) | 5.50 (0.80) |
| <i>n</i> | 16 | 15 | 17 | 12 | 18 |

Analyses are recalculated to 100% (normalised) on a volatile-free basis and expressed as a mean (\pm standard deviation) of *n* analyses in wt%.

*Total Fe expressed as FeO.

- No data

[†]Water by difference (100 minus original analytical total)

n = number of shards analysed. Analyses were undertaken at the Department of Geology, University of Toronto, on a CAMEBAX SX-50, that operates at a 15 kV beam current at 10 to 20 nA, beam focused and in scanning mode. Analyst: B. Alloway (IGNS).

Table 2.3 Electron microprobe analyses of glass shards from Te Henga 1 tephra and probable Waiuku/Potaka tephra correlatives.

2.4.3 Correlation with paleoclimatic records and calculation of uplift rates

Both marine and fluvial terraces were correlated to global paleoclimatic records (Fig. 2.4). Ages and correlation of the marine terrace levels is based on the occurrence of the three tephra layers as chronostratigraphic markers. All marine terrace levels are correlated to an uneven MIS, corresponding with interglacial periods with a sea-level highstand. Oxygen isotope fluctuation and the astronomically tuned timescale of ODP Site 677 were used (Shackleton et al., 1990). Recent ⁴⁰Ar/³⁹Ar dating and magnetostratigraphy of volcanic rock sequences is consistent with the astronomical chronology of this record (Spell and McDougall, 1992) and it is generally regarded as recommendable for global correlation of terraces (Pillans, 1994; Bridgland et al., 2004). Rangitawa tephra has been previously identified and linked to the upper part of MIS 10 (Pillans, 1994), also from deep sea cores close to New Zealand (DSDP 594, Froggatt et al., 1986 and SO-36-61, Hesse, 1993). The same holds for Potaka tephra, which has been previously assigned to MIS 27 (Alloway et al., 1993; Shane, 1994) and Rotoehu tephra, which is placed within MIS 3 (Pillans, 1994; Pillans et al., 1996; Shane and Sandiford, 2003). Uplift rates between terrace levels were calculated by dividing relative altitude difference of terraces by age difference from corresponding sea-level highstands from ODP 677. The uplift rates seem to correspond well with those previously calculated for Auckland and the west coast of Northland (e.g. Chappell, 1975; Richardson, 1985; Pillans, 1986; Gibb, 1986; Table 2.2).

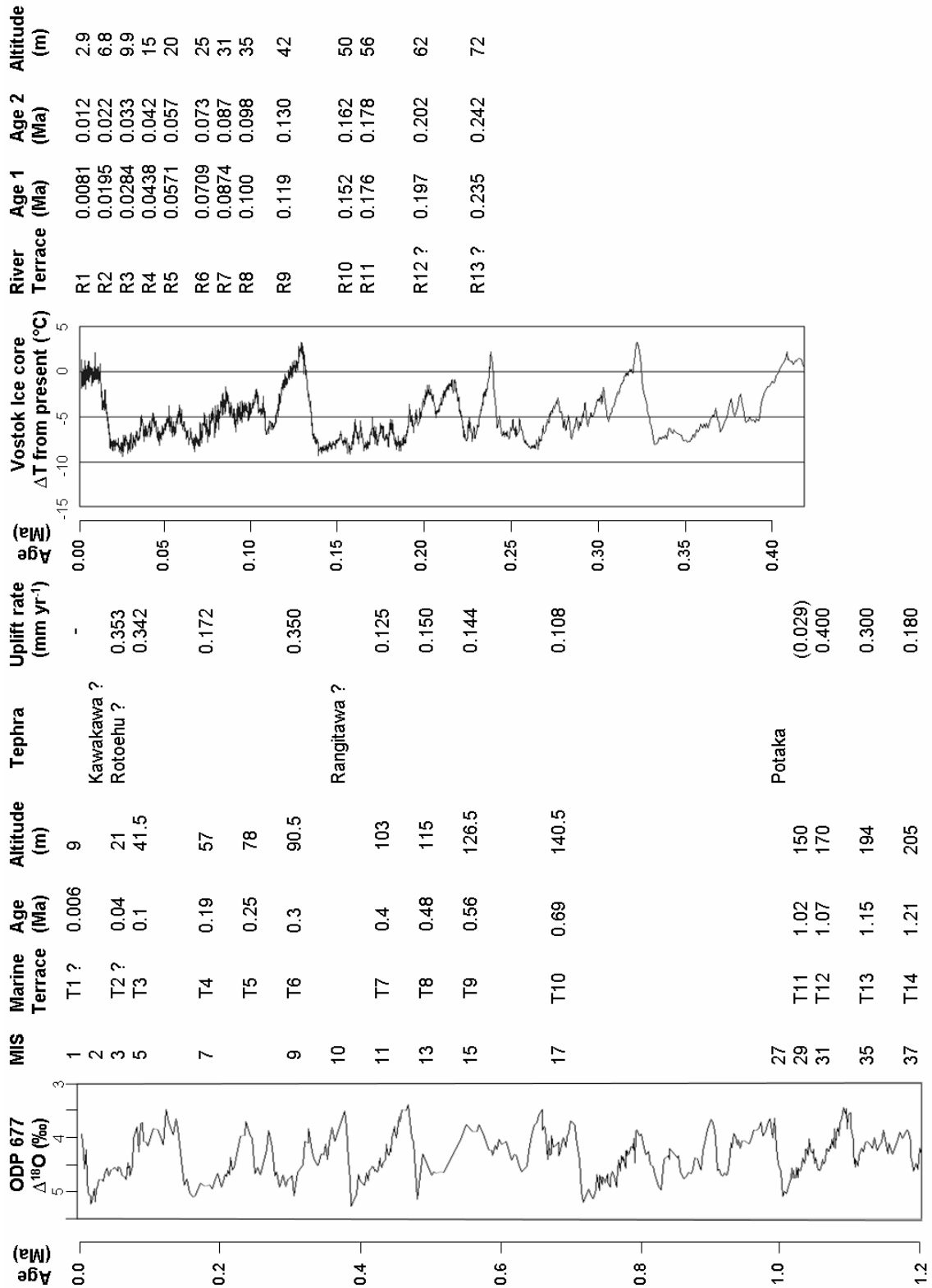


Fig. 2.4 Summary of chronology and correlation of marine- and river terrace levels with paleoclimatic records.

The two youngest marine terrace levels (T1 and T2) were not recognised in the field (possibly destroyed by sea cliff erosion), but inferred on the basis of probable presence of Rotoehu tephra (c. 55 ka) within the youngest terrace level found (T3, 41.5 m; Fig. 2.2). T1 has been aged 6 ka, based on a transgression maximum in New Zealand at that time (Gibb, 1986; Hesp et al., 1999); T2 is inferred to be 40 ka old, corresponding with MIS 3. T5 is interpreted as representing a high sea-level stand around 0.25 Ma, not assigned an MIS (ODP 677). The 300 ka gap between T10 and T11 can be attributed to possible destruction of terrace remnants (probably during MIS 17), because sea-levels during interglacials have been much higher for the last 0.7 Ma (Beu and Edwards, 1984). Consequently, correlation of terrace levels and surely the calculation of uplift rates becomes highly uncertain from MIS 17 and older. The South Taranaki-Wanganui terraces for example have also been interpreted and dated only up till MIS 17 (Pillans, 1994).

Because no hard chronostratigraphic marker was present within the fluvial terrace sequence, fluvial terraces were correlated with the marine sequence by using the mean uplift rates calculated from the marine terraces (0.35 mm yr^{-1} from 0-0.1 Ma and 0.26 mm yr^{-1} from 0.1-0.3 Ma). Ages of fluvial terraces were estimated by dividing terrace height by the calculated uplift rate. Assuming glacial aggradation, incision starts at the end of a cold period. Final fluvial terrace chronology was established by linking estimated terrace ages (from uplift rates, Age 1 in Fig. 2.4) with ages taken from the paleoclimatic records halfway up peaks from stadial to interstadial or glacial to interglacial conditions in the ODP 677 and Vostok records (Age 2 in Fig. 2.4). Kawakawa tephra, likely present in terrace R2 (although probably in reworked form), provides a tentative correlation datum just prior to the Last Glacial Maximum in the lower part of MIS 2 (Pillans, 1994; Shane, 1994).

2.5 Discussion

As mentioned before, there are some issues which complicate the interpretation of marine terraces in the Auckland-Northland region: As in many cases, the marine terrace surfaces are overlain by younger coverbeds and there is hardly any direct evidence for marine processes in the form of e.g. wave-cut surfaces. In the Te Henga-Muriwai section, Pliocene to Pleistocene sands unconformably overlie Miocene Volcanic rocks. Despite the subplanar and staircase-like morphology of the sand surfaces typical for coastal terraces, the material is relatively soft and it is very unlikely that actual wave-cutting would occur and abrasion plateaus would be created and preserved. Instead, the sheet-like sands are sometimes interpreted as deflated dune remnants (Isaac, 1996), also called 'Stokes surfaces' or 'barrier system deposits', of which sediments are supposed to have been transported landwards by waves (McMahon, 1994). Still, these levels could be interpreted as representing shallow marine and intertidal erosion levels (Isaac et al., 1994), forming similar sea-level high stand markers than wave-cut platforms. Furthermore, offshore there are indications of preserved wave-cut platforms (Isaac et al., 1994): (i) flat tops and surfaces cut on Early Miocene volcanoes west of Northland were preserved after rapid subsidence (Herzer, 1995) and (ii) drillholes indicate that erosional paleoterraces underlie Mio-Pleistocene (Awhitu Group) sequences at 70-100 m below sea-level in the Kaipara and Aupouri areas (Isaac et al., 1994).

Another issue is the lack of evidence for convergent tectonic activity (with associated volcanism and displacement of older sediments) after the end of the Early Miocene for the region in general: For Northland, Isaac et al. (1994) summarise several weathered and

dissected 'erosional surfaces' and terrace remnants of Miocene age up to 700 m above sea-level. They are inferred to have been formed by shallow marine and intertidal erosion and are locally overlain by terrestrial sediments of Early Pliocene to Pleistocene age. Late Pliocene to Pleistocene 'constructional and erosional terraces' are interfingering with marine, estuarine and fluvial deposits at up to 30 m above sea-level. Coastal terraces of inferred last interglacial age are present as erosional benches but mostly as constructional surfaces overlying shallow marine sequences and are in general 1-3 m above present high tide level, which correlates with last interglacial sea-levels (Chappell, 1983) and would indicate that the Northland peninsula has been tectonically stable during the last 120 ka (with the exception of Waitakaruru, 12 m uplift during last glacial and Holocene). Based on the position of a carbonaceous paleosol close to present day high-tide level, Alloway et al. (2004) suggest a negligible tectonic uplift experienced in the Auckland area since the deposition of an underlying 1 Ma old tephra deposit. However, a general regional uplift, superimposed on glacio-eustatic sea-level change, is often referred to as the only possible mechanism leading to the maintenance of a considerable relief and active denudation processes inland and the development of raised coastal terraces high in the landscape (e.g. Ballance, 1968; Ballance and Williams, 1992). Coastal terrace surfaces previously found in the Auckland and Northland region maintain broadly similar heights and geological evidence indicates they have formed during the Quaternary (Ballance and Williams, 1992). A generally accepted relatively uniform Quaternary uplift of Northland (Chappell, 1975; Barter, 1976), while very slow in human terms, may be responsible for the maintenance of rugged relief, despite an otherwise stable tectonic situation for 10-15 Ma and deep and rapid chemical weathering of rocks (Ballance and Williams, 1992).

Another point of discussion has been, and still remains, the rate of uplift. A maximum rate of 0.35 mm yr^{-1} , but commonly less, has been calculated for at least the latter part of the Quaternary period (Pillans, 1983 and 1990; Ballance and Williams, 1992). Long term uplift rates can be the result of highly episodic events (e.g. earthquakes) in which sudden displacements of metres are separated by decades or centuries of 'stability'. Geological evidence suggests tectonic activity in the study area is characterised by relative uplift and subsidence of segments along faults, sometimes referred to as block-tilting or -faulting, typically occurring in spasms (e.g. resulting in a widely accepted regional westward tilting; Hayward, 1983; Spörli, 1989; Isaac et al., 1994; Edbrooke, 2001). Therefore, the uplift rates computed from terrace age and altitude differences (Fig. 2.4), have to be regarded as average rates between two preserved terrace levels.

Although there is only a very limited age control over both coastal and fluvial terrace sections, the combined record provides a better insight in the uplift dynamics of the study area. The overall tendency is an overall increase in uplift rate during the last c. 1 Ma (Fig. 2.4), a trend which is globally observed (e.g. Bridgland, 2000; Maddy et al., 2000). Apparently, the plate marginal subduction processes in the North Island of New Zealand increased during this period. A contemporaneous increase in volcanic activity could suggest a causal link, although other theories (differences in shallow mantle temperatures, intra-plate stress, flow in the lower continental crust, erosional isostasy) are still under debate (Goes et al., 2000; Westaway, 2001). A link between Quaternary climate oscillations and crust movements is provided by the observation that when the climate oscillations increased in magnitude during the Middle Pleistocene, the uplift rates as reconstructed from terrace staircases have also increased significantly (van den Berg and van Hoof, 2001).

The fluvial terrace record from the Kumeu River valley appears to register high resolution changes in climate or uplift (given the absolute altitude, sea-level effects can be ruled out). The mechanism of fluvial terrace formation for the North Island of New Zealand is not as straightforward as for the South Island and other parts of the world. First of all, there were no major changes in the main vegetation type and forest has been the dominant land cover throughout the Quaternary in Northland and Auckland: Newnham (1999) e.g. found there was no substantial loss of forest anywhere in Northland at any time during the Last Glacial Maximum. Relative temperature depressions were probably similar to those experienced elsewhere in New Zealand, but in the warmer North, were not sufficient to eliminate forest. For Auckland, only a generally more open conifer-hardwood forest canopy and expansion of small trees and scrubs during glacial periods were demonstrated (Newnham and Lowe, 1991; Sandiford et al., 2002, 2003; Shane and Sandiford, 2003). The main exogenous reason for changes in sediment supply were volcanic eruptions, supplying huge amounts of ash and disrupting the vegetation in the process. The limited sedimentology of the preserved Kumeu River terraces is suggesting very thin layers of sediments, often clayey and containing reworked volcanic ash. Apparently, there were no periods with significant net aggradation in the system. In the meanwhile, a continued incision occurred during the Quaternary due to the high uplift rate, leaving a staircase of so called 'strath' terraces. In this context, the only landscape processes that can be proposed are changes in the frequency of droughts leading to more forest fires. Climatic control may thus be attributed to variations in humidity or aridity rather than to temperature changes (Newnham, 1999; Bridgland et al., 2004). The possible role of changing fire regimes is also suggested by the frequent occurrence of charcoal in the lower terraces. When trees die as a result of burning, this can trigger massive landsliding events in the headwaters (Chapter 6) supplying large amounts of mud into the system. These mudflow deposits do not make a clear recognisable fluvial sedimentary record, especially when they are weathered. This mechanism might explain why the Last Glacial Maximum was a period of widespread, climatologically controlled river aggradation in New Zealand (Pillans et al., 1993; Vucetich et al., 1996). The association of river aggradation with glacial and stadial periods and incision occurring during interglacials has been previously substantiated based on carbon dating and pollen assemblages (Milne, 1973; Vella et al., 1988; Marden and Neall, 1990; Bull, 1991; Pillans, 1994; Berryman et al., 2000; Eden et al., 2001).

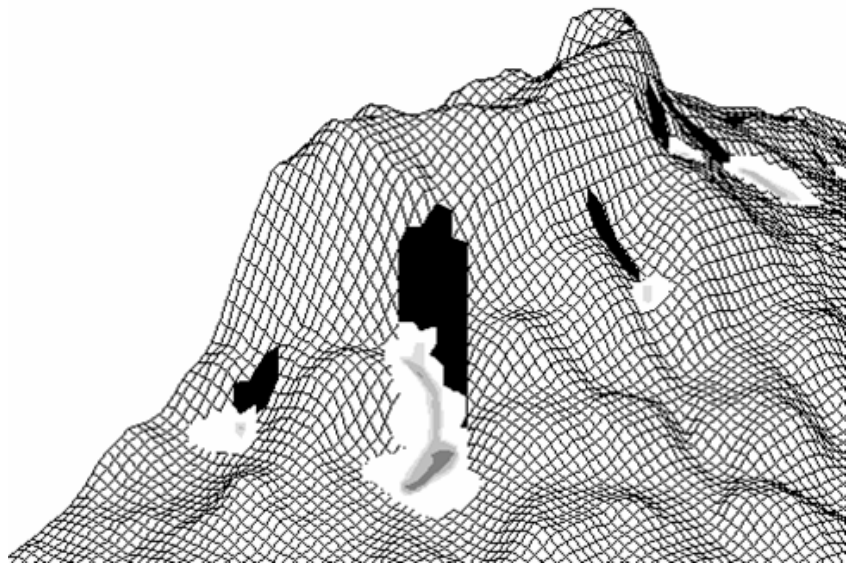
Another reason why the terrace stratigraphy is not that well developed is the relatively rapid uplift regime of the region. The reconstructed uplift rates are at least 3 times the order of magnitude higher than commonly associated with terraces in Europe for example (for NW Europe, uplift rates since the Middle Pleistocene are ranging between $0.04 - 0.1 \text{ mm yr}^{-1}$, Westaway, 2001; Westaway et al., 2001). Such fast uplift rates lead to strath terraces with only thin layers of fluvial sediments limiting their preservation considerably (Veldkamp, 1992).

Given the uncertainties in altitude measurements and age estimates only a semi-quantitative model of the regional uplift and fluvial response can be proposed. The general model is an actively incising river, carving out strath terraces. The incision phases are reactivated by sea-level lowering and interrupted by net aggradation events due to changing fire regimes during the somewhat drier glacials/stadials or volcanic ash falls, all leading to a temporary increased sediment supply. It is very difficult to link these provisional findings to other similar records. A record in a similar setting in the literature was not found. It is hypothesised that the climo-tectonic setting in the Auckland-Northland region will never lead to a classical terrace

sequence with a clear stratigraphy and profound climate control. It is the lack of an obvious and clear terrace record that has led to the systematic underrepresentation of such areas in global terrace literature. It is therefore proposed to make global wide systematic analysis of paleoclimate and uplift rates, in order to identify those areas where well developed terrace staircases can be expected and where they will be more conspicuous.

2.6 Conclusion

A combined coastal/fluvial terrace record demonstrated relatively fast uplift rates (up to 0.4 mm yr^{-1}) for a study area northwest of Auckland. Apparently a c. 1.2 Ma record of marine terrace levels is preserved along the coast. Although some researchers interpret the marine surfaces as aeolian in origin (Stokes surfaces), evidence is presented that these surfaces are essentially erosional coastal terraces with some coverbeds (including tephra). The preserved fluvial record in the Kumeu River valley suggests several terrace units for each glacial-interglacial cycle. The proposed endogenous controlling mechanism on the aggradation/incision dynamics are the climatic changes in humidity/aridity causing different fire regimes. In addition, tephra from the Taupo Volcanic Zone form an exogenous control on increased sediment loads. It is concluded that similar studies are underrepresented in the literature as no classical terraces sequences are formed under similar climo-tectonic settings.



Chapter 3

Landscape Process Modelling

In this chapter, a model to assess the location of shallow landslides and their impact on landscape development within a timeframe of years to decades is proposed. Processes that need to be incorporated in the model are reviewed followed by the proposed modelling framework. The capabilities of the model are explored through an application for a forested 17 km² study catchment in the Waitakere Ranges for which digital elevation data are available with a grid resolution of 25 × 25 m. The model predicts the spatial pattern of landslide susceptibility within the simulated catchment and subsequently applies a spatial algorithm for the redistribution of failed material by effectively changing the corresponding digital elevation data after each timestep on the basis of a scenario of triggering rainfall events, relative landslide hazard and trajectories with runout criteria for failed slope material. The resulting model will form a landslide module within the dynamic landscape evolution model LAPSUS. The model forms a spatially explicit method to address the effects of shallow landslide erosion and sedimentation because digital elevation data are adapted between timesteps and on- and off-site effects over the years can be simulated in this way. By visualisation of the modelling results in a GIS environment, the shifting pattern of upslope and downslope (in)stability, triggering of new landslides and the resulting slope retreat by soil material redistribution due to former mass movements can be simulated and assessed.

3.1 Introduction

Shallow landslides are one of the most common types of landslides, occurring frequently in steep, soil-mantled landscapes in different climatic zones (e.g. Kirkby, 1987; Benda and Cundy, 1990; Selby, 1993). In many cases, failure and transport of slope material by

Based on: Claessens, L., Schoorl, J.M. and Veldkamp A., 2005. Modelling the location of shallow landslides and their effects on landscape dynamics in large watersheds: an application for Northern New Zealand. *Geomorphology*. In press.

© 2005 Elsevier Science B.V.

landsliding is one of the principal processes of soil redistribution and hillslope development in landscapes.

Landslides have traditionally been regarded as key indicators of forest disturbance, particularly in association with logging activities (Douglas et al., 1999; Montgomery et al., 2000; Fannin and Wise 2001), land use and climatic change (Van Beek, 2002; Vanacker et al., 2003) or as response to human imposed changes such as road building (Brand and Hudson, 1982; Larsen and Torres-Sanchez, 1998). Over the past decades most model studies dealing with landslides have mainly focussed on landslide hazards and terrain stability mapping for regional and urban planning (Van Westen, 1993; Guzzetti et al., 1999) and the impact of landslides on basin sediment yield (Burton and Bathurst, 1998). In addition, a number of recent landslide studies have been concerned with identifying rainfall thresholds required to trigger landslide events (Crozier, 1999) or magnitude and frequency of landsliding in a specific catchment (Reid and Page, 2003). However, as a mass movement process, rainfall-triggered landslides have been underestimated as contributors to slope development and denudation in the past (Dykes, 2002). Geomorphological investigations in steeplands show evidence that shallow landslides play a key role in the maintenance of characteristic slope forms and probably also make significant contributions to ecological dynamics (Dykes and Thornes, 1996).

At present relatively few attempts have been made to model the effects of shallow landslides on landscape development. Modelling the relevant processes in a dynamic way requires a methodology aggregating several mechanisms acting at different spatial and temporal scale levels but remaining at least spatially explicit over a timeframe concerning redistribution of soil material. Kirkby (1987) summarises the difficulties in the context of models of longer term landscape development as follows: work on rapid mass movements has concentrated on stability analysis, so that forecasting of destinations for slide debris is very inexact, even for an individual slide. Modelling of slope profile evolution is severely restricted by a lack of studies on the factors controlling travel distances of mobilised material, which are crucial to the development of an overall mass budget in a forecasting context. The second major problem lies in aggregating from the individual slide to the assemblage of slides over a long period, generally without detailed meteorological records. The change of temporal scale requires models that are built from somewhat different premises than those of short-term stability analysis, although plainly they must be compatible.

The practical significance of shallow landsliding has motivated many approaches of mapping and predicting potential landslide initiation (see review in Montgomery and Dietrich, 1994). A recent approach, which is proven to be very practical, is the use of digital elevation models and simple coupled hydrological and slope stability models (Dietrich et al., 1992, 1993 and 1995; Dietrich and Montgomery, 1998; Montgomery and Dietrich, 1994; Montgomery et al., 2000; Wu and Sidle, 1995; Pack et al., 2001; Duan and Grant, 2000; Borga et al., 1998 and 2002; Fernandes et al., 2004). Availability of GIS technology permits then to resolve and display spatial patterns of landslide susceptibility at the same scale and resolution as the digital terrain model.

In general landslides triggered on forested slopes release such energy and mass that a debris flow nearly always develops. This flow erodes the unstable material in its path and continues to move downslope until the gradient falls below that needed to maintain flow (Burton and Bathurst, 1998). To study the role of rainfall-induced landslides within the hierarchy of hillslope erosion processes on the longer term, it is therefore important not only to know the

spatial distribution of possible landslide initiation sites but also to characterise erosion and deposition patterns caused by slope failure. Removal of failed landslide material can potentially increase the local slope by taking away initial support and may trigger subsequent upslope failure. Additional downslope erosion and failure may occur along the debris flow erosional pathway and by loading and steepening downslope material by debris flow deposition. Once a debris flow emerges, the problem of determining its path becomes complicated by the ability of the flow to erode, to spread, to plug, and to alter its direction. The rate of volume transport of a debris flow and its change with time, viscosity and hillslope morphology are some factors important for debris flow erosion and deposition.

Using data from individual events, two-dimensional mathematical models for flows on fans have been calibrated to determine flow depths, velocities, impact forces and areas of deposition (Mizuyama et al., 1987; Mizuyama and Ishikawa, 1990; O'Brien and Fullerton, 1990; Takahashi, 1991). These methods require a large amount of data along with numerous assumptions about the characteristics of the debris flow. Formulations from laws of mass and momentum conservation are complex and more appropriate for examination of the detailed behaviour of an individual debris flow for which the flow material composition and hillslope characteristics are well specified (Bathurst et al., 1997). For the current goal, a simpler, rule-based and spatially explicit approach is used that can easily be applied to multiple landslides occurring throughout a catchment over periods of time ranging from single rainstorms to several years and for which the data specification is more general.

3.2 Materials and methods

3.2.1 Study area

The Waitakere Ranges Regional Parkland lies immediately west of Auckland city, New Zealand (174.8°E, 36.9°S, Fig. 3.1). It is mostly covered in thick virgin and regenerating native forest and popular for wilderness activities and tramping. Most of the land is publicly owned, forming part of Auckland Centennial Memorial Park and water catchment land with restricted entry. Altitude ranges from sea-level to 474m.

The area has a warm and humid subtropical climate with a mean annual rainfall ranging from about 1400 mm near the Tasman coast up to 2030 mm at the higher altitudes (ARC, 2002). Daily rainfall data from 1988-2003 are available from two climate stations in Swanson and at the Arataki visitor's centre. A Magnitude-Frequency Index (MFI) for daily rainfall totals of the study area is calculated according to Ahnert's (1987) method (Fig. 3.2). This results in a MFI of 60.0;10.7, meaning a daily rainfall of 60 mm is reached or exceeded once a year and a daily rainfall of 70.7 mm or more occurs once every ten years.

The rugged topography of the area is caused by the resistant nature of the component rocks. The ranges are formed predominantly of Miocene volcanic breccia and conglomerate (Piha Formation), andesitic to basaltic lava flows (Lone Kauri Formation) and well-bedded volcanic sandstone and siltstone (Nihotupu Formation; Hayward, 1976). The topography is entirely erosional; none of the original volcanic landforms are preserved. In general the landscape is mantled by very deep soils but locally bedrock crops out on steep side slopes, in cliffs, volcanic dikes and intrusions. Soils are classified as haplic Acrisols according to the WRB classification (Deckers et al., 2002). The clay composition of the soils is dominated by kaolinite but varying fractions of smectite, halloysite and vermiculite clays are present.

The Waitakere Ranges have a history of human modification and use extending back less than one thousand years. Especially in the previous century timber milling has modified the area drastically. Farming also resulted in extensive areas being cleared of their original vegetation. With the development of a water supply system for Auckland with reservoir lakes and dams and to ensure the purity of this water supply 2,610 ha of forest was retired from development and allowed to recover naturally (Murdoch, 1991). By now 8,882 ha have some form of protection and are mostly covered in thick virgin and regenerating native forest (Denyer et al., 1993).

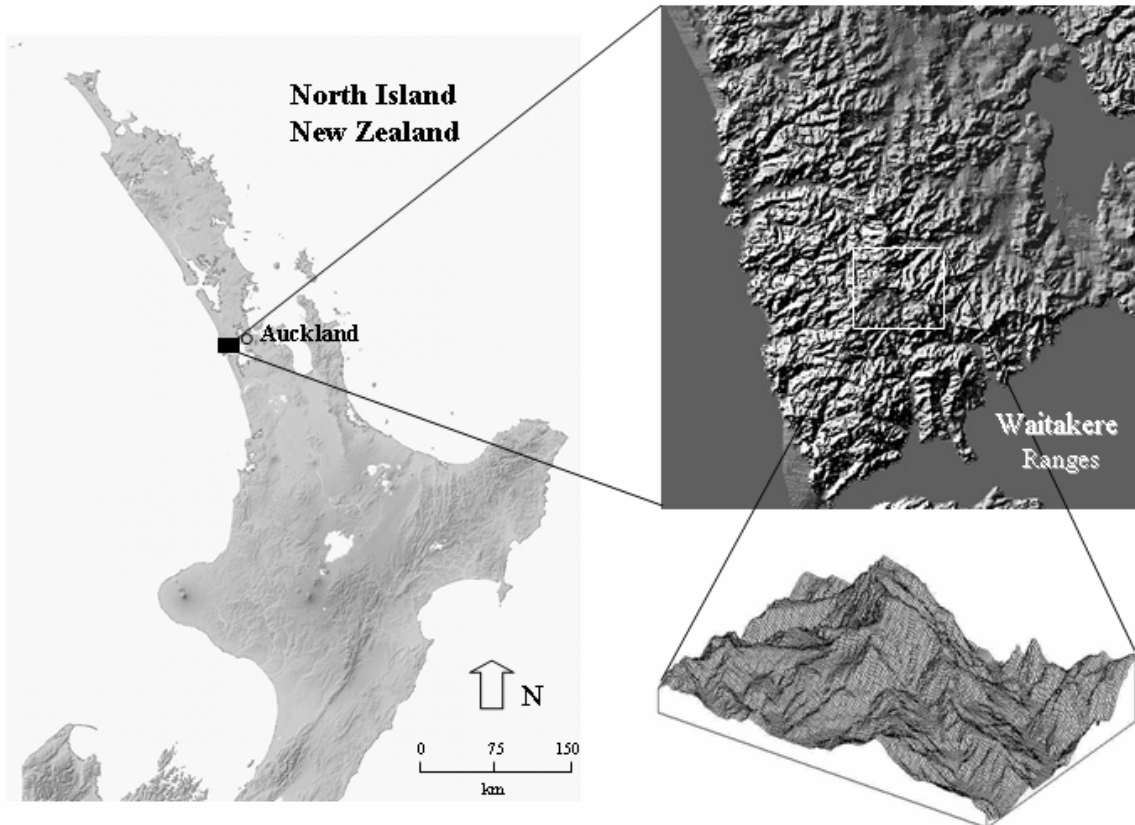


Fig. 3.1 Study area location within New Zealand and 3D representation of the DEM of the Waitakere Ranges study catchment.

Shallow landsliding is an important sediment transport process in the ranges, especially on steep side slopes and in topographic hollows. Slope failure is most common in soils developed in the weak sandstone and siltstone of the Nihotupu Formation but also frequently occurs in the weathered volcanic breccias and lava flows of the Piha and Lone Kauri Formation. Slope failures involving 1 to 40 m³ of soil material are common within moderately to highly weathered rock (particularly the finer grained materials), on slopes steeper than 18° in cleared areas and on slightly steeper slopes in bush covered areas (Hayward, 1983).

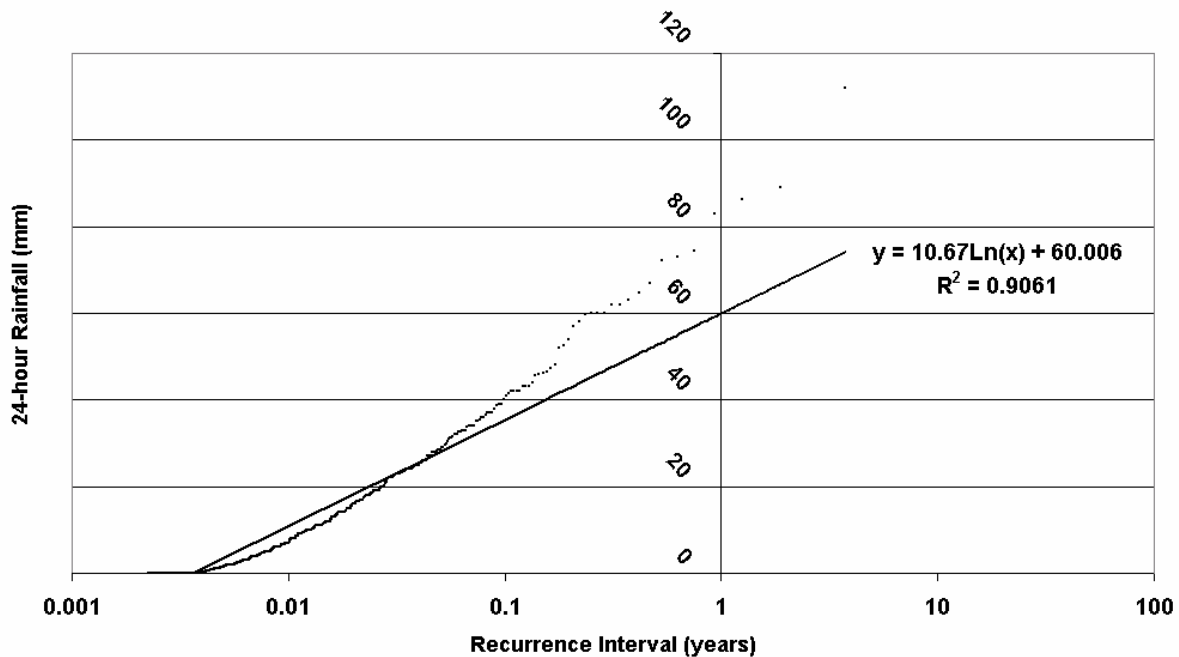


Fig. 3.2 Magnitude-Frequency plot for daily rainfall totals measured at the Arataki visitor centre 1997-2002.

3.2.2 Modelling framework

The modelling environment for embedding the shallow landslide component is comprised by the landscape evolution model LAPSUS (Landscape ProcesS modelling at mUlti dimensions and scaleS; Schoorl et al., 2000). This approach is a finite element model based on early works of Kirkby (1971) and Foster and Meyer (1972 and 1975). It addresses on-site and off-site effects of current and possible water and soil redistribution by water run-off and tillage erosion. Landscape evolution within a timeframe of decades is simulated in a dynamic way by adapting digital elevation data between yearly timesteps according to calculated soil redistribution. The model was developed for a well documented cultivated area in the Mediterranean climate zone of Southern Spain. Calibration of the model was done with the ^{137}Cs technique and different landuse scenarios were applied to yield changes in erosion and sedimentation patterns (e.g. Schoorl and Veldkamp, 2001; Schoorl et al., 2002). For application in the New Zealand catchment, where shallow landsliding is the most dominant soil redistribution process, a new landslide component is added to the existing model structure. A complete integration of all the model components for broader application, dealing with the erosion and sedimentation processes caused by water run-off, tillage erosion and shallow landsliding is foreseen.

3.2.3 Landslide hazard modelling

Montgomery and Dietrich (1994), based on earlier formulations proposed by O'Loughlin (1986), combine a contour based steady state hydrologic model with a deterministic infinite slope stability model to delineate areas prone to landsliding due to surface topographic effects on hydrologic response. The approach in this chapter is based on this method but has two differences (as in Pack et al., 2001):

1. The cohesion term is retained in the infinite slope stability model to account for differences in soil cohesion between geological formations and additional strength by root reinforcement for different vegetation types.
2. Grid-based rather than contour-based DEM methodology.

The infinite slope stability model factor of safety is defined as the ratio of the available shear strength (stabilising forces) to the shear stress (destabilising forces) (e.g. Graham, 1984). With soil depth interpreted as specified perpendicular to the slope surface, rather than measured vertically, the factor of safety (FS) can be written as (Pack et al., 2001):

$$FS = \frac{\left(C + \cos \theta \left[1 - W \left(\frac{\rho_w}{\rho_s} \right) \right] \tan \phi \right)}{\sin \theta} \quad (3.1)$$

where C is combined cohesion [-], W is a relative wetness index [-], θ is local slope angle [°], ρ_s wet soil bulk density [g cm^{-3}], ρ_w the density of water [g cm^{-3}] and ϕ effective angle of internal friction of the soil [°]. The combined cohesion term C is made dimensionless relative to the perpendicular soil thickness and is defined as follows :

$$C = \frac{C_r + C_s}{h\rho_s g} \quad (3.2)$$

with C_r root cohesion [N m^{-2}], C_s soil cohesion [N m^{-2}], h perpendicular soil thickness [m] and g the gravitational acceleration constant (9.81 m s^{-2}). C is thus the ratio of total cohesive strength relative to the soil depth or can be interpreted as the relative contribution to slope stability of the cohesive forces. W is the relative wetness, which is the ratio of local flux at a given steady state rainfall to that at soil profile saturation. For the calculation of W in this application, a steady state hydrologic response model based on the work by O'Loughlin (1986) and Moore et al. (1988) is used in which W can be defined as:

$$W = \frac{Ra}{bT \sin \theta} \quad (3.3)$$

with R steady state rainfall recharge [m day^{-1}], a the upslope contributing drainage area [m^2], b the unit contour length, T soil transmissivity when saturated [$\text{m}^2 \text{ day}^{-1}$] and θ the local slope angle [°]. For b , grid size [m] is taken as the effective contour length, independent upon flow direction as in Pack et al. (2001). Wetness can not exceed 1 because any excess is assumed to form overland flow. Hence the range of values for W is between 0 and 1. By substituting Eq. (3.3) in (3.1), equating the factor of safety to 1, which is the threshold for instability, and solving for R the minimum steady state rainfall predicted to cause slope failure can be determined. Q_{cr} [m day^{-1}] is called the critical rainfall, which can be written as:

$$Q_{cr} = T \sin \theta \left(\frac{b}{a} \right) \left(\frac{\rho_s}{\rho_w} \right) \left[1 - \frac{(\sin \theta - C)}{(\cos \theta \tan \phi)} \right] \quad (3.4)$$

With the boundary conditions for W (between 0 and 1), the conditions for upper and lower thresholds for elements that can possibly fail according to Eq. (3.4) can be expressed. Unconditionally stable areas are predicted to be stable, even when saturated and satisfy:

$$\tan \theta \leq \left(\frac{C}{\cos \theta} \right) + \left(1 - \frac{\rho_w}{\rho_s} \right) \tan \phi \quad (3.5)$$

Unconditionally unstable elements, which are bedrock outcrops in most cases, are unstable even when dry and have:

$$\tan \theta > \tan \phi + \left(\frac{C}{\cos \theta} \right) \quad (3.6)$$

In the model, local slope and wetness are calculated at each grid point and the other parameters are lumped within an area of same parent material and vegetation type. In this way the spatial distribution of critical rainfall values can be calculated as an expression of the potential for shallow landslide initiation. The upslope contributing drainage area used in the calculation of W is interpreted using the concept of multiple downslope flow (Quinn et al., 1991) to represent the convergence or divergence of flow under topographic control.

3.2.4 Trajectories of failed slope material

Most of the empirical approaches found in literature try to quantify the impact of shallow landslides on sediment yield at the catchment scale. Bathurst and others (1997) tested, both with hypothetical hillslopes and field data, four empirical models for determining percentage delivery of sediment to streams for shallow landslides that evolve into debris flows. The best compromise between simplicity and reliability proved to be a model based on a study by Vandre (1985), which is also used by Burton and Bathurst (1998). In the model, debris flow runout distance R [m] is expressed as:

$$R = \phi \Delta y \quad (3.7)$$

where Δy [m] is the elevation difference between the head of the slide and the point at which deposition begins (this point is reached once the gradient falls below a certain slope angle) and ϕ [-] is an empirically derived fraction set at 0.4 (Vandre, 1985; Burton and Bathurst, 1998). For this approach the use of the elevation loss within the erosional phase as a measure of debris flow momentum at the start of deposition is adapted from this method. However the runout distance itself, originally aimed at quantifying percentage sediment delivery to streams, is treated differently. The trajectory of the depositional phase is not routed following steepest descent nor is the debris flow material spread uniformly over the full runout distance. Instead, the importance of hillslope morphology for the spatial deposition pattern is

incorporated by using a combination of multiple flow routing principles and R as a measure for the reach of downslope gridcells receiving material in the depositional phase.

The way soil material is redistributed in the model is as follows: in the erosional phase, the debris flow accumulates unstable soil material following the steepest descent gradient. Johnson and Rodine (1984) express the critical thickness of debris flow material z [m] beginning to flow or stop flowage on an infinite slope depending on local slope and soil geotechnical properties according to:

$$z = \frac{C_s}{\rho_s \cos \theta (\tan \theta - \tan \phi')} \quad (3.8)$$

in which ϕ' is the apparent or bulk angle of internal friction, including the effect of pore water pressure as debris flow initiation mechanism. In this way, flow is impossible if the bulk friction angle is equal to or greater than the slope angle, that is if $\phi' \geq \theta$. Often approximations of a minimum slope gradient for maintaining flow are used (e.g. Ikeya, 1981; Johnson and Rodine, 1984; Benda and Cundy, 1990; Wu and Sidle, 1995; Burton and Bathurst, 1998). It is proposed to put such a slope limit on debris flow movement by inverting Eq. (3.8), substitute ϕ' by a slope angle limit for debris flow movement and estimate the amount of eroded material S [m] depending on soil geotechnical properties and local gradient as:

$$S = \frac{\rho_s \cos \theta (\tan \theta - \tan \alpha) a}{C_s} \quad (3.9)$$

with α [°] minimum local slope for debris flow movement and a [m²] a correction factor for dimensions. In this way, the amount of eroded material is regarded as inversed proportional to the minimal depth for debris flow mobilisation (substituting the bulk internal friction angle ϕ' by a slope limit α). On steeper slopes and for less cohesive soils, more material is eroded.

The point at which deposition begins or where the added erosion material reduces to zero is then reached once the gradient falls below a certain slope angle α (e.g. 10°, depending on the typical landslide dimensions of the area). At this point the number of downslope gridcells involved in the deposition of debris flow material is defined as 'cell-distance' D [-] and this is calculated as:

$$D = \left(\frac{R}{b} \right) \quad (3.10)$$

with R the debris flow runout distance as defined in Eq. (3.7) and b the gridcell resolution [m]. The accumulated soil material is then further routed with a 'double' multiple flow methodology as illustrated in Fig. 3.3. For downslope neighbours of the point where deposition starts the sediment, which is effectively delivered to gridcell n , can be expressed as:

$$S_n = \left(\frac{B_{n-1}}{D_{n-1}} \right) f_n \quad (3.11)$$

The term B_{n-1}/D_{n-1} is the amount of sediment coming from upslope divided by the cell-distance and being deposited in gridcells n . The remaining sediment budget of gridcell n , which is not delivered but passed through to gridcells $n+1$ can be expressed as:

$$B_n = B_{n-1} \left(1 - \frac{1}{D_{n-1}} \right) f_n \quad (3.12)$$

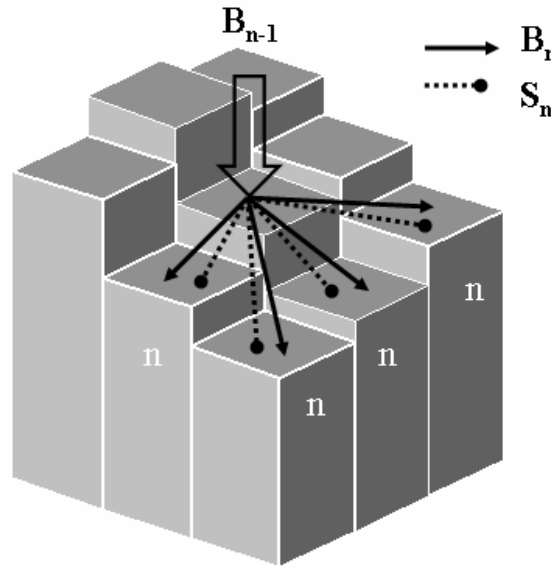


Fig. 3.3 Schematic representation of the ‘double’ multiple-flow methodology. Further explanation is in the text.

In Eqs. (3.11) and (3.12), f_n is the fraction of sediment (S) or sediment budget (B) allocated to each lower neighbour and determined by the multiple flow concept by Quinn et al. (1991). Sediment and sediment budget are divided to all down slope neighbours, using a slope dependent weighting factor for each fraction :

$$f_n = \frac{(\Lambda)_n^p}{\sum_{m=1}^{\max 8} (\Lambda)_m^p} \quad (3.13)$$

where fraction f_n of the total amount out of a cell in direction n , is equal to the slope gradient (tangent) Λ in direction n powered by factor p , divided by the summation of Λ for all (never more than eight) down slope neighbours m powered by factor p . In each downslope grid step, the cell-distance is then lowered by one:

$$D_n = D_{n-1} - 1 \quad (3.14)$$

When $D < 1$ all the remaining sediment is deposited and the debris flow halts.

3.2.5 Input data

Field data of the study area were obtained during systematic field surveys carried out from March to May 2002. To test the predictive power of the landslide hazard model an inventory of shallow landslide features was made. Shallow landslides involving just the soil-mantle are very common and form the main erosional feature in the area. However, due to the dense vegetation in the steep canyon areas, it is difficult to map all the scars, even in the field. Some of the scars are probably several decades old based on the vegetation cover and sharpness of the edges. Using a time series of aerial photography and field inspection with a GPS device, 76 landslide scars were mapped in the study area. The scars are most commonly encountered on the steeper footslopes and at the downstream end of small steep, unchanneled valleys.

Soil properties are strongly related to the parent material. Therefore soil physical parameters used in the model are assumed to be uniform within geological units. Digitising of areas with the same parent material was done according to the 1:50 000 geological map of New Zealand, sheet Q11 (Hayward, 1983). Transmissivity values are estimated on the basis of field measurements of saturated hydraulic conductivity using the inversed augerhole method (Kessler and Oosterbaan, 1974). Saturated bulk densities of the three soil types were determined in the laboratory (Table 3.1). Saturated shear strength of the soil material has been determined by consolidated-drained direct shear tests on undisturbed samples taken from soils developed in the three main parent materials of the area. The undisturbed blocks of clay taken in the field were trimmed to fit inside a shearbox with dimensions $10 \times 10 \times 2.5$ cm. The samples were subjected to normal loads of 28-95 kPa. Results are shown in Fig. 3.4 and Table 3.1.

| Formation | C_s [kPa] \pm S.E. | ϕ [rad] \pm S.E. | ρ_s [g cm ⁻³] | T [m ² day ⁻¹] |
|------------|------------------------|-------------------------|--------------------------------|---|
| Piha | 5.976 \pm 1.946 | 0.678 \pm 0.029 | 1.447 | 18 |
| Lone Kauri | 12.223 \pm 2.157 | 0.688 \pm 0.032 | 1.455 | 15 |
| Nihotupu | 13.352 \pm 2.140 | 0.548 \pm 0.032 | 1.436 | 11 |

Table 3.1 Soil physical model input parameters for the three parent materials.

| Formation | C [-] <i>Kauri</i> | C [-] <i>Podocarp/Broadleaf</i> | C [-] <i>Broadleaf</i> | C [-] <i>Succesional</i> |
|------------|-------------------------|--------------------------------------|-----------------------------|-------------------------------|
| Piha | 0.42 | 0.37 | 0.30 | 0.26 |
| Lone Kauri | 0.64 | 0.59 | 0.52 | 0.48 |
| Nihotupu | 0.69 | 0.63 | 0.56 | 0.53 |

Table 3.2 Combined cohesion values for combinations of the three parent materials and the four vegetation classes.

Root strength of both tree and understory vegetation provides significant apparent cohesion to the soil. To address the relative importance of different vegetation types in increasing the

resistance against shallow landsliding by root reinforcement, a vegetation classification was needed. A survey for the Protected Natural Areas Programme (Denyer et al., 1993) yielded a detailed vegetation map of the Waitakere ecological district. This map was used as a basis to delineate and assign root cohesion values to four main vegetation classes occurring in the catchment. Back analysis of slope failures mapped in the field and by aerial photography interpretation made it possible to calibrate the model for this application by adapting the root cohesion in the combined cohesion term for each vegetation class. The apparent cohesion values attributed to the different vegetation classes are well within range of results obtained by other researchers (e.g. Selby, 1993; Montgomery et al., 2000; Dykes, 2002). An overview of all combined cohesion values per vegetation class and parent material is given in Table 3.2. Digital elevation data for the Waitakere Ranges were available with a 25×25 m grid resolution (see Fig. 3.1). To obtain a hydrologically sound DEM, both sinks and pits, whose height is lower than that of all their connected neighbours, were removed by increasing the elevation of to that of the lowest point in the pit perimeter. The local slope was derived from the DEM and the upslope contributing drainage area was computed using the algorithm of multiple downslope flow (Quinn et al., 1991).

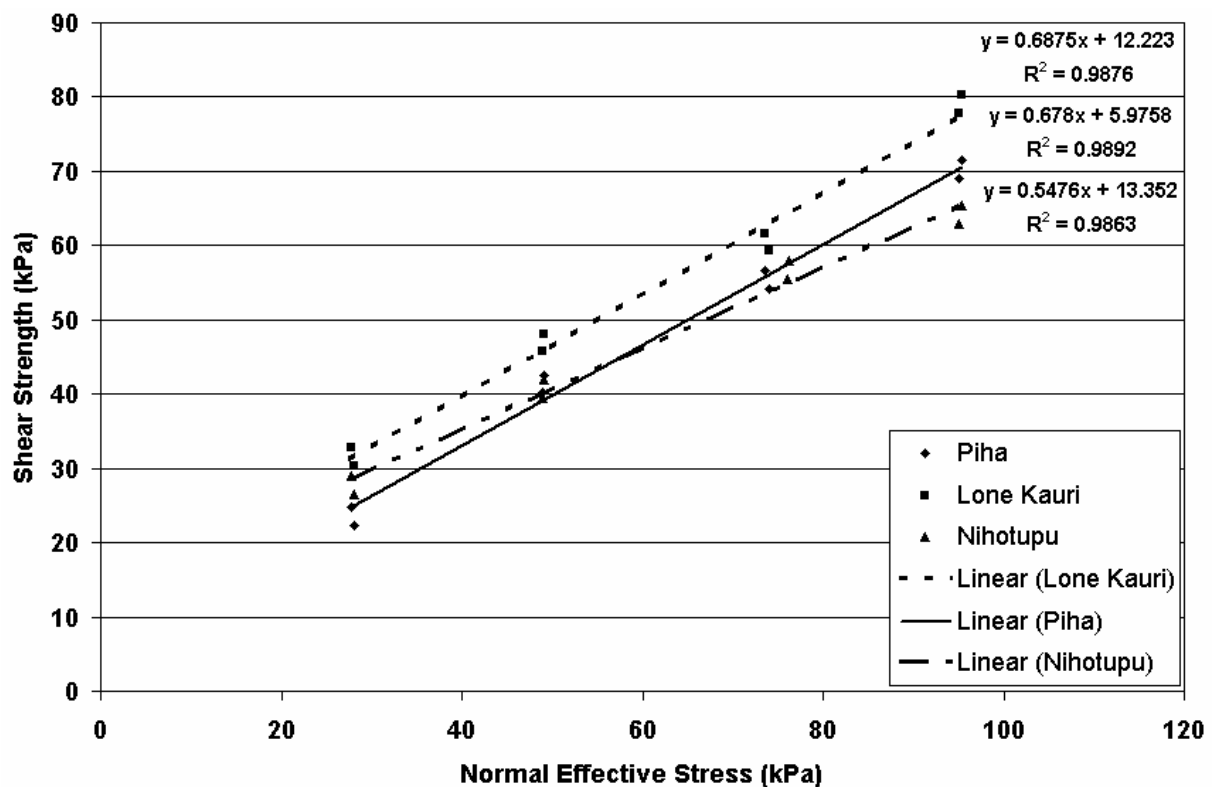


Fig. 3.4 Shear strength envelopes for soils developed in the three main parent materials.

3.3 Results and discussion

3.3.1 Application for Waitakere Ranges catchment

To explore the performance and sensitivity of the described method the model is applied to a forested 17 km^2 catchment within the Waitakere Ranges, which is well documented and

comprises all the variability in parent material and vegetation types. The model was calibrated and parameterised based on field observations and measurements of the input parameters according to Table 3.1 and Table 3.2 and test the component in explaining shallow landsliding phenomena over a longer time period. A realistic scenario for the occurrence of landslide triggering rainstorms with a certain intensity is applied to each timestep of one decade based on long term rainfall records in combination with back analysis of detected landslides on time series of aerial photographs. The model calculates for each timestep the relative potential for sliding and, according to the scenario, redistributes landslide material of failed sites following the transport trajectories described above. After each timestep the digital elevation data are effectively adapted according to these debris flow erosion and deposition patterns.

Because the shallow landsliding in the study area is not weathering- but transport limited soil production rates do not have to be taken into account. Although it has been shown and recognised that both geotechnical and hydrological behaviour are altered as regolith is stripped from hillsides and redeposited on footslopes (Brooks et al., 2002) it is assumed here that sites which failed in one timestep regain their full relative potential for sliding, i.e. their original soil physical parameter setting, in the subsequent timestep. An overview map with visualisations of the regions of debris flow erosion and deposition is shown in Fig. 3.5 and a more detailed area is represented in Fig. 3.6. When the model is ran for several consecutive timesteps it is possible to compare the different landslide hazard maps between the timesteps and get insight in the pattern of upslope and downslope triggering of new landslides and the resulting slope retreat. Fig. 3.7 shows a detail of a comparative operation between the landslide hazard maps after timestep one and five. Higher hazards are found upslope the failed slide due to undercutting and steepening of the slope above the eroded part. Also downslope the failure, parts with a higher landslide potential are encountered caused by steepening of local slopes mainly on the sides of the landslide sediment lobe. Because water from upslope is more canalised towards the steepened eroded part of the landslide, parts bordering the channel have less contributing area and are relieved of some failure potential. In this way the model simulates the mosaic like shifting pattern of upslope and downslope triggering of new landslides over years by soil material redistribution due to former mass movements.

3.3.2 Model validity

Several assumptions have been made to derive the relationships in this approach. The use of C as a dimensionless parameter in the factor of safety calculation is convenient but implies assuming that the soil thickness is constant. Another assumption in the wetness calculation is that saturated hydraulic conductivity, and therefore also transmissivity, are treated as if they do not vary with depth. If a spatially distributed varying soil depth is taken into account, soil production functions should be used and hydraulic conductivity can be treated as vertically varying with depth (Dietrich et al., 1995). The steady state hydrologic model requires the assumption that the predicted spatial pattern of critical steady state rainfall represents that which occurs during an unsteady, landslide producing rainfall event. Furthermore the relative potential for shallow landslides is supposed to be determined by convergence of shallow subsurface flow, following the surface topography and proportional to the upslope contributing area. Small velocity of subsurface flow might prevent a reliable application of the steady state assumption and it is likely that most points receive contributions from only a small proportion of their total upslope contributing area. In general, the notion of critical

rainfall should only be considered as a relative measure of failure potential (Borga et al., 1998, 2002).

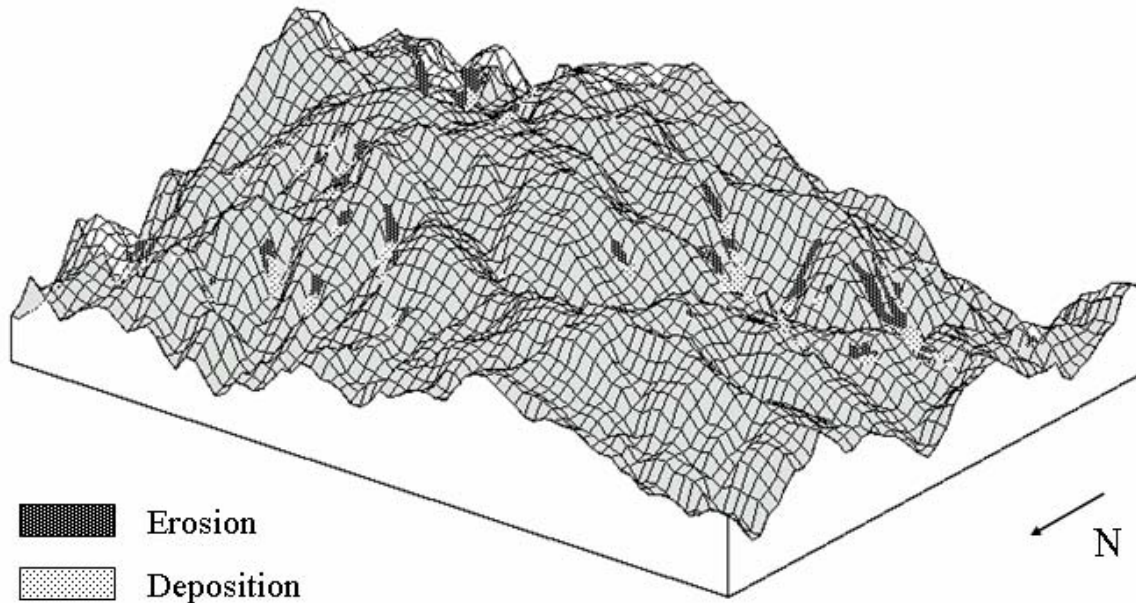


Fig. 3.5 Landslide erosion- and deposition patterns for failures with a critical steady state rainfall of 0.025 m day^{-1} or less. Note that the DEM is displayed in another resolution than that of the model output.

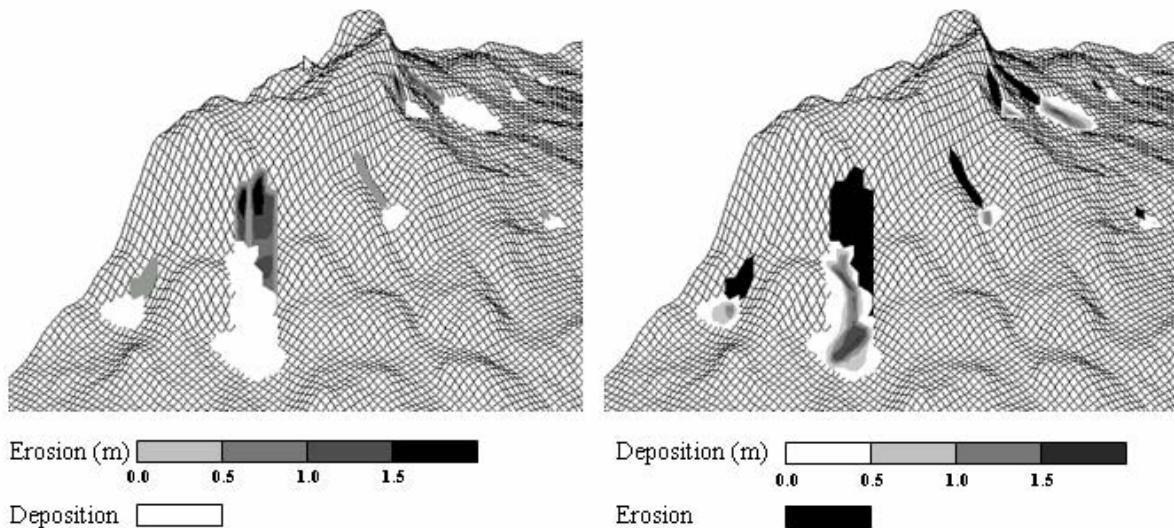


Fig. 3.6 Detail of landslide erosion- and deposition patterns.

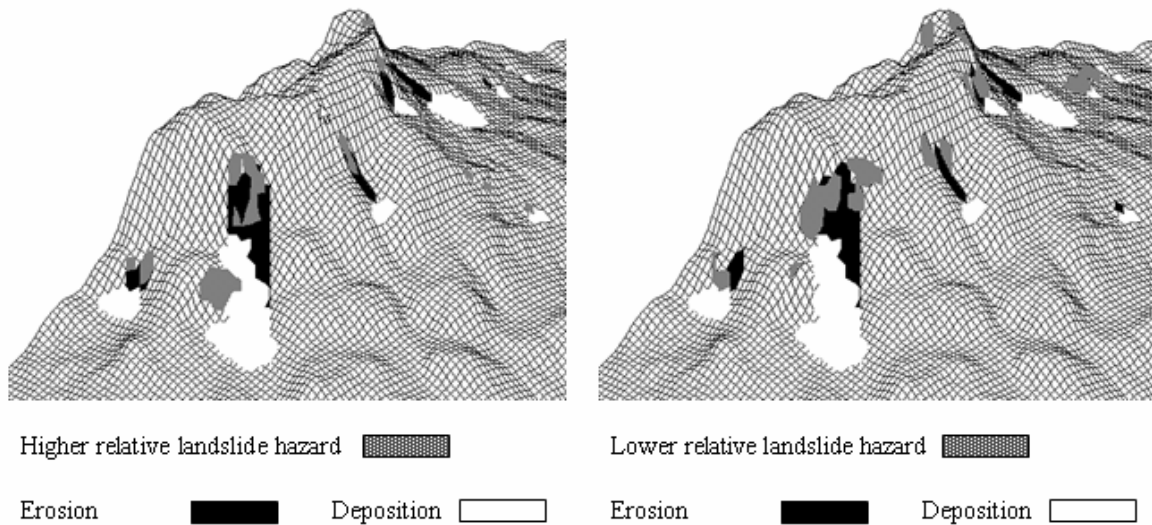


Fig. 3.7 Comparison of hazard maps between timesteps and visualisation of resulting (in)stability patterns.

It should be noted that valid results can only be obtained when the topography of the study area and dimensions of the landslides are well represented by the grid resolution of the digital elevation model used. An elaborate discussion about scale issues and aggregation and disaggregation of spatial data used in landscape process modelling and LAPSUS more specifically can be found in Schoorl et al., 2000. A detailed study on how grid resolution influences the outcome of the proposed landslide model is described in Chapter 4.

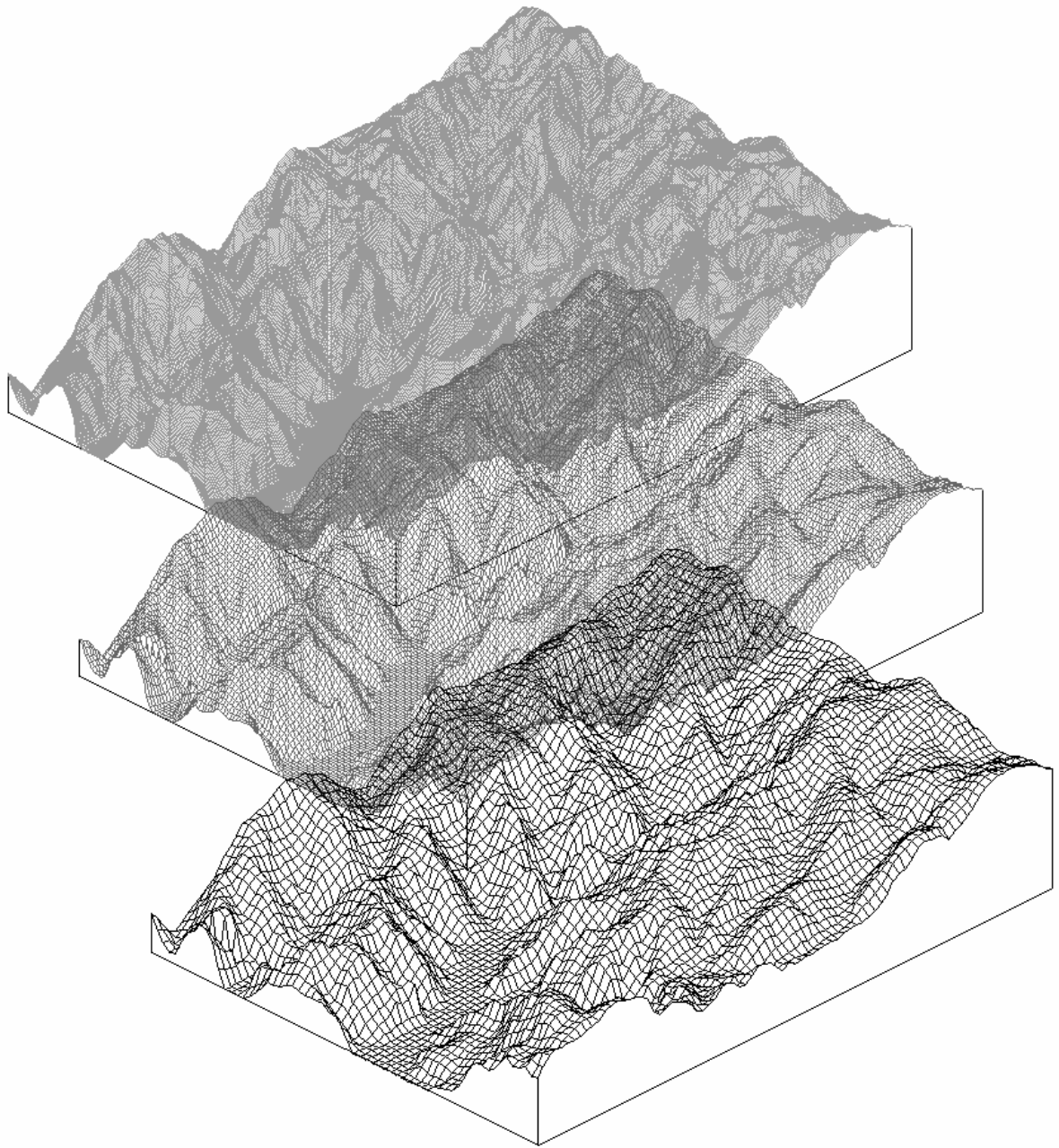
The hypothesis for the present study is that the impact of many rainfall events of different intensity and duration that trigger shallow landslides over years is translated in the failure of all sites with a critical steady state rainfall below a certain value during one timestep. This notion and use of timesteps can be more specified when detailed meteorological data in combination with an inventory of failures triggered by rainfall events with a certain intensity and frequency are available.

The overall aim of the model component is to assess the spatial impacts of shallow landsliding on longer term landscape dynamics; it is not the intention to simulate detailed changes in channel geometry or hillslope geomorphology caused by individual failures. Especially the soil redistribution algorithms (Eqs. (3.9)-(3.14)) are hard to allocate a real physical interpretation. To be able to simulate debris flow movement with process-based formulas, a lot of additional parameters would have to be gathered (e.g. viscosity, debris flow composition, soil depth...). On the landscape level, and dealing with long term simulations, these properties would be hard to quantify in a spatially explicit way. With the aim of developing a model that does not require the rheological properties of a debris flow, this empirical methodology can easily incorporate a slope limit on debris flow movement. It takes into account hillslope morphology for erosion and deposition, is based on elevation differences and therefore convenient when basin topography is represented by a digital elevation model. Bearing in mind its assumptions and limitations this approach has been demonstrated to retain the essence of the physical controls of topography and soil properties

on landsliding and remains parametrically simple for ease of calibration and application in catchment studies.

3.4 Conclusions

In this chapter, principles and modelling techniques of a physically based slope stability model, a steady-state subsurface flow model and debris flow runout criteria were adopted and combined. The resulting model forms a landslide component within the dynamic landscape evolution model LAPSUS, which can contemporaneously simulate soil redistribution by water run-off and tillage erosion. The overall aim of the model component is to assess the impacts of shallow landsliding on longer term landscape dynamics and help to define possible feedbacks with other hillslope processes; it is not the intention to simulate detailed changes in hillslope geomorphology caused by individual shallow landslides. The adopted approach, in combination with field and laboratory measurements, explores the capabilities of the model to calculate relative landslide potentials and visualise the changing pattern of slope instability within a timeframe of years to decades. The model presents a simple and robust method to address the effects of shallow landslide erosion and sedimentation. Digital elevation data are adapted between timesteps and on- and off-site effects over the years can be simulated. The combined infinite slope stability and subsurface flow model performs well in predicting landslide locations with their relative failure potential and is capable of producing results which have a physically realistic interpretation. For determination of debris flow trajectories sophisticated formulations applicable to a well-specified individual debris flow were inappropriate and simpler, empirical formulas were used. Validation of these criteria requires data sets linking landslide events with rainfall conditions triggering their occurrence and their resulting soil redistribution. This is a demanding requirement for large research areas and parameter estimation with resulting uncertainty may therefore be necessary. Improvements of the existing techniques and especially the full integration of all LAPSUS model components are envisaged in the future. Moreover, because the influence of vegetation on soil cohesion is not treated as a lumped parameter input, the model could accordingly be used with different land use cover (change) scenarios addressing the impact on landscape development and natural resources. Consequently, the integration of LAPSUS with the existing land use change model CLUE (Verburg et al., 2002) is the subject of future research.



Chapter 4

DEM Resolution Effects

In this chapter, the effects of DEM resolution on the results of LAPSUS-LS are assessed. Distributions of slope, specific catchment area and relative hazard for shallow landsliding are analysed for four different DEM resolutions (grid sizes of 10, 25, 50 and 100 m) of a 12 km² study catchment in the Waitakere Ranges. The effect of DEM resolution is especially pronounced for the boundary conditions determining a valid hazard calculation. For coarse resolutions, the smoothing effect results in a larger area becoming classified as unconditionally stable or unstable. Simple empirical soil redistribution algorithms are applied for scenarios in which all sites with a certain landslide hazard fail and generate debris flow. The lower initial number of failing cells but also the inclusion of slope (limit) in those algorithms becomes apparent with coarser resolutions. For finer resolutions, much larger amounts of soil redistribution are found, which is attributed to the more detailed landscape representation. Looking at spatial patterns of landslide erosion and sedimentation, the size of the area affected by these processes also increases with finer resolutions. In general, landslide erosion occupies larger parts of the area than deposition, although the total amounts of soil material eroded and deposited are the same. Analysis of feedback mechanisms between soil failures over time shows that finer resolutions show higher percentages of the area with an increased or decreased landslide hazard. When the extent of sites with lower and higher hazards are compared, finer grid sizes and higher landslide hazard threshold scenarios tend to increase the total extent of areas becoming more stable relative to the less stable ones. Extreme care should be taken when quantifying landslide basin sediment yield by applying simple soil redistribution formulas to DEMs with different resolutions. Rather, quantities should be interpreted as relative amounts. For studying shallow landsliding over a longer timeframe, the 'perfect' DEM resolution may not exist, because no resolution can possibly represent the dimensions of all different slope failures scattered in space and time. It is

Based on: Claessens, L., Heuvelink, G.B.M., Schoorl, J.M. and Veldkamp, A., 2005. DEM resolution effects on shallow landslide hazard and soil redistribution modelling. *Earth Surface Processes and Landforms* 30. In press.
© John Wiley & Sons Ltd.

emphasised that the choice of DEM resolution, possibly restricted by data availability in the first place, should always be adapted to the context of a particular type of analysis.

4.1 Introduction

Topographically based modelling of catchment processes has become very popular in recent applied environmental research, mainly due to the advances in availability and quality of digital elevation models (DEMs) (Moore et al., 1991; Goodchild et al., 1993; Wise, 2000). Digital elevation data available from DEMs are sometimes of direct interest (e.g. in erosion, sedimentation and landscape evolution studies), but elevation values are most often used in algorithms to calculate surface derivatives such as slope, aspect, flow direction and upstream contributing area. Catchment boundaries and stream drainage networks can be derived from those topographic attributes as well. The results of these DEM analyses are used in many terrain modelling applications: distributed hydrological modelling (Beven and Moore, 1993), prediction of surface saturation zones (O'Loughlin, 1986; Barling et al., 1994), erosion-deposition models (Desmet and Govers, 1996; Schoorl et al., 2000), hillslope stability and landslide (hazard) models (Montgomery and Dietrich, 1994; Tarboton, 1997; see also Chapter 3), predictive soil mapping (Skidmore et al., 1991; Thompson et al., 2001; Scull et al., 2003), and in land use (change) models (Veldkamp and Fresco, 1996a and 1996b; Verburg et al., 2002; Vanacker et al., 2003).

In general, topographic information in a DEM can be represented and stored as (i) a triangulated irregular network (TIN), (ii) discrete landform elements based on the intersection of flow- and contourlines, or (iii) a grid. The first two methods are in a way superior to the third because they can be adapted to become most representative of the, for the modelling context, important landscape features. However, the grid DEM has been the most commonly used data source for digital terrain analysis because of its simple structure and compatibility with other digitally produced data (Gao, 1998; Wise 2000). Unfortunately, grid DEMs suffer from some drawbacks that arise from the nature of their data structure which remains a representation of the 'real-world' continuous surface and derivatives such as slope and aspect will always be approximations of the real value. As this chapter only deals with this type of constraints, for simplicity, the general term DEM will be used to refer to grid DEMs.

In the extraction of topographical information from DEMs for modelling purposes, two main sources of error are involved: (i) errors in the DEM itself and (ii) errors caused by the algorithms used in the analysis (Wise, 2000). When a DEM is interpolated from contours, apart from the accuracy of the source data, interpolation methods will be a source of error (Li, 1994; Carrara et al., 1997). Relatively small errors in interpolated elevation values can lead to large errors in the calculation of derivatives (Bolstad and Stowe, 1994; Desmet, 1997; Heuvelink, 1998; Wise, 1998 and 2000). Although certain interpolation methods tend to perform better for specific data sources and applications, Wilson and Gallant (2000) conclude that attempts to make generalisations about 'best' methods are very difficult. Simple interpolation methods will give satisfactory results as long as the input data are abundant and well sampled and sophisticated algorithms are likely to produce unsatisfactory results when applied to data of poor quality. The algorithm itself used to compute surface derivatives from a DEM obviously has an influence on the accuracy of a DEM analysis. Quite some research has been done comparing algorithms for slope and aspect (Skidmore, 1989; Srinivasan and Engel, 1991; Dunn and Hickey, 1998; Jones, 1998; Florinsky, 1998; Mizukoshi and Aniya,

2002), or methods for the determination of flow directions or routing algorithms (Quinn et al., 1991; Holmgren, 1994; Wolock and McGabe, 1995; Desmet and Govers, 1996; Tarboton, 1997; Zhou and Liu, 2002).

Another important factor for the analysis of DEMs, is the influence of DEM grid size, i.e. DEM resolution, on modelling results. Although the increasing availability of DEMs and computational capacity allows rapid topographical analysis of large catchments, the degree to which DEM resolution affects the representation of the land surface has not been examined systematically (Zhang and Montgomery, 1994). Several studies did explore the effect of DEM resolution on landscape representation (Hutchinson and Dowling, 1991; Jenson, 1991; Panuska et al., 1991; Quinn et al., 1991). The resolution sensitivity of the topographic index developed by Beven and Kirkby (1979) has received quite some attention and the distribution of this index proves to be to some degree dependent on DEM resolution (Chairat and Delleur, 1993; Band et al., 1993; Wolock and Price, 1994; Zhang and Montgomery, 1994; Quinn et al., 1995; Band and Moore, 1995; Saulnier et al., 1997; Braun et al., 1997; Becker and Braun, 1999). Nevertheless, little is known about the systematic effects of changing resolution upon the results produced by topographically driven geomorphological models (Dietrich and Montgomery, 1998; Wilson and Gallant, 2000; Schoorl et al., 2000). Especially landslide hazard models, very often using (gridded) DEMs, seem to have escaped the attention on resolution effects. Quite some research has been done on landslide hazard delineation and probability modelling but since different terrain analysis methods can produce different topographic attributes, this undoubtedly influences the probabilities derived and should be explored further (Duan and Grant, 2000).

In this chapter a brief overview will be given of work that has already been done on the influence of DEM resolution on terrain analysis and will then focus on the impacts on the outcome of LAPSUS-LS.

4.2 Influence of DEM resolution on digital terrain analysis

4.2.1 DEM resolution and topographic index

Several researchers have specifically addressed the impact of DEM resolution on the distribution of the hydrological similarity index and the complications for its use in TOPMODEL (Beven and Kirkby, 1979; Moore et al., 1991). The index can be expressed as $\ln(a/\tan\beta)$, where a is the specific catchment area and β is the local slope. The index essentially is a measure of the tendency of water to accumulate at one position on a slope. In general, with coarsening resolution, β tends to drop because local variation in terrain is smoothed, whereas the distribution of a tends to shift towards larger values (Band and Moore, 1995; Wilson et al., 2000). Several researchers compared distributions or mean values of $\ln(a/\tan\beta)$ computed with DEMs with differing resolutions (Quinn et al., 1991 and 1995; Band et al., 1993; Chairat and Delleur, 1993; Zhang and Montgomery, 1994; Saulnier et al., 1997). In general, using coarser DEMs, a larger percentage of high index values was obtained. Wolock and Price (1994) argue that, for TOPMODEL, coarse resolution DEMs are not necessarily inappropriate because an implicit assumption is that the water table configuration mimics surface topography and may be smoother and better represented by a coarse resolution DEM. Braun et al. (1997) and Becker and Braun (1999) show that an acceptable

approximation of the 'real' distribution of the topographical index in a catchment can be derived from a low resolution DEM by the use of simple scaling.

4.2.2 DEM resolution and influence on topographical attributes and modelling results

Bates et al. (1998) illustrate the interaction between DEM resolution and model grid size of a hydraulic and hydrological model. They describe DEM resolution as a first filter on topographic information content assimilated into a model. They also point to a second topographic information filter when the grid size of other parameter inputs is set at a lower resolution than that of the DEM. Gains in accuracy supposedly given by producing models that rely on more physically complex descriptions of processes, may be nullified by the lack of sufficient high resolution data. A third concern, also noted by Grayson et al. (1993), is that if the information content of the DEM drops below some threshold, certain assumptions in distributed models, particularly if flow routing is involved, may not be met.

By extracting watershed geometry from a DEM and using it in an event based distributed model for calculating surface runoff, Thielen et al. (1999) found that flow path lengths, drainage density and time to peakflow decreased whereas peak flow rate, maximum total flow length and runoff volume increased with decreasing DEM resolution.

Wilson et al. (2000), using TAPES-G for deriving primary topographic attributes, found decreasing slope gradients, more short flow paths (measured in terms of number of cells) and increasing specific catchment area with increasing cell size. They also delineated channel/net deposition and net erosion cells by the change in sediment transport capacity index (Moore and Burch, 1986) across a grid cell. For the net erosion areas, they also describe the sensitivity to DEM resolution for the Revised Universal Soil Loss Equation length-slope (RUSLE-LS) factor, using flow-path length, and the Moore/Wilson (MW) sediment transport capacity index, using specific catchment area (Moore and Wilson, 1992). The two variables increased with increasing grid size and different statistical and spatial distributions were generated. Furthermore, fundamentally different values were obtained and this is likely to cause additional problems when substituting one for the other in empirical models (see also Mitasova, 1996; Desmet and Govers, 1997).

Applying a simple single process model for erosion and sedimentation on two artificial DEMs with five different resolutions, Schoorl et al. (2000) described an artificial mathematical overestimation of erosion and a realistic natural modelling effect of underestimating resedimentation with coarsening resolution. The first effect could be handled by introducing a systematic correction factor, the second by modelling in a multi-scale framework and using resedimentation rates from finer resolutions in simulations for larger areas with coarser resolution.

Thompson et al. (2001) statistically and visually compared terrain attributes and quantitative soil-landscape models derived from DEMs with different horizontal resolution and vertical precision. They suggest that the vertical precision must increase with increasing horizontal resolution so that it remains greater than the average difference in elevation between grid points in the DEM. Furthermore, they found similar capabilities in predicting A horizon depth for 10 m and 30 m resolution DEMs and therefore state that higher-resolution DEMs may not be necessary for generating useful soil-landscape models.

In general, the significance of shifts in topographical attributes derived from DEMs with different resolution needs to be assessed relative to the sensitivity of the models using this information and landscape features of interest should guide the choice of resolution (Band and

Moore, 1995). Zhang and Montgomery (1994) found that runoff processes in their area were controlled by physical properties of the landscape of about ten meters and suggest a 10 m grid size as a rational compromise between increasing resolution and data volume for simulating geomorphic and hydrological processes. Garbrecht and Martz (1994) found that, for extracting drainage properties from their DEM, the grid area should be less than 5 % of the network reference area to reproduce important drainage features.

4.2.3 DEM resolution and landslide modelling

Models used to delineate the location and calculate the potential for shallow landsliding in a grid based DEM environment are being used with a variety of grid sizes, ranging from as coarse as 4.05 hectares (Ward, 1981) to a few meters (e.g. 2 m, Dietrich and Montgomery, 1998). In general, cell size is selected by the user and should depend on the quality and density of the input data, size of the area to be mapped and accuracy required for the output data (Ward, 1981). Borga et al. (1998 and 2002) use 10 m grids in one basin, 'consistent with the resolution of the original topographic data and the low grid-to-hillslope length ratio', and 5 m grids in another catchment 'to portray individual landslides accurately'. Burton and Bathurst (1998) use a dual resolution approach, modelling basin hydrology at a 200 m resolution, for time and memory requirements, and predicting landslide hazard and potential sediment yield at 20 m resolution, which they consider to be appropriate for landslide simulation. Vanacker et al. (2003) use a 5 m grid size DEM in a factor of safety analysis, a resolution judged suitable for studying the linkage between land-use change and slope stability.

Few studies have been done on the identification and quantification of the influence of DEM resolution on landslide hazard assessment and the resulting soil redistribution pattern. Dietrich and Montgomery (1998) give two examples of how the distribution of the hydrologic ratio, expressed as $\log(q/T)$ (q is steady state rainfall [m day^{-1}], T is transmissivity [$\text{m}^2 \text{day}^{-1}$]), varies with different DEM resolutions in a landscape. They also show a comparison for a shallow landslide location and hazard prediction (with SHALSTAB) between a 30 m and a 6 m DEM and a 10 m and 2 m DEM. For both cases they conclude that, although percentages of the landscape in the moderate landslide hazard classes are similar for coarse and fine resolutions, the spatial patterns in general differ in important ways. In the finer resolution case, patterns of relative slope stability are much more strongly defined by local ridge and valley topography. Low $\log(q/T)$ values (meaning a higher slope instability potential) are more concentrated in steep valleys, rather than spread out across the landscape. They conclude that with finer resolution topography, sites with highest instability increase and can be delineated more precisely, rather than mapping broad zones of instability in the case of coarser resolutions.

4.3 Materials and methods

4.3.1 Study area

Also for this chapter, the field research was conducted in the Waitakere Ranges, described in more detail in Chapters 1 and 2. The study area chosen for this analysis is the ± 3 by 4 km catchment of the Piha and Glen Esk streams and their tributaries (Topographic Map of New Zealand 260-Q11 & Pt. R11, 416728-458697; Fig. 4.1). The geology of this part mainly

consists of Miocene volcanic breccia and conglomerate of the Piha Formation (Hayward, 1976).

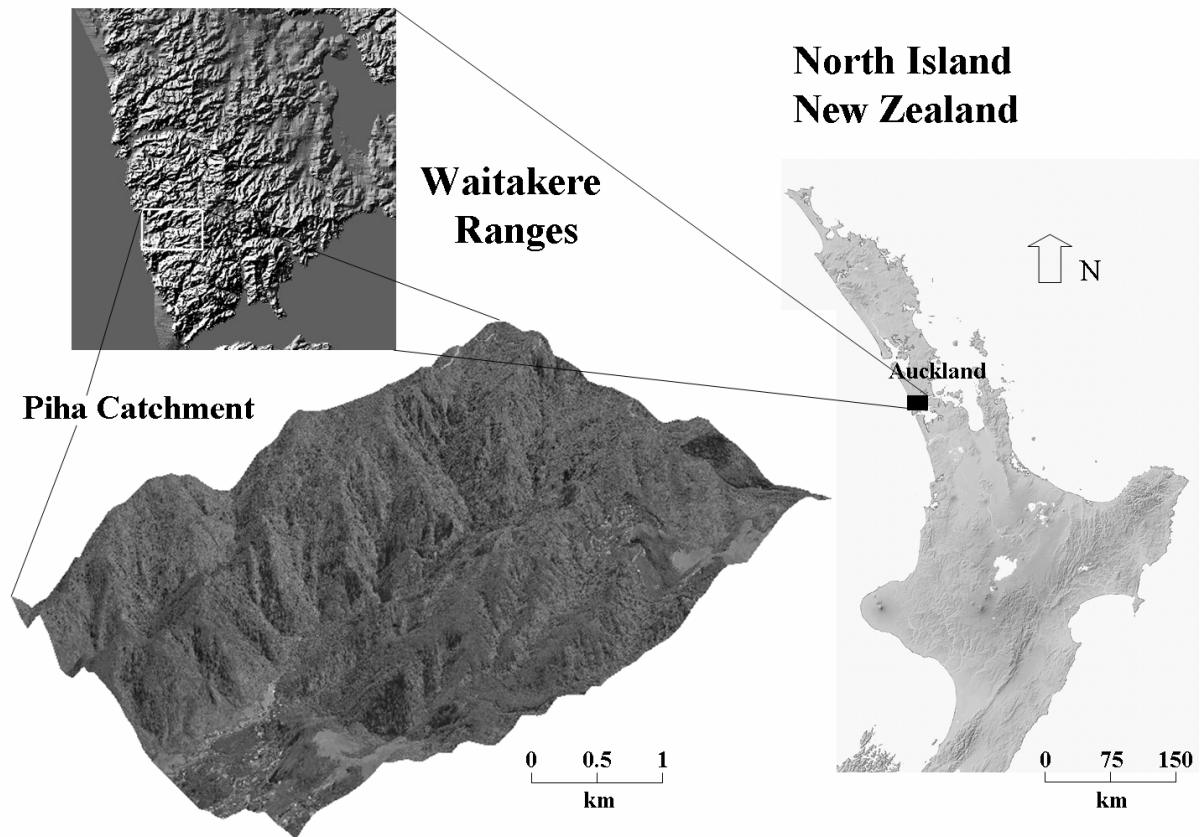


Fig. 4.1 Location of the study area within the Waitakere Ranges and the North Island of New Zealand.

4.3.2 LAPSUS-LS

In Chapter 3 the development, applicability and limitations of the LAPSUS-LS model component were described in detail. LAPSUS-LS is a combination of several modelling steps. First it calculates relative landslide hazard distribution, expressed as critical rainfall Q_{cr} [m day^{-1}], from topographical and geotechnical attributes according to Eq. (3.4). Historical rainfall-landslide distribution datasets and magnitude-frequency scenarios are then used to calibrate and run the model. Unlike some researchers who account for variability and uncertainty of terrain attributes in more probabilistic approaches (Dietrich et al., 1995; Duan and Grant, 2000; Pack et al., 2001; Zaitchik et al., 2003), also this chapter is restricted to a deterministic approach, lumping all but the topographic parameters in the watershed, in this way focusing solely on DEM resolution effects. A sensitivity plot with the relative importance of each variable in the calculation of Q_{cr} [m day^{-1}] following Eq. (3.4) is given in Fig. 4.2. This graph shows the relative change of the critical rainfall value as a function of the relative divergence of each input variable from a given set of default input values. Obviously, T , ρ_s and C show a linear, positive correlation with Q_{cr} . Increasing specific catchment area or slope lowers Q_{cr} , higher internal friction angles yield a lower landslide hazard. Given the set of default input parameters, the negative correlation of slope with Q_{cr} is larger than that of

specific catchment area. Internal friction has the largest positive correlation with Q_{cr} . Hence, in general it is the most effective in lowering relative landslide hazard with increasing input values. A second step in the LAPSUS-LS model is the application of soil redistribution algorithms (Eqs. (3.9)-(3.14)) to quantify and visualise feedbacks between mass movements or interactions with other geomorphic processes.

Although there are reliable field and laboratory measurements of T , C , ρ_s and ϕ for the different parent materials of the study area and these parameters could be treated as spatially distributed (as in Chapter 3), for this application all variables, except slope and contributing area, are lumped in the watershed. Lumping of parameters has also been done by Barling et al. (1994), Dietrich and Montgomery (1998) and Wu and Sidle (1995), due to lack of sufficient measured catchment properties. Lumped input parameters are estimated on the basis of field and laboratory measurements (Table 3.1 and 3.2), and are $15 \text{ [m}^2 \text{ day}^{-1}]$ for T , 0.2 [-] for C , $1.5 \text{ [g cm}^{-3}]$ for ρ_s and $35 \text{ [}^\circ]$ for ϕ . Exponent p of Eq. (3.13) for the determination of the fraction for multiple flow directions is set at 4 (Holmgren, 1994).

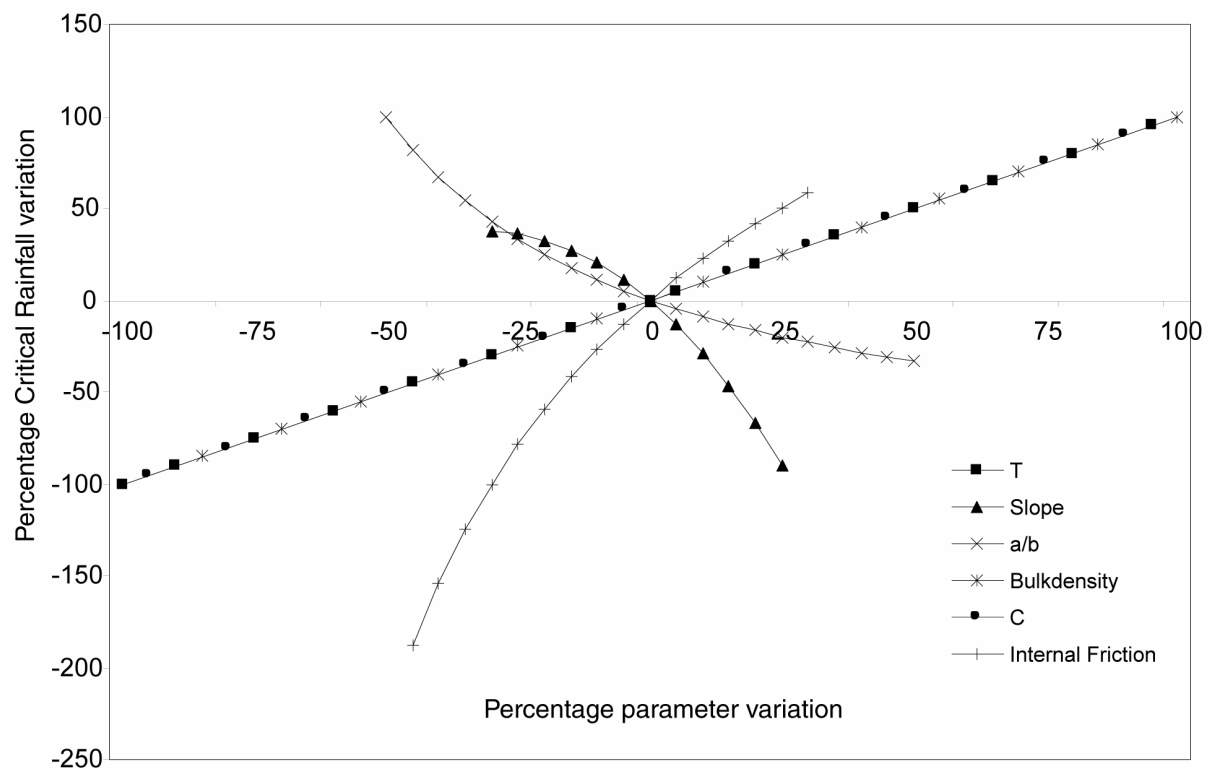


Fig. 4.2 Sensitivity plot for Critical Rainfall (Eq. (3.4)), showing the percentage change of its value as a function of the divergence of each input variable from a given set of default input values.

4.3.3 Terrain analysis: DEM, slope and specific catchment area

To investigate the effect of DEM resolution, 100 m, 50 m and 25 m DEMs were aggregated in ArcView GIS from the same 10 m DEM. The 10 m DEM in turn was derived by TIN interpolation from 10 m elevation contours electronically created from 3D stereo photographs. Although being aware of the possible consequences of the choice of slope and flow routing

algorithms briefly discussed above, these effects will not be explored further here and the focus is solely on the effects of DEM resolution.

For calculation of slope, the local cell-to-cell slope is used, rather than using a smoothing multiple cell window, as done in most GIS procedures. The upslope contributing drainage area is calculated using the concept of multiple flow by Quinn et al. (1991), to represent the convergence or divergence of flow under topographic control. Although Tarboton (1997) correctly points out that this method is ‘dispersive’, Dietrich and Montgomery (1998) discuss that it avoids grid artefacts and gives reasonable estimates for the total drainage area for each cell, when used in Eq. (3.4). Furthermore, grid cell size is taken as effective contour length b in the definition of specific catchment area because other algorithms that calculate b based on the sum of flow directions will be influenced by the orientation of the topography relative to the grid system (Dietrich and Montgomery, 1998).

4.4 Results and discussion

4.4.1 Influence of grid size on slope, specific catchment area and critical rainfall

To explore how different DEM resolutions influence relative shallow landslide hazard distribution, the behaviour of the two topographical attributes derived from the DEM and used in the hazard assessment, i.e. local slope and contributing area, is analysed. These parameters constitute a topographical and hydrological characterisation of the study area, respectively.

Fig. 4.3 shows the cumulative distribution of slope values within the study area for the four DEM resolutions. Although the trends are quite similar (note the same near absence of slopes around 0.20 rad for the four resolutions), it is clear that the coarser resolutions show a larger contribution of lower slope angles and fewer short steep slopes. Both effects become less pronounced towards the finest grid size, reflecting the progressively smaller improvement made by representing the original 10 m contour data of the area with increasingly smaller grid cells. It must be stressed that the method of slope computation is very important when analysing these resolution effects. As mentioned, a cell-to-cell slope computation is used, meaning that slope is calculated over a ‘slope distance’ equal to the DEM resolution, i.e. ranging from 10 to 100 m with coarsening resolution. When using multiple cell windows to compute slope, the ‘slope distance’ will increase and the smoothing effect of coarser resolutions will even be more pronounced. The ‘yardstick’ (Mandelbrot, 1986) used to compute a slope should not automatically depend on the DEM resolution but rather on the process to be simulated.

The cumulative distribution for the computed specific catchment area (contributing area per unit contour length) for the different resolutions is plotted in Fig. 4.4. The minimum values are directly related to the grid size and are equal to the area of one cell divided by the flow width or contour length. In other words, they equal the DEM resolution. Coarser DEM resolutions also have a higher contribution of high specific catchment area values to the distribution: progressively more drainage area tends to accumulate when directing flow down slope towards the outlet cell due to the higher unit contributing area for the larger grid sizes. In the end, the value of contributing area for the outlet cell of the watershed is approximately the same for the four resolutions. Similar smoothing effects of coarser resolutions on derived topographic attributes were found by several researchers for various landscapes (Quinn et al., 1991 and 1995; Wolock and Price, 1994; Zhang and Montgomery, 1994; Moore, 1996; Wilson et al., 2000).

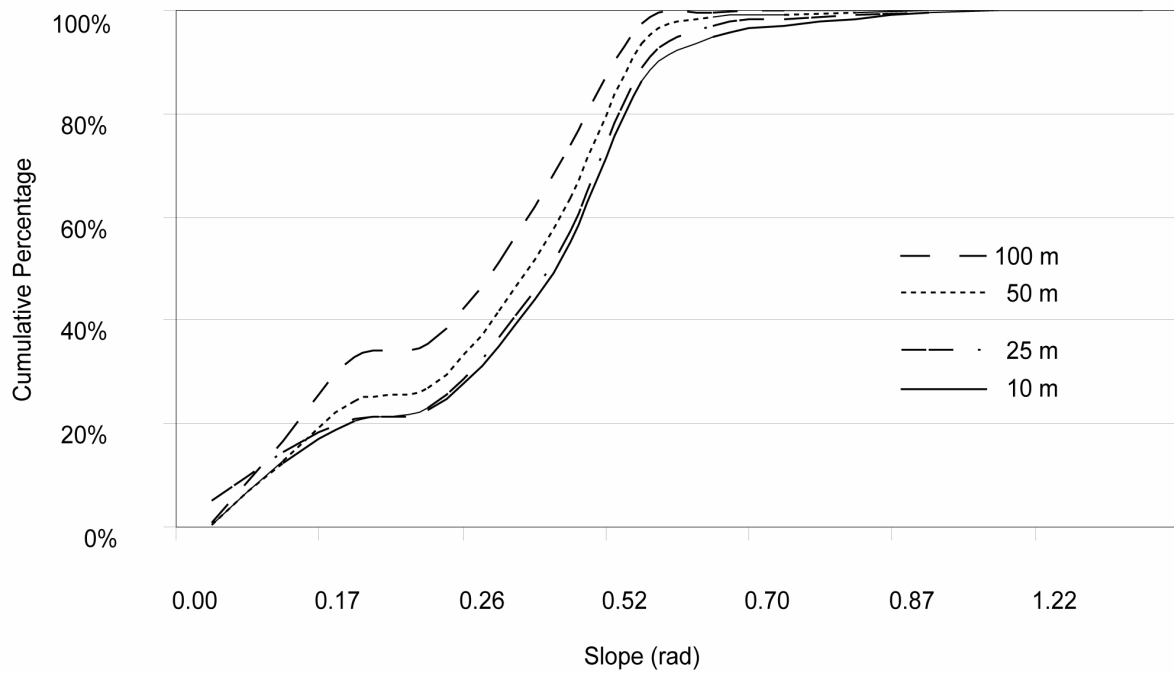


Fig. 4.3 Cumulative distribution of slope values within the study area for the four DEM resolutions.

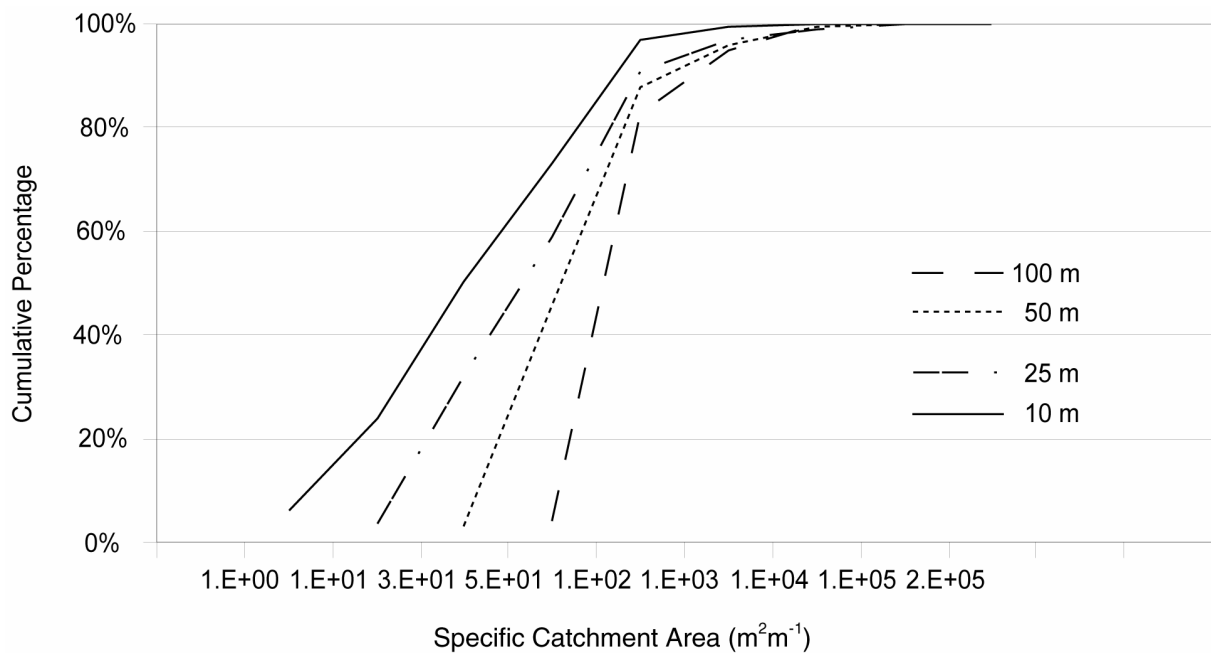


Fig. 4.4 Cumulative distribution of specific catchment area within the study area for the four DEM resolutions.

The effects of resolution on the cumulative distributions of slope and specific catchment area have a direct impact on the calculated values for the critical steady state rainfall for landslide

initiation Q_{cr} [m day^{-1}] (Eq. 3.4). Fig. 4.5 shows, for the different DEM resolutions, the percentage of the study area having a certain critical rainfall value, interpreted as the relative potential for landsliding or becoming ‘unstable’. The most pronounced effect is the influence of slope distribution on the boundary conditions for using Eq. (3.4), i.e. assigning a critical rainfall value to a grid cell. The intercept with the Y-axis or area with ‘zero’ critical rainfall value equals the amount of unconditionally unstable cells according to Eq. (3.6). In this application, this condition is only influenced by the local slope as a variable factor and more unconditionally unstable cells are encountered with more terrain variance and steeper slopes. The other boundary condition (Eq. (3.5)), excluding unconditionally stable areas from landslide hazard calculation, is also completely dependent on local slope distribution and for the same reason, less unconditionally stable cells are found with finer resolutions. In general, the effect of smoothing or filtering of topographic information is very clear and the detail obtained in the lower critical rainfall value ranges is progressively lost with coarsening resolution. Within the range of valid critical rainfall calculations according to Eq. (3.4), besides local slope, also differences in specific catchment area distribution become important. This is more difficult to interpret from Fig. 4.5 but the effect of the coarse resolution DEM having more high specific catchment area values, possibly lowering Q_{cr} , is mostly nullified because those higher values tend to occur in the valley bottom towards the outlet cell, where slopes are generally low enough for classification as unconditionally stable. This is confirmed when comparing specific catchment area descriptive statistics, split up between areas having a possible valid critical rainfall calculation and unconditionally stable parts (Table 4.1).

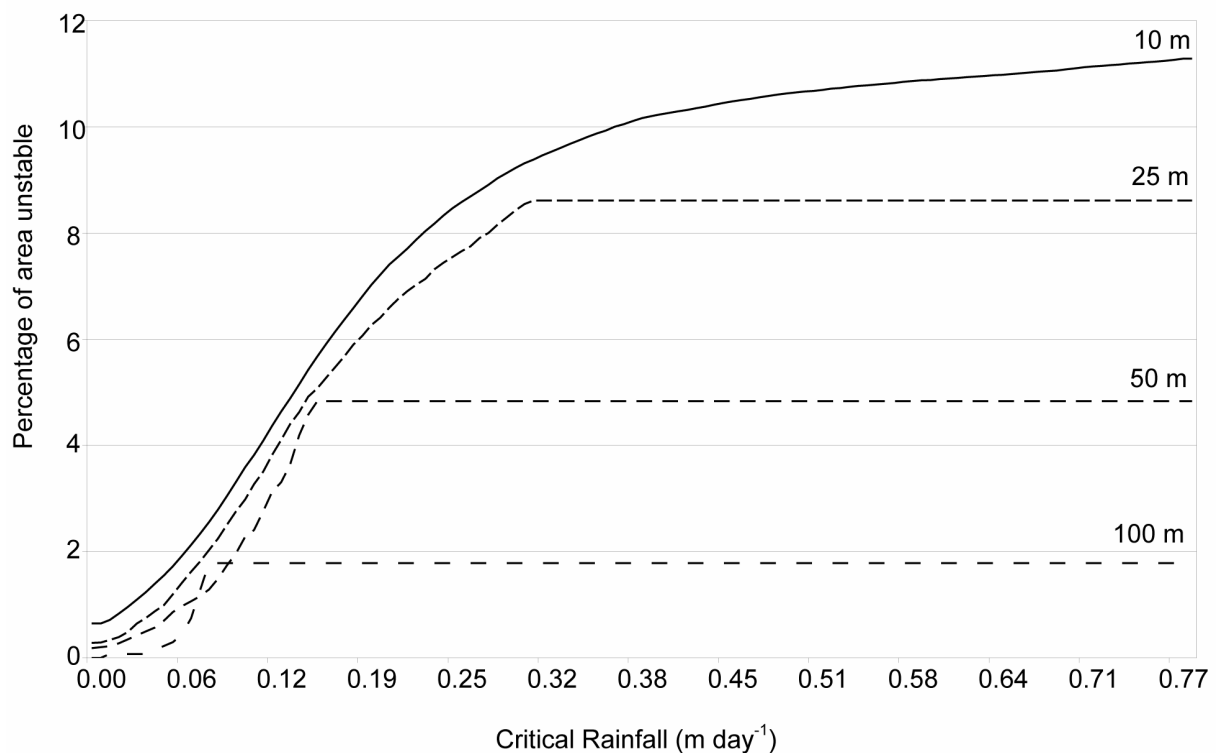


Fig. 4.5 Percentages of the study area having a certain Critical Rainfall value (relative potential for landsliding) for the four different DEM resolutions.

| Grid Size [m] | Landslide Hazard | Specific Catchment Area [m ² m ⁻¹] | | | Slope [°] | | |
|---------------|------------------|---|----------------|---------------|--------------|--------------|--------------|
| | | Min. | Max. | Mean | Min. | Max. | Mean |
| 10 | No | 10.0 | 208948.7 | 616.9 | 0.00 | 31.32 | 16.05 |
| | Yes | 10.0 | 5388.0 | 61.6 | 31.32 | 48.89 | 36.63 |
| 25 | No | 25.0 | 239274.6 | 2480.9 | 90.00 | 31.32 | 16.21 |
| | Yes | 25.0 | 97256.1 | 204.9 | 31.32 | 48.81 | 35.86 |
| 50 | No | 50.0 | 121347.3 | 2350.4 | 0.00 | 31.32 | 15.50 |
| | Yes | 50.0 | 46944.6 | 275.9 | 31.38 | 48.20 | 35.24 |
| 100 | No | 100.0 | 102551.8 | 2326.0 | 0.00 | 30.95 | 13.74 |
| | Yes | 100.0 | 23074.8 | 1068.5 | 31.43 | 41.40 | 34.68 |

Table 4.1 Descriptive statistics for specific catchment area and slope values for the different DEM resolutions.

4.4.2 Influence of grid size on landslide soil redistribution quantities and spatial patterns

After calculating the relative hazard for shallow landsliding Q_{cr} over the catchment, the interactions between possible initial collapse and resulting debris flow soil redistribution can be assessed by applying Eqs. (3.9)-(3.14) as described above. DEM elevation values can then be adapted according to the amounts [m] of landslide erosion (Eq. (3.9)) and deposition (Eq. (3.11)). When, for a next model run or timestep, Q_{cr} is calculated again with the adapted DEM, it is possible to visualise feedbacks between mass movements or interactions with other geomorphic processes by comparing landslide hazard maps between timesteps. Historical rainfall-landslide distribution datasets can provide the link between real rainfall events (with their magnitude and frequency), triggering slope failure at certain locations over time and the critical steady state rainfall value assigned to those cells. In this way, the time frame represented by one timestep or model run can be quantified. Alternatively, since those long term and spatially explicit datasets are rarely available, one timestep can be interpreted as a scenario with the average frequency of many rainfall events of different intensity and duration that trigger shallow landslides over years translated in the failure of all sites with a critical steady state rainfall smaller than a certain value.

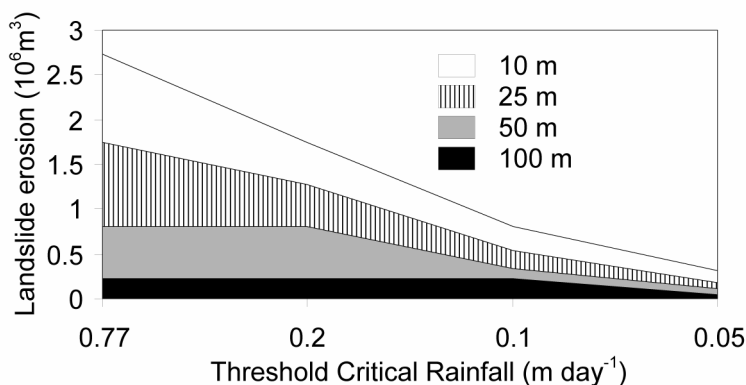


Fig. 4.6 Total amounts of landslide erosion for different critical rainfall thresholds and DEM resolutions.

After running the modelling steps for a certain scenario, the total amounts of eroded and deposited soil material [m^3] can be quantified. These quantities are the same because consecutive fluvial sediment transport out of the catchment is not yet accounted for in the model. Fig. 4.6 gives a comparison of total amounts of erosion for four different scenarios applied to the four DEMs. The maximal Q_{cr} value in the catchment is 0.77 m day^{-1} . The corresponding scenario is a measure of total possible landslide erosion/sedimentation within the catchment or the most extreme case in which all sites with a valid hazard value are triggered. The other scenarios with progressively lower maximal Q_{cr} values represent more realistic situations in which only areas with consecutive higher hazard values are affected. The influence of grid size on critical rainfall distribution (Fig. 4.5) has a direct impact on the amount of sites triggered and the resulting erosion/sedimentation quantities in each scenario. The maximum possible quantities are already reached for lower threshold critical rainfall scenarios when resolution is coarsened and again the smoothing of the landscape becomes apparent. Furthermore because of this, the effect of a higher unit area for the coarser resolutions, used to calculate the amount of soil material in m^3 , is not enough to counteract the diversion of the amounts for smaller grid sizes towards much higher values with increasing critical rainfall threshold.

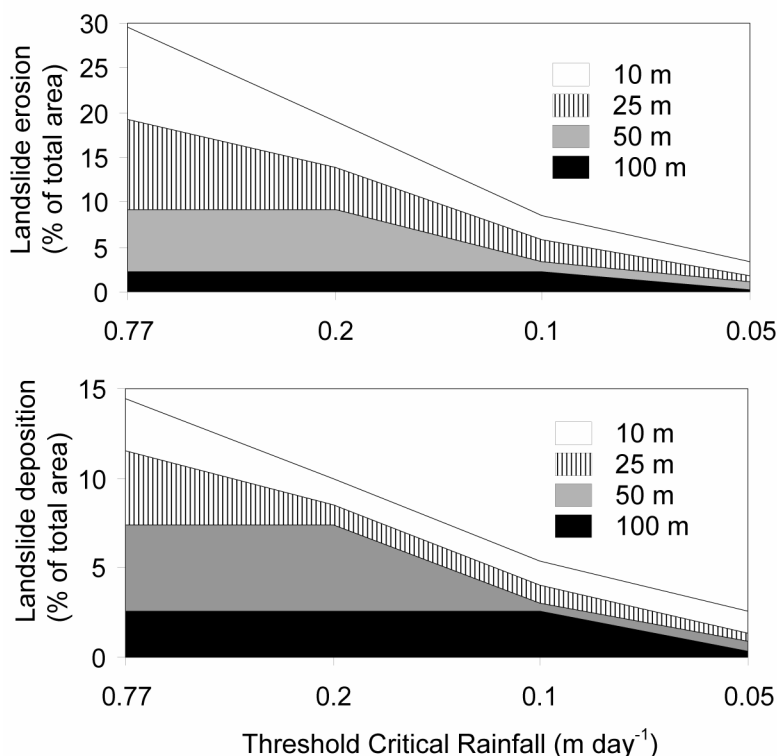


Fig. 4.7 Percentages of the total area affected by erosion and deposition for different critical rainfall thresholds and DEM resolutions.

Bearing in mind this resolution effect, extreme care should be taken when computing e.g. quantitative basin sediment yields with grid based soil redistribution algorithms. Especially

the quantification of landslide erosion and deposition, which involves rather scattered processes within a catchment compared to the more spatially continuous process of water (surface) erosion, is extremely sensitive to the resolution chosen to represent the dimensions of landslides and debris flows typical of a study area. One could even argue that it is impossible to choose one single best resolution to represent the characteristics of all failures occurring in a landscape over time and to quantify their soil redistribution accurately with simple empirical algorithms.

Since the model was not developed for calculating erosion or sediment yields in a quantitative way but for studying spatial patterns of long term soil redistribution and feedback mechanisms, the impact of resolution on these patterns is assessed. In Fig. 4.7, the percentages of the total area affected by erosion and deposition are plotted for different scenarios and DEM resolutions. Almost the same patterns as for the calculated quantities (Fig. 4.6) are visible. Again, the larger unit area for coarser resolutions and thus the larger possible contribution to the percentage of the area affected is not enough to counteract the effect of much more possibly triggered landslide sites and resulting soil redistribution with finer resolutions. Except for the 100 m DEM, larger parts of the area tend to be involved in landslide erosion than deposition (Fig. 4.8), although the amounts of soil material eroded and deposited are the same. Here, the higher unit areas for coarser resolutions do relatively raise the extent of deposition area because of the multiple flow principles used in the sedimentation algorithm. These trends are of course also dependent on the choice of ϕ [-], the empirically derived fraction of the elevation difference between the head of the slide and the point at which deposition begins, set at 0.4 in the deposition algorithm (Eqs. (3.7) and (3.10)).

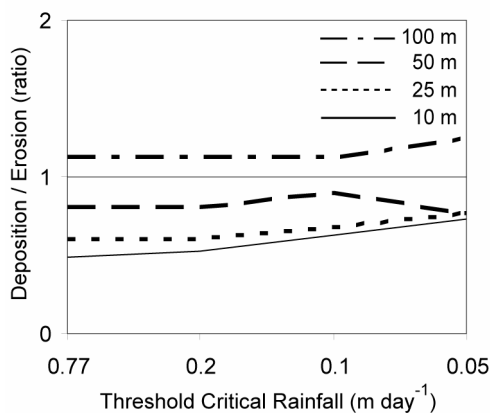


Fig. 4.8 Comparison of percentages of the total area affected by landslide deposition and - erosion for different critical rainfall thresholds and DEM resolutions.

Fig. 4.9 shows percentages of the area becoming relatively less or more stable after comparison of landslide hazard maps before and after a model run scenario with different threshold Q_{cr} values. For finer resolutions, not only more cells are initiated according to the scenario, i.e. having a critical rainfall of the scenario threshold or less, but also the resulting soil redistribution pattern is more detailed. After comparing initial and final hazard maps, more variation is encountered with finer resolutions and higher percentages of the area have a changed (higher and lower) landslide hazard. When the extents of areas with lower and higher hazard are compared (Fig. 4.10), finer resolutions and lower critical rainfall thresholds tend to

increase the total extent of areas becoming more stable relative to the less stable ones. Finer resolution DEMs explain more terrain variance and seem in this way more effective in lowering the overall modelled landslide potential; this effect is more strongly pronounced when dealing with lower critical rainfall thresholds.

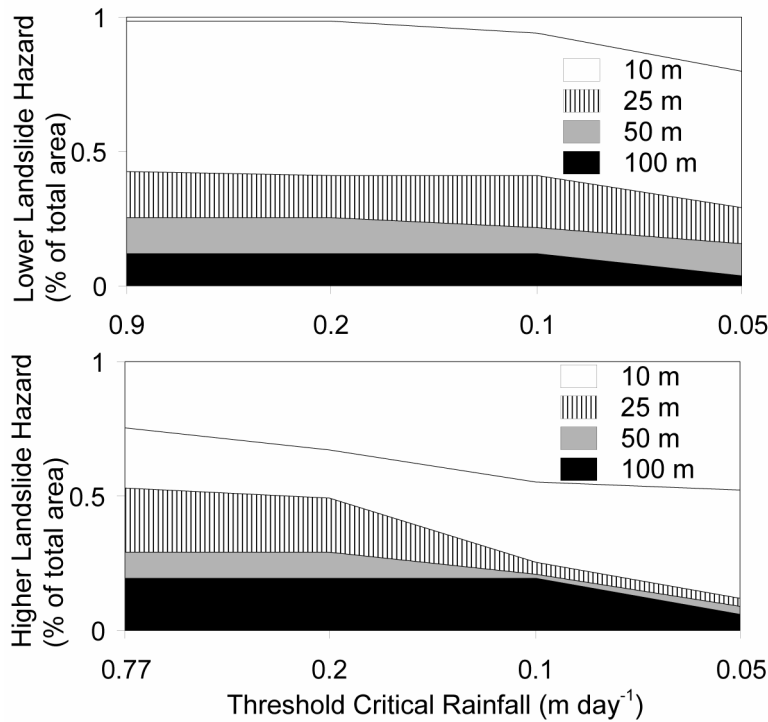


Fig. 4.9 Percentages of the area getting a lower or higher landslide hazard after a model run scenario with different critical rainfall thresholds and DEM resolutions.

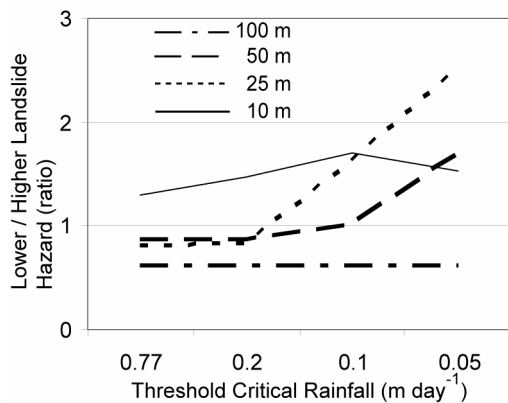
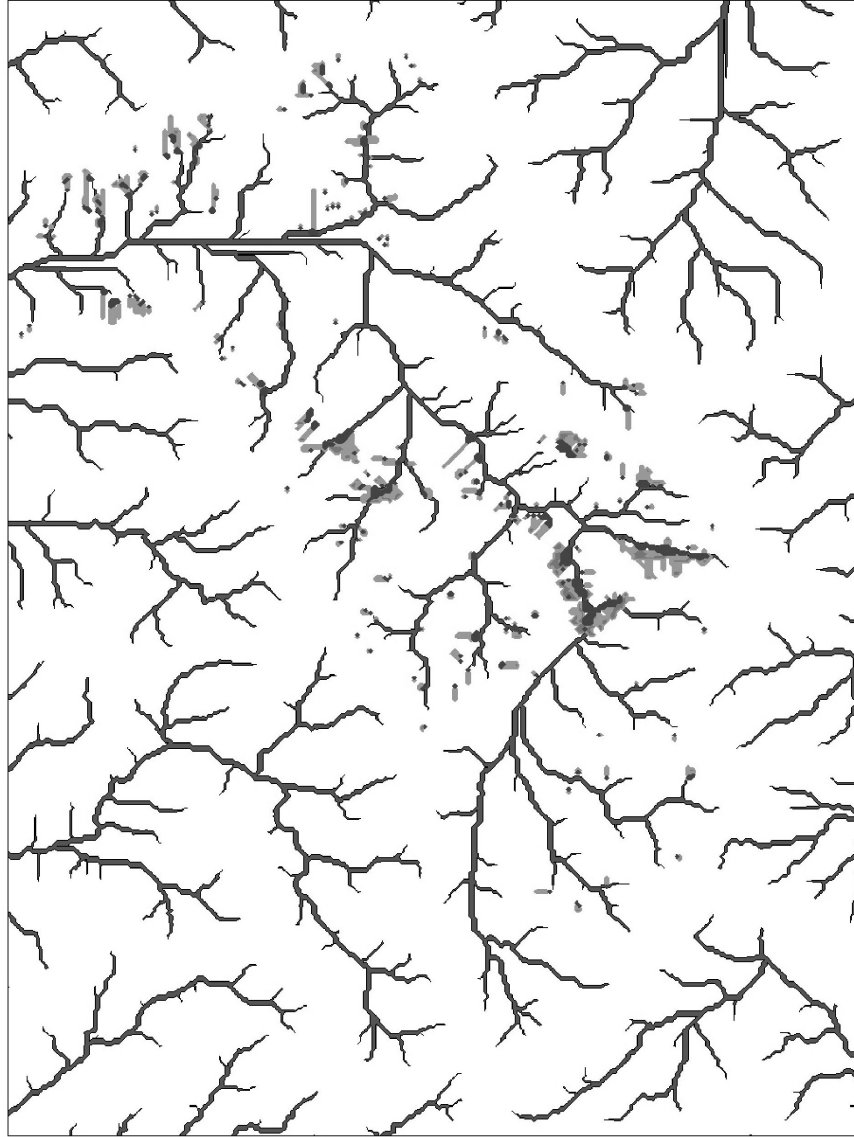


Fig. 4.10 Comparison of percentages of the total area getting a lower and higher landslide hazard for different critical rainfall thresholds and DEM resolutions.

4.5 Conclusions

Coarsening resolution has a smoothing effect on landscape topographical representation. Furthermore, the effect of DEM resolution on these attributes has a major impact on the distribution of the critical steady state rainfall value, interpreted as a relative hazard for shallow landsliding. For coarser resolutions, the smoothing effect results in a larger area being excluded from the valid critical rainfall range and those parts are classified as unconditionally stable or unstable. When applying simple empirical soil redistribution algorithms, not only the lower initial amount of failing cells with coarser resolution but also the inclusion of slope(limit) in the algorithms becomes apparent. Although the model was not developed specifically to address quantitative landslide erosion and sedimentation rates, the amounts of eroded and deposited material were calculated for different scenarios and DEM resolutions. For smaller cell sizes, much higher amounts of soil redistribution were found, all caused by the much more detailed landscape representation. Looking at spatial patterns of landslide erosion/sedimentation, the percentages of the area being affected by erosion or sedimentation show a similar trend. Also larger parts of the area tend to be involved in landslide erosion than deposition in general, although the total quantities of soil material eroded and deposited are the same. When comparing landslide hazard maps between model scenario runs to visualise feedback mechanisms between soil failures over time, more variation is encountered with finer resolutions and higher percentages of the area have an increased or decreased landslide hazard. When the percentages of the area of sites with lower and higher hazard are compared, finer resolutions and lower critical rainfall thresholds tend to increase the total extent of areas becoming more stable.

As a general conclusion it can be stated that extreme care should be taken when quantifying landslide erosion or sediment yield by applying simple soil redistribution formulas to DEMs with different resolutions. Calculation of erosion and sedimentation quantities can still be useful but these should rather be interpreted as relative amounts. For evaluation of shallow landslide distribution and the effect on landscape dynamics over long terms, the 'perfect' DEM resolution will not exist because no resolution can, even for a small study area, represent the dimensions of all possible slope failures scattered in space and time. The choice of DEM resolution may be restricted by data availability in the first place but should always be done in the context of a particular type of analysis. When long term landslide hazards and soil redistribution patterns are for example used to explain vegetation patterns, working at the scale of a single tree, even the 10 m DEM will probably be too coarse, whereas for broader vegetation classes, 50 m cells will possibly give a reasonable result. A coarse resolution DEM may appear to be of very poor quality, but if it can produce good results, then its quality is certainly satisfactory for that particular application. Furthermore it must be stressed that the topographical and hydrological characteristics of different landscapes can vary quite fundamentally. The choice of DEM resolution should always be made against the background of the distribution of these attributes within a study area and a sensitivity analysis of the model using them. Ideally, a DEM should represent the topographical and hydrological properties derived from it in such a way that neglecting features which are possibly 'filtered out' does not harm the quality of the model outcome. DEM resolution is context dependent and in the example in this chapter, creates a threshold of (in)sensitivity to shallow landslide hazard calculation. Assessing these sensitivities forms an essential part of good modelling practice.



Chapter 5

Landslide Magnitude and Frequency

In this chapter, a sediment record is used, in combination with the LAPSUS-LS model, to reconstruct the incidence of high-magnitude/low-frequency landslide events in the upper part of the Waitakere River catchment and the history of the Te Henga wetland at the outlet. Sediment stratigraphy and chronology are interpreted by radiocarbon dating, foraminiferal analysis, and provisional tephrochronology. Gradual impoundment of the wetland began c. 6000 cal yr BP, coinciding with the start of a gentle sea-level fall, but complete damming and initial sedimentation did not begin until c. 1000 cal yr BP. After damming, four well-defined sediment pulses occurred and these are preserved in the form of distinct clay layers in most of the sediment cores. For interpreting the sediment pulses, the LAPSUS-LS model is applied to determine spatially distributed relative landslide hazard, applicable at the catchment scale. An empirical landslide-soil redistribution component is added to determine sediment delivery ratio and the impact on total catchment sediment yield. Sediment volumes are calculated from the wetland cores and corresponding landslide scenarios are defined through back-analysis of modelled sediment yield output. In general, at least four major high-magnitude landslide events, both natural and intensified by forest clearance activities, occurred in the catchment upstream of Te Henga wetland during the last c. 1000 years. Their magnitude can be expressed by a range of critical rainfall thresholds representing a LAPSUS-LS scenario.

5.1 Introduction

In many geomorphological settings, shallow landsliding is one of the most important components of hillslope denudation and therefore can play an important role in determining catchment sediment yield. Because the actual triggering of shallow landslides by rainfall

Based on: Claessens L., Lowe, D.J., Hayward, B.W., Schoorl, J.M. and Veldkamp, A., 2005. Reconstructing high-magnitude/low-frequency landslide events based on soil redistribution modelling and a Late-Holocene sediment record from New Zealand. *Geomorphology*. Submitted.

© 2005 Elsevier Science B.V.

events, and the consequent amounts of erosion and deposition, are highly dependent on (natural or human-induced) land use and land-cover changes, there is an increased need for methodologies that can assess the effects of these changes on landslide occurrence and catchment sediment yield (Burton and Bathurst, 1998; Glade, 2003). Furthermore, there is a lack of understanding of the possible linkages between climate change and corresponding change of geomorphic activity and resulting sediment yield (Evans and Slaymaker, 2004). The relation between sediment production in upland areas and the sediment yield at a basin outlet has been the subject of research for over half a century (Glymph, 1945). Understanding the connections between cause and response, however, remains far from complete (Trustrum et al., 1999). Despite a relatively good understanding of the mechanics of individual landslides (e.g. Selby, 1993), few studies have analysed the cumulative effects of soil redistribution by landsliding over large spatial and (or) temporal scales (Martin et al., 2002; see also Chapter 3). As sediment derived from landsliding is generated and transported mainly during extreme rainfall triggering events with a low frequency of occurrence, studying the link between spatial and temporal occurrence of these events and the resulting sediment yield is of great interest.

A major obstacle when assessing rates of landsliding is the difficulty of obtaining data that are relevant over medium to long time scales. Longer term magnitude-frequency distributions of landslides are usually estimated from rates over decadal time scales derived from large inventories of aerial photographs (Hovius et al., 1997; Jakob, 2000; Martin et al., 2002). Analytic expressions such as power-law models are then fitted through probability density functions for empirically derived landslide properties such as area or volume. Other researchers try to link climate data with landslide inventories and identify e.g. the magnitude of storms that trigger landslides (Crozier, 1996; Glade, 1996). Relationships between the frequency of landslide-generating storms and mean annual rainfall (Hicks, 1995) or between rainstorm magnitude and landslide frequency (Page et al., 1999; Reid and Page, 2003) have also been established.

In general, the temporal resolution for most magnitude-frequency analyses is rather short for the largest events to be properly represented. Sediment yield resulting from landsliding within a catchment could be translated into process magnitude and frequency if it is transported out of the catchment and trapped in a lake or swamp. Lake or swamp sediments are the product of the environmental processes, physical, biological and chemical, that have been operating within the surrounding catchment. They provide a record of the timing and magnitude of environmental processes, both natural and human-induced (Goff et al., 1996; Page and Trustrum, 1997). Unlike on hillslopes, where contemporary processes destroy the evidence of earlier erosion events, lake sediments have the potential to provide an undisturbed record over a long time frame (Brunsdon, 1993). When large rainstorms are the main cause of erosion, as is the case in many New Zealand steeplands (De Rose et al. 1993; Page et al. 1994a; Glade, 2003), lake sediments can provide more information about the cumulative effects of these episodic events (Page and Trustrum, 1997; Trustrum et al., 1999). Furthermore, recent research on sediment budgets, river discharge and suspended sediment load suggests that most of the sediment transported by streams and deposited in lakes or swamps originates from landslides and landslide-gully complexes in the upland catchment (e.g. Page et al., 1994a; Eden and Page, 1998; Hicks et al., 2000). Especially in smaller basins, magnitude-frequency relationships for landslide erosion and sediment deposition seem to be closely related and high-magnitude/low-frequency landsliding events are often responsible for most of the

deposition (Hovius et al., 1997; Trustrum et al., 1999). In larger basins, by contrast, landsliding makes a smaller relative contribution to catchment suspended sediment yield than does that arising from other processes (e.g. gullies, sheetwash, and fluvial erosion).

Many researchers have used sediment records preserved in lakes or swamps to assess magnitude and frequency of sediment production in the upland area and the resulting sediment yield (Owens and Slaymaker, 1993; Page et al., 1994a, 1994b and 2004). Sediment records of lakes are studied mostly by extracting and interpreting sediment cores. The stratigraphy and chronology of these cores is often established by a combination of techniques which include radiocarbon dating, ^{210}Pb and ^{137}Cs dating (Goff et al., 1996; Newnham et al., 1998; Trustrum et al., 1999), pollen and diatom analysis (Page and Trustrum, 1997; Sandiford et al., 2003), and tephrochronology (Lowe and Green, 1987; Eden and Page, 1998; Evans and Slaymaker, 2004).

Calculation of sediment yields is conventionally undertaken by converting sediment thicknesses in individual cores to volumes by averaging across the lake area (Foster et al., 1990). Other approaches incorporate spatial variability within a lake by combining individual core volume estimates with the area of Thiessen polygons constructed around the core location (O'Hara et al., 1993). Evans and Slaymaker (2004) used a regression model of the accumulation surface to predict sediment accumulation with error intervals for each core.

The relation between upland erosion and sediment yield is complex because not all material detached from hillslopes will reach the sediment reservoir (Owens and Slaymaker, 1993). Material deposited in a reservoir may represent only a small fraction of that mobilised within the catchment (Walling, 1983). Several sources of error occur when reservoir sedimentation data are transferred into sediment yield and erosion rates for the upland catchment (see review in Butcher et al., 1993). To make this conversion, it is necessary to know the sediment delivery ratio, the ratio between total erosion on hillslopes within a catchment, and sediment delivery to the stream network. Delivery ratios are scale-dependent and catchments of $<10\text{ km}^2$ show maximum sediment yields per unit area compared with intermediate yields in the largest systems (Butcher et al., 1993). Increasing rainfall also influences the delivery ratio: during high-magnitude events, ratios are usually very high (up to 0.7, Trustrum et al., 1999). Variations in sediment delivery ratio have also been studied to assess the relation between land use change and erosion (Page et al., 1994a; Page and Trustrum, 1997; Trustrum et al. 1999; Glade 2003).

Several studies have attempted to link extrapolated erosion rates from measurements at a particular site (sediment loads) to the total catchment sediment yield (Caine and Swanson, 1989; Hattanji and Onda 2004). Dearing and Foster (1993), however, argued that a monitored record of sediment yield may remain constant or may fluctuate wildly without giving any clues as to what is actually happening in the catchment. Other researchers have analysed landslide characteristics from large field and (or) aerial photograph inventories to estimate landslide volumes, frequencies and sediment yields (e.g. Hovius et al., 1997; Page et al., 1999; Jakob, 2000; Martin et al., 2002). Other methods for estimating total landslide sediment volumes include statistical (sample) techniques applied to field data (Megahan et al., 1991; Page et al. 1994a), or cut-and-fill calculations based on pre-landslide and post-landslide surfaces from a digital elevation model (DEM) (Korup et al., 2004).

Only a few studies have used erosion/sedimentation modelling to calculate amounts of landslide sediment volumes and/or sediment yields from a catchment. Spatially distributed erosion and sedimentation models have long been restricted to processes dealing with surface

erosion by overland flow (e.g. Wicks and Bathurst, 1996). Istanbuloglu et al. (2004) modelled the effects of forest vegetation and disturbances on total sediment production by several erosion processes (runoff, creep, gully erosion and landsliding). Recently, models have been developed to assess the spatial patterns and effects of landslide erosion and deposition within a catchment (e.g. LAPSUS-LS, Chapter 3); some models also deal with the resulting sediment yield and delivery ratio (Burton and Bathurst, 1998). Bathurst et al. (1997) tested several empirical modelling approaches for determining the delivery ratio of landslide sediment to streams and the resulting sediment yield. These models are simple relationships that estimate landslide runout distance from slope geometry. Another statistical model estimating sediment delivery directly has been tested. In general, none of the models was completely accurate. Burton and Bathurst (1998) built on Vandre's (1985) model to estimate runout distance, and incorporated this formula in a spatially distributed landslide hazard and soil redistribution model. Regarding the spatial pattern of landslide sediment delivery, the LAPSUS-LS approach is based on the principles of this model (see also Chapter 3).

5.2 Materials and methods

5.2.1 Study area

Waitakere River catchment

The Waitakere River catchment is situated in the central part of the Waitakere Ranges (Fig. 5.1). The catchment is approximately 31 km² and its mean elevation is 175 m asl. After partial forest clearance by early European farmers during the second half of the 19th century (Hayward and Diamond, 1978), much of the area is now covered with regenerating native vegetation but patches of undisturbed rainforest remain. Although landslides are usually less common under forest than under, e.g. pasture because of protection by vegetation cover and reinforcement by tree root systems (Phillips and Watson, 1994), they are still the dominant erosion process in the study area (see other examples in Crozier et al. 1992; Eden and Page, 1998; Moon et al., 2003). The Waitakere Reservoir was constructed on the headwaters of the Waitakere River in 1910 to contribute to Auckland's water supply. This obviously affected the natural river flow and reduced both the mean stem flow and peak flows (Watercare Services Ltd., 2001).

Te Henga wetland

The Te Henga wetland (also known as Bethells swamp) is situated in the northern part of the Waitakere Ranges and forms the outlet of the Waitakere River to the Tasman Sea. The wetland is ~1.7 km² and was impounded by a landward-prograding dune complex in a similar way to that for nearby Lake Wainamu (Fig. 5.1). The Late Holocene coastal 'blacksand' of the dune complex (Mitiwai Sand, Hayward, 1983; Karioitahi Group, Isaac et al., 1994) is present in beach and dune deposits along the west coast of the Waitakere Ranges. The sands are erosion products primarily of Quaternary andesitic volcanic and volcanoclastic rocks of western Taranaki and the central North Island. They have been transported along shore by shallow marine currents and were subsequently concentrated by wave and wind action into beach and dune lag deposits (Edbrooke, 2001). The moving dune fields have probably accumulated within the last c. 1300 cal years based on entrapment of Te Henga by the equivalent of dune belt 4 (c. 1500-300 ¹⁴C years ago) as described by Schofield (1975) and

Low and Green (1987) for the South Kaipara Barrier that lies to the north. The wetland has a very high ecological value and its extent and quality are of regional significance in the Auckland area (Denyer et al., 1993). Archaeological evidence suggests that forest around the wetland was cleared during early Polynesian (Maori) settlement around the margins of the wetland (Diamond and Hayward, 1979; Hayward and Diamond, 1978). It was filled substantially with sediments from upstream by the time of the arrival of the first European settlers in the early 19th century (Waitakere Ranges Protection Society, 1979). A flax mill operated around the head of the wetland from 1880-1890 (Hayward and Diamond, 1978). In the 1920s, kauri tree logging and milling activities took place and a launch towed logs through the wetland (Diamond and Hayward, 1980). Whereas the Waitakere Dam upstream reduces peak flows in the wetland at present, the flood storage available within the wetland system has a greater impact on hydrological conditions than the influences of the dam (Watercare Services Ltd., 2001). Near the outlet of the wetland, the small Mokoroa and Wainamu streams also drain into the wetland but contribute little to the sediment delivery because of low geomorphic activity and damming by dune-impounded Lake Wainamu upstream, respectively.

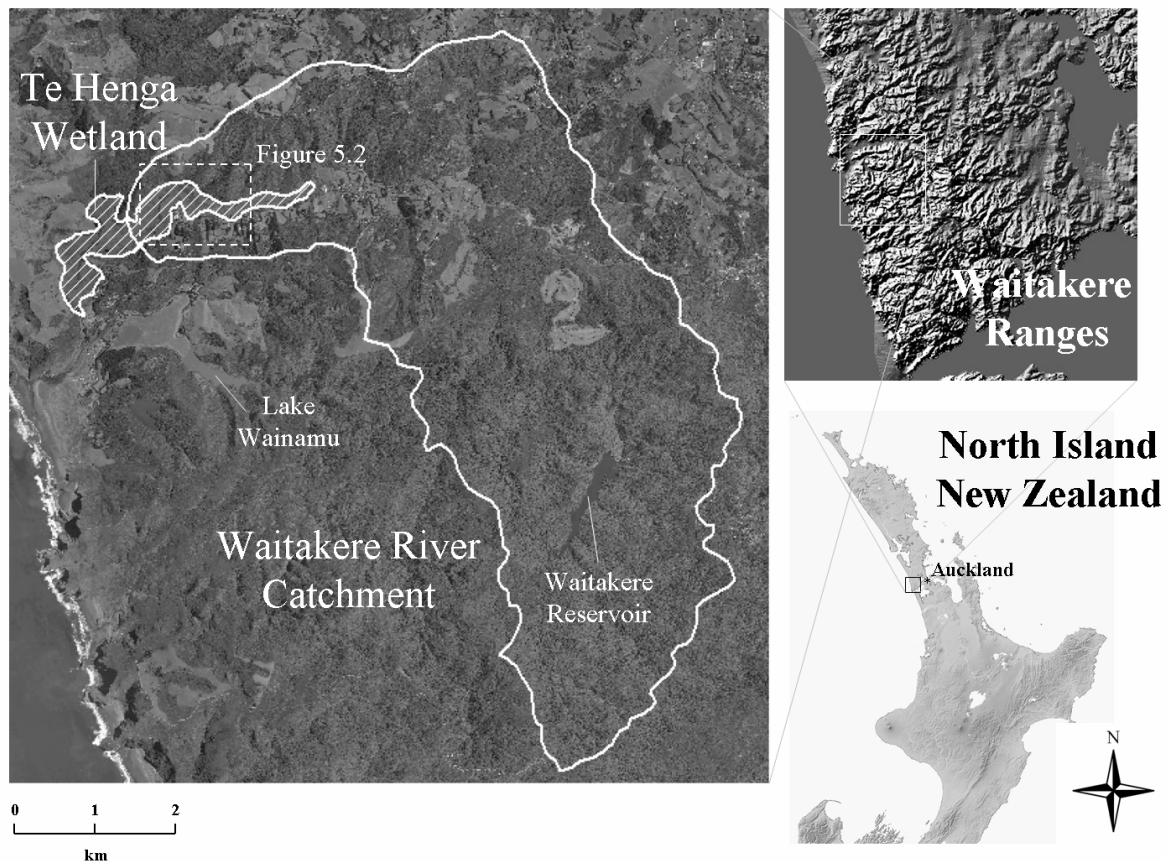


Fig. 5.1 Location of the Waitakere River catchment and other localities referred to in the text.

5.2.2 LAPSUS-LS, delivery ratio and sediment yield

A spatially explicit relative hazard for shallow landsliding is calculated with the LAPSUS-LS model, described in Chapter 3 (Q_{cr} [m day⁻¹], Eq. (3.4)). The impact of landsliding on basin sediment yield depends on whether the eroded material is deposited in, and transported by the

stream network. The percentage delivery or delivery ratio is dependent on the interaction between landslide soil redistribution patterns and channels able to route and transport the material further towards the catchment outlet. Instead of estimating or extrapolating delivery ratios and sediment yields from site measurements or large field inventories, in this application the amount of sediment yield is determined from the modelled spatial pattern of soil redistribution and the consecutive interaction with a topographically delineated stream network. Landslide material displacement was modelled using Eqs. (3.9) to (3.12). For determining the stream network, different methods are available, ranging from specified contributing area and/or slope thresholds (e.g. O’Callaghan and Mark, 1984; Martin et al., 2002) to the use of upward curved grid cells (Tarboton, 2000) and grid network pruning by order (Peckham, 1998). For this application, the sediment transporting stream network was determined by simply specifying a minimum contributing area threshold. Flow direction was assigned according to the steepest descent, and flow accumulation was calculated as a measure of the drainage area in number of grid cells (this method is typically called ‘D8’ algorithm, Fairfield and Leymarie, 1991). All grid cells draining more than a threshold drainage area are defined as part of the stream network and able to transport landslide material to the catchment outlet. When a grid cell, which is part of the depositional pathway of a landslide, intersects with a grid cell from the transporting stream network, the remaining sediment budget of that grid cell, according to Eq. (3.12), is added to the catchment sediment yield.

By modelling the spatial pattern of landslide soil redistribution and the interaction with the channel network, buffering of the depositional response by temporary storage of landslide material on footslopes is taken into account. If the depositional pathway does not cross a transporting channel, the landslide material is not delivered to the outlet but remains on the slope and hence excluded from the sediment yield. The delivery ratio is also determined by use of this method (and does not have to be estimated): deposition that occurs out of reach of a channel able to transport the material is not added to the sediment yield.

Determining the stream network by assigning a threshold value of contributing drainage area, calculated from the DEM, implies that delineated streams are assumed to be able to transport the sediment in its entirety to the catchment outlet. Field evidence supports this assumption: even shortly after sediment-producing events, the streams in the study catchment contain little suspended sediment and stream beds appeared as bare rock.

As described in Chapter 3, data requirements necessary for applying LAPSUS-LS are good quality topographical information and some geotechnical soil parameters. For the study area, a DEM with a 25-m grid resolution was derived from vector line and point data sourced from the topographic database from Land Information New Zealand. Values for T , C , ρ_s and ϕ are based on field and laboratory measurements (Table 3.1 and 3.2). The default settings of the empirical parameters used in the soil redistribution algorithms (Eqs. (3.9)-(3.12)) are based on field evidence and literature and further subjected to a sensitivity analysis. The ‘runout fraction’ ϕ was set at 0.4 and the slope angle α , at which deposition begins, was set at 10° (Vandre, 1985; Burton and Bathurst, 1998). The threshold value of contributing area for stream development and the threshold critical rainfall for landslide initiation are both scenario dependent and also further analysed regarding model sensitivity (paragraph 5.3.1).

As in Chapter 3, calibration concerning the location of landslide initiation sites has been undertaken on the basis of fieldwork and a series of aerial photographs covering a limited timeframe. It is very likely that high-magnitude/low-frequency events are not all correctly

represented and are underestimated in the dataset. Building model scenarios based on the long-term sediment record of the wetland will give an indication about the relative importance of these events over time.

5.2.3 Sediment record

Core stratigraphy and chronology

A corer with a diameter of 2 cm and extensions up to 5 m in total length was used in February and March, 2003, to obtain a detailed record of sediments across the wetland (Fig. 5.2). Stratigraphy, texture, colour, sorting, degree of weathering and type of organic material and content were described.

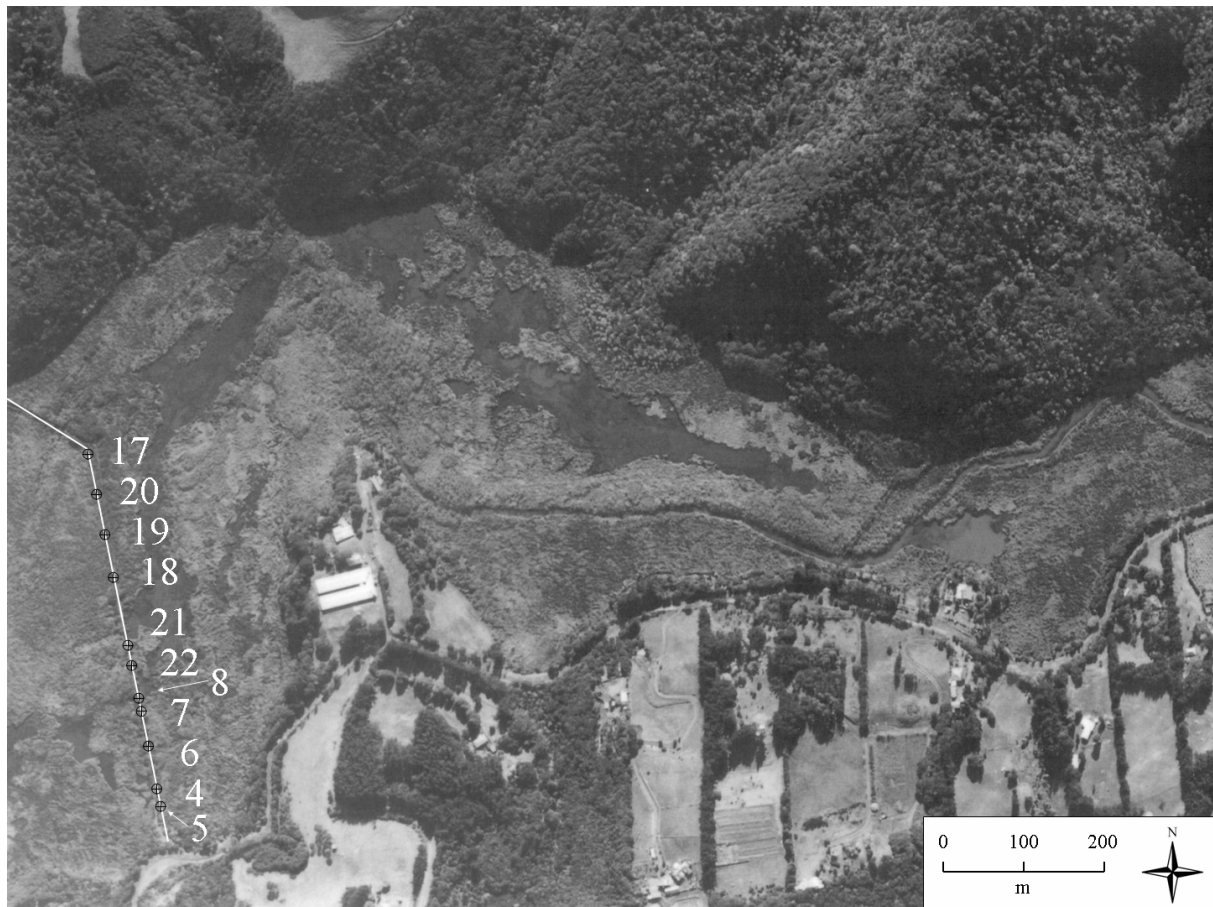


Fig. 5.2 Air photo detail of Te Henga wetland and location of transect and sampling points.

The chronology of the cores was established using radiocarbon ages and tentative tephra correlations based on microprobe analyses of glass. Two samples for ^{14}C dating were taken from core 6 that straddled a well-defined sediment pulse seen in nine of the eleven cores along the transect. It was hypothesised that the dates from this core would indicate the frequency of occurrence of sediment pulses with magnitudes calculable from the stratigraphy. Two other ^{14}C samples were taken from cores 18 and 22 at ~4 m depth, where a thin tephra layer was present. Because this part of the core is situated within the sand phase of the record (i.e. before the lake was completely dammed and sedimentation started), and around the

transition from coarse to fine sand, these dates would enable a maximum age to be assigned to the initial impounding of the wetland.

Correlation and dating of tephra layers for providing a chronology for sedimentary records has been described in Chapter 2 (Section 2.3.2). Two thin rhyolitic tephra deposits were identified in Te Henga wetland, probably reworked in the wetland sediment record rather than in their primary form (e.g. see Moore, 1991). Major element compositions of glass shards of the two tephra deposits were analysed by electron microprobe (see also Section 2.3.2).

Foraminiferal analysis

The occurrence of fossil benthic foraminifera has been documented in many marine and brackish environments around the New Zealand coast (Hayward et al., 1999). Interpretation depends on knowledge of their present-day ecological distribution in sheltered harbours and tidal inlets in northern New Zealand. These studies have shown that tidal elevation and salinity are the major environmental factors influencing benthic foraminiferal distribution in these settings (e.g. Hayward et al., 1999, 2004). Sand layers in core 18 contained shells and benthic foraminifera which could indicate changes in marine or tidal influence and possibly give insight to the sedimentation history of the wetland. For the analysis, an approximate volume of 5-10 cm³ sediment per sample was taken. The mud fraction (<63 µm) of the sediment samples was washed out and the foraminifera were concentrated by floating on heavy liquid for searching with a microscope.

5.3 Results and discussion

5.3.1 LAPSUS-LS and sediment yield

Sensitivity analysis

After calculation of relative landslide hazard for the catchment (Eq. (3.4)), four parameters remain essential in constructing model scenarios for the subsequent soil redistribution and sediment yield. A sensitivity analysis is shown in Fig. 5.3, a plot of the changes in the model caused by varying one parameter but keeping others constant (default value) (Table 5.1). The slope limit for landslide erosion α determines where the erosional phase halts and the deposition begins. If this slope limit is raised, less total landslide erosion (and deposition) occurs and, as a consequence, the delivery ratio and sediment yield are lowered as well. The runout fraction ϕ determines the total reach of the depositional phase. It has no influence on the total amount of erosion but increases the delivery ratio and sediment yield when raised because more material reaches the stream network. By increasing the threshold contributing area for determining a sediment transporting stream, the stream network becomes less dense and a lower sediment yield and delivery ratio are obtained. The model is very sensitive in the lower range of threshold contributing area values; the stream network becomes so dense that almost all landslide material is intercepted and the delivery ratio tends towards 1.0. The critical rainfall threshold (Q_{cr}) represents the landslide scenario and all grid cells with a value equal to or lower than the threshold fail and induce erosion and sedimentation. Much higher amounts of erosion are obtained when the threshold critical rainfall is raised because more grid cells, with a progressively lower landslide hazard, fail and cause soil redistribution.

| Scenario | Threshold Contributing Area [#grids] | Critical Rainfall Threshold [m day ⁻¹] | Landslide Erosion [m ³] | Sediment Yield [m ³] | Delivery Ratio [-] |
|----------|--------------------------------------|--|-------------------------------------|----------------------------------|--------------------|
| Default | 500 | 0.02 | 222857 | 57061 | 0.26 |
| 1 | 100 | 0.02 | 222857 | 86222 | 0.39 |
| 2 | 100 | 0.05 | 511037 | 201761 | 0.39 |

Table 5.1 Modelling results for landslide scenarios with varying thresholds for critical rainfall and contributing area for stream development.

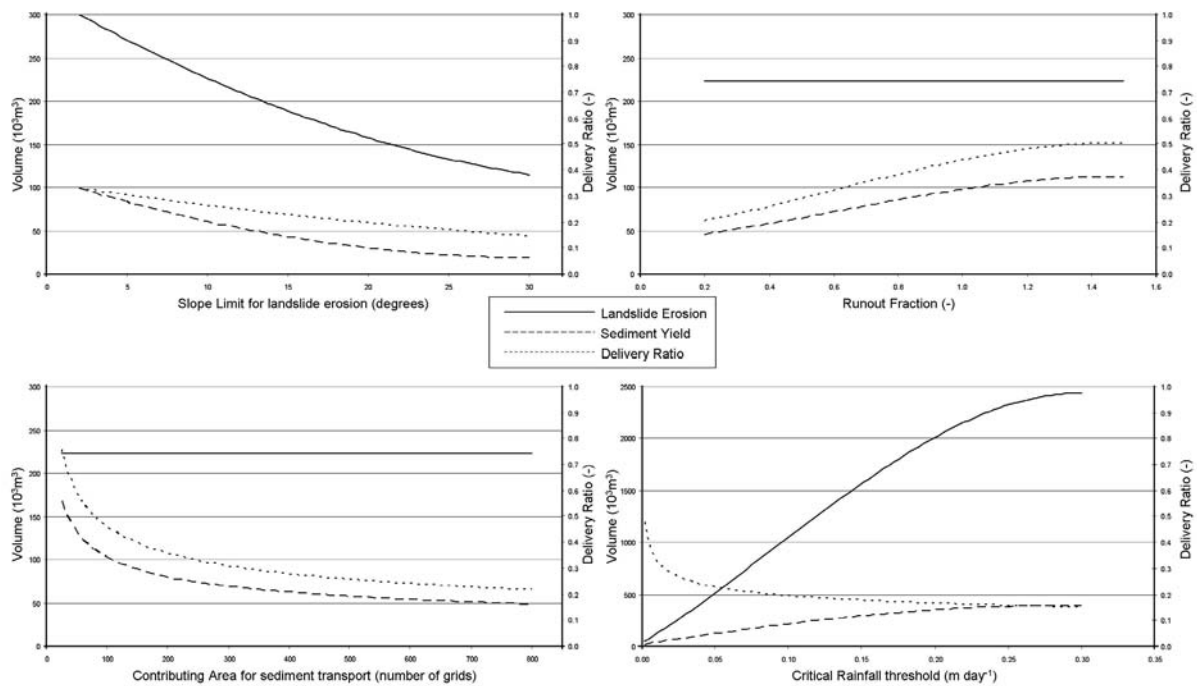


Fig. 5.3 Sensitivity analysis for sediment yield related parameters in LAPSUS-LS.

Landslide scenarios and sediment yield

The sensitivity analysis (Fig. 5.3) shows that the slope limit for landslide erosion and the runout fraction have relatively small influences on modelling results for delivery ratio and sediment yield. Concerning the threshold contributing area for determining the stream network, it is an issue to decide the most appropriate minimal contributing area representing a stream, here capable of transporting sediment, or whether some other attribute such as slope should be part of the threshold (Tarboton et al. 1992; Montgomery and Foufoula-Georgiou 1993). The choice of the threshold value is important in approximating the actual shape of the stream network and in obtaining accurate stream flow hydrographs as well. An arbitrary threshold value is usually chosen on the basis of visual similarity between the extracted network and topographic maps. However, in many cases this method poorly represents channel networks observed in the field because first-order channels and many second- and third-order channels may not be determined. Tarboton et al. (1992) suggested selecting the appropriate contributing area threshold for determining the channel network from an

inflection in the drainage area-slope relation for averaged data. Montgomery and Foufoula-Georgiou (1993), however, discussed conceptual and procedural problems with this approach. Because sediment is transported typically by higher-order streams, a very accurate extraction of all lower-order streams is not required for this application. A threshold contributing area of 400 grid cells (0.25 km²) shows a good visual similarity with streams indicated on the topographic map (sheet Q11 & Pt. R11), which are streams with a minimum length of 500 m (Land Information New Zealand, 2000). Furthermore, the modelling results for delivery ratio and sediment yield are relatively insensitive in this range of contributing area thresholds (300-500 grid cells, see Fig. 5.3).

The critical rainfall threshold largely defines the landslide scenario and strongly influences the modelling outcomes for delivery ratio and sediment yield. Table 5.1 illustrates three examples of scenarios in which the critical rainfall threshold and the threshold contributing area are both varied. Slope limit and runout constant were kept fixed at 10° and 0.4, respectively. Defining a denser channel network in scenario 1 resulted in a higher sediment yield and delivery ratio than for the default scenario. By raising the critical rainfall threshold in scenario 2, landslide erosion and sediment yield increased but there was no change in delivery ratio. The spatial patterns and interactions between landslide processes and channel network delineation for the three scenarios are shown in Fig. 5.4.

5.3.2 Sediment record interpretation

Core stratigraphy and chronology

The stratigraphy of the eleven sediment cores is shown in Fig. 5.5. Depths are given relative to the level of the causeway (which is less than 1 m above the mean wetland water level and 3-4 m above mean sea-level). Below ~3 m depth, the cores consist of Holocene sand. A transition from coarse to finer sand occurs from ~3.5 m upwards. An irregular but clear boundary (varying between 300 and 266 cm) marks the start of sedimentation in the wetland, i.e. after it had become completely dammed by a landward-prograding dune system. The wetland acts as a highly efficient sediment trap, especially in terms of episodic or event-based input fluxes. The wetland is a very shallow lake, densely populated with vegetation (mostly reed), except for the main channels, which are the deeper parts, draining the wetland. In the vegetated 'basins', water flow is seriously reduced, suspended clay particles can easily settle and consequently the thickest clay layers are evident. These basins receive only water-containing sediments when significant extra water enters the wetland, typically during high-magnitude/low-frequency events triggering landsliding in the upstream catchment. In this way, the system works in a similar fashion as occurs, for example, in the marshes in the Wolga delta (Overeem et al., 2003). Most of the cores exhibited four well-defined grey homogeneous clay layers, interspersed with peat and/or organic-rich mud, enabling correlation between cores to be made on the basis of these visible lithological changes. The sediment pulses are interpreted to represent high-magnitude landslide erosion events being preserved as overbank deposits of the main channels draining the wetland. Cores 18 and 21 lacked the sediment pulses, this lack being attributed to the core positions within the main channel draining the wetland where sediment is not preserved. Two fine tephra layers were identified in the sediment cores, both containing rounded pumice gravels/lapilli (3-8 mm in diameter) and so most likely have been reworked. Reworked, stranded tephra deposits are widely reported at coastal sites in New Zealand, especially along the North Island's east coast, and are generally attributed to sea-raftering processes (e.g. McFadgen 1989; Lowe and de Lange,

2000). A very thin tephra layer was present in eight of the eleven cores around ~ 3 m, in the upper part of the (fine) sand phase. A second tephra layer was identified in five cores at a depth of ~ 4 m, around the transition from coarse to fine sand (Fig. 5.5).

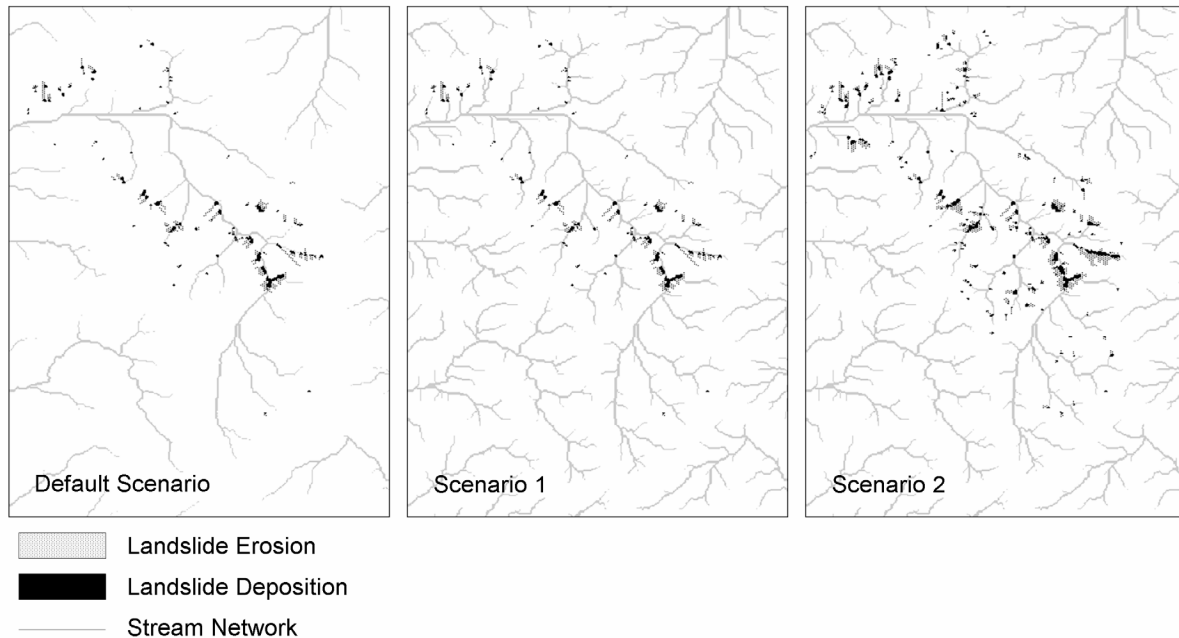


Fig. 5.4 Spatial patterns of landslide soil redistribution for scenarios presented in Table 5.1.

Four stratigraphic positions in cores 6, 22 and 18 were radiocarbon dated (Table 5.2). Electron microprobe analyses of the two tephra beds (T4 and T22), and tentative correlatives, are presented in Table 5.3. The glass shards are rhyolitic, have high FeO and CaO contents and thus are compositionally closely matched with glass from Holocene eruptives of Taupo caldera volcano (e.g. Stokes et al., 1992; Lowe et al., 1999; Shane, 2000). The radiocarbon samples from cores 18 and 22 were taken 15 and 19 cm above the deepest tephra layer (T22), respectively. The radiocarbon ages, stratigraphy and probable reworking in the wetland suggest that tephra T22 probably correlates with Taupo-derived tephras ranging from 6000-10,000 cal yr BP in age. When comparing glass chemistry (Table 5.3), Motutere Tephra (6650 cal yr BP) remains as the most plausible correlative (also referred to as Unit G in Wilson, 1993). Because this sequence is present just under the transition from coarse to finer sand, an approximate date of c. 6000 cal yr BP is proposed as the time when a dune system gained influence and started to gradually block off the valley and impound the wetland. This transition also follows the start of a gentle sea-level fall of ~ 2 m after it reached its maximum height ~7000 cal yr BP (Gibb, 1986) and a change in tidal influence is also confirmed by the foraminiferal record (see below). The second tephra layer T4, which occurs in the upper part of the sand phase, provides a probable marker for the time the dune system completely dammed the wetland and freshwater sedimentation started. However, no dateable material was found in its vicinity. Taking into account the radiocarbon age of material above the first sediment pulse (~ 500 cal yr old, Fig. 5.5), correlation with tephra deposits ranging in age from 1500–3000 cal yr BP is suggested. Based on glass composition, Mapara Tephra (2160

cal yr BP) seems the most plausible correlative for T4 (Table 5.3; Unit X in Wilson, 1993). Taking into account the seemingly slow deposition rates in the sand phase (only ~1 m in 4500 cal yrs), the age of complete damming of the wetland is estimated at c. 1000 cal yr BP. This estimate is consistent with other indications (stratigraphic relationships in unpublished reports), implying moving dune fields on the west coast of Auckland have accumulated within this time period, as noted earlier.

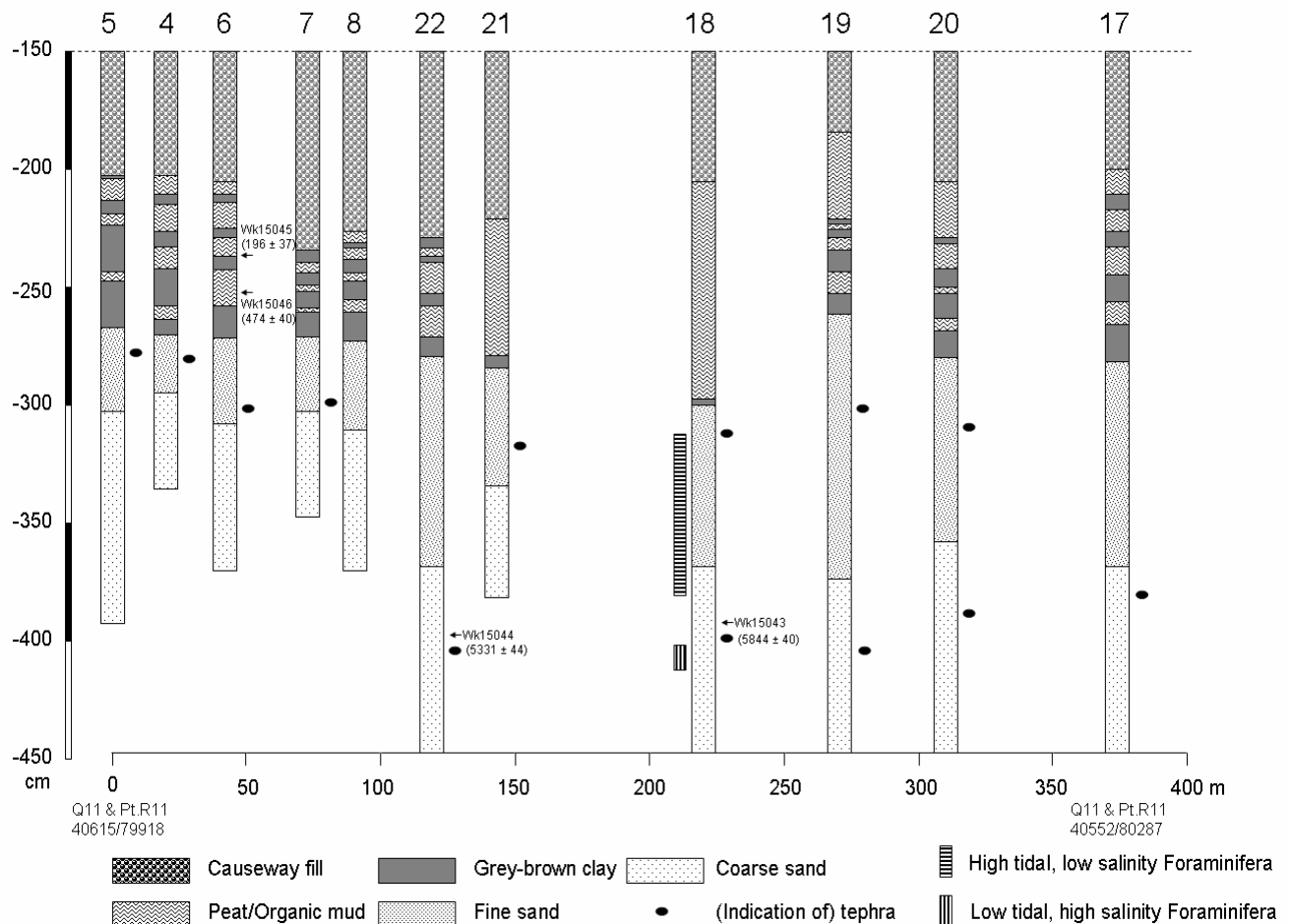


Fig. 5.5 Stratigraphy of Te Henga wetland cores. Wk: Waikato Radiocarbon Dating Laboratory number. Ages in conventional (Libby) radiocarbon years BP (see Table 5.4).

Foraminiferal analysis

The samples from core 18 provided clear evidence that at least a 1-metre interval (320–435 cm) accumulated in a sheltered estuarine environment (Tables 5.4 and 5.5). The upper two foraminiferal samples in this interval (320, 385 cm) contain rare agglutinated foraminifera typical of high tidal, low salinity salt marsh. The shells from the interval 412–435 cm and the lowest foraminiferal sample (431–435 cm) from the same interval comprise faunas that live preferentially in unvegetated, intertidal (low-mid tide) mud or sand flats in sheltered inlets and harbour edge settings with near normal or slightly reduced salinities. The abundance of *Arthritica bifurca* suggests that a lower tidal elevation was more likely. The specimen of the small, narrow limpet *Notoacmea helmsi scapha* provides evidence for the presence of *Zostera*

seagrass because this limpet is adapted to living on its narrow blades. The single specimen of the foraminifer *Zeaflorilus parri* lives only in shallow subtidal exposed environments and must have been washed into the estuary from the open coast. Core 18 contains fossil evidence for the former presence of a sheltered estuary where Te Henga wetland now exists. The interval shallows, presumably with sediment accumulation from low tidal, moderately high salinity, sand flats up to a high tidal lower salinity salt marsh. This transition occurred ~6000 cal yr BP, estimated according to the stratigraphy, the ^{14}C dates and occurrence of (probable) Motutere Tephra (Table 5.3). Subsequent compaction may account for some of the difference between the thickness of the sequence and the indicated shallowing of ~ 2.5-3 m (with respect to the tidal range). The transition also coincides with the start of the ~ 2 m sea-level fall since ~7000 cal yr BP (Gibb, 1986).

| Core number + Depth [cm] | Laboratory Number ^a | Conventional age ^b [^{14}C yr] | Calibrated age range [yr BP] + Probability [%] ^c | $\delta^{13}\text{C}$ [‰] ^d | Material |
|-----------------------------|-----------------------------------|--|---|---|-------------------|
| 18 (400) | Wk15043 NZA20362 | 5844 ± 40 | 6730-6490 (95.4) | -26.8 | Charcoal |
| 22 (420) | Wk15044 NZA20363 | 5331 ± 44 | 6200-5940 (95.4) | -24.5 | Charcoal/ Wood |
| 6 (231) | Wk15045 NZA20221 | 196 ± 37 | 300-60 (79.0) | -28.7 | Peat |
| 6 (242) | Wk15046 NZA20222 | 474 ± 40 | 550-430 (91.6) | -29.2 | Peat |

All ages determined by AMS (Accelerator Mass Spectrometry).

^a Wk refers to Waikato University Radiocarbon Dating Laboratory; NZA refers to the Rafter Radiocarbon Laboratory (Institute of Geological & Nuclear Sciences, Lower Hutt, New Zealand).

^b Ages in conventional radiocarbon years BP (Before Present where 'present' is AD1950) ± 1 Standard Deviation. Ages based on Libby half-life of 5568 for ^{14}C (Stuiver and Pollach, 1977), with correction for isotopic fractionation ($\delta^{13}\text{C}$) applied.

^c All ages were calibrated using the OxCal calibration program applying the IntCal98 calibration curve (Stuiver et al., 1998).

^d Parts per thousand difference (per mille) between the sample carbon 13 content and the content of the international PDB standard carbonate (Aitken, 1990); PDB refers to the Cretaceous belemnite formation at Peedee in South Carolina, USA.

Table 5.2 Radiocarbon dates for core samples from Te Henga wetland.

Sediment pulses and corresponding landslide scenarios

Nine out of the eleven sediment cores, on both sides of the main channel (cores 18 and 21), exhibited four well-defined clay sediment pulses (Fig. 5.5). Sediment thickness and estimated sediment volumes can be used as a surrogate for the amount (magnitude) of erosion in the catchment. Together with some age control, frequencies of occurrence of the sediment producing landslide events can be established. Several sources of error are often involved in sedimentation surveys and especially in the calculation of sediment volumes (Butcher et al., 1993). Various authors have stressed the importance of the variation of the bulk density of sediments both between and within reservoirs and changes of volumes with compaction over time (Rausch and Heineman, 1984; Pizzuto and Schwendt, 1997). Other researchers, however, concluded that the bulk densities of deposits from storm sediment pulses in cores showed little variation both between and within cores (Page et al., 1994b).

| T4 | Mapara (Unit X) [§] | Whakaipo (Unit V) | Waimihia (Subunit S1) | Taupo (Subunit Y5) |
|--------------------------------|------------------------------|--------------------------|--------------------------|---------------------|
| SiO ₂ | 76.27 (0.76) | 77.91 (0.26) | 76.22 (0.19) | 75.79 (0.31) |
| Al ₂ O ₃ | 12.81 (0.07) | 12.48 (0.07) | 13.03 (0.19) | 13.23 (0.13) |
| TiO ₂ | 0.15 (0.06) | 0.16 (0.05) | 0.21 (0.05) | 0.24 (0.04) |
| FeO* | 1.68 (0.24) | 1.52 (0.08) | 1.79 (0.11) | 1.83 (0.11) |
| MnO | 0.05 (0.06) | - | - | - |
| MgO | 0.18 (0.17) | 0.13 (0.01) | 0.19 (0.04) | 0.21 (0.02) |
| CaO | 1.22 (0.13) | 0.98 (0.03) | 1.43 (0.10) | 1.37 (0.11) |
| Na ₂ O | 4.46 (0.30) | 3.62 (0.11) | 4.11 (0.10) | 4.37 (0.19) |
| K ₂ O | 3.04 (0.03) | 3.09 (0.10) | 2.85 (0.15) | 2.79 (0.14) |
| Cl | 0.20 (0.05) | 0.12 (0.02) | 0.16 (0.03) | 0.17 (0.03) |
| Water [¶] | 7.23 (1.55) | 1.55 (0.79) | 4.20 (0.52) | 5.60 (0.90) |
| <i>n</i> | 4 | 11 | 10 | 9 |
| AGE [†] | 2160±25 (c. 2160 cal BP) | 2685±20 (c. 2800 cal BP) | 3230±20 (c. 3450 cal BP) | 1850±10 (AD 232±15) |

| T22 | Motutere (Unit G) 1 | Motutere 2 | Opepe (Unit E) 1 | Opepe 2 | Opepe 3 |
|--------------------------------|--------------------------|--------------|---------------------------|--------------|--------------|
| SiO ₂ | 75.53 (0.59) | 76.82 (0.47) | 75.99 (0.40) | 76.54 (0.63) | 75.98 (0.24) |
| Al ₂ O ₃ | 13.06 (0.55) | 12.95 (0.23) | 12.98 (0.22) | 13.13 (0.14) | 12.94 (0.09) |
| TiO ₂ | 0.24 (0.08) | 0.21 (0.05) | 0.22 (0.04) | 0.27 (0.07) | 0.23 (0.08) |
| FeO* | 1.89 (0.14) | 1.61 (0.16) | 1.85 (0.14) | 1.77 (0.14) | 1.75 (0.10) |
| MnO | 0.11 (0.08) | - | - | 0.13 (0.08) | 0.06 (0.05) |
| MgO | 0.19 (0.08) | 0.20 (0.08) | 0.24 (0.06) | 0.21 (0.03) | 0.13 (0.05) |
| CaO | 1.29 (0.10) | 1.30 (0.15) | 1.63 (0.13) | 1.52 (0.06) | 1.48 (0.06) |
| Na ₂ O | 4.57 (0.10) | 3.88 (0.51) | 3.90 (0.08) | 3.40 (0.60) | 4.22 (0.21) |
| K ₂ O | 3.00 (0.08) | 2.89 (0.21) | 3.01 (0.11) | 2.87 (0.07) | 3.07 (0.04) |
| Cl | 0.15 (0.03) | 0.14 (0.03) | 0.18 (0.05) | 0.15 (0.03) | 0.14 (0.03) |
| Water [¶] | 6.67 (2.43) | 1.77 (1.26) | 5.52 (1.23) | 2.76 (1.11) | 5.85 (1.66) |
| <i>n</i> | 10 | 11 | 11 | 10 | - |
| AGE [†] | c. 5800 (c. 6650 cal BP) | | 9050±40 (c. 10200 cal BP) | | |

Table 5.3 Electron microprobe analyses of glass shards from tephras in Te Henga wetland and analyses of possible correlatives.

Analyses are recalculated to 100% (normalised) on a volatile-free basis and expressed as a mean (±standard deviation) of *n* analyses in wt%.

*Total Fe expressed as FeO.

- No data

[¶] Water by difference (100 minus original analytical total)

n = number of shards analysed. Analyses were undertaken at Auckland University on a Jeol JXA-840 probe fitted with a PGT Prism 2000 EDS detector, absorbed current of 1.5 nA at 15 kV and beam defocussed to 15 µm. Analyst: W. Esler (University of Waikato).

[§] Tephra names are based on Froggatt and Lowe (1990); alternative designations as volcanological units (in parentheses) are from Wilson (1993).

[†] First age given is error-weighted mean age in radiocarbon years BP. Data sources are as follows: Mapara, Whakaipo, Taupo: Froggatt and Lowe (1990); Motutere: Wilson (1993); Waimihia, Opepe: Lowe et al. (1999). Second age (in parentheses) is given in calibrated years BP or as calendar date. Data sources are as follows: Mapara, Whakaipo, Motutere: Wilson (1993); Waimihia, Opepe: Lowe et al. (1999); Taupo: Lowe and de Lange (2000).

EMP data sources are as follows: Mapara: Eden et al. (1993); Whakaipo: Newnham et al. (1995); Motutere (Unit G) 1 : Eden and Froggatt (1996), Motutere (Unit G) 2 : Froggatt and Rogers (1990); Waimihia, Taupo, Opepe 1: Lowe et al. (1999); Opepe 2: Sandiford et al. (2001) (Pukaki Crater, Auckland); Opepe 3: Shane and Hoverd (2002) (Onepoto Basin, Auckland).

| Depth (cm) | Description |
|------------|--|
| 412 | Fragments of unidentifiable bivalve |
| 427 | Double valved (in-situ) cockle, <i>Austrovenus stutchburyi</i> |
| 435 | Double valved (in-situ) small cockle, <i>Austrovenus stutchburyi</i> |
| 412 - 460 | Fragments of cockle, <i>Austrovenus stutchburyi</i> , and small limpet, <i>Notoacmea helmsi</i> , that grazes on algae growing on the cockle shells. |

Table 5.4 Shell samples from core 18.

| Description | Depth (cm): | 320 - 330 | 385 - 400 | 431 - 435 |
|----------------------------------|-------------|-----------|-----------|-----------|
| Foraminifera | | | | |
| <i>Haplophragmoides wilberti</i> | | 1 | 6 | 0 |
| <i>Jadammina macrescens</i> | | 1 | 2 | 0 |
| <i>Miliammina fusca</i> | | 4 | 0 | 0 |
| <i>Trochamminita salsa</i> | | 0 | 2 | 0 |
| <i>Ammonia aoteana</i> | | 0 | 0 | 17 |
| <i>Zeaflorilus parri</i> | | 0 | 0 | 1 |
| Diatoms | | rare | rare | 0 |
| Ostracods | | 0 | 0 | 7 |
| Echinoderm spines | | 0 | 0 | 2 |
| Barnacle plates: | | | | |
| <i>Austrominius australis</i> | | 0 | 0 | 1 |
| Mollusc shells: | | | | |
| <i>Arthritica bifurca</i> | | 0 | 0 | 20 |
| <i>Austrovenus stutchburyi</i> | | 0 | 0 | 7 |
| <i>Notoacmea helmsi</i> | | 0 | 0 | 1 |
| <i>Notoacmea helmsi scapha</i> | | 0 | 0 | 1 |

Table 5.5 Raw census counts from three foraminifera-bearing samples from core 18.

Furthermore, others have argued that the use of volumes is less error-prone than transformations to mass (e.g. Butcher et al., 1933). No corrections were made for bulk density differences between eroded/transported soil and resulting core sediment layers or between sediment layers within the cores. A more accurate measure of sediment yield would also

require more cores to be taken because of the variable nature of the wetland and consequently the spatial variability of sedimentation. Volumes were calculated by multiplying the mean sediment thickness (\pm one standard deviation) for each sediment pulse within the wetland depositional area (1.7 km²). The range of sediment volumes of the four pulses can then be linked to the sediment yield of a corresponding landslide scenario (critical rainfall threshold), modelled with LAPSUS-LS (Fig. 5.6). It is implicitly assumed that the topographic information derived from the present DEM and used in the model is representative for the whole timeframe of the sedimentation phase. The magnitude of the landslide events can be expressed as a critical rainfall threshold range (Table 5.6); sites with a value equal to or lower than this threshold are triggered and enter the soil redistribution and sediment yield algorithms of the model. It should be noted that these magnitudes were probably underestimated because the wetland has not complete trap efficiency. Furthermore, trap efficiency depends on the change in reservoir level and capacity, and high rates of sedimentation will cause it to vary over time, usually decreasing as the reservoir continues to infill (Butcher et al., 1993). Subsequent compaction of sediment, not only by its own weight but also intensified by construction of the overlying causeway, may account for another underestimation of sediment volumes (although most of the compaction probably involved the readily compressible peat or organic mud layers). Holocene compaction ratios of 0.2-0.5 have been recorded for estuarine organic-rich sediments (Pizzuto and Schwendt, 1997). Because of these assumptions, emphasis should be placed on the order of magnitude of the volumetric estimates rather than the precise values.

| Layer Thickness (cm) (\pm 1 SD) | Sediment Volume (m ³) | Minimum Q_{cr} (m day ⁻¹) | Mean Q_{cr} (m day ⁻¹) | Maximum Q_{cr} (m day ⁻¹) |
|---------------------------------------|--------------------------------------|--|---|--|
| 3.94 (\pm 1.81) | 66980 (\pm 30770) | 0.0100 | 0.0248 | 0.0392 |
| 5.72 (\pm 1.62) | 97240 (\pm 27540) | 0.0260 | 0.0390 | 0.0518 |
| 10.67 (\pm 4.77) | 181390 (\pm 81090) | 0.0404 | 0.0783 | 0.1189 |
| 12.33 (\pm 4.00) | 209610 (\pm 68000) | 0.0596 | 0.0919 | 0.1271 |

Table 5.6 Volumes of the four sediment pulses, from top downward, and their corresponding (range of) landslide scenarios.

According to the ages determined in core 6, at least two high-magnitude events (sediment pulses 3 and 4, Figs. 5.5 and 5.6) occurred in pre-European times. These may have been caused by natural landslide activity or the influence of early Polynesian (Maori) settlement around the margins of the wetland (Diamond and Hayward, 1979; Hayward and Diamond, 1978), or both. Similar mud layers have been found in some Waikato lakes and analyses of associated pollen and $\delta^{13}\text{C}$ values have shown the layers coincide with catchment deforestation of an unprecedented scale and thus attributable to Polynesian burning at around 700 cal yr BP (e.g., Hogg et al., 1987; Newnham et al., 1989; Green and Lowe, 1994; see also Hogg et al., 2003). The two younger events occurred over about the last 150 years and may have been caused or at least intensified by logging and quarry operations upstream from the late 1830s to 1940s (Diamond and Hayward, 1980). A more precise timing of the influence of the first European (after 1830) forest clearance operations could be better distinguished from natural impacts by pollen analysis, which can show the introduction of exotic European species (e.g. Wilmshurst et al., 1999). It should be noted that landslide hazards are calculated

with parameter settings for the area at present according to Tables 3.1 and 3.2. In the parts of the area where logging took place, lower root reinforcement (lower C_r values) would result in higher landslide hazards and relatively more sediment yield implying a small overestimation of the critical rainfall thresholds representing the last two landslide scenarios.

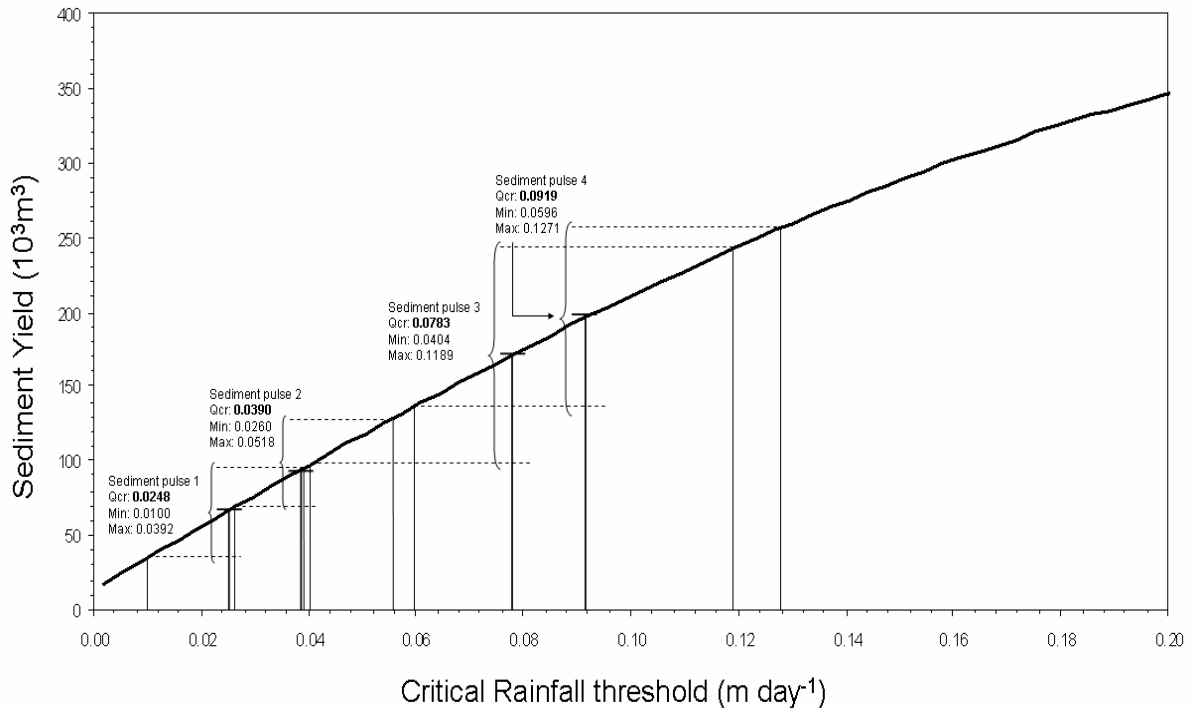
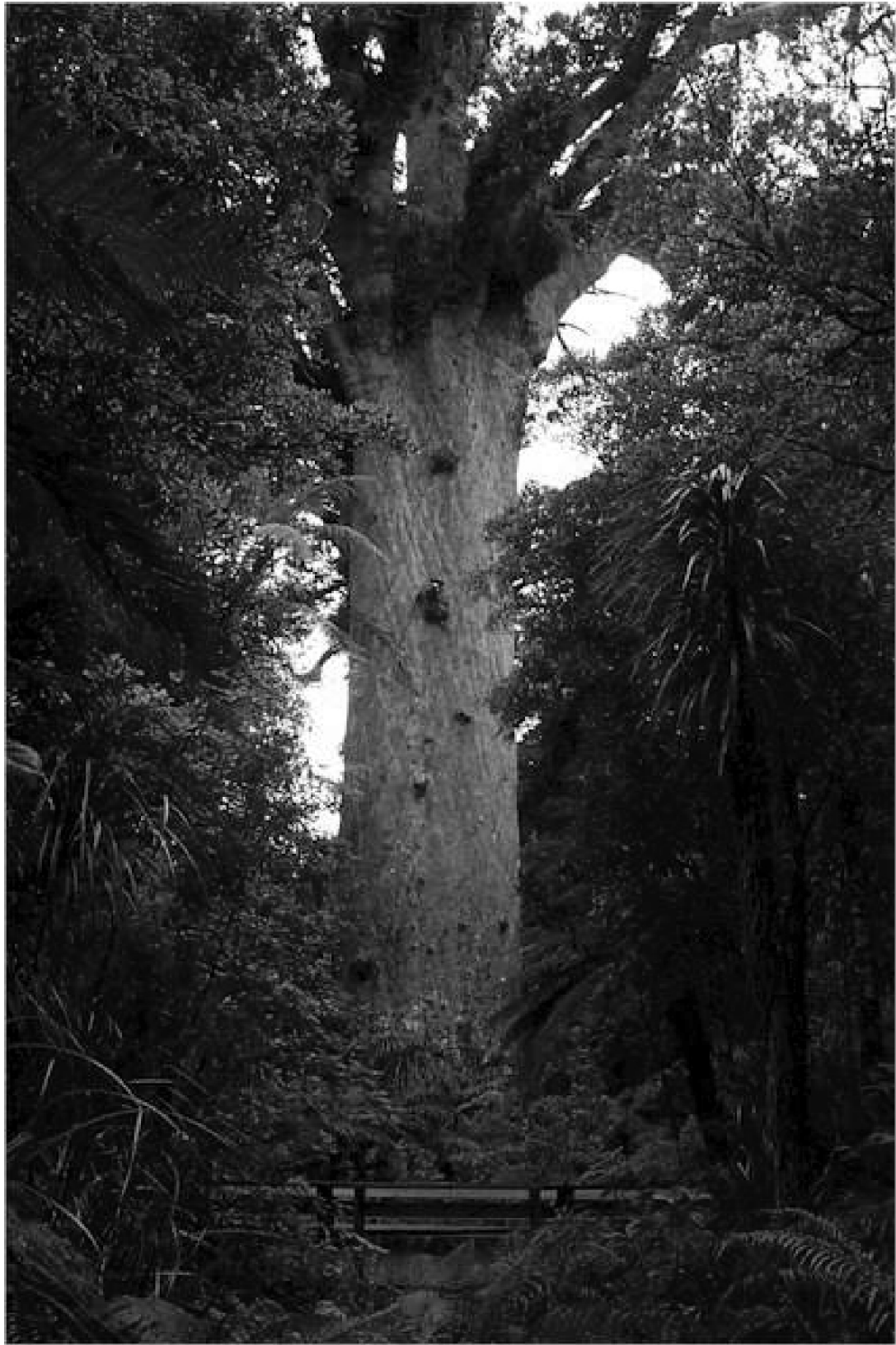


Fig. 5.6 Back-analysis of calculated wetland sediment volumes to corresponding LAPSUS-LS landslide scenarios.

5.4 Conclusions

In this chapter, the possibility of combining a wetland sediment record with the LAPSUS-LS landslide model to reconstruct the sedimentation history of the wetland and the occurrence of high-magnitude/low-frequency landslide events in the catchment upstream was assessed. By using radiocarbon dating, foraminiferal analysis and tephrochronology, the stratigraphy and chronology for eleven sediment cores was established. A small drop in sea-level following the Holocene sea-level maximum is represented in the lower part of the sediment record, dated at c. 6000 cal yr BP, and marked by a transition from coarse to finer sand and a change in foraminiferal content. The actual damming of the wetland by a landward prograding dune system inducing the start of freshwater sedimentation was completed by c. 1000 cal yr BP. At least four clay sediment pulses are recognised in the cores and interpreted as representing high-magnitude landslide events. The two oldest events occurred are either natural phenomena or the result of early Maori settlement, or both, whereas the last two events are most likely caused or intensified by forest clearance and logging activities in the upland catchment from the 1830s to the 1940s. Sediment volumes were calculated from the cores and corresponding landslide scenarios were defined through back-analysis of LAPSUS-LS

sediment yield model output. Although initially not intended to quantify landslide erosion and sediment yield, the model seems capable of linking a catchment scale calculated sediment yield, resulting from a landslide scenario and expressed by a threshold critical rainfall, with Late-Holocene sediment pulses preserved in the wetland at the basin outlet.



Chapter 6

Vegetation Patterns and Landscape Stability

In this chapter, the use of topographical attributes for the analysis of the spatial distribution and ecological cycle of kauri (*Agathis australis*), a canopy emergent conifer tree from northern New Zealand, is studied. Several primary and secondary topographic attributes are derived from a DEM for the Waitakere River catchment and the contribution of these variables in explaining presence or absence of mature kauri is assessed with logistic regression and Receiver Operating Characteristic (ROC) plots. The topographically based landslide hazard index calculated with the LAPSUS-LS model appears to be very useful in explaining the occurrence and ecological dynamics of kauri. It is shown that the combination of topographic -, soil physical - and hydrological parameters in the calculation of this single landslide hazard index, performs better in explaining presence of mature kauri than using topographic attributes calculated from the DEM properties alone. Moreover, this example demonstrates the possibilities of using terrain attributes for representing geomorphological processes and disturbance mechanisms, often indispensable in explaining a species' ecological cycle and forest stand dynamics. The results of this analysis support the 'temporal stand replacement model', involving disturbance as a dominant ecological process in forest regeneration, as an interpretation of the community dynamics of kauri. Furthermore, a certain threshold maturity stage, in which trees become able to stabilise landslide prone sites and postpone a possible disturbance by this process, together with great longevity are seen as major factors making kauri a 'landscape engineer'.

Based on: Claessens L., Verburg, P.H., Schoorl, J.M. and Veldkamp A., 2005. Contribution of topographically based landslide hazard modelling to the analysis of the spatial distribution and ecology of kauri (*Agathis australis*). Landscape Ecology. Submitted.
© Kluwer Academic Publishers.

6.1 Introduction

In the following paragraphs, the use of topographical attributes for the analysis of the spatial pattern and ecological cycle of kauri (*Agathis australis*) (Gardner, 1981) is evaluated. An attempt is made to interpret statistically the presence or absence of mature kauri in association with properties derived from elevation data. Furthermore, the possibilities of using terrain attributes for representing or detecting environmental conditions, relevant geomorphological processes and disturbance regimes are explored. This introduction will focus on kauri and its distribution; in addition an overview is given of general concepts of vegetation patterns and previous research on digital terrain analysis for ecological applications.

6.1.1 Kauri and its distribution

Kauri (*Agathis australis*) is a large conifer tree of the *Araucariaceae* family and endemic to New Zealand. Evergreen rainforests dominated by kauri occur in the north of the North Island and the current natural southern limit is approximately latitude 38° S (Ecroyd, 1982). Kauri trees form an emergent layer (35 m) above a mixed angiosperm canopy (10-20 m) and may, although numerically inferior to the angiosperms, contribute much to forest structure and function (Ogden and Stewart, 1995; Enright, 2001). Conifers usually account for c. 40 % of the stand basal area but represent 50-60 % of above-ground biomass given the combination of large diameter and emergent habit (Enright, 2001). *Agathis australis* changes its form markedly from seedling or juvenile stage to the mature tree: it undergoes a dramatic change from the conical, monopodial pole tree (known as a 'ricker') to the mature lollipop shape (Ogden and Stewart, 1995). Dense stands of size-varying and often even-aged kauri trees form a mosaic pattern in the landscape. Kauri trees can grow to an immense size and age estimates of over 1000 years have been made. Logging operations in the late 19th and 20th centuries all but wiped out the once extensive stands of mature kauri. Fortunately, many trees are now preserved in forest reserves and kauri is no longer commercially felled.

Several authors have tried to explain the population and stand dynamics within kauri dominated forests in relation to local environmental conditions, disturbance and competitive interactions between conifers and angiosperms (Cathersides, 1972; Ogden, 1985; Ahmed and Ogden, 1987; Jessop, 1992; Enright and Ogden, 1995; Ogden and Stewart, 1995; Burns and Leathwick, 1996; Enright et al., 1999). Burns and Leathwick (1996) find two gradients in forest composition, associated with topography (reflecting soil fertility and moisture) and altitude (with varying temperature and precipitation). Conifers tend to occur on infertile soils often found on ridges, whereas angiosperms, although not excluded from ridge top positions, were found on the more fertile lower slopes and in gullies. Jessop (1992) applies climate modelling techniques accounting for topography to demonstrate a strong relationship between the spatial distribution of kauri and a high quantity of solar radiation.

A commonly accepted interpretation of the community dynamics of kauri forests is the 'temporal stand replacement' (or 'lozenge') model, described by Ogden (1985) and Ogden and Stewart (1995). They attribute the preferred occurrence of kauri on ridge tops to more frequent disturbance by windfall and soil slipping, allowing the light-demanding kauri seedlings to establish, rather than because the ridge soils are drier and less fertile. The model identifies multiple stages in the kauri-angiosperm ecosystem (Figure 1; based on Figure 5.6 in Ogden and Stewart (1995)):

- A. A seedling recruitment phase immediately after a disturbance event. A dense cohort of kauri can establish favored by light conditions.
- B. A self-thinning phase in which tree density declines but total biomass remains the same. Possible gaps are filled by lateral growth of surrounding individuals rather than by recruitment from the seedling pool.
- C. A cohort senescence phase in which biomass declines but gaps can be filled by recruitment from a second but less dense cohort of kauri. The second cohort is less dense because of the more competitive environment in comparison with the first.
- D. The tree density decreases further and only a limited number of large trees remain because opportunities for recruitment decline until a new major disturbance event starts the cycle again.
- E. Large-scale exogenous disturbances can cause a return to the initial cohort stage.

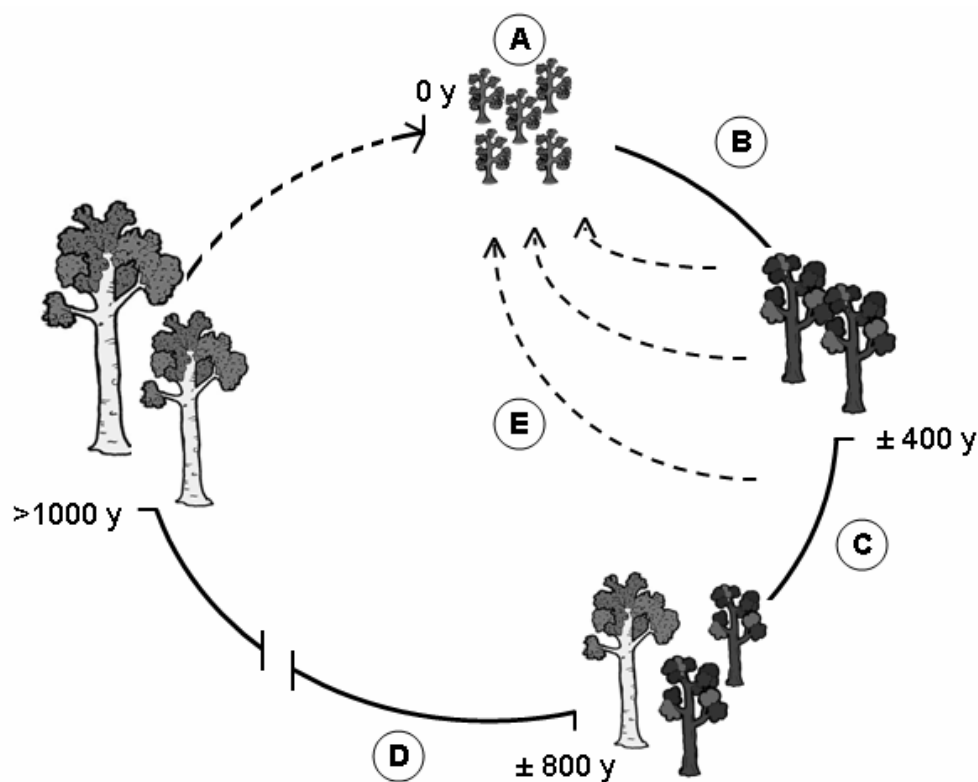


Fig. 6.1 Schematic representation of temporal stand replacement model. For explanation of stages A-E refer to text.

Thus stand regeneration is episodic and dependent upon large scale forest disturbance by cyclonic storms or fire (Ogden, 1985; Ogden et al., 1987). Due to the great longevity of the species, commonly 600 years and sometimes > 1000 years, there is a high probability of this occurring during the life of any cohort (Ogden et al., 1992). The model was tested with field plot data for its validity, not restricted to kauri dominated systems but for forests containing *Araucariaceae* in the western pacific in general, by Enright et al. (1999). Coexistence of the araucarian element with angiosperm forest species was shown to be dependent upon disturbance events, which give the conifers a temporary competitive advantage over the co-

occurring angiosperm tree species. Great longevity relative to most of the angiosperms, and occasional gap phase recruitment, facilitates their long-term persistence in stands through long periods without catastrophic disturbance (Enright et al., 1999). In addition, when kauri becomes able to locally postpone disturbance (by root reinforcement) causing a return to the initial cohort stage, it again exploits its capability to outlive other species.

6.1.2 Vegetation patterns

Patterns of ecosystem structure, composition and function are controlled by landforms and geomorphic processes within a landscape, because of their effect on environmental gradients and patterns and frequency of disturbance (Swanson et al., 1988). Different geological parent materials result in a variety of landforms and local soil conditions. Combined with climate, these local properties can affect the spatial distribution of species within a natural ecosystem. A certain optimal range for those primary environmental resources can form a 'niche' for a certain species (Austin, 1985; Mackey et al., 2000). Another important concept in ecosystem dynamics is 'disturbance', which can be defined as 'any relatively discrete event in time that disrupts ecosystem, community or population structure and changes resources, substrate availability or the physical environment' (White and Pickett, 1985; Bonan and Shugart, 1989). Examples of disturbance include fire, flood, insect infestations, diseases, windthrow, lightning, avalanches and landsliding. The type, severity and spatial heterogeneity of a disturbance all determine a species' post-disturbance response. This response is in turn determined by the typical life-history attributes of a species, e.g. high light level requirement versus shade tolerance. Besides niche conditions and disturbance patterns and frequency, human influence (present and historical landuse) can also have a major impact on vegetation patterns (e.g. Burrows, 1990).

Spatial patterns of vegetation are generally regarded as the result of a combination of both niche environmental conditions and disturbance processes (Mackey et al., 2000). However, the relative contributions of these factors to the resulting pattern and linkages of cause and effect have been shown very difficult to establish. Spatially distributed data in complex landscapes are often hard to quantify, and an amount of uncertainty remains about the relevance of certain conditions for specific ecological processes.

6.1.3 Digital terrain analysis for ecological applications

Topographic attributes derived from digital elevation models (DEMs) are widely used in hydrological, geomorphological and ecological applications (see reviews in Moore et al. (1991 and 1993b) and Wilson and Gallant (2000)). Because digital elevation data are now readily available, considerable research has been done on the extent to which the spatial distribution of certain species is correlated with environmental conditions related to local topography (Davis and Goetz, 1990; Mackey et al., 2000; Hörsch, 2003). DEMs highly correlate with temperature, moisture, geomorphological processes and disturbances (Hörsch, 2003). Topography can influence niche conditions, e.g. through its importance for redistribution of water in the landscape and effects of slope and aspect on solar radiation budgets (Dubayah and Rich, 1995). Regarding disturbance processes, slope angle and length can influence e.g. fire intensity, rate of spread and within-fire heterogeneity (Mackey et al., 2000). Height or local aspect can have influence on exposure to fire, wind or lightning (Kulakowski and Veblen, 2002). Also landslides, involving removal of vegetation and topsoil and thereby altering light and soil conditions, are widely recognised as a disturbance process

often related to population dynamics of certain vegetation types (Swanson et al., 1988; Butler and Walsh, 1994; Shroder and Bishop, 1995; Myster et al., 1997). However, on the landscape level, relatively little attention has been paid to the effects of landslide activity as a determinant of vegetation patterns (compared with the modelling of e.g. fire and windthrow disturbance regimes).

Digital terrain analysis for ecological studies has mainly focused on calculating and modelling spatially and temporally varying solar radiation at the landscape's surface and its consequences for flora or fauna dynamics (Moore et al., 1993a; Jessop, 1992; Brown, 1994; Dubayah and Rich, 1995; Kumar et al., 1997; Franklin, 1998; McKenney et al., 1999; Wilson and Gallant, 2000). Variation in elevation, slope, aspect, and local topographic horizon can cause substantial differences in solar radiation and thereby affect such biophysical processes as air and soil heating, evapotranspiration, and primary production (Dubayah and Rich, 1995; Wilson and Gallant, 2000). These processes may, in turn, affect the distribution and abundance of flora and fauna and many authors have shown that the distributions of solar radiation and vegetation are highly correlated (Kirkpatrick and Nunez, 1980; Jessop, 1992; Moore et al., 1993a).

Disturbance on the landscape level has long been assessed by spatially aggregated approaches not based on spatially explicit topographical information (Clark, 1991; review in Turner and Dale (1990)). Only recently, the value of using topographical attributes for representing 'sensitivity' for certain disturbance mechanisms has been recognised. Mackey et al. (2000) combine the influence of topography on both niche properties and disturbance regimes in a 'domain analysis'. They argue that environmental domains can be identified across a landscape where the probability for the occurrence of a given species is more likely. The method used is a combination of DEM analysis, remotely sensed and field data to find a statistical correlation with the spatial distribution patterns of canopy trees. They find a significant topographic control on the distribution of one pine species, suggested by the stronger predictive power of the topographic index, compared with in situ soil and topography observations. Wetness index, elevation percentile and short-wave radiation, yield a discrimination of the environmental domain of one species compared with the other two. Hörsch (2003) analyses the potential of 24 primary and secondary topographical parameters to explain the spatial distribution of montane and subalpine forests in the central Alps. Several attributes are derived from a DEM and some are treated as indicators for disturbance intensity and frequency. Elevation, slope angle and to a certain degree moisture related variables proved to be the most important parameters to explain both forest habitats. Inaccuracies within the simulation results could partly be attributed to the insufficient parameterisation of geomorphologic activity (Hörsch 2003). Other applications using topographical attributes to represent disturbance gradients include Brown (1994) and Kramer et al. (2001).

Although landslides are recognised as an important mechanism of disturbance in steep terrain, digital terrain analysis to assess landsliding in relation to vegetation dynamics has hardly been applied. Studies relating landslides with vegetation distribution most often focus on post-landslide niche conditions influencing primary succession (Guariguata, 1990; Walker and Boneta, 1995; Walker et al., 1996; Myster et al., 1997; Restrepo, 2003). Butler and Walsh (1994) found that in their alpine study area debris flows can act to depress treeline below its climatic optimum. Tang et al. (1997) use a physically-based model of the topographic influence on landslide initiation to study feedback mechanisms between forest harvest patterns and landscape disturbance.

6.2 Materials and methods

6.2.1 Study area

As for all previous chapters, the study area for this last application is situated in the Waitakere Ranges regional park. The flora in the parkland is diverse, containing 540 indigenous plants; several rare and endangered species are present. Over one third of the vegetation consists of podocarp-broadleaf forest. Other types of vegetation association include coastal edge-, bluff-, wetland- and successional vegetation. In the central part of the ranges, in rugged terrain, extensive patches of mature kauri forest remain in which kauri and the occasional podocarp species emerge over a very low mid tier of cutty grass (*Gahnia*) species, kauri grass (*Astelia trinervia*), kiekie (*Freycinetia baueriana*) and mingimingi (*Leucopogon fasciculatus*) (Denyer et al., 1993). The actual catchment studied in this chapter is the same as described in Chapter 5 (Waitakere River catchment). Being aware that parts of this area are disturbed by historical or present human influence (e.g. forest clearance, farming, Waitakere Reservoir, golf course), only the parts of the forest which are mostly undisturbed by these modifications are considered.

6.2.2 DEM analysis and LAPSUS-LS

For vegetation analysis at the landscape level, a DEM can be used to derive spatially distributed primary and secondary topographic attributes, correlated with temperature, light and moisture conditions and geomorphological process intensity. A 10 m resolution DEM was derived by TIN interpolation from 10 m elevation contours electronically created from 3D stereo photographs flown on 25th January 1999 (Source: Auckland Regional Council).

Slope and aspect are the principal factors determining the variability of global radiation, and hence potential evapotranspiration, received across a landscape (Moore et al., 1993a). Exposure to wind also influences soil moisture and is in turn related to slope and aspect. Elevation (from the DEM) determines vertical eco-climatic zones correlated with rainfall and temperature gradients. The algorithm itself used to compute surface derivatives such as slope, aspect, flow direction or contributing area from a DEM has consequences for the outcome of a DEM analysis (e.g. Florinsky, 1998). For this analysis, it is chosen to calculate both local, cell to cell based slope and the more commonly used procedure of computing slope in a 3x3 cell window.

Upslope contributing area, often referred to as drainage or catchment area, is calculated by the number of cells contributing flow to a cell. This attribute is a representation of soil moisture and can also be associated with the intensity and frequency of processes involving water accumulation. A lot of work has been done on the use of different algorithms for the determination of flow routing and effects on the calculation of contributing or specific catchment area (e.g. Zhou and Liu, 2002). For this analysis, two methods of calculating the contributing area were chosen: the steepest descent (O'Callaghan and Mark, 1984) and the multiple flow routing algorithms (Quinn et al., 1991).

Curvature attributes determine the rate of change of slope (or aspect), usually in a particular direction. The profile curvature shows the rate of change of slope for each cell in the direction of slope and affects the acceleration and deceleration of flow, and therefore influences erosion and deposition. The plan curvature measures the curvature of the surface perpendicular to the maximum slope direction and influences convergence and divergence of flow (Wilson and

Gallant, 2000). The standard algorithms using a 3x3 cell window available in ArcView GIS (ESRI, 1999) were used to calculate profile and plan curvature.

The topographic wetness index describes the spatial distribution and extent of zones of saturation for runoff generation as a function of upslope contributing area, soil transmissivity and slope (Wilson and Gallant, 2000). The equation assumes steady-state conditions and can be written as:

$$W = \ln\left(\frac{A}{T \tan \theta}\right) \quad (6.1)$$

Where A is the specific catchment area (or contributing area per unit contour length) [$\text{m}^2 \text{m}^{-1}$], T is the soil transmissivity when saturated [$\text{m}^2 \text{day}^{-1}$] and θ is the slope [$^\circ$].

For the analysis of shallow landslide hazard, local slope, contributing area, topographic wetness indices and critical rainfall values were calculated with the LAPSUS-LS model (Chapter 3). As described in Chapter 3, the spatial distribution of Q_{cr} values, calculated according to Eq. (3.4), can be interpreted as an expression of the potential for shallow landslide initiation.

6.2.3 Presence-absence analysis

Kauri distribution

A detailed inventory of mature kauri trees (as represented in stage C and D of the temporal stand replacement model) was made by means of detection on aerial photography, intensive fieldwork (georeferencing mature kauri with GPS) and digitising orthorectified imagery of the study area. A 10 m resolution grid presence-absence dataset (142861 gridcells in total) was derived from this inventory. A total of 1494 mature kauri trees were identified in the parts of the study area undisturbed by human activity.

Logistic regression

Statistical models are widely used in exploring the likely occurrence or distribution of species and have become an important tool in conservation planning and wildlife management (Davis and Goetz, 1990; Pearce and Ferrier, 2000; Manel et al., 2001; Aspinall, 2002). Typically, absence-presence data and site measurements from distributed samples are analysed to test the statistical significance of hypotheses relating presence or absence with site variables. At larger spatial scales, presence-absence models are often derived using correlative univariate or multivariate techniques such as discriminant analysis, contingency tables (Pinder III et al., 1997; Hörsch, 2003), principal components analysis (del Barrio et al., 1997; Hörsch, 2003), correspondence analysis (Gottfried et al., 1998; Pfeffer et al., 2003), linear regression (Florinsky and Kuryakova, 1996), artificial neural networks or logistic regression (Davis and Goetz, 1990; Brown, 1994; Manel et al., 1999; Aspinall, 2002).

To model presence-absence of a species Manel et al. (1999) showed that logistic regression should be preferred over discriminant analysis and artificial neural networks. Logistic regression was shown to have clear advantages in developing testable hypotheses and provides the clearest indications of possible causal effects on distribution. The technique also has the advantage that all of the predictors can be binary, a mixture of categorical and continuous or just continuous. The logit transformation of the probability of presence $P(Y=1)$

($Y=1$ represents the occurrence of the dependent variable), produces a linear function called the logistic response function (Neter et al., 1996; Menard, 2001; Agresti, 2002):

$$\text{logit}(Y) = \log(\text{odds}(Y=1)) = \log\left(\frac{P}{1-P}\right) = \beta_0 + \sum_{i=1}^n \beta_i X_i \quad (6.2)$$

Where P is the probability for occurrence of the dependent variable Y (i.e. $Y=1$), β_0 is an intercept, β_i are the regression coefficients to be estimated and X_i are a set of explanatory independent variables.

To facilitate model interpretation, odds ratios are often used. The odds ratio, $\exp(\beta)$, can be interpreted as the change in the odds for the considered event (that is, occurrence of kauri or $Y=1$) upon an increase of one unit in the corresponding independent variable X . However, ‘the odds ratio provides exactly the same information as the logistic regression coefficients β_i , it is only presented in a different way’ (Menard, 2001).

When independent variables are measured in different units, the relationship between the dependent variable and different independent variables can not be judged directly by comparing the regression coefficients, odds ratios or probabilities. To estimate the relative contribution of different variables within a logistic regression model, standardised logistic regression coefficients can be used (Menard, 2001). Standardised coefficients in general indicate how many standard deviations of change in a dependent variable are associated with a one standard deviation increase in the independent variable. Standardised logistic regression coefficients can be estimated as :

$$b_{YX}^* = (b_{YX})(S_X) / \sqrt{\frac{S_{\text{logit}(\hat{Y})}^2}{R^2}} = \frac{b_{YX} S_X R}{S_{\text{logit}(\hat{Y})}} \quad (6.3)$$

where b_{YX}^* is the standardised logistic regression coefficient, b_{YX} is the unstandardised logistic regression coefficient, S_X is the standard deviation of the independent variable X , $S_{\text{logit}(\hat{Y})}^2$ is the variance and $S_{\text{logit}(\hat{Y})}$ the standard deviation of $\text{logit}(\hat{Y})$ ($\text{logit}(\hat{Y})$ is the estimated value of $\text{logit}(Y)$ predicted by the regression equation), and R^2 is the coefficient of determination.

To select the relevant independent variables explaining the occurrence of kauri, a forward stepwise logistic regression method is chosen. This procedure utilises chi-square differences to determine which variables to add or drop from the model. The statistical software package SPSS (version 11.5.0) was used for the analyses.

Model performance

Any approach to ecological modelling has little merit if the statistical model and predictions can not, or are not, assessed for their accuracy using independent data (Fielding and Bell, 1997; Manel et al., 1999). A comparison of different performance measures for presence-absence models including data partitioning techniques can be found in Fielding and Bell (1997) and Manel et al. (2001). One recommended method is based on the use of Receiver Operating Characteristic (ROC) plots (Metz, 1978), indicating model performance independently of the arbitrary probability threshold at which the presence of a target species is assigned to a certain location. Methods involving ROC curves have so far been infrequently

applied to ecological data (Fielding and Bell, 1997; Guisan and Zimmerman, 2000; Pearce and Ferrier, 2000; Manel et al., 2001). The ROC curve forms a measure for goodness of fit of a logistic regression model similar to the R^2 statistic used in Ordinary Least Square regression (Pontius and Schneider, 2001). It evaluates the predicted probabilities by comparing them with the observed values over the whole domain of predicted probabilities instead of only evaluating the percentage of correctly classified observations at a fixed cut-off value. In the ROC graph, the true positive proportion is plotted against the false positive proportion for a range of threshold probabilities. A line is drawn through these points to derive the ROC curve. The closer the curve to the upper left corner, the more accurate the model is in its ability to discriminate between presence and absence. High performance models are characterised by large areas under the ROC curve (Area Under the Curve, AUC; Manel et al., 2001). A random model gives an AUC value of 0.5; a perfect fit results in an AUC of 1.0 (Swets, 1988). Manel et al. (2001) also illustrate that the area under the ROC curve is independent of prevalence (i.e. the frequency of occurrence of a species). ROC curves will be used here to evaluate both the goodness of fit of the logistic regression model and its ability to predict presence or absence of mature kauri.

Spatial autocorrelation

Spatial autocorrelation refers to the lack of independence which is often present among observations in cross-sectional data sets or in geographic data where nearby locations are more closely related than distant locations (Anselin, 1988; Bell and Bockstael, 2000). In the case of occurrence of kauri trees, spatial dependence may be attributed for example to the first phase in the ecological cycle (phase A in the temporal stand replacement model): a first dense cohort of seedlings is established after a disturbance event and this site, having the same environmental conditions and proximity of parent trees for seed dispersal, may exhibit neighbourhood dependence. In general, spatial autocorrelation results in inefficient parameter estimates and inaccurate measures of statistical significance. As Bockstael (1996) indicates, no satisfactory methods are available for addressing spatial autocorrelation in logit models. Methods to test and control for spatial effects have mainly been developed for the linear regression case and form a developing field of research for applicability in logistic regression (Staal et al., 2002). Still, influence of spatial autocorrelation on logistic regression results is often reduced by using a sample of the observations instead of the full data set. Sampling methods include randomly distributed sampling (Aspinall, 2002; Verburg et al., 2004), applying a sampling distance determined empirically with a semivariogram (Davis and Goetz 1990) or a leave-one-out or Jack-knife sampling method (Manel et al., 1999; 2001; Kramer et al., 2001). Presence of spatial autocorrelation can be tested with statistical indices like Moran's I (Overmars et al. 2003). To explicitly address the issue of spatial autocorrelation, neighbourhood characteristics that account for interactions could be included in the model specification (Staal et al., 2002; Verburg et al., 2004). For this application, the effect of spatial autocorrelation is reduced by taking a (50%) random sample of the observations. It is acknowledged that spatial dependence is not fully accounted for in this way and regression coefficient estimates may be partly biased by spatial dependence. However, taking a smaller sample would too radically reduce the number of observations and significance level of this analysis. An additional test that included a potential source of spatial autocorrelation, the distance to the nearest tree, did not indicate that this process is a major factor in the study area and no significant influence on the results was found.

| Variable | Description | Dimensions | Min. | Max. | Mean |
|----------|--------------------------------------|------------------------|---------------------|-------|--------|
| slope1 | local cell-to-cell slope | [°] | 0.0 | 78.24 | 16.53 |
| slope2 | 3x3 window slope | [°] | 0.0 | 68.61 | 16.50 |
| asp1 | 3x3 window aspect | [°] | -1(flat) | 360 | 190 |
| asp2 | 3x3 window aspect | [9 classes] | n.a. | n.a. | n.a. |
| altitude | DEM elevation | [m] | 42.03 | 400.0 | 244.61 |
| casd | contributing area, steepest descent | [#cells] | 1 | 68802 | 115 |
| camf | contributing area, multiple flow | [#cells] | 1 | 68770 | 116 |
| plcurv | plan curvature | [1/100 z units] | -82.37 | 40.33 | 0.016 |
| prcurv | profile curvature | [1/100 z units] | -40.01 | 80.17 | 0.012 |
| twi | topographic wetness index Eq. (6.1) | [-] | 1.11 | 29.91 | 6.69 |
| crain1 | critical rainfall Q_{cr} Eq. (3.4) | [m day ⁻¹] | $1.8 \cdot 10^{-5}$ | 0.78 | 0.16 |
| crain2 | critical rainfall Q_{cr} Eq. (3.4) | [6 classes] | n.a. | n.a. | n.a. |

Table 6.1 Overview of topographically based variables derived from the study area DEM.

6.3 Results

6.3.1 DEM analysis and LAPSUS-LS

Table 6.1 gives an overview of all the explanatory topographic variables derived from the DEM and used in the presence-absence analysis. The spatial distribution of critical rainfall values is calculated according to Eq. (3.4): local slope and contributing area (multiple flow algorithm) are calculated from the DEM for each grid point and the other parameters are lumped within an area of the same parent material. Soil physical parameter inputs for the three parent materials can be found in Table 3.1. For this application root cohesion (C_r in Eq. (3.2)) is set to zero (no vegetation surcharge), so the critical rainfall value reduces to a terrain intrinsic, topographically based relative landslide hazard index. Aspect and critical rainfall were both included as continuous and categorical variables. Aspect values were divided in 9 classes: 1) flat 2) north 3) north-east 4) east 5) south-east 6) south 7) south-west 8) west 9) north-west. Being relative measures of landslide susceptibility rather than physically interpretable absolute numbers, the Q_{cr} values (Eq. (3.4)) were divided in six classes:

1. Unconditionally unstable according to Eq. (3.6)
2. Very high landslide hazard: $0.0 < Q_{cr} < 0.05 \text{ m day}^{-1}$
3. High landslide hazard: $0.05 < Q_{cr} < 0.1 \text{ m day}^{-1}$
4. Moderate landslide hazard: $0.1 < Q_{cr} < 0.2 \text{ m day}^{-1}$
5. Low landslide hazard: $0.2 < Q_{cr} \text{ m day}^{-1}$
6. Unconditionally stable according to Eq. (3.5)

6.3.2 Logistic regression

To investigate the possible contribution of the landslide hazard index to the explanation of presence-absence of mature kauri, two logistic regressions were carried out, one without and one with critical rainfall as an explanatory variable. For fitting the logistic regression model, a random 50% sample of the data set was used. A forward stepwise regression was chosen to select the relevant variables from Table 6.1 explaining occurrence of kauri. This procedure

only includes variables with a significant contribution in the model. Possible collinear independent variables are unlikely to be retained. For categorical explanatory variables (asp2, crrain2), one class is used as a reference. Aspect classes were evaluated relative to class 2 (north), critical rainfall classes relative to class 6 (unconditionally stable). The results for the two logistic regression models can be found in Tables 6.2 and 6.3. AUC values for model fit are 0.737 and 0.750 respectively (Figs. 6.2a and 6.2b).

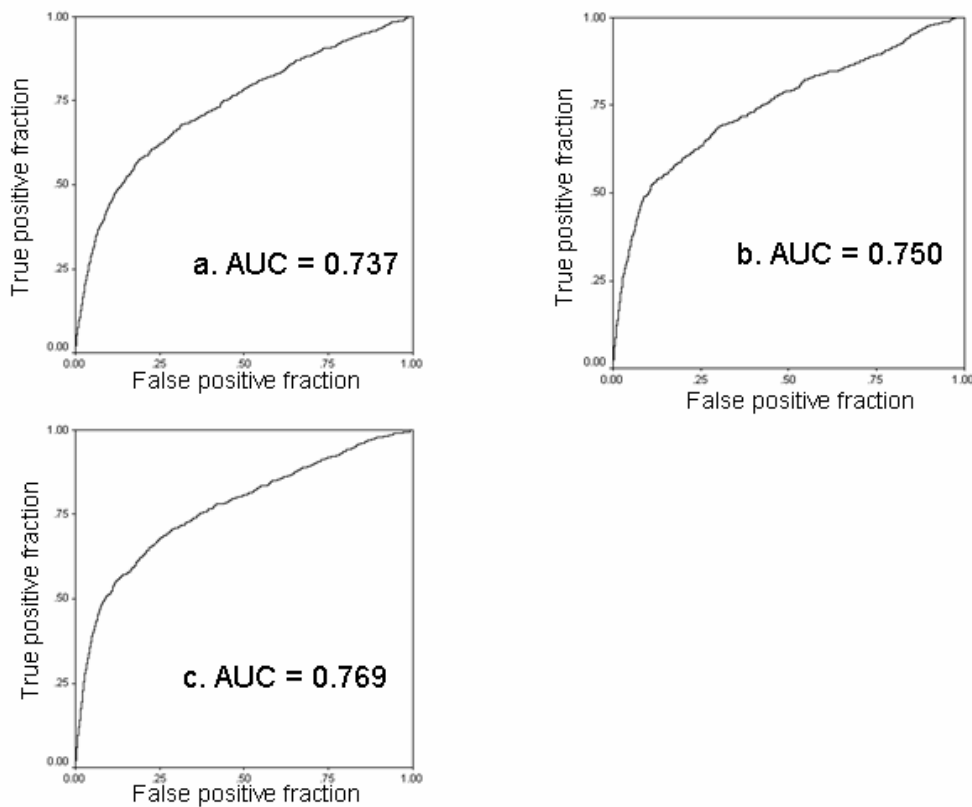


Fig. 6.2 ROC curves and AUC values of the logistic regression models: a. model fit data set without inclusion of landslide hazard as independent variable b. model fit data set with inclusion of landslide hazard as independent variable c. model validation data set.

Model validation was done by applying the logistic regression equation obtained with the calibration data set to the remaining 50% of the data and testing the calculated probabilities against the occurrence of kauri with the ROC statistic. The AUC value is 0.769 (Fig. 6.2c).

For the model without inclusion of landslide hazard as an independent variable, according to the standardised regression coefficients, the occurrence of kauri seems most correlated with slope and topographic wetness index. After inclusion of landslide hazard, moderate to very high landslide hazard areas are highly correlated with the presence of mature kauri. In both cases, west and south-west aspect positions seem to be preferred above north-west and east (with aspect class north as reference). Elevation (DEM) and profile curvature show relatively low correlation with the position of mature kauri. In the ROC graphs the true positive proportion is plotted against the false positive proportion for a range of threshold probabilities. The AUC value of the ROC curve for the regression model including landslide

hazard is higher than the value obtained without landslide hazard as explanatory variable (Figs. 6.2b and 6.2a respectively). Both AUC values are between 0.7 and 0.9 and indicate reasonable discrimination ability (Swets, 1988). The AUC value for the ROC curve obtained by testing probabilities, calculated with the calibration regression equation, for the validation data set (Fig. 6.2c) is higher than the value for the calibration data set itself and indicates good model performance. Probabilities of mature kauri occurrence can be calculated with the regression coefficients of Table 6.3 for the whole study area and are visualised against the kauri inventory dataset (Fig. 6.3).

| Variable | β | S.E. | b* | $\exp(\beta)$ |
|------------|---------|----------|--------|---------------|
| altitude | 0.002* | 0.001 | 0.011 | 1.002 |
| prcurv | 0.063* | 0.013 | 0.009 | 1.065 |
| slope1 | 0.093* | 0.004 | 0.068 | 1.097 |
| twi | 0.089* | 0.013 | 0.027 | 1.093 |
| asp2 | | | | |
| flat | -15.779 | 1686.436 | -0.102 | 0.000 |
| north-east | -0.227 | 0.163 | -0.006 | 0.797 |
| east | -0.830* | 0.218 | -0.018 | 0.436 |
| south-east | -0.108 | 0.183 | -0.002 | 0.898 |
| south | 0.177 | 0.157 | 0.004 | 1.194 |
| south-west | 0.754* | 0.132 | 0.018 | 2.124 |
| west | 0.812* | 0.127 | 0.021 | 2.252 |
| north-west | 0.315* | 0.134 | 0.009 | 1.370 |
| constant | -7.676 | 0.252 | | 0.000 |

* : Significant at 0.05 level.

Table 6.2 Forward stepwise logistic regression results excluding landslide hazard as an independent variable.

6.4 Discussion and conclusions

Topographic attributes alone cannot fully explain all ecologically important processes that influence the spatial distribution of kauri trees or vegetation patterns in general. At least, as this study illustrates, they seem representative of an important part of the environmental conditions and/or processes that constitute a vegetation domain. Besides natural environmental conditions, human impact (both recent and historical), can have a huge impact on the distribution of vegetation types (Tappeiner et al., 1998; Motzkin et al., 1999; Burrows, 1990). Unfortunately, spatially referenced data on tree harvesting, land use history or human disturbance are often lacking or hard to obtain.

The use of logistic regression for this analysis was not primarily intended to predict presence or absence of kauri but to point to the possible benefits of topographical analysis in explaining a species' ecological cycle. The statistical method used was above all intended to be explanatory and chosen to formulate and test hypotheses linking presence of kauri with spatially distributed topographic attributes. To select the relevant variables explaining occurrence of kauri, a forward stepwise logistic regression method was chosen. This procedure utilises chi-square differences to determine automatically which variables to add or

drop from the model. Although stepwise techniques have some disadvantages when used for theory testing, they are considered useful for exploratory purposes (see discussion in Menard , 2001, p. 63).

| Variable | β | S.E. | b* | exp(β) |
|------------------|---------|----------|--------|----------------|
| crrain2 | | | | |
| uncond. unstable | 2.670* | 0.219 | 0.018 | 14.443 |
| very high hazard | 2.095* | 0.139 | 0.033 | 8.125 |
| high hazard | 2.282* | 0.116 | 0.039 | 9.798 |
| moderate hazard | 2.315* | 0.096 | 0.050 | 10.121 |
| low hazard | 0.559* | 0.195 | 0.011 | 1.748 |
| asp2 | | | | |
| flat | -15.867 | 1694.646 | -0.134 | 0.000 |
| north-east | -0.247 | 0.163 | -0.008 | 0.782 |
| east | -0.818* | 0.218 | -0.023 | 0.441 |
| south-east | -0.164 | 0.184 | -0.004 | 0.849 |
| south | 0.152 | 0.158 | 0.004 | 1.164 |
| south-west | 0.718* | 0.133 | 0.022 | 2.050 |
| west | 0.821* | 0.128 | 0.027 | 2.274 |
| north-west | 0.341* | 0.134 | 0.013 | 1.407 |
| altitude | 0.002* | 0.001 | 0.016 | 1.002 |
| constant | -6.011 | 0.180 | | 0.002 |

* : Significant at 0.05 level.

Table 6.3 Forward stepwise logistic regression results including landslide hazard as an independent variable.

In Waipoua Kauri Forest, Burns and Leathwick (1996) found the vegetation pattern to be largely determined by topographical variation in soil fertility and moisture and altitudinally linked temperature and precipitation gradients. However, for this study area, relative elevation seems merely unimportant for the occurrence of mature kauri trees. In contradiction to the results of Jessop (1992), who found kauri preferentially on positions with north, north-east aspect, in this study area mature kauri trees seem to occur more on west, south-west facing slopes. For New Zealand in general, north-east facing slopes receive more solar radiation than south-west facing ones and this effect is more strongly pronounced for steeper slopes (Segal et al., 1985). Thus, the strong relationship between the spatial distribution of (mature) kauri and a high quantity of solar radiation found by Jessop (1992) is not confirmed in this study area.

The use of a topographically based landslide hazard index performs well in explaining the occurrence and ecological dynamics of kauri. The logistic regression models designed show that the combination of topographic -, soil physical - and hydrological parameters in the calculation of one landslide hazard index, has advantages over using solely topographical information calculated from the DEM. Less single explanatory variables are needed and a better model performance, reflected by a slightly higher AUC value, is obtained when including the landslide hazard as independent variable. More important, this example

demonstrates the possibilities of using terrain attributes for representing geomorphological processes, often important in explaining a species' ecological cycle.

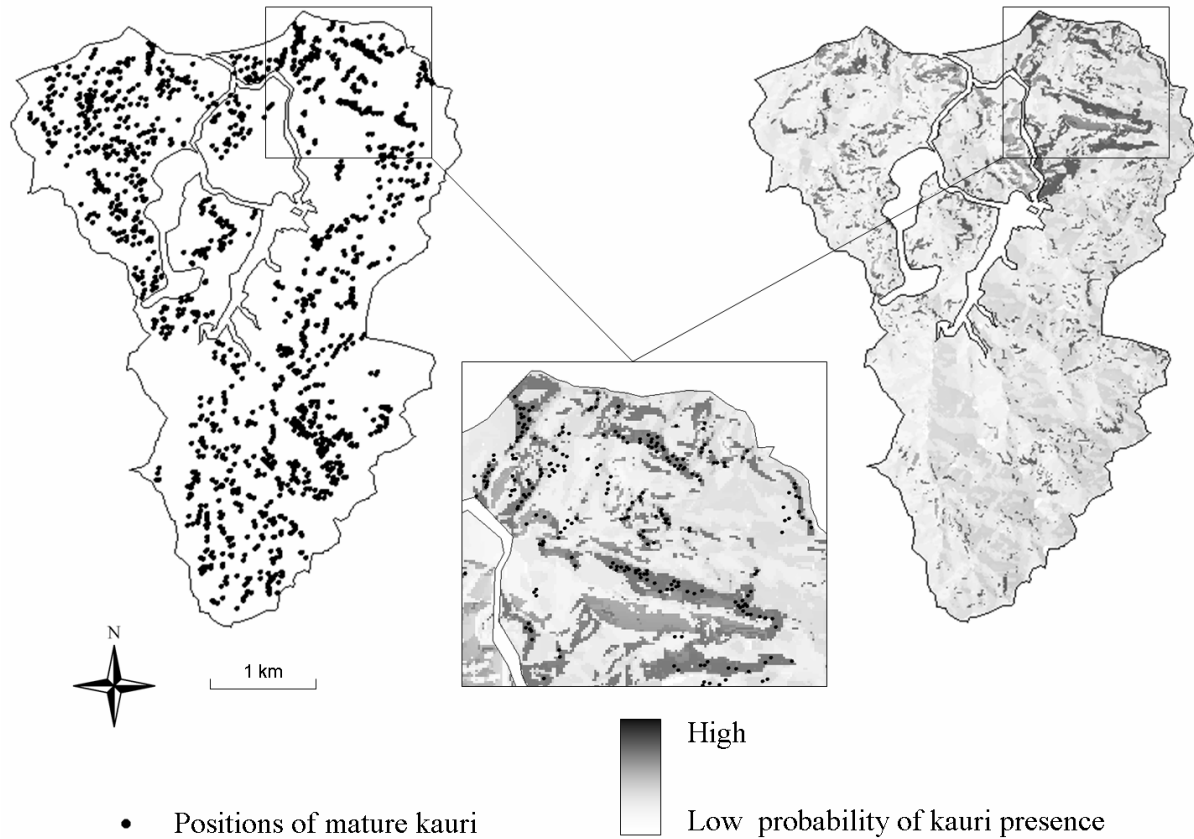


Fig. 6.3 Kauri inventory map for the study catchment and probabilities of occurrence calculated with regression coefficients of Table 6.3. The inset shows a detail of an overlay of the two maps.

The results of this analysis support the temporal stand replacement model (Ogden, 1985; Ogden and Stewart, 1995) as an interpretation of the community dynamics of kauri and additionally point to landsliding as a relevant disturbance mechanism. Mature kauri trees tend to occur preferentially on sites with a moderate to high landslide hazard. Even unconditionally unstable parts (which would fail according to their terrain properties, even without triggering by rainfall), seem to host mature kauri trees. It must be stressed that the landslide hazard is a relative index, calculated from topographic, geotechnical and hydrological terrain intrinsic parameters. The very apparent influence of vegetation, and especially mature kauri trees with dense and strong rooting systems, on 'real' landslide hazard is deliberately not taken into account for the calculation of the index. In this way, the occurrence of mature kauri on landslide prone sites can be explained as representing an equilibrium stage with the tree supporting the unstable landscape position in the last phase of the ecological cycle, i.e. before a disturbance (landslide or maybe also windthrow) event takes place and the cycle starts again. At a certain maturity stage, when the rooting system and tree weight add relevant root reinforcement and vegetation surcharge to the soil cohesion, a threshold phase could be

recognised, in which kauri starts to enhance the effect of its great longevity relative to other species by stabilising its landscape position and postponing possible disturbance by landsliding. In this way, a return to the initial cohort stage by exogenous disturbance (Fig. 6.1, phase E) is avoided or at least postponed and kauri fully exploits its ability to outlive other species. A field observation that additionally supports this idea is that only dead or damaged mature kauri trees seem to be subject to landsliding or windthrow.

Although not primarily intended for prediction of presence of kauri, the method used in this chapter could be adopted to delineate favorable sites or areas for possible kauri forest regeneration (see e.g. Fig. 6.3) and could accordingly be used for nature conservation planning and management in areas similar to the study area.

Chapter 7

Chapter 2

Tectonics
& terraces

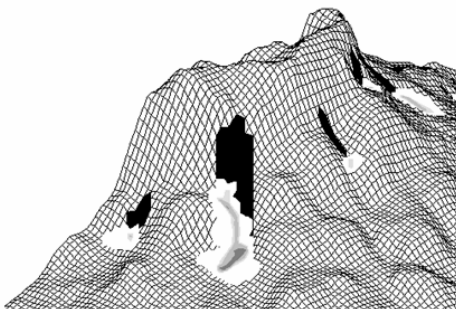


Chapter 1

Introduction
& geology study area

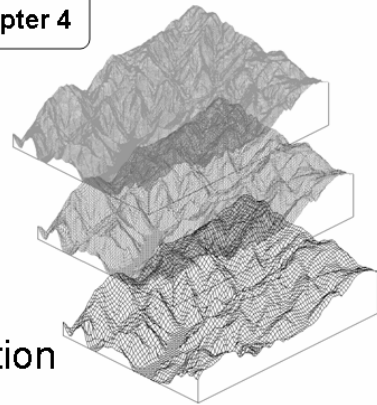
Chapter 3

LAPSUS-LS: landslide
model development



Chapter 4

DEM
resolution
effects



Chapter 5

Magnitude
& frequency
of landslide soil
redistribution



Chapter 6

Kauri ecology
& landscape
stability



Chapter 7

Synthesis

This final chapter will reflect on the most important conclusions from this thesis and discuss the main objectives and research questions postulated in Chapter 1. The next paragraphs will elaborate on three general themes covering the previous chapters. Finally some ideas for future research are put forward.

7.1 Tectonic uplift, paleoclimate and geomorphic activity

Shallow landsliding has been and still is a highly active geomorphic process in the Waitakere Ranges study area. On the long term, continued hillslope denudation, not restricted to landsliding, can only be accomplished if the potential energy for transport of material is provided by base level lowering. This is in turn provoked by local tectonic uplift or global sea-level fluctuations, or a combination of both, forcing graded rivers to incise, undermine hillslopes and in this way triggering upslope (headward) soil erosion processes. In this context, trying to identify local uplift and quantify long term uplift rates for the study area in the form of fluvial- and marine terrace analysis was justified (Chapter 2). Although there seems to be some form of controversy about the uplift history and especially the preservation of terraces in the Auckland and Northland region, a general regional uplift, superimposed on glacio-eustatic sea-level change, is interpreted here to be the only possible mechanism leading to the maintenance of a considerable relief and active denudation processes inland. Due to limited field evidence (fluvial and marine sediments) and dateable keybeds, the analysis of the terraces and calculation of uplift rates was chiefly based on geomorphic criteria. The interpretation of planar landforms as terraces or erosion surfaces and the subsequent translation to uplift history remains open for debate. Whether the marine- and river terraces can be defined as such in *sensu stricto*, is maybe less essential regarding the context of this thesis; within this research they provide the only tool to assess the long term background signal of uplift, responsible for triggering shallow landslides or hillslope denudation in general. Furthermore, terrace research is now mainly conducted in geological settings where formation and preservation of terrace surfaces are very likely, usually with ample supply and clear exposure of sediments. This part of the thesis can possibly motivate future researchers to focus on terraces in 'less favorable' conditions, similar to the study area (i.e. high uplift settings with limited supply of hardly distinguishable sediments).

7.2 Dynamic landscape process modelling: LAPSUS-LS

7.2.1 Validity of the LAPSUS-LS model

Shallow landslides, identified as constituting the dominant soil redistribution mechanism in the study area, are triggered by complex relationships between many controlling factors, including hillslope morphology, vegetation, soil properties, and hillslope hydrology. A geomorphic model is by definition a strong simplification of real conditions and processes and is developed with a specific goal, for example to gain more insight in certain phenomena or quantify specific (sub)processes, rather than aiming at completely simulating or mimicking the full extent of actual conditions. In addition, the development of the LAPSUS-LS model in this thesis (Chapter 3) involves a trade-off between the degree to which the model is 'physically based' and the type and number of model parameters (with increasing uncertainty, error propagation, time and costs to obtain etc.). The overall aim of the model component according to the research questions is to assess the impacts of shallow landsliding on longer term landscape dynamics and to help to define possible feedbacks with other hillslope processes. In this way it is not the intention to simulate detailed changes in hillslope geomorphology caused by individual shallow landslides. Still, modelling the relevant processes in a dynamic way requires a methodology aggregating several mechanisms acting at different spatial and temporal scale levels but remaining at least spatially explicit over a timeframe concerning redistribution of soil material and its effects. The hypothesis for the present study is that the impact of many rainfall events of different intensity and duration that trigger shallow landslides over years is translated in the failure of all sites with a certain landslide hazard during one timestep. For this purpose, the combination of the infinite slope stability and subsurface flow model performs well in predicting landslide locations with their relative failure potential. This methodology determining landslide hazards has been frequently applied before and the assumptions and boundary conditions are described in detail in Chapter 3. The subsequent soil redistribution however is assessed with essentially new spatial algorithms. Sophisticated formulations applicable to well-specified individual landslides would require a lot of additional parameters to be gathered (e.g. viscosity, debris flow composition, soil depth etc.). On the landscape level, and dealing with long term simulations, these properties would be hard to quantify in a spatially explicit way so simpler, empirical formulas are developed. These soil redistribution algorithms are only partly based on theoretical principles but they are capable of producing results which have a physically realistic interpretation serving the aim of studying spatial effects of landslide erosion, sedimentation and feedback mechanisms. A fairly new modelling practice applied in LAPSUS(-LS) is that digital elevation data are adapted between timesteps according to landslide scenarios and soil redistribution algorithms and on- and off-site effects over the years can be simulated in a spatially explicit way.

The calibration of LAPSUS-LS is done by back analysis of slope failures mapped in the field, aerial photography interpretation and adaptation of the root reinforcement parameters for each vegetation class accordingly. Because it is impossible to map all slope failures in space and time for the study area, this procedure can only be regarded as 'semi-calibration'; the model is only tuned to fit a restricted set of field data. Using the root cohesion as a calibration parameter serves two purposes: (i) it is possible to differentiate the landscape regarding landslide susceptibility within one lumped unit of parent material (of which properties are

measured) and (ii) determining root cohesion of vegetation proves to be difficult and in a highly diverse, natural setting as the study area, it seems even impossible to scale up properties from a single root to the root system of different growing stages of a tree or scrub, towards a gridcell within one vegetation class. As far as validation is concerned, only the locations of a restricted number of slope failures can be evaluated because there are simply no datasets covering long term landslide magnitude, frequency or quantities and spatial patterns of soil redistribution at the catchment scale. In this context, some researchers mention that it may finally have to be accepted that sometimes model validation is impossible, especially for slope modelling over the longer term (De Roo, 1996; Mroczkowski et al., 1997). There has been considerable change in attitude among modellers in recent years concerning appropriate validation strategies, why validation is carried out and whether it is necessary to validate models at all (Brooks, 2003).

7.2.2 DEM resolution

In Chapter 4 the effects of DEM resolution on the results of geomorphic models are assessed, with the LAPSUS-LS model serving as an example. For this specific application, the effect of DEM resolution appears to be particularly pronounced for the boundary conditions determining a valid landslide hazard calculation. Furthermore it is shown that extreme care should be taken when quantifying total amounts of landslide erosion and sedimentation by applying simple soil redistribution formulas as used in LAPSUS-LS to DEMs with different resolutions. So what is the most appropriate DEM resolution for landscape process modelling in general? From the LAPSUS-LS example it can be stated that the 'perfect' DEM resolution may not always exist as the choice of grid size should always be made against the background of the distribution of the attributes which are represented by or derived from it. A sensitivity analysis of the specific model using DEM attributes as model input parameters is highly recommended. Ideally, a DEM should represent the properties derived from it in such a way that neglecting features which are possibly 'filtered out' with coarsening resolution does not harm the quality of the model outcome. A coarse resolution DEM may appear to be of very poor quality, but if it can produce good results, then its quality is certainly satisfactory for that particular application.

7.2.3 Magnitude-frequency

When studying longer term landscape evolution and dynamics, addressing the magnitude and frequency of geomorphic processes is essential though often hard to quantify. This is especially the case for shallow landsliding, because it is linked with intensities and frequency of rainfall events, making the process rather scattered in time and fluctuating regarding total quantities of transported material. A major obstacle when assessing rates of landsliding is the difficulty of obtaining data that are relevant over longer time scales. Magnitude-frequency distributions of landslides are usually estimated from rates over decadal time scales derived from large inventories of aerial photographs. Moreover, high-magnitude/low-frequency events, often responsible for the major part of long term hillslope denudation, are underrepresented within the temporal resolution of data sets for most magnitude-frequency analyses. In Chapter 5, a wetland sediment record is used in combination with LAPSUS-LS modelling scenarios to reconstruct the incidence of high-magnitude/low-frequency landslide events in the upland catchment and the sedimentation history of the wetland at the basin outlet. Because the model is initially not intended to quantify landslide erosion and sediment

yield, some algorithms are added to determine a spatially explicit sediment delivery ratio and to calculate impact of landslide scenarios on total catchment sediment yield. Despite some limitations and assumptions (bulk density of sediments, compaction, stream density, trap efficiency, etc.), this method seems capable of linking a catchment scale calculated sediment yield, resulting from a LAPSUS-LS landslide scenario, with sediment pulses preserved in the wetland at the basin outlet.

7.3 Kauri as a soil-landscape engineer ?

One of the objectives of the overall research project is to investigate the interrelation between the ecology and stand dynamics of kauri trees and landscape and soil forming processes. There are several indications that kauri trees locally decrease rootability and deplete the underlying soil in nutrients relatively more than other species do. Sandy soils under kauri for example are known to undergo excessive podzolisation (finally resulting in gigantic ‘egg-cup’ podzols, sometimes associated with impermeable ironpans) and growth of other trees, including kauri seedlings, might be strongly reduced on these positions. In this way kauri could be seen as an extreme example of a tree making local conditions worse to a level it endures better than its competitors and by doing so increasing its own fitness. Whether soil formation processes under kauri are influenced or enhanced by tree, leaf or root components (e.g. polyphenols) more than for other trees, or depleted soils are mostly the result of the longevity of the species itself remains the subject of ongoing research within other parts of this research programme. In any way, as a survival strategy for kauri it seems inevitable to have some form of landscape rejuvenation to undo kauri’s destructive effects on soil productivity, permitting its own seedlings to colonise newly created open spaces with freshly exposed parent material. Moreover, the mosaic-like pattern of occurrence of dense stands of mostly even-aged mature kauri trees on specific landscape positions, often on or near ridge tops, directed several researchers already to the hypothesis that disturbance might be a dominant factor in the ecological cycle of kauri.

As this thesis is focussing on the soil distribution and landscape processes within the study area, trying to establish a link between the dominant geomorphic activity (in this case shallow landsliding) as a disturbance mechanism and the occurrence of kauri in the landscape is justified. Although geomorphic processes in general have been recognised as important ways of disturbance, besides fire or windthrow for example, few studies have used models to assess vegetation patterns in relation to landscape dynamics. Disturbance on the landscape level has long been assessed by spatially aggregated approaches not based on spatially explicit topographical information. In the case of landsliding, most studies focus on post-landslide niche conditions influencing primary succession. If a model or digital terrain analysis is used for ecological studies, the focus has mainly been on calculating spatially and temporally varying solar radiation at the landscape’s surface and its consequences for vegetation dynamics. Chapter 6 however demonstrates the possibilities of using the topographically based landslide hazard index, calculated with LAPSUS-LS, in explaining the occurrence and ecological dynamics of kauri in the study area. A major cause of concern is the fact that almost no part of the Waitakere Ranges has been preserved from forest clearing in the late 19th and early 20th centuries, and there are only few remnants of pristine kauri dominated forest for studying long term natural ecological processes. Fortunately, the Waitakere River catchment is virtually undisturbed, at least since the construction of a water supply dam in the

headwaters and obviously disturbed parts were ‘masked’ from the analysis. Another possible source of error is the inventory of mature kauri trees, which was made predominantly on the basis of aerial photograph interpretation. The possibilities of missing individual trees or erroneously including other similar looking species remain. Anyhow, the value of using topographical attributes and geomorphic process models for representing ‘sensitivity’ for certain disturbance mechanisms in a spatially explicit way can be substantiated. By designing logistic regression models it is shown that the combination of topographic -, soil physical - and hydrological parameters in the calculation of the landslide hazard index, has advantages over using solely topographical information from the DEM. A feedback mechanism between landscape stability and the ecology of kauri trees can be recognised in a threshold maturity stage when trees become able to stabilise landslide prone sites, postpone possible disturbance and take advantage of their great longevity relative to most other trees.

Because of this feedback to landscape stability, the relative amount of mature kauri within a landscape is of direct influence to the supply of sediment to streams, which ultimately determines river aggradation. In Chapter 2, the mechanism of fluvial terrace formation in the study area is interpreted. The climatic control on terrace formation is attributed to variations in humidity or aridity rather than to temperature changes. Net aggradation during the somewhat drier glacials/stadials is seen as a response to an increase in forest fires leading to a temporary increased sediment supply. A drier climate can influence the ecological pathway of kauri, described in Chapter 6: when the frequency of disturbance (by fire, but also e.g. windthrow) increases, kauri would more often and earlier return to the initial cohort stage (Fig. 6.1), nullifying the advantage of its longevity relative to other species. Moreover, this has a negative feedback to landscape stability, triggering more landslides and supplying large amounts of mud to the system, causing river aggradation. These mud deposits (also represented in the sediment record of the Te Henga wetland in Chapter 5) do not make a clear recognisable fluvial sedimentary record, especially when they are weathered, and make fluvial terrace interpretation less straightforward (Chapter 2).

7.4 Ideas for future research

From the previous sections it becomes clear that the original research questions in turn raise new questions, and that several improvements or additions can be made to the methodologies applied in the different chapters of this thesis. In the following paragraphs some ideas for future research are raised.

7.4.1 Tectonic history, uplift rates and terraces in the Auckland-Northland area

The controversy about the uplift history and especially the preservation of terraces in the Auckland and Northland region is mainly due to the lack of studies providing field evidence and dateable keybeds to strengthen interpretations. There is a need to conduct more fieldwork and potentially find evidence in the form of clear fluvial sediments, in the case of river terraces, or signs of marine origin (dateable shell fragments, bored surfaces etc.) within the planar landforms interpreted as marine terraces in Chapter 2. Furthermore, the chronology of both the marine and river terrace sequences is rather weak. Due to some practical problems (only one sample out of 12 yielded enough glass shards for electron microprobe analysis), it was not possible to identify and date all key tephra beds used for interpretation of terrace ages and regional uplift history. Resampling, geochemical characterisation, correlation and/or

dating of all key tephra layers is highly recommendable to further underpin the tectonic history of the study area. Suitable technique for dating tephras are isothermal plateau fission track (ITPFT) dating of glass shards (Westgate, 1989) or ^{40}Ar - ^{39}Ar dating of feldspar preparates (e.g. Shane, 2000).

7.4.2 Improvements LAPSUS-LS

Vegetation

The influence of vegetation (root reinforcement) on the calculation of the relative landslide hazard is included in the LAPSUS-LS modelling structure in the form of the root cohesion parameter (C_r in Eq. (3.2)). Still, at this stage, this parameter is only used to perform a semi-calibration of the model by back analysing slope failures mapped in the field and adapt the root cohesion for each vegetation class accordingly. For this study area, determining root cohesion for a gridcell within one (highly diverse) vegetation class proves to be difficult, because of scaling up issues (see also section 7.2.1). When applying LAPSUS-LS to areas with a more homogeneous landcover, measuring root strength and assigning root cohesion values to grid cells becomes more feasible and should be looked at.

'Legacy-effect'

When soil is removed and redeposited on hillslopes, it is known that both geotechnical and hydrological behaviour are altered. In the present version of LAPSUS-LS, we assume that sites where soil is eroded or deposited regain their full relative potential for shallow landsliding (retaining their original soil physical parameter setting), in the subsequent timestep. This is an assumption which can be justified for soil mantled landscapes, where landsliding is not weathering- but transport limited. In this case no hard rock is surfacing when soil is eroded: the time to return to initial soil conditions (homogenisation) is relatively short and soil development rates can be safely neglected using yearly timesteps. To apply LAPSUS-LS in areas where soils are shallow and landsliding is weathering (or supply) limited, soil production rates (both physical and chemical weathering) to develop a sufficiently deep soil profile similar to initial conditions have to be taken into account.

Long term landscape evolution: 'event-resistance'

The present LAPSUS-LS model is developed to assess the location of shallow landslides and their impact on landscape development within a timeframe of years to decades. When simulating soil redistribution over progressively longer timer periods, a certain 'event-resistance' will emerge: the total potential for landsliding will decrease and in the end an equilibrium situation will develop where no material is displaced. After all, the long term impetus for continued hillslope denudation is base level lowering, forcing rivers to incise, undermine hillslopes by removing sediment out of the system and in this way providing potential energy for upslope soil erosion processes. Neither a background signal of uplift, nor removal of sediment out of the system is currently accounted for in the model. This would be necessary when simulating longer term (hundreds to thousands of years) landscape evolution.

Sinks and flats

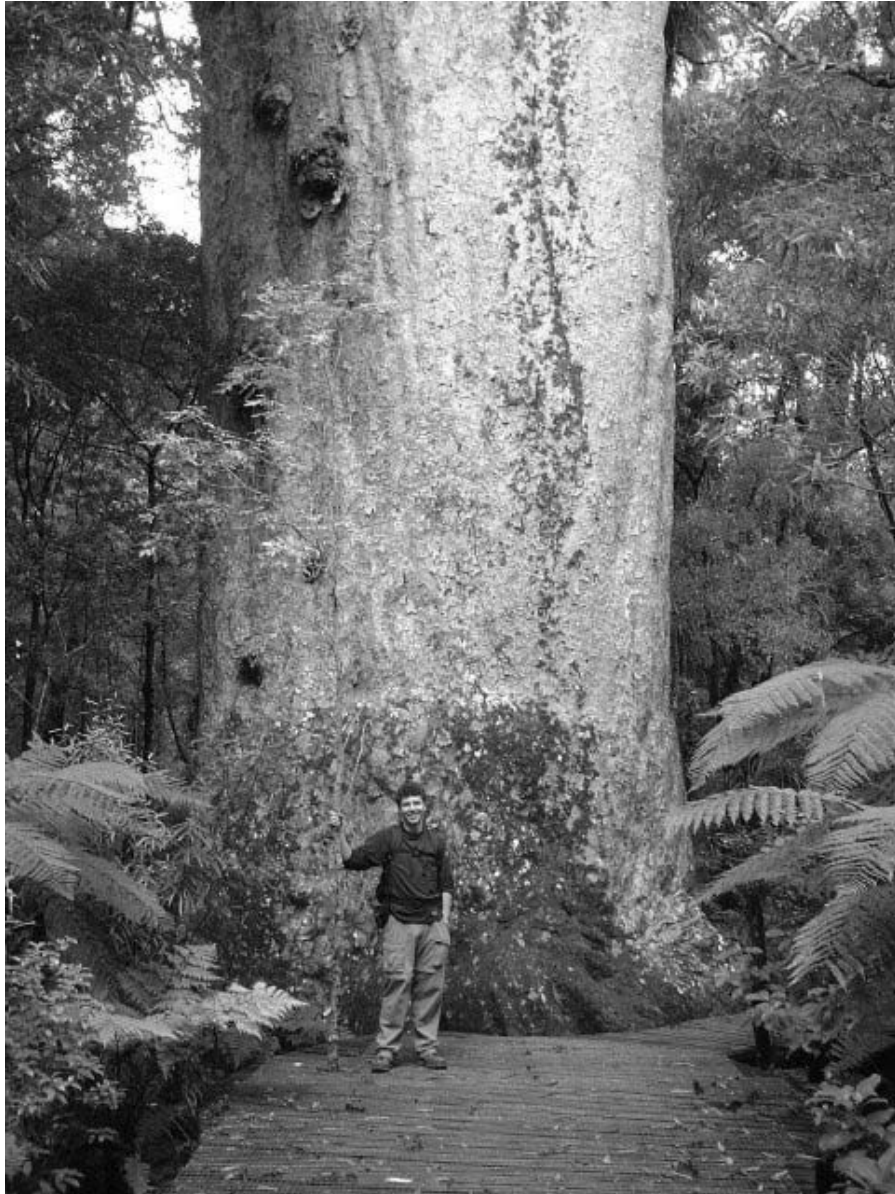
Sinks and flats are common problems encountered when using DEMs to represent landscape topography. Sinks are locations in the DEM that are surrounded only by higher neighbouring gridcells. Flats are multiple adjacent gridcells with exactly the same altitude, hence without

any gradient or flow direction to be derived. Both features can be artificial or natural attributes of a landscape. Artificial sinks and flats mostly arise from the applied interpolation technique to create the DEM and from issues of DEM precision and resolution. Most standard GIS packages have standard procedures to fill sinks, filling them to the same height as the outlet or spill, in this way creating a new flat. Flats are then forced to drain in the direction of the spill, often using a steepest descent routing procedure, thereby creating an unrealistic 'fishbone' drainage structure. Also in LAPSUS(-LS), both artificial sinks and flats need to be removed: the model is based on landscape-wide topographic gradients and multiple flow routing principles, for transport of both water and soil, and therefore the DEM needs to be 'hydrologically sound'. However, sinks and flats are not always DEM artefacts and can be natural phenomena as well. This is especially the case when soil is eroded and deposited by landsliding and DEM elevation data are adapted during subsequent timesteps of the model: 'spoons' and 'toes' of eroded and deposited landslide material can both result in sinks and flat areas, in this case representing the result of a 'natural' process. Accordingly, new algorithms, dealing with water and sediment transport in and through natural sinks and flats should be developed, tested and applied.

7.4.3 Integration of geomorphic process models and landuse change models

As explained in Chapter 3, LAPSUS-LS is developed as a model component within the LAPSUS modelling framework (LandscApe ProcesS modelling at mUlti dimensions and scaleS; Schoorl et al., 2000). Originally LAPSUS is a dynamic landscape process model to address spatial patterns of soil redistribution by water run-off and tillage erosion. LAPSUS-LS was developed separately, specifically for the New Zealand study area, where shallow landsliding is the most dominant denudation process. It should be noted that deep-seated landsliding, although an important process in the Waitakere Ranges on the long term, is not included in the model at this stage. When extending applications of LAPSUS to study sites where several or all of these different geomorphic processes are acting together, a full integration of the different model components, making it possible to cope with interactions and possible feedback mechanisms, is conceivable.

Geomorphic processes acting on hillslopes are significantly influenced by land cover through the effects on soil physical conditions and erodibility. Consequently, land use change may have a large impact on erosion and sedimentation processes. Moreover this is a dynamic relationship and landscape processes can in turn cause land use change. These connections bring about the need to integrate the LAPSUS modelling framework with landuse change models that can account for spatial, temporal, biophysical and socio-economic factors (Veldkamp and Verburg, 2004). In this context LAPSUS-LS is well suited because the influence of vegetation on soil cohesion can be made spatially explicit by assigning root cohesion values to different landuse types (C_r in Eq. (3.2)). Consequently, the integration of LAPSUS with e.g. the existing land use change model CLUE (the Conversion of Land Use and its Effects; Veldkamp and Fresco, 1996a and 1996b; Verburg et al., 2002) is regarded as an important subject for future research.



References

- Agresti, A., 2002. *Categorical Data Analysis*, Second Edition. John Wiley and Sons, New York, US.
- Ahmed, M. and Ogden, J., 1987. Population dynamics of the emergent conifer *Agathis australis* (D. Don) Lindl. (kauri) in New Zealand. 1. Population structure and tree growth rates in mature stands. *New Zealand Journal of Botany* 25, 217-229.
- Ahnert, F., 1987. An approach to the identification of morphoclimates. In: Gardiner, V. (Ed.), *International Geomorphology 1986*. Wiley, Chichester, UK, pp 159-188.
- Aitken, M.J., 1990. *Science-based Dating in Archaeology*. Longman, London, UK.
- Alloway, B.V. and Newnham, R.M., 1995. A preliminary assessment of the threat posed by distal silicic volcanism based in the Middle-Late Quaternary tephrostratigraphic record. *Geological Society of New Zealand Miscellaneous Publication* 81B, 73-83.
- Alloway, B.V., Pillans, B.J., Sandhu, A.S. and Westgate, J.A., 1993. Revision of the marine chronology in the Wanganui Basin, New Zealand, based on the isothermal plateau fission-track dating of tephra horizons. *Sedimentary Geology* 82, 299-310.
- Alloway, B., Westgate, J., Pillans, B., Pearce, N., Newnham, R., Byrami, M. and Aarburg, S., 2004. Stratigraphy, age and correlation of middle Pleistocene silicic tephra in the Auckland region, New Zealand: A prolific distal record of TVZ volcanism. *New Zealand Journal of Geology and Geophysics* 47, 447-479.
- Anselin, W., 1988. *Spatial Econometrics: Methods and Models*. Kluwer, Boston, US.
- Aspinall, R.J., 2002. Use of logistic regression for validation of maps of spatial distribution of vegetation species derived from high spatial resolution hyperspectral remotely sensed data. *Ecological Modelling* 157, 301-312.
- Auckland Regional Council, 2002. *Auckland Water Resource Quantity statement 2002*, TP 171. ARC, Auckland, New Zealand.
- Austin, M.P., 1985. Continuum concept, ordination methods, and niche theory. *Annual Review of Ecology and Systematics* 16, 39-61.
- Ballance, P.F., 1968. The physiography of the Auckland district. *New Zealand Geographer* 24, 23-49.
- Ballance, P.F., 1976a. Evolution of the upper Cenozoic magmatic arc and plate boundary in northern New Zealand. *Earth and Planetary Letters*, 28, 356-370.
- Ballance, P.F., 1976b. Stratigraphy and bibliography of the Waitemata Group of Auckland. *New Zealand Journal of Geology and Geophysics* 19, 897-932.
- Ballance, P.F. and Williams, P.W., 1992. The geomorphology of Auckland and Northland. In: Soons, J.M. and Selby, M.J. (Eds.), *Landforms of New Zealand Second Edition*. Longman Paul, Auckland, New Zealand, pp 210-232.
- Ballance, P.F., Hayward, B.W. and Wakefield, L.L., 1977. Group nomenclature of Late Oligocene and Early Miocene rocks in Auckland and Northland, New Zealand: and an Akarana Supergroup. *New Zealand Journal of Geology and Geophysics*, 20, 673-686.
- Band, L.E. and Moore, I.D., 1995. Scale: landscape attributes and geographical information systems. *Hydrological Processes* 9, 401-422.
- Band, L.E., Patterson, P., Nemani, R. and Running, S.W., 1993. Forest ecosystem processes at the watershed scale: incorporating hillslope hydrology. *Agricultural and Forest Meteorology* 63, 93-126.

- Barling, R.D., Moore, I.D. and Grayson, R.B., 1994. A quasi-dynamic wetness index for characterizing the spatial distribution of zones of surface saturation and soil water content. *Water Resources Research* 30, 1029-1044.
- Barter, T.P., 1976. The Kaihu Group (Plio-Quaternary) of the Awhitu Peninsula, south-west Auckland. Unpublished PhD thesis, University of Auckland, New Zealand.
- Bates P.D., Anderson, M.G. and Horritt, M., 1998. Terrain information in geomorphological models: stability, resolution and sensitivity. In: Lane, S.N, Richards, K.S and Chandler, J.H (Eds), *Landform monitoring, modelling and analysis*. John Wiley & Sons Ltd., New York, US, pp 279-309.
- Bathurst J.C., Burton A. and Ward T.J., 1997. Debris flow run-out and landslide sediment delivery model tests. *Journal of Hydraulic Engineering* 123, 410-419.
- Becker, A. and Braun, P., 1999. Disaggregation, aggregation and spatial scaling in hydrological modelling. *Journal of Hydrology* 217, 239-252.
- Bell, K.P. and Bockstael, N.E., 2000. Applying the generalized-moments estimation approach to spatial problems involving microlevel data. *The Review of Economics and Statistics* 82, 72-82.
- Benda, L.E. and Cundy, T.W., 1990. Predicting deposition of debris flows in mountain channels. *Canadian Geotechnical Journal* 27, 409-417.
- Bender, M.L., Fairbanks, R.G., Taylor, F.W., Matthews, R.K., Goddard, J.G. and Broecker, W.S., 1979. Uranium-series dating of the Pleistocene reef tracts of Barbados, West Indies. *Geological Society of America Bulletin* 90, 577-594.
- Berryman, K., 1993. Age, height, and deformation of Holocene marine terraces at Mahia Peninsula, Hikurangi subduction margin, New Zealand. *Tectonics* 12, 1347-1364.
- Berryman, K., Marden, M., Eden, D., Mazengarb, C., Ota, Y., and Moriya, I., 2000. Tectonic and paleoclimatic significance of Quaternary river terraces of the Waipaoa River, east coast, North Island, New Zealand. *New Zealand Journal of Geology and Geophysics* 43, 229-245.
- Beu, A.G. and Edwards, A.R., 1984. New Zealand Pleistocene and late Pliocene glacio-eustatic cycles. *Palaeogeography, Palaeoclimatology, Palaeoecology* 46, 119-142.
- Beven, K.J. and Kirkby, M.J., 1979. A physically based, variable contributing area model of basin hydrology. *Hydrological Sciences Bulletin* 24, 43-69.
- Beven K.J. and Moore, I.D. (Eds.), 1993. *Terrain Analysis and Distributed Modelling in Hydrology*. John Wiley & Sons, New York, US.
- Black, T.M., Shane, P.A.R., Westgate, J.A. and Froggatt, P.C., 1996. Chronological and palaeomagnetic constraints on widespread welded ignimbrites of the Taupo volcanic zone, New Zealand. *Bulletin of Volcanology* 58, 226-238.
- Bockstael, N.E., 1996. Modelling economics and ecology: the importance of a spatial perspective. *American Journal of Agricultural Economics* 78, 1168-1180.
- Bolstad, P.V. and Stowe, T., 1994. An evaluation of DEM accuracy: elevation, slope and aspect. *Photographic Engineering and Remote Sensing* 60, 1327-1332.
- Bonan, G.B. and Shugart, H.H., 1989. Environmental factors and ecological processes in boreal forests. *Annual Review of Ecology and Systematics* 20, 1-28.
- Borga, M., Dalla Fontana, G., Da Ros, D. and Marchi, L., 1998. Shallow landslide hazard assessment using a physically based model and digital elevation data. *Environmental geology* 35, 81-88.
- Borga, M., Dalla Fontana, G., Gregoretti, C. and Marchi, L., 2002. Assessment of shallow landsliding by using a physically based model of hillslope stability. *Hydrological Processes* 16, 2833-2851.
- Bradley, R.S., 1999. *Paleoclimatology, Reconstructing Climates of the Quaternary (Second Edition)*. Academic Press, San Diego, US.
- Bradshaw, J.D., 1989. Cretaceous geotectonic patterns in the New Zealand region. *Tectonics* 8, 803-820.
- Brand E.W. and Hudson, R.R., 1982. CHASE – an empirical approach to the design of cut slopes in Hong Kong soils. *Proc. 7th S.E. Asian Geotechnical Conf., Hong Kong, Vol.1*, 1-16.
- Braun, P., Molnar, T. and Kleeberg, H.B., 1997. The problem of scaling in grid-related hydrological process modelling. *Hydrological Processes* 11, 1219-1230.
- Bridgland, D.T., 2000. River terrace systems in north-west Europe: an archive of environmental change, uplift and early human occupation. *Quaternary Science Reviews* 19, 1293-1303.
- Bridgland, D., Maddy, D. and Bates, M., 2004. River terrace sequences: templates for Quaternary geochronology and marine-terrestrial correlation. *Journal of Quaternary Science* 19, 203-218.

- Brooks, S.M., 2003. Slopes and slope processes: research over the past decade. *Progress in Physical Geography* 27, 130-141.
- Brooks S.M., Crozier, M.J., Preston, N.J. and Anderson, M.G., 2002. Regolith stripping and the control of shallow translational hillslope failure: application of a two-dimensional coupled soil hydrology-slope stability model, Hawke's Bay, New Zealand. *Geomorphology* 45, 165-179.
- Brothers, R.N., 1954. The relative Pleistocene chronology of the South Kaipara District, New Zealand. *Transactions of the Royal Society of New Zealand* 82, 677-694.
- Brown, D.G. 1994. Predicting vegetation types at treeline using topography and biophysical disturbance variables. *Journal of Vegetation Science* 5, 641-656.
- Brunsdon, D., 1993. Mass movement; the research frontier and beyond: a geomorphological approach. *Geomorphology* 7, 85-128.
- Bull, W.B., 1991. Climate and landscape change in a humid fluvial system. In: Bull, W.B., 1991. *Geomorphic Responses to Climatic Change*. Oxford University Press, New York, US, pp 227-269.
- Burns, B.R. and Leathwick, J.R., 1996. Vegetation-environment relationships at Waipoua Forest, Northland, New Zealand. *New Zealand Journal of Botany* 34, 79-92.
- Burrows, C., 1990. *Processes of Vegetation Change*. Unwin Hyman, London, UK.
- Burton A. and Bathurst, J.C., 1998. Physically based modelling of shallow landslide sediment yield at a catchment scale. *Environmental Geology* 35, 89-99.
- Butcher, D.P., Labadz, J.C., Potter, W.R. and White, P., 1993. Reservoir sedimentation rates in the Southern Pennine Region, UK. In: McManus, J., Duck, R.W. (Eds.), *Geomorphology and Sedimentology of Lakes and Reservoirs*. Wiley, New York, US, pp 73-92.
- Butler, D.R. and Walsh, S.J., 1994. Site characteristics of debris flows and their relationship to alpine treeline. *Physical Geography* 15, 181-199.
- Caine, N. and Swanson, F.J., 1989. Geomorphic coupling of hillslope and channel systems in two small mountain basins. *Zeitschrift für Geomorphologie* 33, 189-203.
- Calavache, V.M.L., 1984. Evaluation report of some aspects of Parakai Bore № 1. Geothermal Institute, University of Auckland, New Zealand.
- Campbell H., 1998. Our place. In: Hicks G. and Campbell H. (Eds.), *Awesome Forces: The natural hazards that threaten New Zealand*. Te Papa Press, Wellington, New Zealand, pp 3-17.
- Campbell, I.B., 1973. Late Pleistocene alluvial pumice deposits in the Wanganui Valley. *New Zealand Journal of Geology and Geophysics* 16, 717-721.
- Carrara A., Bitelli, G. and Carla, R., 1997. Comparison of techniques for generating digital terrain models from contour lines. *International Journal of Geographical Information Science* 11, 451-473.
- Carter, L., 1980. Ironsand in continental shelf systems off western New Zealand – a synopsis. *New Zealand Journal of Geology and Geophysics*, 23, 455-468.
- Carter, L., Nelson, C.S., Neil, H.L. and Froggatt, P.C., 1995. Correlation, dispersal, and preservation of the Kawakawa Tephra and other late Quaternary tephra layers in the Southwest Pacific Ocean. *New Zealand Journal of Geology and Geophysics* 38, 29-46.
- Cathersides, P.S., 1972. A geographical appraisal of the geocological distribution of *Agathis australis*, *Beilschmiedia tawa*, and *Dacrydium cupressinum* communities in selected areas of the North Island, New Zealand. Unpublished MA thesis, University of Auckland, New Zealand, 154 pp.
- Chairat, S. and Delleur, J.W., 1993. Effects of Topographic Index Distribution on Predicted Runoff Using GRASS. *Water Resources Bulletin, American Water Resources Association* 29, 1029-1034.
- Chappell, J., 1974. Geology of coral terraces, Huon Peninsula, New Guinea: a study of Quaternary tectonic movements and sea-level changes. *Geological Society of America Bulletin* 85, 553-570.
- Chappell, J., 1975. Upper Quaternary warping and uplift rates in the Bay of Plenty and west coast, North Island, New Zealand. *New Zealand Journal of Geology and Geophysics* 18, 129-155.
- Chappell, J., 1983. A revised sea-level record for the last 300 000 years from Papua New Guinea. *Search* 14, 99-101.
- Chappell, J. and Veeh, H.H., 1978. Late Quaternary tectonic movements and sea-level changes at Timor and Atauro Island. *Geological Society of America Bulletin* 89, 356-368.
- Chappell, J., Ota, Y. and Berryman, K., 1996. Late Quaternary coseismic uplift history of Huon Peninsula, Papua New Guinea. *Quaternary Science Reviews* 15, 7-22.

- Claessens, L. and Veldkamp, A., 2005a. A Quaternary uplift record for the northern Waitakere Ranges, Te Henga-Muriwai, New Zealand, based on marine-terrestrial correlations of coastal and fluvial terraces. *Quaternary Science Reviews*. Submitted.
- Claessens, L., Schoorl, J.M. and Veldkamp, A., 2005b. Modelling the location of shallow landslides and their effects on landscape dynamics in large watersheds: an application for Northern New Zealand. *Geomorphology*. In press.
- Claessens, L., Heuvelink, G.B.M., Schoorl, J.M. and Veldkamp, A., 2005c. DEM resolution effects on shallow landslide hazard and soil redistribution modelling. *Earth Surface Processes and Landforms* 30. In press.
- Claessens, L., Lowe, D.J., Hayward, B.W., Schoorl, J.M. and Veldkamp, A., 2005d. Reconstructing high-magnitude/low-frequency landslide events based on soil redistribution modelling and a Late-Holocene sediment record from New Zealand. *Geomorphology*. Submitted.
- Claessens, L., Verburg, P.H., Schoorl, J.M. and Veldkamp, A., 2005e. Contribution of topographically based landslide hazard modelling to the analysis of the spatial distribution and ecology of kauri (*Agathis australis*). *Landscape Ecology*. Submitted.
- Clark, R.H., 1948. Evolution of drainage of area between southern shores of Kaipara Harbour and Waitemata Harbour. Unpublished MSc thesis, University of Auckland, New Zealand.
- Clark, J.S., 1991. Disturbance and tree life history on the shifting mosaic landscape. *Ecology* 72, 1102-1118.
- Cooper, A.F., Barreiro, A.B., Kimbrough, D.L. and Mattison, J.M., 1987. Lamprophyre dike intrusion and age of the Alpine Fault, New Zealand. *Geology* 15, 941-944.
- Crozier, M.J., 1996. Magnitude/frequency issues in landslide hazard assessment. *Heidelberger Geographische Arbeiten* 104, 221-236.
- Crozier, M.J., 1999. Prediction of rainfall-triggered landslides: a test of the antecedent water status model. *Earth Surface Processes and Landforms* 24, 825-833.
- Crozier, M.J., Gage, M., Pettinga, J.R., Selby, M.J. and Wasson, R.J., 1992. The stability of hillslopes. In: Soons, J.M., Selby, M.J. (Eds.), *Landforms of New Zealand*. Longman, Auckland, New Zealand, pp 63-90.
- Davis, F.W. and Goetz, S., 1990. Modeling vegetation pattern using digital terrain data. *Landscape Ecology* 4, 69-80.
- Day, M.J., 1980. Landslides in the Gunung Mulu National Park. *Geographical Journal* 146, 7-13.
- Dearing, J.A. and Foster, I.D.L., 1993. Lake Sediments and Geomorphological Processes: Some Thoughts. In: McManus, J., Duck, R.W. (Eds.), *Geomorphology and Sedimentology of Lakes and Reservoirs*. Wiley, New York, US, pp 5-14.
- Deckers, J.A., Driessen, P.M., Nachtergaele F.O. and Spaargaren, O.C., 2002. World Reference Base for Soil Resources. In: Lal, R. (Ed.), *Encyclopedia of Soil Science*. Marcel Dekker Inc., New York, US, pp 1446-1452.
- Del Barrio, G., Alvera, B., Puigdefabregas, J. and Diez, C., 1997. Response of high mountain landscape to topographic variables: Central Pyrenees. *Landscape Ecology* 12, 95-115.
- Denyer, K., Cutting, M., Campbell, G., Green, C. and Hilton, M., 1993. Waitakere Ecological District, Survey Report for the Protected Natural Areas Programme. Auckland Regional Council, Newton, Auckland, New Zealand.
- De Ploey, J. and Cruz, O., 1979. Landslides in the Serra do Mar, Brazil. *Catena* 6, 111-122.
- DeRoo, A.P.J., 1996. Validation problems of hydrological and soil erosion catchment models: examples from a Dutch erosion project. In: Anderson, M.G. and Brooks, S.M. (Eds.), *Advances in hillslope processes*. John Wiley and Sons Ltd, Chisester, UK, pp 669-684.
- De Rose, R.C., Trustrum, N.A. and Blaschke, P.M., 1993. Post-deforestation soil loss from steep land hillslopes in Taranaki, New Zealand. *Earth Surface Processes and Landforms* 18, 131-144.
- Desmet, P.J.J., 1997. Effects of interpolation errors on the analysis of DEMs. *Earth Surface Processes and Landforms* 22, 563-580.
- Desmet, P.J.J. and Govers, G., 1996. Comparison of routing algorithms for digital elevation models and their implication for predicting ephemeral gullies. *International Journal of Geographical Information Science* 10, 311-331.
- Desmet, P.J.J. and Govers, G., 1997. Comment on 'Modelling topographic potential for erosion and deposition using GIS'. *International Journal of Geographical Information Science* 11, 603-610.
- Diamond, J.T. and Hayward, B.W., 1979. The Maori history and legend of the Waitakere Ranges. Lodestar Press, Auckland, New Zealand.

- Diamond, J.T. and Hayward, B.W., 1980. Waitakere Kauri: A pictorial history of the Kauri timber industry in the Waitakere Ranges, West Auckland. Lodestar Press, Auckland, New Zealand.
- Dietrich, W.E. and Montgomery, D.R., 1998. SHALSTAB: a digital terrain model for mapping shallow landslide potential. <http://socrates.berkeley.edu/~geomorph/shalstab/> [08-12-2004].
- Dietrich, W.E., Wilson, C.J., Montgomery, D.R., McKean J. and Bauer, R., 1992. Erosion thresholds and land surface morphology. *Geology* 20, 675-679.
- Dietrich, W.E., Wilson, C.J., Montgomery, D.R. and McKean J., 1993. Analysis of erosion thresholds, channel networks and landscape morphology using a digital terrain model. *Journal of Geology* 101, 161-180.
- Dietrich, W.E., Reiss, R., Hsu, M. and Montgomery, D.R., 1995. A process-based model for colluvial soil depth and shallow landsliding using digital elevation data. *Hydrological Processes*, 9, 383-400.
- Douglas, I., 1999. Hydrological investigations of forest disturbance and land cover impacts in South-East Asia: a review. *Philosophical Transactions of the Royal Society of London, Series B* 354, 1725-1738.
- Douglas, I., Bidin, K., Balamurugan, G., Chappell, N.A., Walsh, R.P.D., Greer, T. and Sinun, W., 1999. The role of extreme events in the impacts of selective forestry on erosion during harvesting and recovery phases at Danum Valley, Sabah. *Philosophical Transactions of the Royal Society of London, Series B* 354, 1749-1761.
- Duan J. and Grant, G.E., 2000. Shallow landslide delineation for steep forest watersheds based on topographic attributes and probability analysis. In: Wilson, J.P. and Gallant, J.C. (Eds.), *Terrain Analysis: Principles and Applications*. John Wiley & sons, New York, US, pp 311-329.
- Dubayah, R. and Rich, P.M., 1995. Topographic solar radiation models for GIS. *International Journal of Geographic Information Systems* 9, 405-419.
- Dunn, M. and Hickey, R., 1998. The effect of slope algorithms on slope estimates within a GIS. *Cartography* 27, 9-15.
- Dykes, A.P., 2002. Weathering-limited rainfall-triggered shallow mass movements in undisturbed steep land tropical rainforest. *Geomorphology* 46, 73-93.
- Dykes, A.P. and Thornes, J.B., 1996. Tectonics and relief in tropical forested mountains: the Gipfelflur hypothesis revisited. In: Anderson, M.G., Brooks, S.M. (Eds.), *Advances in Hillslope Processes*, vol. 2. Wiley, Chichester, UK, pp 975-994.
- Ecroyd, C.E., 1982. Biological Flora of New Zealand 8. *Agathis australis* (D. Don) Lindl. (Araucariaceae) Kauri. *New Zealand Journal of Botany* 24, 17-36.
- Edbrooke, S.W. (compiler), 2001. *Geology of the Auckland area*. Institute of Geological and Nuclear Sciences 1:250 000 geological map 3. 1 sheet + 74p. Institute of Geological and Nuclear Sciences Limited, Lower Hutt, New Zealand.
- Eden, D.N., 1989. River terraces and their loessial cover beds, Awatere River Valley, South Island, New Zealand. *New Zealand Journal of Geology and Geophysics* 32, 487-497.
- Eden, D.N. and Froggatt, P.C., 1996. A 6500 year-old history of tephra deposition recorded in the sediments of Lake Tutira, eastern North Island, New Zealand. *Quaternary International* 34-36, 55-64.
- Eden, D.N. and Page, M.J., 1998. Palaeoclimatic implications of a storm erosion record from late Holocene lake sediments, North Island, New Zealand. *Palaeogeography, Palaeoclimatology, Palaeoecology* 139, 37-58.
- Eden, D.N., Palmer, A.S., Cronin, S.J., Marden, M. and Berryman, K.R., 2001. Dating the culmination of river aggradation at the end of the last glaciation using distal tephra compositions, eastern North Island, New Zealand. *Geomorphology* 38, 133-151.
- Enright, N.J., 2001. Nutrient accessions in a mixed conifer-angiosperm forest in northern New Zealand. *Austral Ecology* 26, 618-629.
- Enright, N.J. and Ogden, J., 1995. The southern conifers – a synthesis. In: Enright, N.J. and Hill, R.S. (Eds.), *Ecology of the southern conifers*. Melbourne University Press, Melbourne, Australia, pp 271-287.
- Enright, N.J., Ogden, J. and Rigg, L.S., 1999. Dynamics of forests with Araucariaceae in the western Pacific. *Journal of Vegetation Science* 10, 793-804.
- Environmental Systems Research Institute (ESRI), 1999. ArcView GIS version 3.2, Redlands, California, US.
- Evans, M. and Slaymaker, O., 2004. Spatial and temporal variability of sediment delivery from alpine lake basins, Cathedral Provincial Park, southern British Columbia. *Geomorphology* 61, 209-224.
- Fair, E.E., 1968. Structural, tectonic and climate control of the fluvial geomorphology of the Manawatu River west of the Manawatu Gorge, Unpublished MSc thesis, Massey University, Palmerston North, New Zealand.
- Fairfield, J. and Leymarie, P., 1991. Drainage networks from grid digital elevation models. *Water Resources Research* 27, 709-717.

- Fannin R.J. and Wise, M.P., 2001. An empirical-statistical model for debris flow travel distance. *Canadian Geotechnical Journal* 38, 982-994.
- FAO, 2001. Lecture notes on the major soils of the world. World Soil Resources Report no. 94. FAO, Rome. Italy
- Fielding, A.H. and Bell, J.F., 1997. A review of methods for the assessment of prediction errors in conservation presence/absence models. *Environmental Conservation* 24, 38-49.
- Finlay, P.J., Fell, R. and Maguire, P.K., 1997. The relationship between the probability of landslide occurrence and rainfall. *Canadian Geotechnical Journal* 34, 811-824.
- Florinsky, I.V., 1998. Accuracy of local topographic variables derived from digital elevation models. *International Journal of Geographical Information Science* 12, 47-61.
- Florinsky, I.V. and Kuryakova, G.A., 1996. Influence of topography on some vegetation cover properties. *Catena* 27, 123-141.
- Formento-Trigilio, M.L., Burbank, D.W., Nicol, A., Shulmeister, J. and Rieser, U., 2002. River response to an active fold-and-thrust belt in a convergent margin setting, North Island, New Zealand. *Geomorphology* 49, 125-152.
- Foster, G.R. and Meyer, L.D., 1972. A closed-form soil erosion equation for upland areas. In: Shen, H.W. (Ed.), *Sedimentation: symposium to honour professor H.A. Einstein*. Colorado State University, Fort Collins, Colorado. 12.1-12.19.
- Foster, G.R. and Meyer, L.D., 1975. Mathematical simulation of upland erosion by fundamental erosion mechanics. In: Anonymous (Ed.), *Present and perspective technology for predicting sediment yields and sources*. Proceedings Sediment Yield Workshop, Oxford 1972. United States Department of Agriculture, Washington D.C., 190-207.
- Foster, I.D.L., Dearing, J.A., Grew, R. and Orend, K., 1990. The sedimentary database. In: Walling, D.E., Yair, A., Berkowicz, S. (Eds.), *Erosion, Transport, and Deposition Processes*, IAHS Publication 189, Wallingford, UK, pp 19-43.
- Franklin, J., 1998. Predicting the distribution of shrub species in southern California from climate and terrain-derived variables. *Journal of Vegetation Science* 9, 733-749.
- Froggatt, P.C., 1983. Towards a comprehensive Upper Quaternary tephra and ignimbrite stratigraphy of New Zealand using electron microprobe analysis of glass shards. *Quaternary Research* 19, 188-200.
- Froggatt, P.C. and Lowe, D.J., 1990. A review of Quaternary silicic and some other tephra formations from New Zealand: their stratigraphy, nomenclature, distribution, volume, and age. *New Zealand Journal of Geology and Geophysics* 33, 89-109.
- Froggatt, P.C., Nelson, C.S., Carter, L., Griggs, G. and Black, K.P., 1986. An exceptionally large late Quaternary eruption from New Zealand. *Nature* 319, 578-582.
- Gage, M., 1953. The study of Quaternary strand-lines in New Zealand. *Transactions of the Royal Society of New Zealand* 81, 27-34.
- Gao, J., 1998. Impact of sampling intervals on the reliability of topographic variables mapped from grid DEMs at a micro-scale. *International Journal of Geographical Information Science* 12, 875-890.
- Garbrecht, J. and Martz, L., 1994. Grid size dependency of parameters extracted from digital elevation models. *Computers and Geosciences* 20, 85-87.
- Gardner, R.O., 1981. Some species lists of native plants of Auckland region. *Tane* 27, 196-174.
- Gibb, J.G., 1986. A New Zealand regional Holocene eustatic sea-level curve and its application for determination of vertical tectonic movement. *Bulletin of the Royal Society of New Zealand* 24, 377-395.
- Glade, T., 1996. The temporal and spatial occurrence of landslide-triggering rainstorms in New Zealand. *Heidelberger Geographische Arbeiten* 104, 237-250.
- Glade, T., 1998. Establishing the frequency and magnitude of landslide-triggering rainstorm events in New Zealand. *Environmental Geology* 35, 160-174.
- Glade, T., 2003. Landslide occurrence as a response to land use change: a review of evidence from New Zealand. *Catena* 51, 297-314.
- Glymph, L.M., 1945. Studies of sediment yields from watersheds. *International Association of Hydrological Sciences Publication* 36, 173-191.
- Goes, S., Loohuis, J.J.P., Wortel, M.J.R. and Govers, R., 2000. The effect of plate stresses and shallow mantle temperatures on tectonics of north-western Europe. *Global and Planetary Change* 27, 23-38.
- Goff, J.R., Hicock, S.R. and Hamilton, T.S., 1996. Recent Holocene changes in sedimentation in a landslide-dammed lake in the Cascade Mountains, southwestern British Columbia, Canada. *The Holocene* 6, 75-81.

- Goldie, P.J., 1975. Quaternary geology of an area north of Houhora. Unpublished MSc thesis, University of Auckland, New Zealand.
- Goodchild, M.F., Parks, B.O. and Steyaert, L.T., 1993. Environmental Modeling with GIS. Oxford University Press, Oxford.
- Gottfried, M., Pauli, H. and Grabherr, G., 1998. Prediction of vegetation patterns at the limits of plant life: a new view of the alpine-nival ecotone. *Arctic and Alpine Research* 30, 207-221.
- Graham, J., 1984. Methods of stability analysis. In: Brunsdon, D., Prior D.B. (Eds.), *Slope Instability*. John Wiley and Sons, New York, US, pp 171-215.
- Grayson, R.B., Bloschl, G., Barling, R.D. and Moore, I.D., 1993. Process, scale and constraints to hydrologic modeling in GIS. HydroGIS conference. IAHS Publ. 211, 83-92.
- Green, J.D. and Lowe, D.J., 1994. Origins and development. In: Clayton, J.S., de Winton, M.D. (Eds.), *Lake Rotoroa: Change in an Urban Lake*. NIWA Ecosystems Publication 9, Hamilton, New Zealand, pp 13-23.
- Guariguata, M.R., 1990. Landslide disturbance and forest regeneration in the upper Luquillo mountains of Puerto Rico. *Journal of Ecology* 75, 814-832.
- Guisan, A. and Zimmerman, N.E., 2000. Predictive habitat distribution models in ecology. *Ecological Modelling* 135, 147-186.
- Hattanji, T. and Onda, Y., 2004. Coupling of runoff processes and sediment transport in mountainous watersheds underlain by different sedimentary rocks. *Hydrological Processes* 18, 623-636.
- Hayward, B.W., 1976. Lower Miocene stratigraphy and structure of the Waitakere Ranges, North Auckland, New Zealand and the Waitakere Group (new). *New Zealand journal of geology and geophysics* 19, 871-895.
- Hayward, B.W., 1983. Geological Map of New Zealand 1:50 000 Sheet Q11 Waitakere. Map (1 sheet) and notes. New Zealand Department of Scientific and Industrial Research, Wellington, New Zealand, 28 pp.
- Hayward, B.W., 1993. The tempestuous 10 million year life of a double arc and intra-arc basin – New Zealand's Northland Basin in the Early Miocene. In: Ballance, P.F. (Ed.), *South Pacific sedimentary basins. Sedimentary basins of the world 2*. Elsevier, Amsterdam, pp 113-142.
- Hayward, B.W. and Diamond, J.T., 1978. Prehistoric archaeological sites of the Waitakere Ranges and West Auckland, New Zealand. Auckland Regional Authority, Auckland, New Zealand.
- Hayward, B.W., 1979. Eruptive History of the Early to Mid Miocene Waitakere Volcanic Arc, and Palaeogeography of the Waitemata Basin, Northern New Zealand. *Journal of the Royal Society of New Zealand* 9, 297-320.
- Hayward, B.W., Grenfell, H.R., Reid, C. and Hayward, K.A., 1999. Recent New Zealand shallow water benthic foraminifera – taxonomy, ecological distribution, biogeography and use in paleoenvironmental assessment. *Institute of Geological & Nuclear Sciences Monograph* 21, Lower Hutt, New Zealand, 258 pp.
- Hayward, B. W., Scott, G. H., Grenfell, H. R., Carter, R. and Lipps, J.H., 2004. Techniques for estimation of tidal elevation and confinement (~salinity) histories of sheltered harbours and estuaries using benthic foraminifera: Examples from New Zealand. *The Holocene* 14, 218-232.
- Heerdegen, R.G. and Sheperd, M.J., 1992. Manawatu landforms - Product of tectonism, climate change and process. In: Soons, J.M and Selby, M.J. (Eds.), *Landforms of New Zealand*. Longman Paul, Auckland, New Zealand.
- Herzer, R.H., 1995. Seismic stratigraphy of a buried volcanic arc, Northland, New Zealand and implications for Neogene subduction. *Marine and Petroleum Geology* 12, 511-531.
- Hesp, P.A., Shepherd, M.J. and Parnell, K., 1999. Coastal geomorphology in New Zealand. 1989-99. *Progress in Physical Geography* 23, 501-524.
- Hesse, P.P., 1993. A Quaternary record of the Australian environment from aeolian dust in Tasman Sea sediments. Unpublished PhD thesis, Australian National University, Canberra, Australia.
- Heuvelink, G.B.M., 1998. Error Propagation in Environmental Modelling with GIS. Taylor & Francis, London, UK.
- Hicks, D.L., 1975. Geomorphic development of the southern Aupouri and Karikari peninsulas, with special reference to sand dunes. Unpublished MA thesis, University of Auckland, New Zealand.
- Hicks, D.L., 1995. A way to estimate the frequency of rainfall-induced mass movements (note). *Journal of Hydrology (New Zealand)* 33, 59-67.
- Hicks, D.M., Gomez, B. and Trustrum, N.A., 2000. Erosion thresholds and suspended sediment yields, Waipaoa River Basin, New Zealand. *Water Resources Research* 36, 1129-1142.
- Hogg, A.G., Lowe, D.J. and Hendy, C.H., 1987. University of Waikato radiocarbon dates I. *Radiocarbon* 29, 263-301.

- Hogg, A.G., Higham, T.F.G., Lowe, D.J., Palmer, J., Reimer, P. and Newnham, R.M., 2003. A wiggle-match date for polynesian settlement of New Zealand. *Antiquity* 77, 116-125.
- Holmgren, P., 1994. Multiple flow direction algorithm for runoff modeling in grid based elevation models: an empirical evaluation. *Hydrological Processes* 8, 327-334.
- Hörsch, B., 2003. Modelling the spatial distribution of montane and subalpine forests in the central Alps using digital elevation models. *Ecological Modelling* 168, 267-282.
- Hovius, N., Stark, C.P. and Allen, P.A., 1997. Sediment flux from a mountain belt derived by landslide mapping. *Geology* 25, 231-234.
- Hunt, T.M., 1978. Stokes Magnetic Anomaly System. *New Zealand Journal of Geology and Geophysics*, 21, 595-606.
- Hutchinson, M.F. and Dowling, T.I., 1991. A continental hydrological assessment of a new grid-based digital elevation model of Australia. *Hydrological Processes* 5, 45-58.
- Ikeya, H., 1981. A method for designation for area in danger of debris flow. In: Davies, T.R.H., Pearce A.K. (Eds.), *Erosion and Sediment Transport in Pacific Rim Steeplands*. International Association of Hydrological Sciences Publication 132, pp 281-288.
- Isaac, M.J. (compiler), 1996. *Geology of the Kaitaia area*. Institute of Geological and Nuclear Sciences 1:250 000 geological map 1. 1 sheet + 44p. Institute of Geological and Nuclear Sciences Limited, Lower Hutt, New Zealand.
- Isaac, M.J., Herzer, R.H., Brook, F.J. and Hayward, B.W., 1994. Cretaceous and Cenozoic sedimentary basins of Northland, New Zealand. *Institute of Geological and Nuclear Sciences Monograph* 8, Lower Hutt, New Zealand, 203 pp.
- Istanbulluoglu, E., Tarboton, D.G., Pack, R.T. and Luce, C.H., 2004. Modeling of the interactions between forest vegetation, disturbances, and sediment yields. *Journal of Geophysical Research* 109, doi:10.1029/2003JF000041.
- Jakob, M., 2000. The impacts of logging on landslide activity at Clayoquot Sound, British Columbia. *Catena* 38, 279-300.
- Jenson, S.K., 1991. Applications of hydrologic information automatically extracted from digital elevation models. *Hydrological Processes* 5, 31-44.
- Jessop, R., 1992. The use of meso-scale climate modelling in an examination of the distribution of Kauri. Unpublished MSc thesis, University of Auckland, New Zealand, 97 pp.
- Johnson, A.M. and Rodine, J.R., 1984. Debris flow. In: Brunsten, D., Prior D.B. (Eds.), *Slope Instability*. John Wiley and Sons Ltd., New York, US, pp 257-361.
- Jones, K.H., 1998. A comparison of algorithms used to compute hill slope as a property of the DEM. *Computers and Geosciences* 24, 315-323.
- Kamp, P.J.J., 1988. Tectonic geomorphology of the Hikurangi Margin surface manifestations of different modes of subduction. *Zeitschrift für Geomorphologie* 69, 55-67.
- Kamp P.J.J., 1992a. Tectonic architecture of New Zealand. In: Soons J.M. and Selby M.J. (Eds.), *Landforms of New Zealand*. Longman Paul Ltd., Auckland, New Zealand, pp 1-27.
- Kamp, P.J.J., 1992b. Landforms of Hawke's Bay and their origin: a plate tectonic interpretation. In: Soons, J.M. and Selby, M.J. (Eds.), *Landforms of New Zealand Second Edition*. Longman Paul, Auckland, New Zealand, pp 344-366.
- Kermode L., 1992. *Geology of the Auckland Urban Area*. Scale 1:50 000. Institute of Geological & Nuclear Sciences geological map 2. Institute of Geological & Nuclear Sciences Ltd., Lower Hutt, New Zealand, 1 sheet + 63 pp.
- Kessler, J. and Oosterbaan, R., 1974. Determining hydraulic conductivities of soils. In: *Drainage principles and applications*. Publication 16, III, International institute for land reclamation and improvement, Wageningen, The Netherlands, 253-296.
- Kirkby, M.J., 1971. Hillslope process-response models based on the continuity equation. In: Brunsten, D. (Ed.), *Slopes, forms and processes*. Inst. Of Brit. Geographers, Spec. Pub., pp 15-30.
- Kirkby, M.J., 1987. General models of long-term slope evolution through mass movement. In: Anderson, M.G., Richards, K.S., 1987. *Slope stability*. John Wiley & Sons Ltd., New York, US, pp 359-379.
- Kirkpatrick, J.B. and Nunez, M., 1980. Vegetation-radiation relationships in mountainous terrain: eucalypt-dominated vegetation in the Risdon hills, Tasmania. *Journal of Biogeography* 7, 197-208.
- Korup, O., McSaveney, M.J. and Davies, T.R.H., 2004. Sediment generation and delivery from large historic landslides in the Southern Alps, New Zealand. *Geomorphology* 61, 189-207.

- Kramer, M.G., A.J. Hansen, M.L. Taper and Kissinger, E.J., 2001. Abiotic controls on long-term windthrow disturbance and temperate rain forest dynamics in southeast Alaska. *Ecology* 82(10), 2749-2768.
- Kukla, G. and Cílek, V., 1996. Plio-Pleistocene megacycles: record of climate and tectonics. *Palaeogeography, Palaeoclimatology, Palaeoecology* 120, 171-194.
- Kulakowski, D. and Veblen, T.T., 2002. Influences of fire history and topography on the pattern of a severe wind blowdown in a Colorado subalpine forest. *Journal of Ecology* 90, 806-819.
- Kumar, L., Skidmore, A.K. and Knowles, E. 1997. Modelling topographic variation in solar radiation in a GIS environment. *International Journal of Geographical Information Science* 11, 475-497.
- Land Information New Zealand, 2000. Technical Standards for the Production of New Zealand 260 Series Topographic Maps. Land Information New Zealand, Wellington, New Zealand.
- Larsen, M.C. and Simon, A., 1993. A rainfall intensity-duration threshold for landslides in a humid-tropical environment, Puerto Rico. *Geografiska Annaler, Series A* 75, 13-23.
- Larsen, M.C. and Torres-Sanchez, A.J., 1998. The frequency and distribution of recent landslides in three montane tropical regions of Puerto Rico. *Geomorphology* 24, 309-331.
- Lavé, J. and Avouac, J.P., 2000. Active folding of fluvial terraces across the Siwaliks Hills, Himalayas of central Nepal. *Journal of Geophysical Research* 105, 5735-5770.
- Leitch, E.C., 1966. The geology of the North Cape area. Unpublished MSc thesis, University of Auckland, New Zealand.
- Lensen, G.J. and Vella, P., 1971. The Waiohine river faulted terrace sequence. *Royal Society of New Zealand Bulletin* 9, 117-119.
- Li, Z., 1994. A comparative study of the accuracy of digital terrain models (DTMs) based on various data models. *ISPRS Journal of Photogrammetry and Remote Sensing* 49, 2-11.
- Lowe, D.J. 1988. Late Quaternary volcanism in New Zealand: towards an integrated record using distal airfall tephra in lakes and bogs. *Journal of Quaternary Science* 3, 111-120.
- Lowe, D.J. and Green, J.D., 1987. Origins and development of the lakes. In: Viner, A.B. (Ed.), *Inland Waters of New Zealand*. New Zealand Department of Scientific and Industrial Research Bulletin 241, pp 1-64.
- Lowe, D.J. and de Lange, W.P., 2000. Volcano-meteorological tsunamis, the c. 200 AD Taupo eruption (New Zealand) and the possibility of a global tsunami. *The Holocene* 10, 401-407.
- Lowe, D.J., Newnham, R.M. and Ward, C.M., 1999. Stratigraphy and chronology of a 15 cal yr sequence of multi-sourced silicic tephra in a montane peat bog, eastern North Island, New Zealand. *New Zealand Journal of Geology and Geophysics* 42, 565-579.
- Lowe, D.J., Tippet, J.M., Kamp, P.J.J., Liddell, I.J., Briggs, R.M. and Horrocks, J.L., 2001. Ages on weathered Plio-Pleistocene tephra sequences, western North Island, New Zealand. In: Juvigné, E.T. and Raynal, J-P. (Eds.), *Tephra: chronology, Archaeology, CDERAD éditeur, Goudet. Les Dossiers de l'Archéo-Logis* 1, pp 45-60.
- Mackey, B.G., Mullen, C.I., Baldwin, K.A., Gallant, J.C., Sims, R.A. and McKenney, D.W., 2000. Towards a spatial model of boreal forest ecosystems: the role of digital terrain analysis. In: Wilson, J.P. and Gallant, J.C. (Eds.), *Terrain Analysis: Principles and Applications*. John Wiley & Sons, New York, US, pp 391-422.
- Maddy, D., Bridgland, D.R. and Green C.P., 2000. Crustal uplift in southern England: evidence from the river terrace records. *Geomorphology* 33, 167-182.
- Mandelbrot, B., 1982. *The fractal geometry of nature*. W.H. Freeman, San Francisco, US.
- Manel, S., Dias, J.M. and Ormerod, S.J., 1999. Comparing discriminant analysis, neural networks and logistic regression for predicting species' distributions: a case study with a himalayan river bird. *Ecological Modelling* 120, 337-347.
- Manel, S., Williams, H.C. and Ormerod, S.J., 2001. Evaluating presence-absence models in ecology: the need to account for prevalence. *Journal of Applied Ecology* 38, 921-931.
- Marden, M. and Neall, V.E., 1990. Dated Ohakean terraces offset by the Wellington Fault near Woodville, New Zealand. *New Zealand Journal of Geology and Geophysics* 33, 449-453.
- Martin, Y., Rood, K., Schwab, J.W. and Church, M., 2002. Sediment transfer by shallow landsliding in the Queen Charlotte Islands, British Columbia. *Canadian Journal of Earth Science* 39, 189-205.
- McFadgen, B.G., 1989. Late Holocene depositional episodes in coastal New Zealand. *New Zealand Journal of Ecology (Supplement)* 12, 145-149.
- McKenney, D.W., Mackey, B.G. and Zavitz, B.L., 1999. Calibration and sensitivity of a spatially-distributed solar radiation model. *International Journal of Geographical Information Science* 13, 49-65.

- McMahon, T.J., 1994. The Quaternary geology of the South Kaipara Barrier. Unpublished MSc thesis, University of Auckland, New Zealand.
- Megahan, W.F., Monsen, S.B. and Wilson, M.D., 1991. Probability of sediment yields from surface erosion on granitic roadfills in Idaho. *Journal of Environmental Quality*, 20, 53-60.
- Menard, S., 2001. Applied logistic regression analysis. Sage University Papers Series: Quantitative applications in the social sciences. Paper 07-106. Thousand Oaks, London, UK.
- Metz, C.E., 1978. Basic principles of ROC analysis. *Seminars in Nuclear Medicine* 8, 283-298.
- Millener, L.H., 1965. Forest, scrub and fresh water communities. *Science in Auckland*, 11th New Zealand Science Congress. Auckland Institute and Museum, Auckland, New Zealand, pp 36-47.
- Milne, J.D.G., 1973. Mount Curl Tephra, a 230,000-year-old marker bed in New Zealand and its implications for Quaternary chronology. *New Zealand Journal of Geology and Geophysics* 16, 519-532.
- Mitasova, H., Hofierka, J., Zlocha, M. and Iverson, L.R., 1996. Modelling topographic potential for erosion and deposition using GIS. *International Journal of Geographical Information Systems* 10, 629-641.
- Mizukoshi H. and Aniya, M., 2002. Use of Contour-Based DEMs for Deriving and Mapping Topographic Attributes. *Photogrammetric Engineering & Remote Sensing* 68, 83-93.
- Mizuyama, T. and Ishikawa, Y., 1990. Prediction of debris flow prone areas and damage. American Society of Civil Engineers, Proceedings of International Symposium Hydraulics/Hydrology of Arid Lands, San Diego, California, US, pp 712-717.
- Mizuyama, T., Yazawa, A. and Ido, K., 1987. Computer simulation of debris flow depositional processes. *International Association of Hydrological Sciences, Publication* 165, 179-190.
- Molnar, P., Brown, E.T., Burchfiel, B.C., Deng, Q., Feng, X., Li, J., Raisbeck, G.M., Shi, J., Wu, Z., Yiou, F. and You, H., 1994. Quaternary climate change and the formation of river terraces across growing anticlines on the north flank of the Tien Shan, China. *Journal of Geology* 102, 583-602.
- Montgomery, D. R. and Foufoula-Georgiou, E., 1993. Channel network source representation using digital elevation models. *Water Resources Research* 29, 3925-3934
- Montgomery, D.R. and Dietrich, W.E., 1994. A physically based model for the topographic control on shallow landsliding. *Water Resources Research* 30, 1153-1171.
- Montgomery, D.R., Schmidt, K.M., Greenberg, H.M. and Dietrich, W.E., 2000. Forest clearing and regional landsliding. *Geology* 28, 311-314.
- Moon, V.G., de Lange, A. and de Lange, W.P., 2003. Mudslides developed on Waitemata Group rocks, Tawharanui Peninsula, North Auckland. *New Zealand Geographer* 59, 44-53.
- Moore, C.L., 1991. The distal terrestrial record of explosive rhyolitic volcanism: an example from Auckland, New Zealand. *Sedimentary Geology* 74, 25-38.
- Moore, I.D., 1996. Hydrologic modeling and GIS. In: Goodchild, M.F., Steyaert, L.T., Parks, B.O., Crane, M.P., Johnston, C.A., Maidment, D.R. and Glendinning, S.(Eds.), *GIS and Environmental Modeling: Progress and Research Issues*. GIS World Books, Fort Collins, US, pp 143-148.
- Moore, I.D. and Burch, G.J., 1986. Sediment transport capacity of sheet and rill flow: application of unit stream power theory. *Water Resources Research* 22, 1350-1360.
- Moore, I.D. and Wilson, J.P., 1992. Length-slope factors for the Revised Universal Soil Loss Equation: simplified method of estimation. *Journal of Soil and Water Conservation* 47, 23-428.
- Moore, I.D., O'Loughlin, E.M. and Burch, G.J., 1988. A contour based topographic model for hydrological and ecological applications. *Earth Surface Processes and Landforms* 13, 305-320.
- Moore, I.D., Grayson, R.B. and Ladson, A.R., 1991. Digital terrain modeling: a review of hydrological, geomorphological and biological applications. *Hydrological Processes* 5, 3-30.
- Moore, I.D., Norton, T.W. and Williams, J.E., 1993a. Modeling environmental heterogeneity in forested landscapes. *Journal of Hydrology* 150, 717-747.
- Moore, I.D., Turner, A.K., Wilson, J.P., Jenson, S.K. and Band, L.E., 1993b. GIS and land surface-subsurface modelling. In: Goodchild, M.F., Parks, B.O. and Steyaert, T. (Eds.), *Environmental Modeling with GIS*. Oxford University Press, New York-Oxford, US, pp 196-230.
- Motzkin, G., Wilson, P., Foster, D.R. and Allen, A., 1999. Vegetation patterns in heterogeneous landscapes: the importance of history and environment. *Journal of Vegetation Science* 10, 903-920.
- Mroczkowski, M., Raper, G.P. and Kuczera, G., 1997. The quest for more powerful validation of conceptual catchment models. *Water Resources Research* 33, 2325-2336.
- Murdoch, G.J., 1991. Cultural influences on the Ecology of the Waitakere Ranges. Unpublished report, Auckland Regional Council, Resource Management Division, Auckland, New Zealand.

- Murray-Wallace, C.V., 2002. Pleistocene coastal stratigraphy, sea-level highstands and neotectonism of the southern Australian passive continental margin – a review. *Journal of Quaternary Science* 17, 469-489.
- Myster, R.W., Thomlinson, J.R. and Larsen, M.C., 1997. Predicting landslide vegetation in patches on landscape gradients in Puerto Rico. *Landscape Ecology* 12, 299-307.
- Naish, T., Kamp, P.J.J., Alloway, B.V., Pillans, B., Wilson, G.S. and Westgate, J.A., 1996. Integrated tephrochronology and magnetostratigraphy for cyclothem marine strata, Wanganui Basin: implications for the Pliocene-Pleistocene boundary in New Zealand. *Quaternary International* 34-36, 29-48.
- Neall, V.E., 1992. Landforms of Taranaki and the Wanganui lowlands. In: Soons, J.M and Selby, M.J. (Eds.), *Landforms of New Zealand*. Longman Paul, Auckland, New Zealand, pp 287-307.
- Nelson, C.S., Mildenhall, D.C., Todd, A.J. and Pocknall, D.T., 1988. Subsurface stratigraphy, paleoenvironments, palynology, and depositional history of the late Neogene Tauranga Group at Ohinewai, Lower Waikato Lowland, South Auckland, New Zealand. *New Zealand Journal of Geology and Geophysics*, 31, 21-40.
- Neter, J., Kutner, M.H., Nachtsheim, C.J. and Wasserman, W., 1996. *Applied linear statistical models*, 4th edition. Irwin, Burr Ridge, Illinois, US.
- Newnham, R.M., 1999. Environmental change in Northland, New Zealand during the last glacial and Holocene. *Quaternary International* 57/58, 61-70.
- Newnham, R.M. and Lowe, D.J., 1991. Holocene vegetation and volcanic activity, Auckland Isthmus, New Zealand. *Journal of Quaternary Science* 6, 177-193.
- Newnham, R. M., Lowe, D. J. and Green, J. D., 1989. Palynology, vegetation, and climate of the Waikato lowlands, North Island, New Zealand, since c. 18 000 years ago. *Journal of the Royal Society of New Zealand* 19, 127-150.
- Newnham, R.M., Lowe, D.J. and Matthews, B.W., 1998. A late Holocene and prehistoric record of environmental change from Lake Waikaremoana, New Zealand. *The Holocene* 8, 443-454.
- Newnham, R.M., Lowe, D.J. and Alloway, B., 1999. Volcanic hazards in Auckland, New Zealand: a preliminary assessment of the threat posed by central North Island silicic volcanism based on the Quaternary tephrostratigraphical record. *Volcanoes in the Quaternary*. London Geological Society Special Publication 161, 27-45.
- Newnham, R.M., Lowe, D.J., Green, J.D., Turner, G.M., Harper, M.A., McGlone, M.S., Stout, S.L., Horie, S. and Froggatt, P.C., 2004. A discontinuous ca. 80 ka record of Late Quaternary environmental change from Lake Omapere, Northland, New Zealand. *Palaeogeography, Palaeoclimatology, Palaeoecology* 207, 165-198.
- O'Brien, J.S. and Fullerton, W.T., 1990. Two-dimensional modeling of alluvial fan flows. *American Society of Civil Engineers, Proceedings of International Symposium Hydraulics/Hydrology of Arid Lands*, San Diego, California, US, pp 263-273.
- O'Callaghan, J.F. and Mark, D.M., 1984. The extraction of drainage networks from digital elevation data. *Computer Vision, Graphics and Image Processing* 28, 323-344.
- Ogden, J., 1985. An introduction to plant demography with special reference to New Zealand trees. *New Zealand Journal of Botany* 23, 751-772.
- Ogden, J., Wardle, G.M. and Ahmed, M., 1987. Population dynamics of the emergent conifer *Agathis australis* (D. Don) Lindl. (kauri) in New Zealand. 2. Seedling population sizes and gap-phase regeneration. *New Zealand Journal of Botany* 25, 231-242.
- Ogden, J., Wilson, A., Hendy, C., and Newnham, R.M., 1992. The late Quaternary history of kauri (*Agathis australis*) in New Zealand and its climatic significance. *Journal of Biogeography* 19, 611-622.
- Ogden, J. and Stewart, G.H., 1995. Community dynamics of the New Zealand conifers. In: Enright, N.J. and Hill, R.S. (Eds.), *Ecology of the southern conifers*. Melbourne University Press, Melbourne, Australia, pp 81-119.
- O'Hara, S.L., Street-Perrott, F.A. and Burt, T.P., 1993. Accelerated soil erosion around a Mexican highland lake caused by pre-Hispanic agriculture. *Nature* 362, 48-51.
- O'Loughlin, E.M., 1986. Prediction of surface saturation zones in natural catchments by topographic analysis: *Water Resources Research* 22, 794-804.
- Overeem, I., Kroonenberg, S. B., Veldkamp, A., Groenesteijn, K., Rusakov, G. V. and Svitoch, A. A., 2003. Small-scale stratigraphy in a large ramp delta: recent and Holocene sedimentation in the Volga delta, Caspian Sea. *Sedimentary Geology* 159, 133-157.

- Overmars, K.P., de Koning, G.H.J. and Veldkamp, A., 2003. Spatial autocorrelation in multi-scale land use models. *Ecological Modelling* 164, 257-270.
- Owens, P. and Slaymaker, O., 1993. Lacustrine sediment budgets in the coast mountains of British Columbia, Canada. In: McManus, J., Duck, R.W. (Eds.), *Geomorphology and Sedimentology of Lakes and Reservoirs*. Wiley, New York, US, pp 105-123.
- Pack, R.T., Tarboton D.G. and Goodwin, C.N., 2001. Assessing Terrain Stability in a GIS using SINMAP. 15th annual GIS conference, GIS 2001, Vancouver, British Columbia.
- Page, M.J. and Trustrum, N.A., 1997. A late Holocene lake sediment record of the erosion response to land use change in a steep-land catchment, New Zealand. *Zeitschrift für Geomorphologie Neue Folge* 41, 369-392.
- Page, M.J., Trustrum, N.A. and Dymond, J.R., 1994a. Sediment budget to assess the geomorphic effect of a cyclonic storm, New Zealand. *Geomorphology* 9, 69-188.
- Page, M.J., Trustrum, N.A. and DeRose, R.C., 1994b. A high resolution record of storm-induced erosion from lake sediments, New Zealand. *Journal of Paleolimnology* 11, 33-348.
- Page, M.J., Reid, L.M. and Lynn, I.H., 1999. Sediment production from Cyclone Bola landslides, Waipaoa catchment. *Journal of Hydrology (NZ)* 38, 289-308.
- Page, M., Trustrum, N., Brackley, H. and Baisden, T., 2004. Erosion-related soil carbon fluxes in a pastoral steep-land catchment, New Zealand. *Agriculture, Ecosystems and Environment* 103, 561-579.
- Pain, C.F. and Bowler, J.M., 1973. Denudation following the November 1970 earthquake at Madang, Papua New Guinea. *Zeitschrift fuer Geomorphologie, Supplementband* 19, 92-104.
- Panuska, J.C., Moore, I.D. and Kramer, L.A., 1991. Terrain analysis: integration into the agriculture non-point source (AGNPS) pollution model. *Journal of Soil and Water Conservation* 46, 59-64.
- Pearce, J. and Ferrier, S., 2000. Evaluating the predictive performance of habitat models developed using logistic regression. *Ecological Modelling* 133, 225-245.
- Peckham, S.D., 1998. Efficient extraction of river networks and hydrologic measurements from digital elevation data. In: Barndorff-Nielsen O.E. (Ed.), *Stochastic Methods in Hydrology: Rain, Landforms and Floods*. World Scientific, New Jersey, US, pp 173-203.
- Petit J.R., Jouzel J., Raynaud D., Barkov N.I., Barnola J.M., Basile I., Bender M., Chappellaz J., Davis J., Delaygue G., Delmotte M., Kotlyakov V.M., Legrand M., Lipenkov V., Lorius C., Pépin L., Ritz C., Saltzman E. and Stievenard M., 1999. Climate and Atmospheric History of the Past 420,000 years from the Vostok Ice Core, Antarctica. *Nature* 399, 429-436.
- Pfeffer, K., Pebesma, E.J. and Burrough, P.A., 2003. Mapping alpine vegetation using vegetation observations and topographic attributes. *Landscape Ecology* 18, 759-776.
- Phillips, C. and Watson, A., 1994. Structural tree root research in New Zealand: a review. *Landcare Research Science Series*, vol. 71., Manaaki Whenua Press, Lincoln, New Zealand.
- Pillans, B., 1983. Upper Quaternary marine terrace chronology and deformation, South Taranaki, New Zealand. *Geology* 11, 292-297.
- Pillans, B., 1990. Pleistocene marine terraces in New Zealand: a review. *New Zealand Journal of Geology and Geophysics* 33, 219-231.
- Pillans, B., 1994. Direct marine-terrestrial correlations, Wanganui Basin, New Zealand: the last 1 million years. *Quaternary Science Reviews*, 13, 189-200.
- Pillans, B., McGlone, M., Palmer, A., Mildenhall, D., Alloway, B. and Berger, G., 1993. The last glacial maximum in central and southern North Island, New Zealand: a paleoenvironmental reconstruction using Kawakawa tephra formation as a chronostratigraphic marker. *Palaeogeography, Palaeoclimatology, Palaeoecology* 101, 283-304.
- Pinder III, J.E., Kroh, G.C., White, J.D. and Basham May, A.M., 1997. The relationship between vegetation type and topography in Lassen Volcanic National Park. *Plant Ecology* 131, 17-29.
- Pirazzoli, P.A., Radke, U., Hantoro, W.S., Jouannic, C., Oang, C.T. Causse, C., and Borel Best, M., 1991. Quaternary raised coral-reef terraces on Sumba Island, Indonesia. *Science* 252, 1834-1836.
- Pizzuto, J.E. and Schwendt, A.E., 1997. Mathematical modelling of autocompaction of a Holocene transgressive valley-fill deposit, Wolfe Glade, Delaware. *Geology* 25, 57-60.
- Pontius, R.G. and Schneider, L.C., 2001. Land use change model validation by an ROC method for the Ipswich watershed, Massachusetts, USA. *Agriculture, Ecosystems & Environment* 85, 239-248.
- Quinn, P., Beven, K., Chevallier, P. and Planchon, O., 1991. The prediction of hillslope flow paths for distributed hydrological modelling using digital terrain models. *Hydrological Processes* 5, 59-79.

- Quinn, P.F., Beven, K.J. and Lamb, R., 1995. The $\ln(a/\tan\beta)$ index: how to calculate it and how to use it within the topmodel framework. *Hydrological Processes* 9, 161-182.
- Rausch, D.D. and Heinemann, H.G., 1984. Measurement of reservoir sedimentation. In: Hadley, R.F. and Walling D.E. (Eds.), *Erosion and Sedimentation Yield*. GeoBooks, Norwich, UK, pp 179-200.
- Reid, L.M. and Page, M.J., 2003. Magnitude and frequency of landsliding in a large New Zealand catchment. *Geomorphology* 49, 71-88.
- Restrepo, C., Vitousek, P. and Neville, P., 2003. Landslides significantly alter land cover and the distribution of biomass: an example from the Ninole ridges of Hawai'i. *Plant Ecology* 166, 131-143.
- Richardson, R.J.H., 1985. Quaternary geology of the North Kaipara barrier, Northland, New Zealand. *New Zealand Journal of Geology and Geophysics* 28, 111-127.
- Ricketts, B.D., 1975. Quaternary geology of the Parengarenga-Te Kao district. Unpublished MSc thesis, University of Auckland, New Zealand.
- Rockwell, T., Keller, E.A., Clark, M.N. and Johnson, D.L., 1984. Chronology and rates of faulting of Ventura River terraces, California. *Geological Society of America Bulletin* 95, 1466-1474.
- Sandiford, A., Horrocks, M., Newnham, R., Ogden, J. and Alloway, B., 2002. Environmental change during the last glacial maximum (c. 25 000-c. 16 500 years BP) at Mt Richmond, Auckland Isthmus, New Zealand. *Journal of the Royal Society of New Zealand* 32, 155-167.
- Sandiford, A., Newnham, R., Alloway, B. and Ogden, J., 2003. A 28 000-7600 cal yr BP pollen record of vegetation and climate change from Pukaki Crater, northern New Zealand. *Palaeogeography, Palaeoclimatology, Palaeoecology* 201, 235-247.
- Saulnier, G., Obled, C. and Beven, K., 1997. Analytical compensation between DTM grid resolution and effective values of saturated hydraulic conductivity within the TOPMODEL framework. *Hydrological Processes* 11, 1331-1346.
- Schofield, J.C., 1967. Geological Map of New Zealand 1:250 000. Sheet 3 Auckland. Department of Scientific and Industrial Research, Wellington, New Zealand.
- Schofield, J.C., 1975. Sea-level fluctuations cause periodic, post-glacial progradation, South Kaipara Barrier, North Island, New Zealand. *New Zealand Journal of Geology and Geophysics* 18, 295-316.
- Schoorl, J.M. and Veldkamp, A., 2001. Linking land use and landscape process modeling: a case study for the Alora region (South Spain). *Agriculture, Ecosystems and Environment* 85, 281-292.
- Schoorl, J.M., Sonneveld, M.P.W. and Veldkamp, A., 2000. Three-dimensional landscape process modeling: the effect of DEM resolution. *Earth Surface Processes and Landforms* 25, 1025-1043.
- Schoorl, J.M., Veldkamp, A. and Bouma, J., 2002. Modelling water and soil redistribution in a dynamic landscape context. *Soil Science Society of America Journal* 66, 1610-1619.
- Schumm, S.A., 1993. River response to baselevel change: implications for sequence stratigraphy. *Journal of Geology* 101, 279-294.
- Scull P., Franklin J., Chadwick O.A. and McArthur D., 2003. Predictive soil mapping: a review. *Progress in physical geography* 2, 171-197.
- Searle, E.J., 1944. Geology of the Southern Waitakere Hills Region West of Auckland City. *Transactions of the Royal Society of New Zealand* 74, 49-70.
- Segal, M., Mahrer, Y., Pielke, R.A. and Ookouchi, Y., 1985. Modeling transpiration patterns of vegetation along south and north facing slopes during the subtropical dry season. *Agricultural and Forest Meteorology* 36, 19-28.
- Selby, M., 1993. *Hillslope Materials and Processes*. Oxford University Press, Oxford, US.
- Shackleton, N.J., A. Berger, and W.R. Peltier, 1990. An alternative astronomical calibration of the lower Pleistocene timescale based on ODP Site 677. *Transactions of the Royal Society of Edinburgh: Earth Sciences* 81, 251-261.
- Shane, P., 1994. A widespread, early Pleistocene tephra (Potaka tephra, 1 Ma) in New Zealand: character, distribution and implications. *New Zealand Journal of Geology and Geophysics* 37, 25-35.
- Shane, P., 2000. Tephrochronology: a New Zealand case study. *Earth-Science Reviews* 49, 223-259.
- Shane, P. and Hoverd, J., 2002. Distal record of multi-sourced tephra in Onepoto Basin, Auckland, New Zealand: implications for volcanic chronology, frequency and hazards. *Bulletin of Volcanology* 64, 441-545.
- Shane, P. and Sandiford, A., 2003. Paleovegetation of marine isotope stages 4 and 3 in Northern New Zealand and the age of the widespread Rotoehu tephra. *Quaternary Research* 59, 420-429.

- Shane, P., Alloway, B., Black, T. and Westgate, J., 1996a. Isothermal plateau fission-track ages of tephra beds in an early-middle Pleistocene marine and terrestrial sequence, Cape Kidnappers, New Zealand. *Quaternary International* 34-36, 49-53.
- Shane, P., Black, T.M., Alloway, B.V. and Westgate, J., 1996b. Early to middle Pleistocene tephrochronology of North Island, New Zealand: Implications for volcanism, tectonism, and paleoenvironments. *Geological Society of America Bulletin* 108, 915-925.
- Shroder, J.F., Jr. and Bishop, M.P., 1995. Geobotanical assessment in the Great Plains, Rocky Mountains and Himalaya. *Geomorphology* 13, 101-119.
- Skidmore A.K., 1989. A comparison of techniques for calculating gradient and aspect from a gridded digital elevation model. *International Journal of Geographical Information Systems* 3, 323-334.
- Skidmore, A.K., Ryan, P.J., Dawes, W., Short, D. and O'Loughlin, E.O., 1991. Use of an expert system to map forest soils from a geographical information system. *International Journal of Geographical Information Science* 5, 431-445.
- Spell, T.L. and McDougall, I., 1992. Revisions to the age of the Brunhes-Matuyama boundary and the Pleistocene geo-magnetic polarity timescale. *Geophysical Research Letters* 19, 1181-1184.
- Spörli, K.B., 1989. Tectonic framework of Northland, New Zealand. *Royal Society of New Zealand Bulletin* 26, 3-13.
- Srinivasan, R. and Engel, B.A., 1991. Effect of slope prediction methods on slope and erosion estimates. *Applied Engineering in Agriculture* 7, 779-783.
- Staal, S.J., Baltenweck, I., Waithaka, M.M., deWolff, T., and Njoroge, L., 2002. Location and uptake: integrated household and GIS analysis of technology adaptation and landuse, with application to smallholder dairy farms in Kenya. *Agricultural Economics* 27, 295-315.
- Stokes, S., Lowe, D.L. and Froggatt, P.C., 1992. Discriminant function analysis and correlation of late Quaternary tephra deposits from Taupo and Okataina volcanoes, New Zealand, using glass shard major element compositions. *Quaternary International* 13/14, 103-120.
- Stuiver, M. and Polach, H.A., 1977. Discussion: Reporting of ¹⁴C data. *Radiocarbon* 19, 355-363.
- Stuiver, M., Reimer, P.J., Bard, E., Beck, J.W., Burr, G.S., Hughen, K.A., Kromer, B., McCormac, G., van der Plicht, J. and Spurk, M., 1998. INTCAL1998 radiocarbon age calibration, 24,000-0 cal B.P.. *Radiocarbon* 40, 1041-1083.
- Swanson, F.J., Kratz, T.K., Caine, N. and Woodmansee, R.G., 1988. Landform effects on ecosystem patterns and processes. *Bioscience* 38, 92-98.
- Swets, J.A., 1988. Measuring the accuracy of diagnostic systems. *Science* 240, 1285-1293.
- Takahashi T., 1991. *Debris Flow*. A.A. Balkema, Rotterdam, The Netherlands.
- Tang, S.M., Franklin, J.F. and Montgomery, D.R., 1997. Forest harvest patterns and landscape disturbance processes. *Landscape Ecology* 12, 349-363.
- Tappeiner, U., Tasser, E. and Tappeiner, G., 1998. Modelling vegetation patterns using natural and anthropogenic influence factors: preliminary experience with a GIS based model applied to an Alpine area. *Ecological Modelling* 113, 225-237.
- Tarboton, D.G., 1997. A new method for the determination of flow directions and upslope areas in grid digital elevation models. *Water Resources Research* 32, 309-319.
- Tarboton, D.G., 2000. TARDEM, A suite of programs for the Analysis of Digital Elevation Data. <http://www.engineering.usu.edu/cee/faculty/dtarb/tardem.html> [08-12-2004].
- Tarboton, D. G., Bras, R. L. and Rodriguez-Iturbe, I., 1992. A physical basis for drainage density. *Geomorphology* 5, 59-76.
- ten Broeke, E., 2002. Pleistocene coastal terrace chronology of the south-west coast of Northland, New Zealand. Unpublished MSc thesis, Wageningen University, the Netherlands.
- Thielen, A.H., Lücke, A., Diekkrüger, B. and Richter, O., 1999. Scaling input data by GIS for hydrological modelling. *Hydrological Processes* 13, 611-630.
- Thompson, J.A., Bell, J.C. and Butler, C.A., 2001. Digital elevation model resolution: effects on terrain attribute calculation and quantitative soil-landscape modelling. *Geoderma* 100, 67-89.
- Trenhaile, A.S., 2001. Modelling the Quaternary evolution of shore platforms and erosional continental shelves. *Earth Surface Processes and Landforms* 26, 1103-1128.
- Trustrum N.A., Gomez, B., Page, M.J., Reid, L.M. and Hicks, M., 1999. Sediment production, storage and output: The relative role of large magnitude events in steepland catchments. *Zeitschrift fuer Geomorphologie Neue Folge Supplement band* 115, 71-86.

- Turner, M.G. and Dale, V.H., 1990. Modeling landscape disturbance. In: Turner, M.G. and Gardner, R.H. (Eds.), *Quantitative Methods in Landscape Ecology*. Springer-Verlag, New York, US, pp 323-351.
- Vanacker, V., Vanderschaeghe, M., Govers, G., Willems, E., Poesen, J., Deckers, J. and De Bievere, B., 2003. Linking hydrological, infinite slope stability and land-use change models through GIS for assessing the impact of deforestation on slope stability in high Andean watersheds. *Geomorphology* 52, 299-315.
- Van Beek, L.P.H., 2002. The effect of land use and climatic change on slope stability in the Alcoy region (Spain). PhD thesis, Faculty of Geographical Sciences, Utrecht University, The Netherlands.
- Van den Berg, M.W. and van Hoof, T., 2001. The Maas terrace sequence at Maastricht, SE Netherlands evidence for 200 m of late Neogene and Quaternary surface uplift. In: Maddy, D., Macklin, M. and Woodward, J. (Eds.), *River Basin Sediment Systems: Archives of Environmental Change*. Balkema, Rotterdam, The Netherlands, pp 469-484.
- Vandre, B.C., 1985. Rudd Creek debris flow. In: Bowles, D.S. (Ed.) *Delineation of landslide, flash flood, and debris flow hazards in Utah*. General Series Rep UWRL/G-85/03, Utah Water Research Laboratory, Utah State University, Logan, Utah, pp 117-131.
- Van Westen, C.J., 1993. Application of geographical information systems to landslide hazard zonation. ITC Publication no.15, ITC, Enschede, The Netherlands.
- Veldkamp, A., 1992. A 3-D model of fluvial terrace development in the Allier basin (Limagne, France). *Earth Surface Processes and Landforms* 17, 487-500.
- Veldkamp, A. and Fresco, L.O., 1996a. CLUE: a conceptual model to study the conversion of land use and its effects. *Ecological Modelling* 85, 253-270.
- Veldkamp, A. and Fresco, L.O., 1996b. CLUE-CR: an integrated multi-scale model to simulate land use change scenarios in Costa Rica. *Ecological Modelling* 91, 231-248.
- Veldkamp, A. and Tebbens, L.A., 2001. Registration of abrupt climate changes within fluvial systems: insights from numerical modelling experiments. *Global and Planetary Change* 28, 129-144.
- Veldkamp, A. and Verburg, P.H., 2004. Modelling land use change and environmental impact. *Journal of Environmental Management* 72, 1-3.
- Vella, P., Kaewyana, W. and Vucetich, C.G., 1988. Late Quaternary terraces and their cover beds, north-western Wairarapa, New Zealand, and provisional correlations with oxygen isotope stages. *Journal of the Royal Society of New Zealand* 18, 309-324.
- Verburg, P.H., Soepboer, W., Veldkamp, A., Limpiada, R., Espaldon, V. and Sharifah Mastura, S.A., 2002. Modeling the spatial dynamics of regional land use: the CLUE-S model. *Environmental Management* 30, 391-405.
- Verburg, P.H., Ritsema van Eck, J., de Nijs, T.C.M., Dijst, M.J. and Schot, P., 2004. Determinants of land use change patterns in the Netherlands. *Environment and Planning B* 31, 125-150.
- Vloemans, H., 2004. A reconstruction of the Late Quaternary tectonic history of the Waitakere Ranges, using the fluvial terrace sequence of the Kumeu River, Northland, New Zealand. Unpublished MSc thesis, Wageningen University, the Netherlands.
- Vucetich, C.G., Vella, P. and Warnes, P.N., 1996. Antepenultimate glacial to last glacial deposits in southern Wairarapa, New Zealand. *Journal of the Royal Society of New Zealand* 26, 469-482.
- Waitakere Ranges Protection Society, 1979. *Wainamu-Te Henga - A Study*. Auckland, New Zealand, 106 pp.
- Walker, L.R. and Boneta, W., 1995. Plant and soil responses to fire on a fern-covered landslide in Puerto Rico. *Journal of Tropical Ecology* 11, 473-479.
- Walker, L.R., Zarin, D.J., Myster, R.W. and Johnson, A.H., 1996. Ecosystem development and plant succession on landslides in the Caribbean. *Biotropica* 28, 566-576.
- Walling, D.E., 1983. The sediment delivery problem. *Journal of Hydrology* 65, 209-237.
- Ward, T.J., 1981. Use of a mathematical model for estimating potential landslide sites in steep forested drainage basins. In: *Erosion and Sediment Transport in Pacific Rim Steeplands*. IAHS Publication 132, Christchurch, New Zealand, pp 21-41.
- Wardle, P., 1991. *Vegetation of New Zealand*. Cambridge Press, Cambridge, UK.
- Watercare Services Limited, 2001. *Waitakere Ranges Infrastructure - Waitakere Dam – Assessment of Environmental Effects*. Watercare Services Ltd., Auckland, New Zealand.
- Westaway, R., 2001. Flow in the lower continental crust as a mechanism for the Quaternary uplift of the Rhenish Massif, north-west Europe. In: Maddy, D., Macklin, M. and Woodward, J. (Eds.), *River Basin Sediment Systems: Archives of Environmental Change*. Balkema, Rotterdam, The Netherlands, pp 71-151.

- Westaway, R., Maddy, D. and Bridgland, D., 2001. Flow in the lower continental crust as a mechanism for the Quaternary uplift of south-east England: constraints from the Thames record. *Quaternary Science Reviews* 79, 23-36.
- Westgate, J.A., 1989. Isothermal plateau fission track ages of hydrated glass shards from silicic tephra beds. *Earth and Planetary Science Letters* 95, 226-234.
- White, P.S. and Pickett, S.T.A., 1985. Natural disturbance and patch dynamics: an introduction. In: Pickett, S.T.A. and White, P.S.(Eds.), *The ecology of natural disturbance and patch dynamics*. New York Academic Press, New York, US, pp 3-13.
- Wicks, J.M. and Bathurst, J.C., 1996. SHESED: a physically-based, distributed erosion and sediment yield component for the SHE hydrological modelling system. *Journal of Hydrology* 175, 213-238.
- Williams, P.W., 1977. Progradation at Whatipu Beach 1844-1976, Auckland, New Zealand. *New Zealand Geographer* 33, 84-89.
- Williams, P.W., 1982. Speleothem dates, Quaternary terraces and uplift rates in New Zealand. *Nature* 298, 257-260.
- Wilmshurst, J.M., Eden, D.N. and Froggatt, P.C., 1999. Late Holocene forest disturbance in Gisborne, New Zealand: a comparison of terrestrial and marine pollen records. *New Zealand Journal of Botany* 37, 523-540.
- Wilson, C.J.N., 1993. Stratigraphy, chronology, styles and dynamics of late Quaternary eruptions from Taupo Volcano, New Zealand. *Philosophical Transactions of the Royal Society London A343*, 205-306.
- Wilson C.J.N., Houghton, B.F., Kamp, P.J.J. and McWilliams, M.O., 1995. An exceptionally widespread ignimbrite with implications for pyroclastic flow emplacement. *Nature* 378, 605-607.
- Wilson J.P. and Gallant, J.C. (Eds.), 2000. *Terrain analysis: Principles and applications*. John Wiley and Sons, New York, US.
- Wilson, J.P., Repetto, P.L. and Snyder, R.D., 2000. Effect of data source, grid resolution and flow-routing method on computed topographic attributes. In: Wilson J.P. and Gallant, J.C. (Eds.), *Terrain analysis: Principles and applications*. John Wiley & sons, New York, US, pp 133-161.
- Wise, S.M., 1998. The effect of GIS interpolation errors on the use of digital elevation models in geomorphology In: Lane, S.N., Richards, K.S. and Chandler, J.H. (Eds.), *Landform monitoring, modelling and analysis*. John Wiley & Sons Ltd., New York, US, pp 139-164.
- Wise S.M., 2000. Assessing the quality for hydrological applications of digital elevation models derived from contours. *Hydrological Processes* 14, 1909-1929.
- Wolock, D.M. and McGabe, G.J., 1995. Comparison of single and multiple flow direction algorithms for computing topographical parameters in TOPMODEL. *Water Resources Research* 31, 1315-1324.
- Wolock, D.M. and Price, C.V., 1994. Effects of digital elevation model map scale and data resolution on a topography based watershed model. *Water Resources Research* 30, 1665-1680.
- Wu, W. and Sidle, R.C., 1995. A distributed slope stability model for steep forested basins. *Water Resources Research* 31, 2097-2110.
- Zaitchik, B.F., van Es, H.M. and Sullivan, P.J., 2003. Modeling slope stability in Honduras: Parameter sensitivity and scale of aggregation. *Soil Science Society of America Journal* 67, 268-278.
- Zhang, W. and Montgomery, D.R., 1994. Digital elevation model grid size, landscape representation, and hydrologic simulations. *Water Resources Research* 30(4), 1019-1028.
- Zhou, Q. and Liu, X., 2002. Error assessment of grid-based flow routing algorithms used in hydrological models. *International Journal of Geographical Information Science* 16, 819-842.

Summary

The research resulting in this thesis entitled '*Modelling Landslide Dynamics in Forested Landscapes*' with the subtitle '*Addressing landscape evolution, landslide soil redistribution and vegetation patterns in the Waitakere Ranges, west Auckland, New Zealand*' covers the geological, geomorphological and landscape ecology related themes of the project '*Podzolisation under Kauri (Agathis australis): for better or worse?*' supported by the Netherlands Organisation for Scientific Research (NWO). The general objective of this thesis is to investigate landscape, soil and vegetation dynamics in the Waitakere Ranges Regional Park on the North Island of New Zealand, where also all the fieldwork was carried out. The main core of the thesis consists of the development of a dynamic landscape process model to simulate soil redistribution by shallow landsliding. Resulting spatial patterns of erosion and deposition, changes in landslide susceptibility over time and the relation of spatially explicit landscape attributes with vegetation patterns are further explored.

- **Chapter 1** is a general introduction elaborating on the geology, climate and socio-economic setting of the study area and explains the main objectives and research questions. The contents and overall structure of the thesis are also illustrated. Following this introductory chapter, the thesis is composed of 5 chapters based on scientific papers published in or submitted to peer reviewed journals.

- **Chapter 2** deals with the general tectonic setting of the study area. Quaternary coastal and fluvial terrace morphology and chronology are explored to reconstruct the tectonic history of the south-west coast of the Northland region in New Zealand. This chapter is situated on the geological timescale (1.8 Ma BP till present) and places the subsequent chapters dealing with the landscape process model and its applications, acting on a timescale of years to decades, in a broader spatio-temporal perspective. Field surveys and the analysis of aerial photography yield an inventory of 13 fluvial and 12 marine terrace levels. Due to poor exposure of clear field evidence in the form of e.g. wave-cut platforms or distinct river sediments, planar landscape morphology forms the main criterion for terrace remnant identification. Based on the record of terrace height spacings, sparse tephra age control and correlation with global paleoclimatic records, an attempt is made to reconstruct the regional Quaternary uplift rates. Because no hard chronostratigraphic marker is present within the fluvial terrace sequence, fluvial terrace levels are linked to the marine sequence by using the mean uplift rates calculated from the marine terraces (0.35 mm yr^{-1} from 0- 0.1 Ma and 0.26 mm yr^{-1} from 0.1-

0.3 Ma). Both sets of terraces are then correlated with oxygen isotope fluctuations and the astronomically tuned timescale from ODP Site 677 and the Vostok ice core paleoclimatic records. Oldest marine and fluvial terrace levels are estimated 1.21 Ma and 0.242 Ma respectively. Although there seems to be some form of controversy about the uplift history and especially the preservation of terraces in the study area, a general regional uplift, superimposed on glacio-eustatic sea-level changes, is substantiated as the only possible mechanism leading to the maintenance of a considerable relief and active denudation processes inland.

- **Chapter 3** deals with the development and application of the LAPSUS-LS landscape process model. The model is constructed as a component of the LAPSUS modelling framework (LandscApe ProcesS modelling at mUlti dimensions and scaleS; -LS: LandSlide, refers to the process specific model component). LAPSUS-LS delineates the location of shallow landslide initiation sites and simulates the effects on spatial patterns of soil redistribution and resulting landslide hazard for a large watershed within the study area. Processes that need to be incorporated in the model are reviewed followed by the proposed modelling framework. The model predicts the spatial pattern of landslide susceptibility within the simulated catchment and subsequently applies a spatial algorithm for the redistribution of failed material on the basis of a scenario of triggering rainfall events, relative landslide hazard and trajectories with runout criteria for failed slope material. The model forms a spatially explicit method to address the effects of shallow landslide erosion and sedimentation because digital elevation data are adapted between timesteps and on- and off-site effects over the years can be simulated in this way. By visualisation of the modelling results in a GIS environment, the shifting pattern of upslope and downslope (in)stability, triggering of new landslides and the resulting slope retreat by soil material redistribution due to former mass movements is simulated and assessed.

- **Chapter 4** zooms in on a more theoretical aspect of the LAPSUS-LS model and evaluates digital elevation model (DEM) resolution effects on model results. The focus is on influences of grid size on landslide soil redistribution quantities and resulting spatial patterns and feedback mechanisms. Distributions of slope, specific catchment area and relative hazard for shallow landsliding are analysed for four different DEM resolutions (grid sizes of 10, 25, 50 and 100 m) for a 12 km² study catchment in the Waitakere Ranges. The effect of DEM resolution proves to be especially pronounced for the boundary conditions determining a valid landslide hazard calculation. For coarse resolutions, the smoothing effect results in a larger area becoming classified as unconditionally stable or unstable. Simple empirical soil redistribution algorithms are applied for scenarios in which all sites with a certain landslide hazard fail and generate debris flow. The lower initial number of failing cells but also the inclusion of slope (limit) in those algorithms becomes apparent with coarser resolutions. For finer resolutions, much larger amounts of soil redistribution are found, which is attributed to the more detailed landscape representation. Looking at spatial patterns of landslide erosion and sedimentation, the size of the area affected by these processes also increases with finer resolutions. In general, landslide erosion occupies larger parts of the area than deposition, although the total amounts of soil material eroded and deposited are the same. Analysis of feedback mechanisms between soil failures over time shows that finer resolutions show higher percentages of the area with an increased or decreased landslide hazard. When the extent of sites with lower and higher hazards are compared, finer grid sizes and higher landslide hazard threshold scenarios tend to increase the total extent of areas becoming more

stable relative to the less stable ones. It is concluded that extreme care should be taken when quantifying landslide basin sediment yield by applying simple soil redistribution formulas to DEMs with different resolutions. Rather, quantities should be interpreted as relative amounts. For studying shallow landsliding over a longer timeframe, the 'perfect' DEM resolution may not exist, because no resolution can possibly represent the dimensions of all different slope failures scattered in space and time. It is emphasised that the choice of DEM resolution, possibly restricted by data availability in the first place, should always be adapted to the context of a particular type of analysis.

- **Chapter 5** and **6** describe two distinct applications of the LAPSUS-LS model: in **Chapter 5**, a sediment record is used, in combination with the LAPSUS-LS model, to reconstruct the incidence of high-magnitude/low-frequency landslide events in the upper part of the Waitakere River catchment and the history of the Te Henga wetland at the outlet. Sediment stratigraphy and chronology are interpreted by radiocarbon dating, foraminiferal analysis, and provisional tephrochronology. Gradual impoundment of the wetland began c. 6000 cal yr BP, coinciding with the start of a gentle sea-level fall, but complete damming and initial sedimentation did not begin until c. 1000 cal yr BP. After damming, four well-defined sediment pulses occurred and these are preserved in the form of distinct clay layers in most of the sediment cores. For interpreting the sediment pulses, the LAPSUS-LS model is applied to determine spatially distributed relative landslide hazard, applicable at the catchment scale. An empirical landslide soil redistribution component is added to determine sediment delivery ratio and the impact on total catchment sediment yield. Sediment volumes are calculated from the wetland cores and corresponding landslide scenarios are defined through back-analysis of modelled sediment yield output. In general, at least four major high-magnitude landslide events, both natural and intensified by forest clearance activities, occurred in the catchment upstream of Te Henga wetland during the last c. 1000 years. Their magnitude can be expressed by a range of critical rainfall thresholds representing a LAPSUS-LS scenario.

- **Chapter 6** is a more ecologically focused application of the model and links digital terrain analysis and landslide modelling with the spatial distribution of mature kauri trees. The use of topographical attributes for the analysis of the spatial distribution and ecological cycle of kauri (*Agathis australis*), a canopy emergent conifer tree from northern New Zealand, is studied. Several primary and secondary topographic attributes are derived from a DEM for the Waitakere River catchment and the contribution of these variables in explaining presence or absence of mature kauri is assessed with logistic regression and Receiver Operating Characteristic (ROC) plots. The topographically based landslide hazard index calculated with the LAPSUS-LS model appears to be very useful in explaining the occurrence and ecological dynamics of kauri. It is shown that the combination of topographic -, soil physical - and hydrological parameters in the calculation of this single landslide hazard index, performs better in explaining presence of mature kauri than using topographic attributes calculated from the DEM properties alone. Moreover, this example demonstrates the possibilities of using terrain attributes for representing geomorphological processes and disturbance mechanisms, often indispensable in explaining a species' ecological cycle and forest stand dynamics. The results of this analysis support the 'temporal stand replacement model', involving disturbance as a dominant ecological process in forest regeneration, as an interpretation of the community dynamics of kauri. Furthermore, a certain threshold maturity stage, in which trees become able to stabilise landslide prone sites and postpone a possible

disturbance by this process, together with great longevity are seen as major factors making kauri a 'landscape engineer'.

- Synthesising, **Chapter 7** reflects on the most important conclusions from the research resulting in this thesis and discusses the achievement of the main objectives and answers to the research questions postulated in Chapter 1. Three general themes are put forward covering the previous chapters. Finally some ideas for future research are suggested.

Samenvatting

Het onderzoek resulterend in dit proefschrift getiteld ‘*Het modelleren van dynamiek van aardverschuivingen in beboste landschappen*’ met als ondertitel ‘*landschapsevolutie, bodemherverdeling door aardverschuivingen en vegetatie patronen in de Waitakere Ranges, west Auckland, Nieuw-Zeeland*’ behandelt de geologische, geomorfologische en landschaps-ecologische thema’s van het project ‘*Podzolvorming onder Kauri (Agathis australis): in voor- en tegenspoed?*’ ondersteund door de Nederlandse Organisatie voor Wetenschappelijk Onderzoek (NWO). Het algemene doel van dit proefschrift is het onderzoeken van landschap, bodem en vegetatie dynamiek in het regionale park de Waitakere Ranges op het noordeiland van Nieuw-Zeeland, waar ook al het veldwerk werd uitgevoerd. De kern van het proefschrift bestaat uit de ontwikkeling van een dynamisch landschapsprocesmodel om bodemherverdeling door aardverschuivingen te simuleren. De resulterende spatiële patronen van erosie en depositie, veranderingen in het risico op aardverschuivingen in de tijd en het verband tussen spatiëel expliciete landschapskenmerken en vegetatie patronen worden verder onderzocht.

- **Hoofdstuk 1** vormt een algemene inleiding waarin de geologie, het klimaat en de socio-economische situatie van het studiegebied worden behandeld en de algemene doelstellingen en onderzoeksvragen worden uiteengezet. De inhoud en algemene structuur van het proefschrift worden ook geïllustreerd. Volgend op dit inleidende hoofdstuk, is het proefschrift samengesteld uit 5 hoofdstukken die gebaseerd zijn op wetenschappelijke artikels gepubliceerd in of ingediend bij gerecenseerde tijdschriften.

- **Hoofdstuk 2** behandelt de algemene tektonische situatie van het studiegebied. De morfologie en chronologie van Kwartaire kust- en rivierterrassen worden bestudeerd om de tektonische geschiedenis van de zuid-west kust van de regio Northland in Nieuw-Zeeland te reconstrueren. Dit hoofdstuk situeert zich op de geologische tijdschaal (1.8 miljoen jaar geleden tot nu) en plaatst de erop volgende hoofdstukken, die het landschapsprocesmodel en de toepassingen ervan behandelen, in een breder spatiëel en temporeel perspectief. Veldonderzoek en de analyse van luchtfoto’s resulteren in een totaal van 13 rivier- en 12 kustterrasniveaus. Duidelijke aanwijzingen in het veld zoals bvb abrasievlakken of riviersedimenten ontbreken en een vlakke morfologie van het landschap vormt het voornaamste criterium om terrasresten te identificeren. Gebaseerd op de hoogteniveaus van de terrassen, een zwakke tijdscontrole door vulkanische assen en de correlatie met globale

paleoklimatologische data, wordt een poging gedaan om de Kwartaire oplichtsnelheden van de regio te reconstrueren. Omdat er zich geen duidelijke chronostratigrafische referentie bevindt in de rivierterras sequentie worden de rivierterras niveaus gelinkt aan de mariene sequentie door de gemiddelde oplichtsnelheden berekend met de kustterrassen te gebruiken (0.35 mm per jaar van 0-0.1 miljoen jaar en 0.26 mm per jaar van 0.1-0.3 miljoen jaar geleden). Beide series terrassen worden dan gecorreleerd aan zuurstof isotoop fluctuaties en de astronomisch gekalibreerde tijdschaal van diepzeeboring ODP677 en de Vostok ijsboring. De oudste kust- en rivierterras niveaus worden respectievelijk geschat op 1.21 en 0.242 miljoen jaar oud. Ondanks de controverse in de literatuur over de oplichtgeschiedenis en vooral de preservatie van terrassen in het studiegebied, wordt een algemene regionale oplicht, gecombineerd met glacio-eustatische schommelingen in zeeniveau, gezien als het enige mogelijke mechanisme dat leidt tot het behoud van een behoorlijk reliëf en actieve denudatieprocessen landinwaarts.

- **Hoofdstuk 3** behandelt de ontwikkeling en toepassing van het landschapsprocesmodel LAPSUS-LS. Het model is ontworpen als een deelcomponent van het algemene LAPSUS erosie/sedimentatie model (LandscApe ProcesS modelling at mUlti dimensions and scaleS; -LS: LandSlide, verwijst naar aardverschuiving, het specifieke landschapsproces van deze component). LAPSUS-LS duidt plaatsen waar ondiepe aardverschuivingen kunnen starten aan en simuleert de effecten op spatiële patronen van bodemherverdeling en resulterend risico op aardverschuivingen voor een groot stroomgebied in het studiegebied. De processen die in het model moeten opgenomen worden, worden behandeld alsook de voorgestelde modelstructuur. Het model voorspelt het spatiële patroon van gevoeligheden voor aardverschuivingen binnen het stroomgebied en past daarna een algoritme toe dat de resulterende bodemherverdeling simuleert op basis van een regenval scenario, relatief risico op aardverschuivingen en de bestemmingstrajecten van bodemmateriaal gebaseerd op uitloop criteria. Het model vormt een spatiëel expliciete methode om de effecten van erosie en sedimentatie door ondiepe aardverschuivingen te analyseren omdat digitale hoogtegegevens aangepast worden tussen verschillende tijdstappen en zo de lokale effecten en gevolgen op langere afstand kunnen worden gesimuleerd. Door de model resultaten te visualiseren in een Geografisch Informatie Systeem, kan het steeds veranderende patroon van het al dan niet veroorzaken van nieuwe aardverschuivingen boven- en onderaan de helling door oudere aardverschuivingen in de tijd worden getoond.

- **Hoofdstuk 4** zoomt in op een meer theoretisch aspect van het LAPSUS-LS model en evalueert de effecten van verschillende resoluties van een digitaal hoogtemodel (DTM) op model resultaten. De nadruk ligt op invloeden van grid resolutie op hoeveelheden bodemherverdeling door aardverschuivingen, resulterende spatiële patronen en terugkoppeling mechanismen. Verdelingen van helling, specifieke vanggebied oppervlakte en relatief risico op aardverschuivingen worden geanalyseerd voor vier verschillende DTM resoluties (10, 25, 50 and 100 m) voor een stroomgebied van 12 km² in de Waitakere Ranges. Het effect van DTM resolutie blijkt vooral uitgesproken te zijn bij het opstellen van de randvoorwaarden die een geldige berekening van het risico op aardverschuivingen bepalen. Voor grove resoluties resulteert een nivellerend effect in een groter gebied dat als onvoorwaardelijk stabiel of instabiel wordt geclassificeerd. Eenvoudige empirische bodemherverdeling algoritmes worden dan toegepast voor scenario's waarbij op alle posities in het landschap met een bepaald risico op aardverschuivingen een aardverschuiving wordt gesimuleerd. Voor steeds grovere resoluties wordt het effect duidelijk van het initieel lagere aantal gridcellen waar een aardverschuiving optreedt alsook de aanwezigheid van een

hellingslimiet in de algoritmes voor bodemherverdeling. Bij fijnere resoluties worden veel grotere hoeveelheden bodemherverdeling gevonden, te wijten aan de meer gedetailleerde voorstelling van het landschap. De grootte van de oppervlakte betrokken bij erosie en sedimentatie door aardverschuivingen neemt ook toe bij fijnere resoluties. In het algemeen neemt erosie door aardverschuivingen een grotere oppervlakte in dan depositie, ondanks het feit dat totale hoeveelheden gelijk zijn. De analyse van terugkoppelingseffecten tussen processen in de tijd toont aan dat fijnere resoluties een hoger percentage van het gebied met een veranderd risico op aardverschuivingen veroorzaken. Wanneer de oppervlakte van plekken met een hoger of lager risico op aardverschuivingen worden vergeleken, blijkt dat fijnere resoluties samen met hogere scenario drempelwaarden voor risico op aardverschuivingen de totale oppervlakte van stabielere plekken relatief verhogen ten opzichte van minder stabielere plekken. Er wordt geconcludeerd dat hoge voorzichtigheid is aangewezen wanneer totale hoeveelheden sediment veroorzaakt door aardverschuivingen voor een stroomgebied worden berekend met eenvoudige algoritmes voor bodemherverdeling toegepast op DTMs met verschillende resolutie. Hoeveelheden moeten eerder als relatieve dan als absolute hoeveelheden geïnterpreteerd worden. Waarschijnlijk bestaat de ideale resolutie voor een DTM voor het bestuderen van ondiepe aardverschuivingen op langere termijn niet, omdat geen enkele resolutie alle dimensies van verschillende aardverschuivingen in tijd en ruimte kan vertegenwoordigen. Er wordt benadrukt dat de keuze van de resolutie van een DTM, waarschijnlijk in de eerste plaats al beperkt door de beschikbaarheid van data, bovenal moet worden gemaakt rekening houdend met de specifieke toepassing waarvoor het gebruikt moet worden.

• **Hoofdstukken 5 en 6** beschrijven twee verschillende toepassingen van het LAPSUS-LS model: in **Hoofdstuk 5** wordt gebruik gemaakt van een sediment opname in het Te Henga moeras, gecombineerd met het LAPSUS-LS model, om het voorkomen van aardverschuivingen met een grote omvang en lage frequentie te reconstrueren voor het bovenstroomgebied van de Waitakere Rivier, en vat te krijgen op de geschiedenis van het moeras zelf dat de monding van de rivier vormt. Sediment stratigrafie en chronologie worden geïnterpreteerd door gebruik te maken van C14 datering, analyse van foraminiferae en tephrochronologie. Een geleidelijke afdamming van het moeras begon ongeveer 6000 jaar geleden en viel samen met de start van een kleine verlaging van het zeeniveau. De volledige afdamming en de start van sedimentatie in het moeras begon echter pas ongeveer 1000 jaar geleden. Na deze afdamming vonden vier fases van sedimentatie plaats en deze zijn bewaard als duidelijke kleilagen in sediment boringen. Om deze sediment pulsen te interpreteren wordt het LAPSUS-LS model toegepast om het relatieve risico op aardverschuivingen te berekenen voor het stroomgebied. Er wordt een empirische bodemherverdeling component toegevoegd om de hoeveelheid sediment die in rivieren terechtkomt en de totale hoeveelheid sediment die door het stroomgebied wordt afgeleverd te bepalen. De volumes van de sediment pulsen worden berekend uit de boringen in het moeras en een scenario voor aardverschuivingen dat hiermee overeenkomt wordt bepaald door het terugrekenen van gemodelleerde hoeveelheden sediment. Minstens vier periodes met grote aardverschuivingen, zowel natuurlijk als veroorzaakt door menselijke activiteiten, blijken te zijn voorgekomen in het bovenstroomgebied van het Te Henga moeras gedurende de laatste 1000 jaar. De omvang van deze gebeurtenissen kan worden uitgedrukt door een marge van drempelwaarden voor kritische regenval die op hun beurt een LAPSUS-LS scenario vertegenwoordigen.

- **Hoofdstuk 6** is een meer ecologisch toegespitste toepassing van het model die digitale terrein analyse en het modelleren van aardverschuivingen linkt met de spatiële verdeling van volwassen kauri bomen. Het gebruik van topografische eigenschappen voor de analyse van de spatiële verdeling en ecologische cyclus van kauri (*Agathis australis*), een conifeer uit noord Nieuw-Zeeland, wordt bestudeerd. Verschillende primaire en secundaire topografische eigenschappen worden afgeleid uit een digitaal hoogtemodel voor het stroomgebied van de Waitakere rivier en de bijdrage van deze variabelen voor de verklaring van aanwezigheid van volwassen kauri bomen wordt bestudeerd met logistische regressie en Receiver Operating Characteristic (ROC) grafieken. De topografisch gebaseerde index voor het risico op aardverschuivingen berekend met het LAPSUS-LS model blijkt erg nuttig in het verklaren van de aanwezigheid van kauri bomen en hun ecologische dynamiek. Er wordt aangetoond dat de combinatie van topografische-, bodemfysische- en hydrologische parameters in de berekening van deze ene index voor risico op aardverschuivingen, beter presteert in het verklaren van aanwezigheid van volwassen kauri bomen dan wanneer enkel topografische eigenschappen berekend uit het DTM worden gebruikt. Bovendien toont dit voorbeeld de mogelijkheden van het gebruik van terrein eigenschappen om geomorfologische processen en verstoringmechanismen voor te stellen aan, die vaak onmisbaar zijn in de verklaring van de ecologische cyclus van een boomsoort en de dynamiek van standplaatsen in een bos. De resultaten van deze analyse spreken voor het ‘temporal stand replacement model’, waarbij verstoring als een dominant ecologisch proces bij bosregeneratie wordt gezien, als interpretatie voor de ecologie van kauri. Bovendien worden een zekere ouderdomsgrens, waarbij bomen onstabiele plaatsen beginnen te stabiliseren en op die manier een mogelijke verstoring door een aardverschuiving uitstellen, samen met het feit dat kauri bomen heel oud kunnen worden, gezien als belangrijke factoren die kauri bomen ‘landschapsingenieurs’ maken.
- **Hoofdstuk 7** is een synthese hoofdstuk dat terugblijkt op de belangrijkste resultaten van het onderzoek in dit proefschrift en waarin het behalen van de belangrijkste streefdoelen en het beantwoorden van de onderzoeksvragen uit hoofdstuk 1 worden bediscussieerd. Drie algemene thema’s worden naar voor gebracht die de vorige hoofdstukken samenbrengen. Tot slot worden enkele ideeën voor toekomstig onderzoek voorgesteld.

Curriculum Vitae

Lieven Claessens was born on the 2nd of January 1975 in Sint-Niklaas (Belgium). He completed secondary school at the Sint-Jan Berchmanscollege in Antwerp in 1993. The same year he started his study at the Faculty of Agricultural and Applied Biological Sciences, Catholic University of Leuven, where he obtained a Bachelor in Applied Bioscience and Engineering. In 1998 he moved to Wageningen University to study the MSc program Soil & Water. Research for his MSc thesis was conducted at Agritex, Harare (Zimbabwe), calibrating a crop growth model for maize based cropping systems to serve early warning applications. In January 2000 he graduated 'cum laude', with specialisations in Soil Science, Crop Science and GIS. After this he worked for URS Corporation in Brussels as a GIS consultant for soil remediation projects in Belgium and Germany. In October 2000 he started the research leading to this PhD thesis at the Laboratory of Soil Science and Geology, Wageningen University in the project entitled 'Podzolisation under Kauri (*Agathis australis*): for better or worse', funded by the Netherlands Organisation for Scientific Research (NWO). Within this project he studied soil-, landscape- and vegetation dynamics in the Waitakere Ranges Regional Park on the North Island of New Zealand. At the moment he is employed as Associate Teacher at the Laboratory of Soil Science and Geology, responsible for developing and renewing courses on landscape process modelling and sustainable land use and writing new project proposals for future research on soil-landscape-vegetation interactions.